foreword by
NOBEL LAUREATE ROALD HOFFMANN

molecular orbitals of transition metal complexes

YVES JEAN

OXFORD

Molecular Orbitals of Transition Metal Complexes

This page intentionally left blank

Molecular Orbitals of Transition Metal Complexes

Yves Jean

Laboratoire de Chimie Physique,
Université Paris-Sud

Translated by
Colin Marsden

Laboratoire de Physique Quantique,
Université Paul Sabatier,
Toulouse

OXFORD
UNIVERSITY PRESS

OXFORD
UNIVERSITY PRESS

Great Clarendon Street, Oxford OX2 6DP

Oxford University Press is a department of the University of Oxford.
It furthers the University's objective of excellence in research, scholarship,
and education by publishing worldwide in

Oxford New York

Auckland Bangkok Buenos Aires Cape Town Chennai
Dar es Salaam Delhi Hong Kong Istanbul Karachi Kolkata
Kuala Lumpur Madrid Melbourne Mexico City Mumbai Nairobi
São Paulo Shanghai Taipei Tokyo Toronto

Oxford is a registered trade mark of Oxford University Press
in the UK and in certain other countries

Published in the United States
by Oxford University Press Inc., New York

Original French edition:
Les orbitales moléculaires dans les complexes ISBN 2 7302 1024 5

First published 2005

A catalogue record for this title is available from the British Library

Library of Congress Cataloging in Publication Data

(Data available)

ISBN 0 19 853093 5 (Hbk)

10 9 8 7 6 5 4 3 2 1

Typeset by Newgen Imaging Systems (P) Ltd., Chennai, India
Printed in Great Britain
on acid-free paper by
Antony Rowe, Chippenham

Foreword

We are so divided. By the formal structure of university instruction—organic chemistry, inorganic chemistry, physical chemistry. By the incredible and unnecessary specialization of our journals. The molecular bounty we have ourselves created seems simply overwhelming—no wonder we seek compartmentalization in self-protection: It is easy to say, 'I'm an expert in Field x. And while I will listen to a seminar in y or z (when I have time), please . . . let me be happy just in keeping up with my own field.'

The dangers of specialization are obvious—inbreeding, lack of scope, a kind of rococo elaboration of chemical complexity within a field. And we know that new ideas often come from an almost metaphorical importation of a way of thinking or a technique from another area.

Meanwhile, all along, nature persists in subverting the compartmentalizing simplicity of our minds. Through enzymes whose seeming magic is done by metal atoms and clusters at the active site, inorganic chemistry and biochemistry are rejoined. Transition metal carbides put organic carbon into some most unusual, patently inorganic environments. And, beginning in 1950, the explosion in organometallic chemistry has given us an incredible riches of structures and reactions—from ferrocene to olefin metathesis, metal–metal multiple bonds, to C—H activation, and remarkable olefin polymerization catalysts. All from a combination of inorganic and organic chemistry.

Organometallic chemistry from its beginning also depended on, and also built, another bridge. This is to theoretical chemistry. The first, rationalizing accounts of the electronic structure of ferrocene and the Dewar–Chatt–Duncanson picture of metal–olefin bonding were followed by milestones such as the prediction of cyclobutadiene–iron tricarbonyl and Cotton's beautiful elaboration of the idea of a metal–metal quadruple bond. The work of Leslie Orgel played a very important role in those early days. There were fecund interactions all along—compounds leading to calculations, and calculations pushing experimentalists to make new molecules. Often the theory was done by the experimentalists themselves, for the best kind of theory (the one that keeps the fertile dance of experiment moving) is a portable one. As easy to use molecular orbital theory, the theory of choice of the times, most certainly was and is.

It is hard to imagine a contemporary course in organometallic chemistry which does not contain a hefty, albeit qualitative component of molecular orbital theory. Yves Jean (with François Volatron) earlier wrote a classic teaching text on the orbitals of organic molecules. Here he has applied his great pedagogical skills to the construction of a beautifully thought through exposition of bonding in organometallic chemistry. Our undergraduate and graduate students will enjoy this book. And they, the chemists of the future, will use the knowledge gained here to enlarge our experience with new organometallic molecules, subverting once again the arbitrary division of organic and inorganic chemistry. Molecules whose beauty and utility we still cannot imagine.

Roald Hoffmann

Acknowledgements

I would like to thank several colleagues who accepted to read and re-read the manuscript during its preparation, and whose remarks and comments were extremely useful to me: O. Eisenstein and C. Iung (Montpellier 2), J. Y. Saillard (Rennes 1), A. Strich (Strasbourg 1), I. Demachy (Paris Sud, Orsay), P. Le Floch and his group (D. Moores, M. Melaimi, N. Mezailles, M. Doux) at the Ecole Polytechnique (Palaiseau), R. Hoffmann (Cornell). My thanks also go to J. Courtieu (Paris Sud, Orsay), thanks to whom I have been able to give a lecture course on orbital interactions to chemistry students since 1987, and to A. Lledos (Barcelona), who encouraged me to write this book at a time when I was hesitating. For various reasons, I am grateful to F. Mathey (Director of the 'Hétéroéléments et Coordination' laboratory at the Ecole Polytechnique), L. Salem (founder of the laboratory 'Chimie Théorique' at Orsay), C. Pouchan (Pau), J. C. Rayez (Bordeaux 1), J. L. Rivail (Nancy 1), A. Fuchs (Director of the 'Laboratoire de Chimie Physique' at Orsay), M. and P. Jean, for their help.

This book also owes a large debt to the students who have followed my lectures. In order to transmit knowledge *and understanding*, even in an area which is completely familiar, it is necessary to clarify one's ideas so as to make a consistent and, if possible, attractive presentation. Students' comments, remarks, and questions really help the teachers to achieve this goal. When it comes to writing a manuscript, one realizes just how useful the slow development and maturation of ideas has been.

I am very honoured that Roald Hoffmann accepted to write the preface, and the reader will discover during the chapters just how much the book owes to him.

Ecole Polytechnique (Palaiseau)
Université Paris Sud (Orsay)
April 2004

Introduction

This book starts from the most elementary ideas of molecular orbital theory, and it leads the reader progressively towards an understanding of the electronic structure, of the molecular geometry and, in some cases, the reactivity of transition metal complexes.

The use of simple notions, such as symmetry, overlap, and electronegativity, allows a *qualitative* method of analysis of the electronic structure of complexes, and of the properties which follow from it such as geometry or reactivity, to be developed. Qualitative in the sense that, for example, it enables us to understand *why* the structure of a particular complex is tetrahedral rather than planar, without being able to provide a reliable numerical value of the energy difference between these two structures. The *quantitative* level can be attained elsewhere—as is now standard practice in our laboratories—by more accurate methods such as *ab initio* or density functional theories. But to interpret the results provided by more complex calculations, it is often necessary to return to the fundamental notions of symmetry, overlap, and electronegativity.

The qualitative approach used here is mainly based on the analysis of orbital interactions (atomic or molecular). Its application to transition metal complexes developed rapidly from about 1975, the leading exponent being Roald Hoffmann, winner of the Nobel prize for chemistry in 1981 with Kenichi Fukui. As a result, many experimental results can be rationalized, that is to say *understood*, on the basis of analyses and using a language that are accessible to every chemist. A colleague, Marc Bénard, spoke in the introduction to one of his lectures of the prodigious decade 1975–85 . . . Moreover, it has been possible to apply this approach to *all of chemistry* (organic, inorganic, organometallic, and the solid state), which is one of its strongest points. These are no doubt the main reasons for its success which has spread far beyond the realm of specialists: as Roald Hoffmann writes in the preface, it is a transferable theory which has marked our time.

It is certainly *transferable* to students, and the aim of this book is to encourage that process. By learning this method for the theoretical analysis of molecular electronic structure, a method which has so profoundly changed our approach to chemistry, the reader may be

encouraged to continue his exploration of the methods of quantum chemistry which nowadays are part of all chemical research.

In the first chapter, we present the rules for electron counting in transition metal complexes, the different coordination modes adopted by ligands and the essential properties of the orbitals that are involved on the metal and on the ligands. The main ligand fields are studied in the second chapter, where we limit ourselves to σ-type interactions between the metal and the ligands. The structure of the d block is established; knowledge of this structure, which is essential for transiton metal complexes, enables us to explore the relationships between the electronic configuration of complexes and their geometry. In the third chapter, we study the ways in which the analysis is changed when the ligands have π-type interactions with the metal (both π-donor and π-acceptor ligands). All these ideas are then used in the fourth chapter, which is a series of examples that illustrate how, starting from a knowledge of the orbital structure of complexes, we can understand their geometrical structure and, sometimes, their reactivity. The fifth chapter discusses the 'isolobal analogy' which shows how the electronic structures of transition metal complexes and of organic molecules can be related. A bridge is thus constructed between these two areas of chemistry that allows us to understand several resemblances (in particular, concerning structures) between species that appear to be very different. The last chapter contains a presentation of basic Group Theory, with applications to some of the complexes studied in the earlier chapters. This chapter is placed at the end of the book so as not to disrupt the flow of the more chemical aspects of the presentation, but the reader may consult it, if necessary, as and when reference is made to it in the book.

Setting the scene

Transition metal complexes are molecules containing one or more metallic centres (Ti, Fe, Ni, etc.) bound to a certain number of 'ligands'. These latter may be atoms (H, O, Cl, etc.), molecular fragments (CR_3, NR_2, SH, etc.), or molecules that are themselves stable in the absence of any interaction with a metal (NR_3, PR_3, $R_2C{=}CR_2$), benzene, etc.). In this book, we shall study the electronic structure of these complexes by molecular orbital (MO) theory. We shall seek to establish the shape, the energetic ordering, and the electronic occupation of the MO; starting from this detailed description of the electronic structure, we shall consider problems of geometry and reactivity.

Certain important aspects of electronic structure can nevertheless be obtained from a far simpler description, which aims merely at providing a formal analysis of the electron distribution in the complex. Although much simpler and more limited in its applications, this approach to electronic structure turns out to be extremely useful, for at least two reasons:

1. It uses classical ideas and 'language' that are common to all chemists, such as electronegativity or Lewis structures for the ligands. It provides important information, such as the oxidation state (or number) of the metal in the complex, the number of electrons in the immediate environment of the metal, and what one normally calls the 'electronic configuration' of the complex.
2. In a way which can be a little surprising at first sight, it is very useful in the orbital approach when one wishes, for example, to know the number of electrons that must be placed in the complex's nonbonding MO.

There are two ways to obtain this formal distribution of the electrons (or electron count) in a complex. The first, based on a 'covalent' model of the metal–ligand bond, is mostly used in organometallic chemistry, that is, in complexes which possess one or more metal–carbon bonds. The second, based on an 'ionic' model of the metal–ligand bond in which the two electrons are automatically attributed to the ligand, is more frequently employed for inorganic complexes. In fact, the choice between the two methods is largely a matter of taste, as they lead, as we shall see, to identical conclusions.

1.1. Electron count in a complex: the covalent model

Consider a monometallic complex in which the transition metal M is bound to a certain number of ligands $(Lig)_i$, that may be either atoms or molecules. It is important to note that, *in the covalent model, one always considers the ligands in their neutral form* (H, Cl, O, CO, CN, PR_3, CH_3, etc.). Before making the formal electronic assignment for the complex, one must first categorize the ligands according to the nature of their electronic structure.

1.1.1. Ligand classification (L or X)

The main distinction is linked to the number of electrons that the ligand supplies to the metal's coordination sphere: if it supplies a pair of electrons, it is a ligand of type L, whereas a ligand that supplies just one electron is of type X. However, some ligands can supply more than two electrons to the metal. This notation, introduced by M. L. H. Green, is generalized to yield ligands of type $L_\ell X_x$.

1.1.1.1. L-*type ligands*

The simplest case concerns molecules which are coordinated to the metal through a lone pair located on one of their atoms (**1-1**). These molecules are L-type ligands, the metal–ligand bond being formed by the two electrons supplied by the ligand. Examples include amines NR_3 and phosphines PR_3 which contain a lone pair on the nitrogen or phosphorus atom, the water molecule or any ether (OR_2) which can bind to the metal through one of the lone pairs on the oxygen atom. Carbon monoxide is also an L-type ligand, due to the lone pair on the carbon atom.[1]

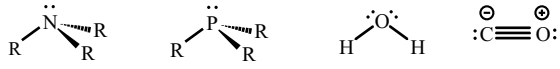

1-1

There are other cases in which the two electrons supplied by the ligand L form a bond between two atoms of that ligand, rather than a lone pair. This can be a π-bond, as in the ethylene molecule, or, more surprisingly, a σ-bond, as in the dihydrogen molecule (**1-2**).[2]

In these examples, two atoms of the ligand are bound in an equivalent way to the metal centre. The *hapticity* of the ligand is said to be 2. This type of bond is indicated by the Greek letter η, the nomenclature used being η^2-C_2H_4 or η^2-H_2, respectively (**1-2**).

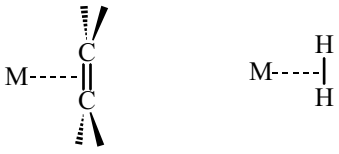

1-2

[1] There is also a lone pair on the oxygen atom. We shall see later why CO binds preferentially through the carbon atom (§ 1.5.2.4 and Chapter 3, § 3.2.2).

[2] Complexes in which a dihydrogen molecule is bound to a transition metal were first characterized in the mid-1980s, and have since been extensively studied by both experimental and theoretical methods (Chapter 4, § 4.1.4).

1.1.1.2. X-*type ligands*

These ligands supply only one electron to the metal's coordination sphere. As neutral entities, X-type ligands are radicals and the metal–ligand bond is formed by the unpaired electron of the ligand and a metal electron. Hydrogen (H) is an X-type ligand, as are the halogens (F, Cl, Br, I), alkyl radicals (CR_3), the amido (NR_2), alkoxy (OR), and cyano (CN) groups (**1-3**), etc.

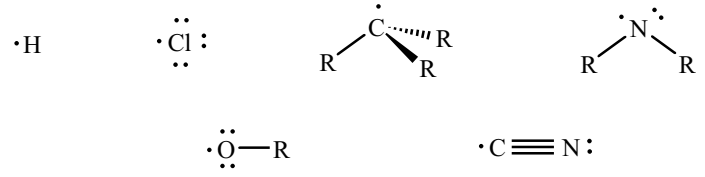

1-3

It should be noted that in some of the examples given above, the radical centre also possesses one or more lone pairs, so that one might have considered it to be an L-type ligand. However, the use of a lone pair for bond formation would lead to a complex with an unpaired electron on the metal (.L:—M). This electronic structure is less stable than that in which the unpaired electron and a metal electron are paired to form the metal–ligand bond (:X–:–M). It can be seen that in this case, all the electrons are paired, either as bonding pairs or as lone pairs.

1.1.1.3. *Ligands of* $L_\ell X_x$ *type*

In a more general notation, ligands can be represented as $L_\ell X_x$ when they use ℓ electron pairs and x unpaired electrons to bind to the metal.

In the ground state, the oxygen atom possesses two unpaired electrons (**1-4a**).[3] It is therefore a ligand of X_2 type, which can bind to a transition metal to form an 'oxo' complex. The sulfido (S) and imido (N-R) (**1-4a**) ligands behave similarly. Atomic nitrogen, with three unpaired electrons, is an X_3 ligand (**1-4b**), giving 'nitrido' complexes. In each case, one therefore considers all the unpaired electrons on the atom bound to the metal.

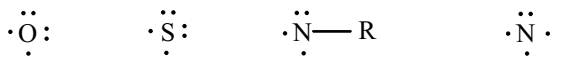

1-4a (X_2) **1-4b** (X_3)

Conjugated polyenes constitute an important family of molecules which are ligands of $L_\ell X_x$ type; they form π*-complexes* with the metal, that is, complexes in which the π system of the ligand interacts with the metal centre. Consider, for example, the cyclopentadienyl ligand

[3] The ground-state electronic configuration for oxygen is $1s^2 2s^2 2p^4$. In the electronic ground state, two electrons are paired in one *p* orbital, while the two other *p* orbitals are singly occupied by electrons with parallel spin (a triplet, following Hund's rules). For nitrogen ($1s^2 2s^2 2p^3$), there are three unpaired electrons, one in each *p* orbital.

C_5H_5 (also represented Cp), whose Lewis structure (**1-5**) shows that the π system contains five electrons (two π bonds and one unpaired electron).

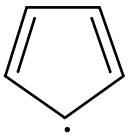

1-5

If this ligand is bound so that all five atoms are essentially at the same distance from the metal centre (η^5-C_5H_5 coordination), the five π electrons are involved in the metal–ligand bonds, so that cyclopentadienyl is classified as an L_2X ligand. Two graphical representations are therefore possible, depending on whether one gives a localized or delocalized description of the ligand's π system (**1-6**).

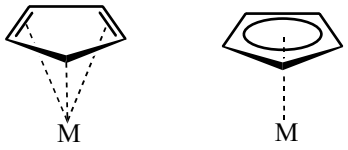

1-6 (η^5, L_2X)

Ferrocene is a particularly interesting π complex [Fe(η^5-$C_5H_5)_2$] (a 'sandwich' complex, in which an iron atom is placed between the planes of two cyclopentadienyl ligands, **1-7**). At first sight, one could consider it either as a complex with two ligands, $[Fe(Lig)_2]$ where Lig = C_5H_5, or as one with 10 ligands, $[Fe(Lig)_{10}]$, since the iron is bonded equivalently to all 10 carbon atoms. However, the L/X ligand classification shows us that each cyclopentadienyl ligand is of the L_2X type, so ferrocene is therefore an $[FeL_4X_2]$ complex in which the iron must be considered as surrounded by *six* ligands, rather than *two* or *ten*. In fact, it is a pseudo-octahedral complex of $[Fe(Lig)_6]$ type!

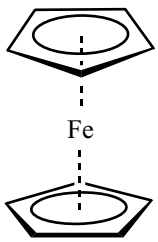

1-7

Two other coordination modes can be imagined for the cyclopentadienyl ligand, and they are indeed observed in some complexes. If only three π electrons (a double bond and the unpaired electron) are supplied to the metal's coordination sphere, C_5H_5 acts as a ligand of LX type. In this case, only three carbon atoms are bound to the metal, and the coordination mode is η^3-C_5H_5 (**1-8**). Finally, the metal can bind just to the radical centre (X-type ligand), giving an η^1-C_5H_5 coordination (**1-9**). In this latter case, one can no longer describe it as a π complex, since the metal centre interacts with only one of the ring carbon atoms, with which it forms a σ bond.

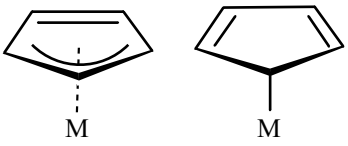

1-8 (η^3, LX) **1-9** (η^1, X)

This diversity of coordination behaviour is also found for other conjugated polyenes. Thus, butadiene can act as an L_2 ligand if the electrons of the two π bonds are involved (η^4-butadiene, **1-10**) or as an L ligand involving a single π bond (η^2-butadiene, **1-11**).

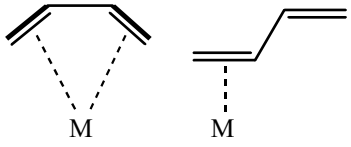

1-10 (η^4, L_2) **1-11** (η^2, L)

In the same way, benzene can bind in the η^6 (L_3 ligand, **1-12**), η^4 (L_2 ligand, **1-13**), or η^2 modes (L ligand, **1-14**) (see Exercise 1.5). In the η^4 and η^2 coordination modes, the six carbon atoms become non-equivalent

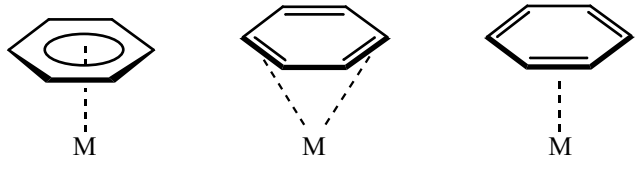

1-12 (η^6, L_3) **1-13** (η^4, L_2) **1-14** (η^2, L)

(four or two, respectively, are bound to the metal), perturbing the π-electron conjugation. As a result, the ring becomes non-planar.

A slightly different case arises for ligands which can bind to a metal centre through several different sites without any conjugation of the electrons involved. These ligands are said to be polydentate (bidentate, tridentate, . . .), in contrast to monodentate ligands such as PR_3, CR_3, etc. For example, 1,2-bis(dimethylephosphino)ethane is a bidentate ligand, since it can bind through its phosphino sites (**1-15**). As each of these has a lone pair, it behaves as an L_2 ligand towards the metal. 1,2-dioxyethane (O-CH_2-CH_2-O) is also a bidentate ligand (**1-16**), but each oxygen atom supplies only one electron to the metal (an X_2 ligand).

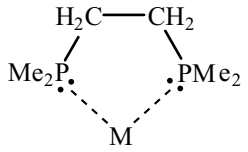

1-15 (L_2)

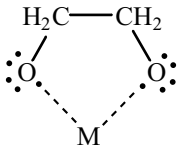

1-16 (X_2)

We end this section by discussing several ligands whose classification as L- or X-type can create difficulties.

The usual Lewis structure for the dioxygen molecule, O_2, shows a double bond and two lone pairs on each oxygen atom. One might therefore conclude that it is an L-type ligand, and that the coordination would be either η^1 (through a lone pair) or η^2 (involving the π bond). However, this Lewis structure, in which all the elctrons are paired, is not satisfactory since the magnetic moment measured experimentally shows that there are *two unpaired electrons* with parallel spin (the ground state is a triplet).[4] This is why O_2 behaves as an X_2 ligand rather than an L ligand.

Carbene ligands, CR_1R_2, provide another example. These species contain two electrons on the carbon atom that do not participate in the formation of the C-R_1 and C-R_2 bonds. Depending on the nature of the R_1 and R_2 atoms or groups, the ground state is either *diamagnetic*, in which case the two nonbonding electrons are paired, forming a lone pair on the carbon atom (**1-17a**), or *paramagnetic*, in which case the two electrons are unpaired, giving a triplet state **1-17b**). In the first case, it is logical to consider the carbene as an L-type ligand, whereas it is an X_2 ligand in the second case.

These two ways of describing a CR_1R_2 ligand are indeed used, and this distinction is at the origin of the two families of carbene complexes in organometallic chemistry: the Fischer-type (L) and the Schrock-type (X_2) carbenes. We shall return to this difference and offer an orbital interpretation (Chapter 4, § 4.3).

[4] This property is readily explained by molecular orbital theory: two electrons must be placed in two degenerate π^*_{oo} orbitals. The most favourable arrangement contains one electron in each orbital, with their spins parallel (a triplet state).

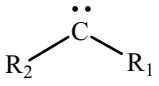

1-17a (L)

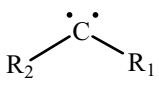

1-17b (X_2)

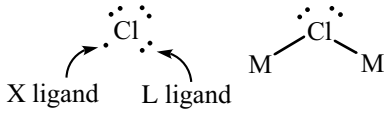

1-18

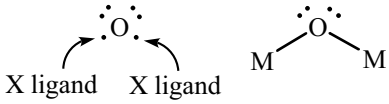

1-19

1.1.1.4. *Bridging ligands*

In bimetallic complexes, some ligands can be 'bridging', that is, bound simultaneously to the two metal centres. These cases are indicated by the nomenclature μ. If one considers a bridging chlorine atom ($M_2(\mu\text{-Cl})$, **1-18**), it behaves as an X ligand towards the first metal centre, thanks to its unpaired electron, but as an L ligand towards the second, thanks to one of its lone pairs (the roles of the two metal centres can, of course, be interchanged). Overall, the chlorine atom is therefore an LX ligand; it supplies three electrons to the pair of metal centres. Other ligands in which an atom has an unpaired electron and at least one lone pair, such as OR, SR, NR_2, PR_2, etc. are analogous. A bridging oxygen atom is an X-type ligand towards each of the two metal centres, since it has two unpaired electrons (**1-19**), so it therefore acts as an X_2 ligand overall.

1.1.2. Electron count and the 18-electron rule

Once the nature of the ligands has been established, the second stage of our analysis of the electronic structure of transition metal complexes will require us to count the number of electrons around the metal and then to assign them, in a formal way, either to the metal or to the ligands. In what follows, we shall consider complexes written as $[ML_\ell X_x]^q$, in which the metal M is bound to ℓ ligands of L type and to x ligands of X type, the overall charge being q.

1.1.2.1. *Total number of electrons, the 18-electron rule*

Each ligand L supplies two electrons to the metal's environment, while each ligand X supplies a single electron. The total number of electrons supplied by the ligands is therefore equal to $2\ell + x$. Only the valence electrons are considered for the transition metal, as, following the spirit of Lewis theory, we assume that core electrons play a negligible role. In what follows, we shall limit our analysis to transition elements corresponding to the progressive filling of the $3d$, $4d$, and $5d$ sub-shells (the transition metals of the d block, see Table 1.1). The valence-electron configuration of these elements is of the type $nd^a(n+1)s^b$, where n equals 3, 4, or 5, for the first, second, or third transition series, respectively.[5] The metal therefore supplies $(a + b)$ electrons. We note that some authors do not consider zinc to be a transition element, as its d sub-shell is full (valence-electron configuration $3d^{10}4s^2$). This remark also applies to cadmium (Cd, $4d^{10}5s^2$) and to mercury (Hg, $5d^{10}6s^2$).

When we take account of the overall charge q of the complex, the total number of valence electrons, N_t, is:

$$\boxed{N_t = m + 2\ell + x - q} \qquad (1.1)$$

[5] There are two other transition series that correspond to the filling of the $4f$ (lanthanides) and $5f$ (actinides) sub-shells.

Table 1.1. Electron configuration and number of valence electrons, m, for the d-block transition metals

1st series	Sc	Ti	V	Cr	Mn	Fe	Co	Ni	Cu	Zn
	$3d^1 4s^2$	$3d^2 4s^2$	$3d^3 4s^2$	$3d^5 4s^1$	$3d^5 4s^2$	$3d^6 4s^2$	$3d^7 4s^2$	$3d^8 4s^2$	$3d^{10} 4s^1$	$3d^{10} 4s^2$
2nd series	Y	Zr	Nb	Mo	Tc	Ru	Rh	Pd	Ag	Cd
	$4d^1 5s^2$	$4d^2 5s^2$	$4d^4 5s^1$	$4d^5 5s^1$	$4d^5 5s^2$	$4d^7 5s^1$	$4d^8 5s^1$	$4d^{10} 5s^0$	$4d^{10} 5s^1$	$4d^{10} 5s^2$
3rd series	Lu	Hf	Ta	W	Re	Os	Ir	Pt	Au	Hg
	$5d^1 6s^2$	$5d^2 6s^2$	$5d^3 6s^2$	$5d^4 6s^2$	$5d^5 6s^2$	$5d^6 6s^2$	$5d^7 6s^2$	$5d^9 6s^1$	$5d^{10} 6s^1$	$5d^{10} 6s^2$
m	3	4	5	6	7	8	9	10	11	12

Several examples of the application of this rule are given below:

Complex	m	2ℓ	x	q	N_t
$[Fe(CO)_5]$	8	10	0	0	18
$[Ir(CO)(Cl)(PPh_3)_2]$	9	6	1	0	16
$[Mn(CO)_6]^+$	7	12	0	+1	18
$[Ni(CN)_5]^{3-}$	10	0	5	−3	18
$[Zn(Cl)_4]^{2-}$	12	0	4	−2	18
$[V(Cl)_4]$	5	0	4	0	9
$[Cr(CO)_3(\eta^6\text{-}C_6H_6)]$	6	12	0	0	18
$[Fe(\eta^5\text{-}C_5H_5)_2]$	8	8	2	0	18
$[Cu(\eta^5\text{-}C_5H_5)(PMe_3)]$	11	6	1	0	18
$[Zr(\eta^5\text{-}C_5H_5)_2(CH_3)]^+$	4	8	3	+1	14
$[Ti(PR_3)_2(Cl)_3(CH_3)]$	4	4	4	0	12
$[W(PR_3)_2(CO)_3(\eta^2\text{-}H_2)]$	6	12	0	0	18
$[Ir(PR_3)_2(Cl)(H)_2]$	9	4	3	0	16
$[Ni(H_2O)_6]^{2+}$	10	12	0	+2	20

By analogy with the octet rule, it has been proposed that a transition metal tends to be surrounded by the number of valence electrons equal to that of the following rare gas (electron configuration $nd^{10}(n+1)s^2(n+1)p^6$). One thereby obtains *the 18-electron rule*, for which we shall provide a first theoretical justification in this chapter (§ 1.6.3). However, in light of the examples given above, one must note that there are many exceptions to this rule; we shall analyse them in greater detail in the following chapters.

1.1.2.2. *Oxidation state*

In order to determine the oxidation state of the metal in the complex, one performs a *fictitious* dissociation of all the ligands, supposing that

Table 1.2. The Allred–Rochow electronegativity scale: (a) for the transition metals and (b) for the light elements

(a)

Sc	Ti	V	Cr	Mn	Fe	Co	Ni	Cu	Zn
1.20	1.32	1.45	1.56	1.60	1.64	1.70	1.75	1.75	1.66
Y	Zr	Nb	Mo	Tc	Ru	Rh	Pd	Ag	Cd
1.11	1.22	1.23	1.30	1.36	1.42	1.45	1.35	1.42	1.46
Lu	Hf	Ta	W	Re	Os	Ir	Pt	Au	Hg
1.14	1.23	1.33	1.40	1.46	1.52	1.55	1.44	1.41	1.44

(b)

H						
2.2						
Li	Be	B	C	N	O	F
1.0	1.5	2.0	2.5	3.1	3.5	4.1
Na	Mg	Al	Si	P	S	Cl
1.0	1.2	1.5	1.7	2.1	2.4	2.8

each of them, either L or X, takes with it the electron pair that created the metal–ligand bond. The remaining charge on the metal after this decomposition is the *oxidation state* of the metal in the complex. This distribution of the electrons, which 'assigns' the bond pair to the ligand, can be partially justified when one notes that this latter is usually a more electronegative entity than is the transition metal (see Table 1.2, the Allred–Rochow electronegativity scale). The metal–ligand bonds are therefore polarized, and the electron pair is more strongly localized on the ligand than on the metal. To assign the two electrons of the bond just to the ligand is, however, a *formal* distribution, which exaggerates the tendency linked to the difference in electronegativity.

In the *fictitious* dissociation that we are considering, a ligand L leaves with the two electrons that it had supplied, so the number of electrons on the metal is not changed in any way. However, an X-type ligand, which had supplied only a single electron to make the bond, leaves in its anionic form X^-, carrying the two electrons from the bond with it. It therefore 'removes' an electron from the metal, that is, it oxidizes it by one unit. The result of this dissociation is therefore written:

$$[ML_\ell X_x]^q \rightarrow \ell L + xX^- + M^{(x+q)} \tag{1.2}$$

The oxidation state (*no*) of the metal in the complex is therefore equal to the algebraic sum of the number of X-type ligands and the charge on the complex:

$$\boxed{no = x + q} \tag{1.3}$$

In a widely used notation to specify the oxidation state of the metal in a complex, the chemical symbol of the metal is followed by the oxidation state written in Roman letters (Mn(I), Fe(II), Cr(III), etc.).

Examples

Complex	x	q	no	Oxidation state
$[Fe(CO)_5]$	0	0	0	Fe(0)
$[Ir(CO)(Cl)(PPh_3)_2]$	1	0	1	Ir(I)
$[Mn(CO)_6]^+$	0	+1	1	Mn(I)
$[Ni(CN)_5]^{3-}$	5	−3	2	Ni(II)
$[Zn(Cl)_4]^{2-}$	4	−2	2	Zn(II)
$[V(Cl)_4]$	4	0	4	V(IV)
$[Cr(CO)_3(\eta^6\text{-}C_6H_6)]$	0	0	0	Cr(0)
$[Fe(\eta^5\text{-}C_5H_5)_2]$	2	0	2	Fe(II)
$[Cu(\eta^5\text{-}C_5H_5)(PMe_3)]$	1	0	1	Cu(I)
$[Zr(\eta^5\text{-}C_5H_5)_2(CH_3)]^+$	3	+1	4	Zr(IV)
$[Ti(PR_3)_2(Cl)_3(CH_3)]$	4	0	4	Ti(IV)
$[W(PR_3)_2(CO)_3(\eta^2\text{-}H_2)]$	0	0	0	W(0)
$[Ir(PR_3)_2(Cl)(H)_2]$	3	0	3	Ir(III)
$[Ni(H_2O)_6]^{2+}$	0	+2	2	Ni(II)

In bimetallic complexes, the oxidation state is calculated by supposing that the metal–metal bond(s), if any, is/are broken homolytically. This procedure is justified by the fact that the electronegativities of the two metal centres are equal if they are identical, or similar in heteronuclear complexes (see Table 1.2(a)). The presence of one or more bonds between the metals therefore has no effect on their oxidation state. For example, the complex $[Mo(Cl)_2(PR_3)_2]_2$ can initially be considered to be decomposed into two monometallic neutral fragments $[Mo(Cl)_2(PR_3)_2]$ in which the oxidation state of molybdenum is +2.

In conclusion, we note that the oxidation state must not be equated to *the real charge* on the metal in the complex, as it is obtained from a formal distribution of the electrons between the metal and the ligands.

1.1.2.3. d^n *Configuration of a metal*

The oxidation state of the metal, which supplies m valence electrons, is equal to no after complex formation. The formal number of electrons remaining on the metal, n, is therefore given by the relationship:

$$\boxed{n = m - no} \tag{1.4}$$

We are considering here n electrons which are not involved in the formation of metal–ligand bonds, in other words 'nonbonding' electrons. The electron configuration of the metal in the complex is represented as d^n.

Examples

Complex	*no*	*m*	Configuration
$[Fe(CO)_5]$	0	8	d^8
$[Ir(CO)(Cl)(PPh_3)_2]$	1	9	d^8
$[Mn(CO)_6]^+$	1	7	d^6
$[Ni(CN)_5]^{3-}$	2	10	d^8
$[Zn(Cl)_4]^{2-}$	2	12	d^{10}
$[V(Cl)_4]$	4	5	d^1
$[Cr(CO)_3(\eta^6\text{-}C_6H_6)]$	0	6	d^6
$[Fe(\eta^5\text{-}C_5H_5)_2]$	2	8	d^6
$[Cu(\eta^5\text{-}C_5H_5)(PMe_3)]$	1	11	d^{10}
$[Zr(\eta^5\text{-}C_5H_5)_2(CH_3)]^+$	4	4	d^0
$[Ti(PR_3)_2(Cl)_3(CH_3)]$	4	4	d^0
$[W(PR_3)_2(CO)_3(\eta^2\text{-}H_2)]$	0	6	d^6
$[Ir(PR_3)_2(Cl)(H)_2]$	3	9	d^6
$[Ni(H_2O)_6]^{2+}$	+2	10	d^8

This notation might seem surprising at first sight, as it implies that all the nonbonding electrons on the metal occupy *d*-type atomic orbitals (AO). Yet, for every metal except palladium, the *s* orbital is at least partially occupied in the ground state of the isolated atom (see Table 1.1). A detailed study of the electronic structure of complexes, presented in Chapter 2, will show us that the nonbonding electrons on the metal do indeed occupy pure *d*-type orbitals, or molecular orbitals whose main component is a *d*-type atomic orbital.

1.2. An alternative model: the ionic model

There is a second method for counting the electrons in a complex and deducing the metal's oxidation state and electronic configuration. This is the ionic model, in which one supposes that a complex is formed by a metal centre and by ligands which *always act as Lewis bases*, supplying one (or several) pairs of electrons.

1.2.1. Lewis bases as ligands

In the covalent model, neutral ligands L (or L_n) supply one (or n) electron pair(s) to the metal: for example, one for amines (NR_3), phosphines (PR_3), the carbonyl group (CO), and derivatives of ethylene ($R_2C{=}CR_2$), and three for benzene (C_6H_6) in the η^6 coordination

mode. As these ligands already behave as Lewis bases in the covalent model, we shall continue to consider them in their neutral form L (or L_n) in the ionic model.

However, an X-type ligand in the covalent model is a radical species which supplies only a single electron to the metal. To 'transform' it into a Lewis base, one must add an electron and therefore consider it in its *anionic form* X^-. In this way, the radical ligands H (hydrogen), Cl (chlorine), and CH_3 (methyl radical) of the covalent model become the H^- (hydride), Cl^- (chloride), and CH_3^- (methyl anion) ligands in the ionic model. Analogously, X_x ligands in the covalent model, which have x unpaired electrons, become X^{x-} ligands in the ionic model. For example, O (X_2) and N (X_3) are now described as O^{2-} and N^{3-}. In general, *one completes the ligand's valence-electron shell so that the octet rule is satisfied*.

This is generalized for ligands of $L_\ell X_x$ type in the covalent model, which quite naturally become $L_\ell X_x^{x-}$ ligands in the ionic model. The cyclopentadienyl radical (Cp), a neutral species with five π electrons (an L_2X ligand, **1-5**), is therefore considered in its monoanionic form (Cp^- with six π electrons). Table 1.3 presents the numbers of electrons attributed to the principal ligands that have been considered so far in the covalent and ionic models.

The additional electron supplied to an X-type ligand to transform it into a Lewis base comes, of course, from the metal. The metal–ligand ensemble is therefore described as an X^- ligand interacting with a metallic cation M^+, thereby giving a purely ionic description of the metal–ligand bond. As a consequence, a complex which was written $ML_\ell X_x$ in the covalent model is represented, in the ionic model, as a metallic cation of charge x bound to $(\ell + x)$ Lewis bases (1.5).

$$[ML_\ell X_x]\ \text{(covalent model)} \rightarrow [M^{(x)+}(L)_\ell(X^-)_x]\ \text{(ionic model)}. \tag{1.5}$$

If the complex has an overall charge q, the charge on the metallic centre in the ionic model becomes $(x + q)$ (1.6).

$$[ML_\ell X_x]^q\ \text{(covalent model)} \rightarrow [M^{(x+q)+}(L)_\ell(X^-)_x]\ \text{(ionic model)}. \tag{1.6}$$

This 'redistribution' of the electrons within the complex can be justified by the higher electronegativity of the ligands than of the metals (see Table 1.2): an X-type ligand 'attracts' the two electrons of the metal–ligand bond to itself, and becomes X^-. In conclusion, we note that the name given to several complexes is directly linked to the ionic model. Thus, complexes with several H ligands ($[ReH_9]^{2-}$, for example) are called 'polyhydrides'.

Table 1.3. Number of electrons supplied by several common ligands according to the covalent and ionic models

Covalent model		Ionic model	
Ligand (type)	Number of electrons	Ligand	Number of electrons
H, Cl, OR, NR_2, CR_3, CN (X ligands)	1e	H^-, Cl^-, OR^-, NR_2^-, CR_3^-, CN^-	2e
CO, NR_3, PR_3, H_2, $R_2C{=}CR_2$ (L ligands)	2e	CO, NR_3, PR_3, H_2, $R_2C{=}CR_2$	2e
O, S, NR (X_2 ligands)	2e	O^{2-}, S^{2-}, NR^{2-}	4e
	4e		4e
η^4-diene (L_2 ligand)		η^4-diene	
	5e		6e
η^5-Cp (L_2X ligand)		η^5-Cp^-	
	6e		6e
η^6-arene (L_3 ligand)		η^6-arene	
μ-Cl (LX ligand)	3e	μ-Cl^-	4e
μ-O (X_2 ligand)	2e	μ-O^{2-}	4e

1.2.2. Equivalence of the covalent and ionic models: examples

1.2.2.1. *Oxidation state and d^n electronic configuration*

In the covalent model, the oxidation state of the metal, *no*, is equal to the charge left on the metal after having carried out a fictitious dissociation of the complex in which all the ligands take the two bonding electrons with them (§ 1.1.2.2). For a complex whose general formula is $[ML_\ell X_x]^q$, one therefore obtains $no = x + q$ (see equations (1.2) and (1.3)). In the ionic formulation of this same complex, (see equation (1.6)), the charge on the metal is just equal to $x + q$, so the ionic and covalent models lead to the same oxidation state *no* for the metal. It follows that the same electronic configuration d^n is obtained by the two models, since n is equal to the number of valence electrons on the metal (m), minus its oxidation state *no* (equation (1.4)).

Examples

Covalent model	Ionic model
$[Ir(CO)(Cl)(PPh_3)_2]$	
$[Ir(L)_3(X)]$ type	$(Ir^+)(CO)(Cl^-)(PPh_3)_2]$
$x = 1; q = 0 \Rightarrow no = +1$	$no = +1$
$m = 9 \Rightarrow n = 9 - 1 \Rightarrow d^8$	$m = 9 \Rightarrow Ir^+: d^8$
$[Fe(\eta^5\text{-}Cp)_2]$	
$[Fe(L_2X)_2]$ type	$[(Fe^{2+})(Cp^-)_2]$
$x = 2; q = 0 \Rightarrow no = +2$	$no = +2$
$m = 8 \Rightarrow n = 8 - 2 \Rightarrow d^6$	$m = 8 \Rightarrow Fe^{2+}: d^6$
$[Mn(CO)_6]^+$	
$[Mn(L)_6]^+$ type	$[(Mn^+)(CO)_6]$
$x = 0; q = +1 \Rightarrow no = +1$	$no = +1$
$m = 7 \Rightarrow n = 7 - 1 \Rightarrow d^6$	$m = 7 \Rightarrow Mn^+: d^6$
$[Ni(CN)_5]^{3-}$	
$[Ni(X)_5]^{3-}$ type	$[(Ni^{2+})(CN^-)_5]$
$x = 5; q = -3 \Rightarrow no = +2$	$no = +2$
$m = 10 \Rightarrow n = 10 - 2 \Rightarrow d^8$	$m = 10 \Rightarrow Ni^{2+}: d^8$

1.2.2.2. *Total number of electrons*

The equivalence of the two models for the calculation of the total number of electrons in a complex (N_t) is shown by a further look at the four examples above.

Covalent model		Ionic model	
$[Ir(CO)(Cl)(PPh_3)_2]$			
$[Ir(L)_3(X)]$ type		$[(Ir^+)(CO)(Cl^-)(PPh_3)_2]$	
Ir	9e	Ir^+	8e
1 CO	2e	1 CO	2e
$2PPh_3$	4e	2 PPh_3	4e
1 Cl	1e	1 Cl^-	2e
N_t	16e	N_t	16e
$[Fe(\eta^5\text{-}Cp)_2]$			
$[Fe(L_2X)_2]$ type		$[(Fe^{2+})(Cp^-)_2]$	
Fe	8e	Fe^{2+}	6e
2 Cp	10e	2 Cp^-	12e
N_t	18e	N_t	18e
$[Mn(CO)_6]^+$			
$[Mn(L)_6]^+$ type		$[(Mn^+)(CO)_6]$	
Mn	7e	Mn^+	6e
6 CO	12e	6 CO	12e
Charge	−1e	N_t	18e
N_t	18e		
$[Ni(CN)_5]^{3-}$			
$[Ni(X)_5]^{3-}$ type		$[(Ni^{2+})(CN^-)_5]$	
Ni	10e	Ni^{2+}	8e
5 CN	5e	5 CN^-	10e
Charge	3e	N_t	18e
N_t	18e		

1.3. Principles of orbital interactions

When we use molecular orbital (MO) theory, the term 'orbital structure' of a complex, or of any molecule, means the shape and the energetic order of the MO. Usually, these orbitals are expressed as Linear Combinations of Atomic Orbitals (LCAO) of the different atoms that make up the system being studied. The shape of an MO is determined by the relative magnitudes and the signs of the different coefficients. The electronic structure is then obtained by placing electrons in these orbitals, filling first those which are lowest in energy.

To construct the MO, it is often advantageous to decompose the molecular system being studied into two simpler sub-systems whose orbitals, either atomic or molecular, are already known. The MO of the complete system are then obtained by allowing the orbitals of the two fragments to interact. In this paragraph, we shall remind the reader of the principal rules which control the interaction between two orbitals on two fragments. For simplicity, we shall treat atomic orbitals, but this limitation will not affect the general nature of our conclusions in any way.

1.3.1. Interaction between two orbitals with the same energy

Consider, for example, the interaction between two identical orbitals of *s* type, χ_1 and χ_2 (Figure 1.1).

The interaction produces a bonding (ϕ_+) and an antibonding MO (ϕ_-). The first is the in-phase combination of the two orbitals χ_1 and χ_2 (coefficients with the same sign), while the second is the out-of-phase combination (coefficients with opposite signs) of these same orbitals. In each MO, the coefficients of χ_1 and χ_2 have the same magnitude, since the interacting orbitals are identical.

In energy terms, the bonding MO is lower in energy than the initial AO, but the antibonding MO is higher. It is important to notice that the destabilization of the antibonding level (ΔE^-) is larger than the stabilization of the bonding level (ΔE^+). It can be shown that these

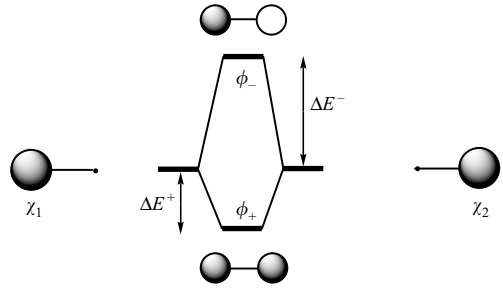

Figure 1.1. Interaction diagram for two orbitals with the same energy.

two quantities are proportional to the overlap S between the interacting orbitals.[6] Therefore, as this overlap increases, the stabilization of the bonding MO and the destabilization of the antibonding MO both become larger.

We shall often be interested later in this book by interactions involving either two or four electrons. In the first case (**1-20**), after the interaction the two electrons both occupy the bonding MO, producing a stabilization of the electronic energy equal to $2\Delta E^{+}$.[7] We deduce that *the stabilization associated with a two-electron interaction between orbitals of the same energy is proportional to the overlap S.*

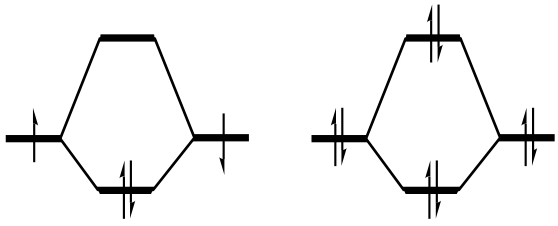

1-20 **1-21**

In the case of a four-electron interaction (**1-21**), both the bonding and antibonding orbitals are doubly occupied. Since ΔE^{-} is larger than ΔE^{+}, the four-electron interaction is destabilizing, and *it can be shown that the destabilization is proportional to the square of the overlap,* S^2.

1.3.2. Interaction between two orbitals with different energies

We now consider the more general case, where the two orbitals χ_1 and χ_2, have different energies ($\varepsilon_1 < \varepsilon_2$, Figure 1.2). Their interaction leads to the formation of a bonding orbital (ϕ_+), lower in energy than the lowest orbital (χ_1), and an antibonding orbital (ϕ_-), higher in energy than the highest orbital (χ_2). As in the preceding case, the stabilization (ΔE^{+}) of the bonding orbital, compared to the energy of χ_1, is smaller than the destabilization (ΔE^{-}) of the antibonding orbital compared to the energy of χ_2 (Figure 1.2). It can be shown that these two quantities are both proportional to the square of the overlap between the orbitals and inversely proportional to their energy difference ($\Delta\varepsilon$), that is, proportional to $S^2/\Delta\varepsilon$. A strong interaction therefore requires both a good overlap between the orbitals and a small energy difference between them.

Comment

This formula is approximate and cannot be used when the two orbitals are too close in energy. It is clear that the expression tends to infinity as $\Delta\varepsilon$ tends

[6] The overlap S_{ij} between two orbitals ϕ_i and ϕ_j is equal to the integral evaluated over all space of the product of the functions ϕ_i^* (the complex conjugate function of ϕ_i) and ϕ_j : $S_{ij} = \langle\phi_i^*|\phi_i\rangle$. For real functions, the integral of the product of the two functions is evaluated over all space.

[7] We assume here that the total electronic energy is equal to the sum of the individual electronic energies. This relationship, which has the advantage of being simple, is obtained when the electronic Hamiltonian is written as a sum of monoelectronic Hamiltonians, as in the Hückel and extended Hückel methods. This approximate formula has, of course, limited application, but it is acceptable for a qualitative analysis of orbital interactions. Further details may be found in *Structure électronique des molécules*, by Y. Jean and F. Volatron, Volume 2, Chapter 13, Dunod, Paris (2003).

towards zero (orbitals of the same energy). For orbitals whose energies are only *slightly different*, it is safer to use the result from the preceding paragraph (proportional to S). An example will be discussed in Chapter 4, § 4.1.3.

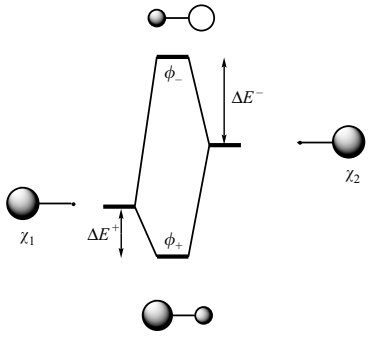

Figure 1.2. Interaction diagram for two orbitals with different energies.

As far as the coefficients are concerned, the bonding orbital (ϕ_+) is concentrated on the centre (or the fragment) that has the lowest-energy orbital (χ_1 here), whereas the opposite polarization is found for the antibonding orbital (ϕ_-), where the coefficient is larger for χ_2 (Figure 1.2). From a chemical viewpoint, this means that the bonding MO is mainly based on the more electronegative centre (or fragment), but the antibonding MO on the less electronegative centre (or fragment).

If we consider a two-electron interaction between doubly occupied χ_1 and empty χ_2 (**1-22**), the two electrons are stabilized by $2\Delta E^+$. *The stabilization associated with a two-electron interaction between two orbitals of different energy is therefore proportional to the square of the overlap and inversely proportional to the energy difference between the two orbitals, that is, proportional to* $S^2/\Delta\varepsilon$. However, a four-electron interaction is destabilizing, since ΔE^- is larger than ΔE^+ (**1-23**). It can be shown that *this four-electron destabilization is proportional to the square of the overlap*, S^2.

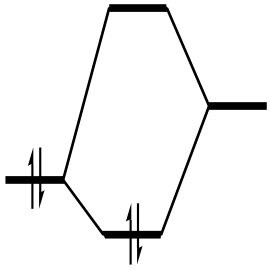

1-22

The two-orbital interaction diagrams (**1-20** to **1-23**) enable us to establish a link between the idea of a bonding pair in the Lewis sense and the MO description. The bonding pair corresponds to double occupation of the bonding MO with the antibonding MO empty. There is thus a single bond in H_2 (identical orbitals, **1-20**) and in HeH^+ (different orbitals, **1-22**). However, if four electrons are involved, the antibonding orbital is doubly occupied and no chemical bond exists between the two atoms. This is the situation in He_2, for example (identical orbitals, **1-21**), and HeH^- (different orbitals, **1-23**), species where the two atoms remain separate.

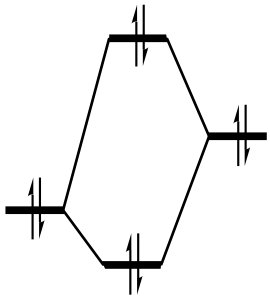

1-23

1.3.3. The role of symmetry

The interaction between two orbitals χ_1 and χ_2 leads to a stabilization (destabilization) of the bonding (antibonding) MO, proportional to the overlap if the orbitals have the same energy but to $S^2/\Delta\varepsilon$ if their energies are different. In both cases, there is clearly no interaction if the overlap is zero. Now S is equal to the integral over all space of the product of the functions χ_1^* and χ_2. In order for this integral to be non-zero, these two functions must be bases for the same irreducible representation of the molecular symmetry group, or, in simpler terms, they must have the same symmetry (Chapter 6, § 6.5.1). If they have different symmetries, the integral is exactly equal to zero, and one says that the overlap is zero by symmetry.

In the general case, where two fragments each with several orbitals interact, this comment allows us to simplify the interaction diagrams very considerably: *only orbitals of the same symmetry interact*.

1.3.4. σ and π interactions

1-24 (σ)

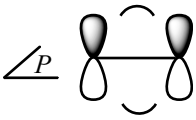

1-25 (π)

Two types of interactions are often distinguished: σ interactions, which concern an *axial* orbital overlap, and π interactions, where the orbital overlap occurs *laterally*, or '*sideways*'. These two types of overlap are illustrated in **1-24** and **1-25**, respectively, for two p orbitals whose axes of revolution are either co-linear (axial overlap) or parallel (sideways overlap). Notice that another way to characterize π interactions is to observe that the orbitals involved share a common nodal plane (P, **1-25**).

In general, σ interactions are stronger than π interactions, since axial overlap is more efficient than sideways overlap. The energy separation between the resulting orbitals is therefore larger for σ (bonding) and σ^* (antibonding) MO than for the π and π^* MO.

The ethylene molecule provides a typical example. The construction of the σ_{CC} and π_{CC} MO from nonbonding orbitals (represented by n_σ and n_p) of the CH_2 fragments is presented in Figure 1.3: the order of the four resulting MO, in terms of increasing energy, is $\sigma_{CC} < \pi_{CC} < \pi^*_{CC} < \sigma^*_{CC}$.

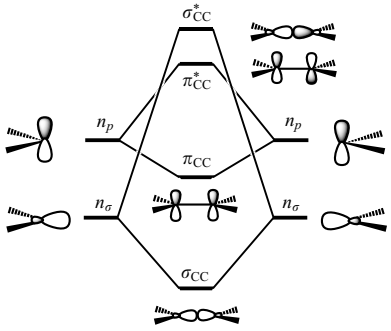

Figure 1.3. Construction of the σ_{CC} and π_{CC} MO in ethylene from n_σ and n_p orbitals on each CH_2 fragment.

1.4. Metal orbitals

In the case of monometallic transition metal complexes, it seems quite natural to construct the MO by allowing the orbitals on the metal centre to interact with those on the ligands. We are now going to examine just which orbitals one must consider on the metal (§ 1.4) and on the ligands (§ 1.5) so as to obtain, after interaction, a satisfactory description of the orbital structure of the complex.

For the metal centre, the atomic orbitals (AO) describing the core electrons will not be considered for the construction of the complex's MO. This approximation can be justified by noting that the amplitude of these orbitals is significant only close to the nucleus, so they can therefore play only a negligible role in bond formation. One must, however, consider the valence AO that are occupied in the ground state of the isolated atom (nd and $(n+1)s$), see Table 1.1), together with the $(n+1)p$ orbitals, which, even though they are empty in the isolated atom, do contribute to bond formation in the complexes of transition metals. There are, therefore, *nine atomic orbitals in all* which participate on the metal, five d-type orbitals, one s-type, and three p-type orbitals.

1.4.1. Description of the valence orbitals

For the s and p orbitals, we shall use the usual conventional representation[8] (**1-26**) which takes their essential features into account:

1. The spherical symmetry of the s orbital.
2. The existence of an axis of revolution for the p_x, p_y, and p_z orbitals (the Ox, Oy, or Oz directions, respectively) and of a nodal plane perpendicular to this axis (the yOz, xOz, or xOy planes, respectively), that is, a plane in which the orbital amplitude is zero. The p orbitals change sign on crossing the nodal plane, which is why they are represented by two 'lobes', one grey (positive amplitude), the other white (negative amplitude).

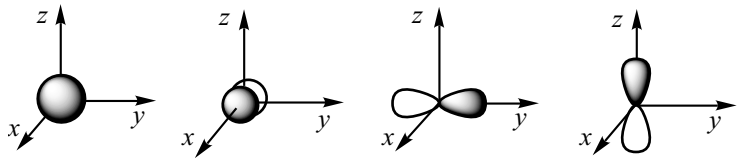

s p_x p_y p_z

1-26

It should be noted that the representation of the orbital whose axis of revolution is perpendicular to the plane of the page (p_x, **1-26**) poses a special problem. This function is exactly zero in this plane (the nodal plane yOz), the positive lobe being directed towards the reader and the negative lobe away from him or her. When one takes account of the symmetry of revolution around the Ox axis, the intersections of these lobes with planes parallel to the nodal plane, either 'above' or 'below' it, are circles. The conventional representation of this orbital shows two offset circles, which represent each lobe seen in perspective.

The presence of five valence d-type orbitals is, of course, the chief characteristic of the metals of the first three transition series. For hydrogenoïd atoms (those with only one electron but a nuclear charge equal to $+Z$), exact analytical solutions to the Schrödinger equation can be obtained (which is not the case for polyelectronic atoms in general). The expressions for the $3d$ orbitals are given below (formulae (1.7)–(1.12)), where both the radial ($R_{3,2}(r)$) and angular parts are normalized.[9] Analogous expressions are obtained for the $4d$ and $5d$ orbitals of the hydrogenoïd atoms, only the radial part of the functions ($R_{4,2}$

[8] Y. Jean and F. Volatron in *An Introduction to Molecular Orbitals*, Oxford University Press, NY. (1993). Chapter 2.

[9] In these expressions, the angular part is expressed using the ratios x/r, y/r, and z/r rather than the spherical coordinates (r, θ, and ϕ). This transformation enables us to make the link between the analytical expression of the orbital and the name which is attributed to it.

and $R_{5,2}$) being modified.

$$3d_{xy} = R_{3,2}(r)\sqrt{\frac{60}{16\pi}}\frac{xy}{r^2} \tag{1.7}$$

$$3d_{xz} = R_{3,2}(r)\sqrt{\frac{60}{16\pi}}\frac{xz}{r^2} \tag{1.8}$$

$$3d_{yz} = R_{3,2}(r)\sqrt{\frac{60}{16\pi}}\frac{yz}{r^2} \tag{1.9}$$

$$3d_{x^2-y^2} = R_{3,2}(r)\sqrt{\frac{15}{16\pi}}\frac{x^2-y^2}{r^2} \tag{1.10}$$

$$3d_{z^2} = R_{3,2}(r)\sqrt{\frac{5}{16\pi}}\frac{2z^2-x^2-y^2}{r^2}, \tag{1.11}$$

where

$$R_{3,2}(r) = \frac{4}{81\sqrt{30}}\sqrt{\frac{Z^3}{a_0^3}}\left(\frac{Zr}{a_0}\right)\exp\left(-\frac{Zr}{3a_0}\right)^2. \tag{1.12}$$

In this last expression (1.12), a_0 is the Bohr radius, equal to 0.529 Å, and Z is the nuclear charge. To what extent are these hydrogenoïd orbitals suitable to describe the d orbitals of transition metals? In polyelectronic atoms, it is only the radial part of the orbitals that is different from hydrogenoïd orbitals; it is modified to take account of the charge on the nucleus and the screening effect created by the other electrons. Since the angular part of the orbitals is conserved, the expressions that are obtained for the $3d$ orbitals of hydrogenoïd atoms enable us to analyse the symmetry properties of the d orbitals of *all* the transition metals.

We note first that the names given to these orbitals ($d_{xy}, d_{xz}, d_{yz}, d_{x^2-y^2}, d_{z^2}$) are directly related to the formulae of their angular parts. At a given distance r from the nucleus, the amplitude of the d_{xz} orbital is directly proportional to the product of the x and z coordinates for that point (formula (1.8)). The same applies for the d_{yz}, d_{xy}, and $d_{x^2-y^2}$ orbitals. But the d_{z^2} orbital is a special case. Its name suggests that it is concentrated wholly along the z-axis. But in fact, this orbital also has a small amplitude, of opposite sign, in the xy plane, so according to formula (1.11), it would be more logical to call it $d_{2z^2-(x^2+y^2)}$.

It is important to define carefully the graphical representations that we shall use for these orbitals throughout this book. They show the orbitals' symmetry properties, the regions of space where their amplitudes are largest and where they are zero (nodal surfaces), all important aspects for our subsequent analysis of interactions between the d orbitals

and orbitals on the ligands. Consider the d_{yz} orbital as an example. Its analytical expression (formula (1.9) shows that its amplitude is zero if $y = 0$ (i.e. at all points in the xz plane) and if $z = 0$ (xy plane): xz and xy are therefore two nodal planes for the d_{yz} orbital. In contrast, the amplitude is greatest along the bisectors of the y- and z-axes. Finally, it is positive where y and z have the same sign, but negative otherwise. All of these properties are clearly shown by the graphical representation **1-27**.

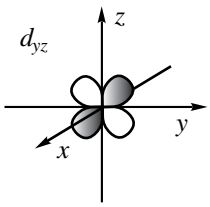

1-27

The d_{xy} and d_{xz} orbitals (formulae (1.7) and (1.8)) may be obtained from the d_{yz} orbital by a rotation of 90° around the y- and z-axes, respectively. They have analogous symmetry properties, with two nodal planes (xz and yz for d_{xy}, xy and yz for d_{xz}), a maximum amplitude along the bisectors of the (x, y) or (x, z) axes and alternating signs for the lobes. Their graphical representation poses the same problem as that already met for the p_x orbital (**1-26**), since the plane of the page is one of the nodal planes. In the same way as before, we represent the intersection of the lobes with planes parallel to the plane of the page (yz), placed either in front or behind, with the back part of the orbital being partly hidden by the front part (**1-28** and **1-29**).

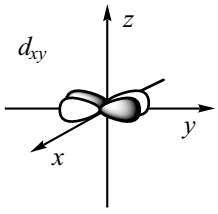

1-28

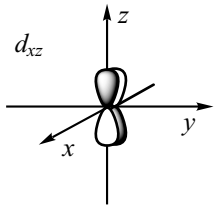

1-29

The $d_{x^2-y^2}$ orbital (formula ((1.10)) has its maximum amplitude along the x- and y-axes, and it also possesses two nodal planes which are the planes bisecting the x- and y-axes (**1-30a**). An alternative representation of this orbital is given in **1-30b**, where the x-axis is perpendicular to the plane of the page. The lobes directed along this axis are now represented by two offset circles.

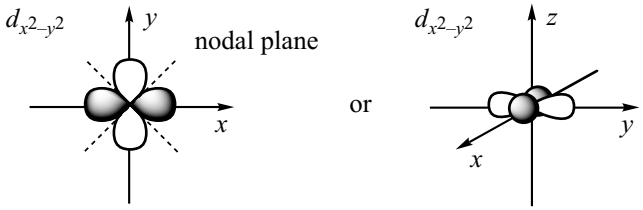

1-30a **1-30b**

The shape of the d_{z^2} orbital is very different from those we have already seen. Its analytical expression (formula (1.11)) shows that its maximal amplitude lies along the z-axis, and that it is positive for both positive and negative z. But it is negative in the xy plane ($z = 0$), and this change in sign implies the existence of a nodal surface. The equation of this surface, $z^2 = (x^2 + y^2)/2$ from formula (1.11), defines a *cone* whose apex angle, θ, is equal to 109.5° (the tetrahedral angle). All of these properties are reproduced by the conventional representation given in **1-31**.

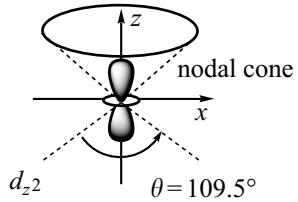

1-31

We close this section by noting that the sign in the analytical expressions of the orbitals is arbitrary. The same remark applies for

Table 1.4. Energies (in eV) of the *s* and *d* orbitals for d-block transition elements obtained from spectroscopic data.

1st series	Sc	Ti	V	Cr	Mn	Fe	Co	Ni	Cu	Zn
ε_{3d}	−7.92	−9.22	−10.11	−10.74	−11.14	−11.65	−12.12	−12.92	−13.46	−17.29
ε_{4s}	−6.60	−7.11	−7.32	−7.45	−7.83	−7.90	−8.09	−8.22	−8.42	−9.39
2nd series	Y	Zr	Nb	Mo	Tc	Ru	Rh	Pd	Ag	Cd
ε_{4d}	−6.48	−8.30	−8.85	−9.14	−9.25	−9.31	−9.45	−9.58	−12.77	−17.85
ε_{5s}	−6.70	−7.31	−7.22	−7.24	−7.21	−7.12	−7.28	−7.43	−7.57	−8.99
3rd series	Lu	Hf	Ta	W	Re	Os	Ir	Pt	Au	Hg
ε_{5d}	−5.28	−6.13	−7.58	−8.76	−9.70	−10.00	−10.21	−10.37	−11.85	−15.58
ε_{6s}	−7.04	−7.52	−8.45	−8.51	−8.76	−8.81	−8.83	−8.75	−9.22	−10.43

their graphical representations. This means that one can change *all* the signs in the representation of an orbital, for example, representing the $d_{x^2-y^2}$ orbital by negative (white) lobes along the x-axis and positive (grey) lobes along the y-axis. All the orbital's properties, such as the regions of maximum amplitude, the changes in sign between neighbouring lobes or the nodal surfaces, are retained in this new representation.

Notation

In the interest of simplification, the five *d* orbitals are often written xy, xz, yz, $x^2 - y^2$, and z^2. This is the notation that we shall use henceforth.

1.4.2. Orbital energies

It is possible to determine the energy of the nd and $(n+1)s$ orbitals for transition metals in their ground-state electronic configuration nd^a $(n+1)s^b$ from spectroscopic data.[10]

The values that are obtained are presented in Table 1.4. They invite several comments which will be helpful when we come to the construction of diagrams for the interaction between metal and ligand orbitals. On moving from left to right in a given series, the energy of both the *s* and *d* orbitals decreases (becoming more negative). This decrease in orbital energy arises from the increase in nuclear charge which strengthens the interaction between the nucleus and the electrons. The variation is nonetheless less pronounced for the *s* orbitals than for the *d* orbitals, because the $(n+1)s$ electrons are strongly shielded by the nd electrons. As a consequence, the *effective* charge $Z^*_{(n+1)s}$

[10] J. B. Mann, T. L. Meek, E. T. Knight, J. F. Capitani, L. C. Allen *J. Amer. Chem. Soc.* *122*, 5132 (2000). The calculations use the ionization potential of the atom and the energy of the atom in its ground state, as well as the energy of the cation formed by removal of an electron from the *s* orbital or from a *d* orbital.

(the nuclear charge Z reduced by the screening $\sigma_{(n+1)s}$) experienced by the s electrons varies little from one element to the next: the increase of the nuclear charge by one unit is largely cancelled by the presence of an additional d electron with its screening effect. However, the d electrons are only weakly screened by the s electrons, so the effective charge Z^*_{nd} increases by close to one unit from one element to the next, leading to a substantial stabilization of the energy of the d orbitals. When we consider the variation within a group, the energetic ordering of the d orbitals in the first four columns is $\varepsilon_{3d} < \varepsilon_{4d} < \varepsilon_{5d}$, but there is an inversion of the $4d$ and $5d$ levels for the four following groups ($\varepsilon_{3d} < \varepsilon_{4d} > \varepsilon_{5d}$). For all the elements except four (Y, Lu, Hf, and Ta), *the nd orbital is lower in energy than the* $(n+1)s$ *orbital*. The $(n+1)p$ orbital is always higher in energy than the $(n+1)s$, as it is everywhere in the periodic table. For the great majority of the d-block transition metals, the orbital energy ordering is therefore, $\varepsilon_{nd} < \varepsilon_{(n+1)s} < \varepsilon_{(n+1)p}$.

1.5. Ligand orbitals

It is not possible to define a single set of orbitals that can be used to describe the interactions with the metal for any type of ligand. Two conditions must be met: the ligand orbitals must be close in energy to those on the metal, and their overlap must also be substantial (§ 1.3.2). Depending on the nature of the ligand, one or several orbitals may satisfy these criteria.

1.5.1. A single ligand orbital: σ interactions

The case where it is clearest that only one orbital need be considered involves the ligand H, since it possesses only one valence orbital, 1_{s_H}. This orbital, which contains one electron (an X-type ligand), can be used to form a $\sigma_{M—H}$ bond by combination with a metal orbital such as the z^2 orbital (**1-32**).[11]

[11] A σ bond means, in this context, a bond described by an MO that possesses cylindrical symmetry about the M-ligand axis. This notation is widely used by chemists for single bonds (see § 1.3.4). However, in group theory, the σ notation is reserved for linear molecules.

$1s_H$ $\sigma_{M–H}$

1-32

For certain more complicated ligands, it is also possible, *as a first approximation*, to consider only a single orbital to describe the metal–ligand interaction. This is the case for ligands of the type AH_3 (or more generally AR_3) whose orbital structure is summarized in Figure 1.4. Therefore, for an amine or phosphine (L-type ligands), it is in general sufficient to consider the nonbonding orbital $2a_1$ (Figure 1.4) that characterizes the lone pair on the nitrogen or phosphorus atom (**1-33a**). Analogous remarks may be made for the methyl ligand, CH_3, or more generally for an alkyl radical CR_3, the nonbonding orbital being only singly occupied in this case (an X-type ligand) (**1-33b**). This is the highest occupied orbital on the ligand, and its energy is not very different from that of the d orbitals for most of the transition metals. Moreover, its

overlap with a metal orbital (e.g. z^2, **1-34**) is substantial since it is a hybrid orbital polarized towards the metal centre. The resulting interaction produces a bonding and an antibonding MO. If the former is doubly occupied and the latter is empty, there is a σ bond between the metal and the ligand (σ_{M-PR3}, or σ_{M-CR3}, **1-34**).

NR_3, PR_3 CR_3 σ_{M-L}

1-33a **1-33b** **1-34**

If we consider only the nonbonding orbital on ligands such as NR_3, PR_3, or CR_3, we are effectively supposing that the interactions of the other MO with the metal orbitals are much weaker than the σ interaction already described. This hypothesis can be justified by analysing the orbital structure of pyramidal AH_3 molecules (Figure 1.4), where we see three bonding molecular orbitals (σ_{A-H}) that account for the A-H bonds, the nonbonding orbital that is concentrated on the central atom, and three antibonding orbitals $\left(\sigma^*_{A-H}\right)$. The bonding orbitals of the ligand can interact with the metal orbitals. But they are far too low in energy, since they are orbitals describing the σ_{A-H} bonds. Moreover, they are partially distributed over the hydrogen atoms, that is, in the direction away from the metal.

For both these reasons (substantial energy gap and poor overlap), the interactions involving the bonding orbitals are weaker than those concerning the nonbonding orbital. In a similar way, interactions between the antibonding σ^*_{A-H} orbitals and the metal centre are usually negligible for the description of the metal–ligand bond; these MO are at high energy and partially oriented away from the metal.

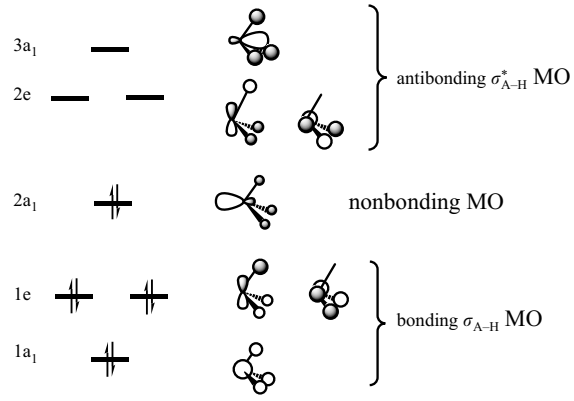

Figure 1.4. Molecular orbitals for AH_3 pyramidal molecules (with the electronic occupation appropriate for molecules with eight valence electrons, such as NH_3 or PH_3).

Comment

It must, however, be noted that the antibonding orbitals can be strongly stabilized by very electronegative substituents, as, for example, in trifluorophosphine, PF_3. In such a case, these orbitals can interact to a non-negligible extent with the *d* orbitals of the metal centre. This is particularly important for the 2e orbitals (Figure 1.4) which can be involved in π-type interactions (see Chapter 3).

1.5.2. Several orbitals: σ and π interactions

For other ligands the situation is more complicated, since it is necessary to take several orbitals into account to obtain a satisfactory description of the bond with the metal. As a first example, we shall consider bent AH_2 molecules.

1.5.2.1. *Ligands of the* AH_2 *type*

The orbital structure of bent AH_2 molecules (or more generally AR_2), see Figure 1.5, shows that there are two bonding orbitals, which describe the σ_{A-H} bonds, the two corresponding antibonding orbitals σ^*_{A-H}, and at an intermediate energy level, two nonbonding molecular orbitals: the $2a_1$ orbital, which is a hybrid pointing in the direction away from the hydrogen atoms, and the $1b_1$ orbital, which is a pure *p* atomic orbital perpendicular to the molecular plane, (see Chapter 6, § 6.5.2). Depending on the nature of the atom A, these two orbitals can contain one electron (BH_2, AlH_2), two (CH_2, SiH_2), three (NH_2, PH_2), or four (OH_2, SH_2).

As in the previous example, the bonding and antibonding orbitals can, in a first approximation, be neglected for the description of the metal–ligand interactions. However, it is necessary to take *both nonbonding orbitals* into account, as they are close in energy and both can lead to interactions with the metal centre. The $2a_1$ orbital plays the

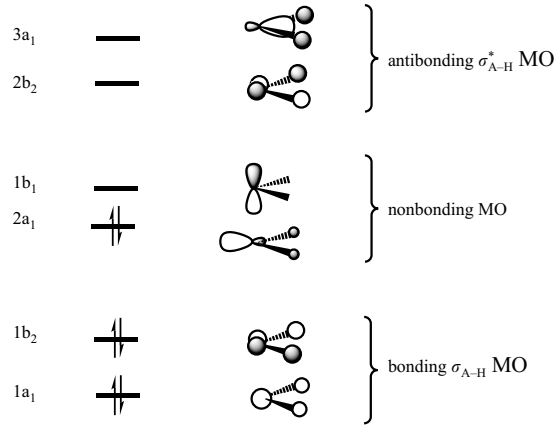

Figure 1.5. Molecular orbitals for AH_2 molecules (with the electronic occupation appropriate for molecules with six valence electrons, such as CH_2 or SiH_2 in their lowest singlet state).

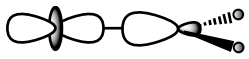

σ_{M-L}

1-35

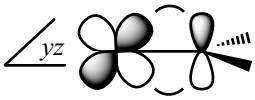

π_{M-L}

1-36

same role as the $2a_1$ orbital in AH_3 molecules, and its interaction with a metal orbital (z^2, for example) leads to the formation of an MO that characterizes a σ bond (**1-35**).

The $1b_1$ orbital (p_x) has the correct symmetry to interact with the *xz* orbital: the overlaps above and below the *yz* plane have the same sign, so that the total overlap (the sum of the partial overlaps) is non-zero (**1-36**). This new metal–ligand interaction is said to be a π *interaction*, since the orbitals concerned share a *common nodal plane* (*yz*). It leads to the formation of two MO, one bonding, π_{M-L}, represented schematically in **1-36**, and one antibonding, π^*_{M-L}. This interaction is particularly important for the description of the metal–ligand bond when two electrons are concerned: the bonding molecular orbital (**1-36**) is then doubly occupied but the antibonding orbital is empty. A π-type interaction therefore adds to and reinforces the σ interaction (**1-35**), giving a double-bond character to the metal–ligand bond. It should be noted that there is an important difference between the σ (**1-35**) and π (**1-36**) interactions concerning the change in the overlap when there is a rotation about the M-L bond: the σ overlap does not change, as it possesses cylindrical symmetry with respect to the bond direction, but the π overlap is eliminated by a rotation of 90°.

Comment

This is exactly analogous to what happens in an organic molecule such as ethylene (Figure 1.3), in which there is a σ_{CC} bond for any relative orientation of the two methylene groups, whereas the existence of a π_{CC} bond depends on the two groups being coplanar.

1.5.2.2. *AH ligands*

Following the reasoning developed in the previous paragraph, *three* molecular orbitals need to be considered for an A-H (or A-R) ligand (see Figure 1.6): the nonbonding orbital 2σ, analogous to the $2a_1$ orbital in AH_3 and AH_2 ligands, which allows a metal–ligand σ bond to be formed, and the two degenerate π orbitals (p_x and p_y) which may be involved in π interactions with the metal centre. Depending on the nature of A, these three orbitals may contain two electrons (BH, AlH), three (CH, SiH), four (NH, SH), five (OH, SH), or six (FH, ClH).

1.5.2.3. *Monoatomic ligands A*

With the exception of the ligand H, for which there is only a single valence orbital $1s_H$ to consider (a σ interaction), one must treat all the valence *s* and *p* orbitals on a monoatomic ligand A. Now the *s* orbital is usually much lower in energy than the *d* orbitals on the metal, especially

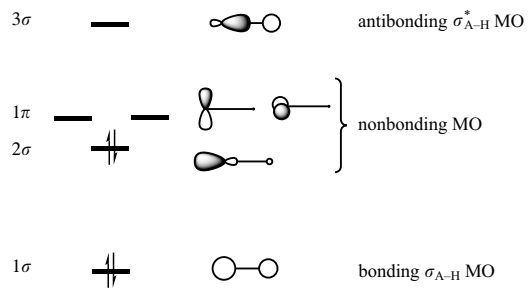

Figure 1.6. Molecular orbitals for AH molecules (with the electronic occupation appropriate for molecules with four valence electrons, such as BH or AlH in their lowest singlet state).

if A is a fairly electronegative element. In this case, one can therefore neglect the interaction of the *s* orbital (which, if it is doubly occupied, therefore describes a lone pair localized on A), and only consider the three *p* orbitals on the ligand, which are higher in energy and therefore closer to the metal *d* orbitals. The one which points towards the metal centre (p_z, **1-37**) is used for the σ interaction, and the two orbitals whose axis of revolution is perpendicular to the bond (p_x and p_y) can lead to π interactions (**1-38**).

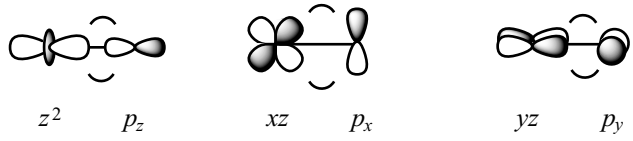

1-37 **1-38**

Comment

In a more sophisticated model of the σ orbitals, one can suppose that p_z and *s* are mixed, to form two *s*–*p* hybrid orbitals, one pointing towards the metal to form the σ bond, and the other in the opposite direction, so as to describe a lone pair of σ type on A. This new approach does not fundamentally change anything in the simplified description given above.

The preceding examples show that one must always consider the atomic or molecular orbital on the ligand that allows a σ bond to be formed with the metal. This orbital may be a nonbonding *s* orbital (H), a hybrid *s*–*p* orbital (AH_3, AH_2, and AH molecules), or a *p* orbital which points towards the metal centre (A atoms). When the atom bound to the metal also possesses nonbonding *p* orbitals perpendicular to the metal–ligand bond (AH_2, AH, A), it is also necessary to consider them, since they lead to π-type interactions with the metal orbitals.

Even though it is an approximation to neglect the other MO on the ligand, this usually leads to an acceptable description of the bond with

the metal centre. It is particularly appropriate when the neglected ligand orbitals are very low in energy and the antibonding orbitals very high. These conditions are usually satisfied when the orbitals are involved in the σ *bonds* of the ligand. However, when the ligand possesses one or more π *bonds*, its π bonding and π^* antibonding molecular orbitals must usually be taken into account.

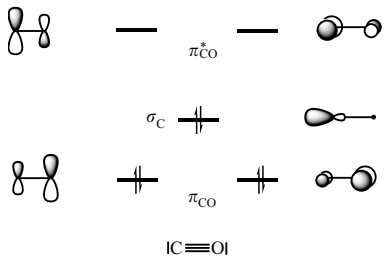

Figure 1.7. Electronic stucture of CO (three highest occupied and two lowest empty orbitals).

1.5.2.4. *Ligands with a π system: the example of CO*

When the ligand possesses a π bond involving the atom bound to the metal (η^1 coordination), this leads to the presence of a π bonding and π^* antibonding orbital on the ligand. In general, the π orbital is higher in energy than the MO that describe the σ bonds, while the π^* orbital is lower than the σ^* MO (§1.3.4). Although none of these π or π^* orbitals is nonbonding, in contrast to the *p* orbitals of AH_2, AH, and A ligands, their energy level is neither sufficiently low (π) nor sufficiently high (π^*) for one to be able, a priori, to neglect their role in the metal–ligand interaction.

Carbon monoxide, CO, also called the carbonyl ligand, is an example which illustrates these points nicely. The essential features of its electronic structure are shown in Figure 1.7. The highest occupied orbital is a nonbonding σ orbital, mainly concentrated on the carbon atom and polarized in the direction away from the oxygen atom. This orbital, which describes the lone pair on the carbon atom, is the one which allows a $\sigma_{M—CO}$ bond to be formed (L-type ligand). The two π_{CO} bonding orbitals associated with the π bonds in C≡O are lower in energy. They are mainly concentrated on oxygen, as that atom is more electronegative than carbon. The lowest empty orbitals are the antibonding π^*_{CO} orbitals, which have a larger contribution from carbon than oxygen. These four orbitals can lead to π-type interactions with orbitals of suitable symmetry on the metal, similar to those we have already seen with the nonbonding *p* orbitals of the AH_2 and AH molecules.

We shall therefore have to study a set of *five orbitals* (one σ, two π, and two π^*) when we wish to analyse the metal–carbonyl bond.[12]

[12] A more detailed analysis will enable us to show that one can, in a first approximation, reduce this number of orbitals to three: the σ orbital and the two π^* orbitals (Chapter 3, § 3.2.2).

1.5.2.5. *π complexes*

In the examples studied so far, the ligand is bound to the metal centre by only one of its atoms. The situation is different when several atoms of the ligand are bound in an equivalent manner to the metal centre (η^x coordination). This is the case for π complexes, in which the π system of the ligand is oriented towards the metal. All the π orbitals of the ligand, both occupied and empty, must now be considered to describe the metal–ligand bonds. As an example, we shall treat an η^2-ethylene complex in detail in Chapter 3 (§ 3.4).

1.6. Initial orbital approach to ML_ℓ complexes

The shape and the energy of the molecular orbitals of a complex depend on the number of ligands and their geometrical arrangement around the metal. It is possible to obtain some important information on the MO without defining the particular complex studied. The purpose of this paragraph is thus to derive the general characteristics of the orbital structure which do not depend (or depend only slightly) on the complex.

1.6.1. Simplified interaction diagram

We shall consider, for simplicity, a complex in which the metal is surrounded by ℓ identical ligands, each with just *a single orbital* that can take part in the metal–ligand interaction (a σ interaction, § 1.5.1).

A simplified diagram for the interaction between the ℓ ligand orbitals and the nine atomic orbitals on the metal (five *d* orbitals, one *s* orbital, and three *p* orbitals, without distinction) is given in Figure 1.8. In this diagram, the metal orbitals are placed higher in energy than those on the ligands, since the latter are more electronegative. The ℓ ligand orbitals interact with ℓ metal orbitals, to form ℓ bonding MO and the associated ℓ antibonding MO. There are therefore $(9 - \ell)$ nonbonding orbitals that remain on the metal.

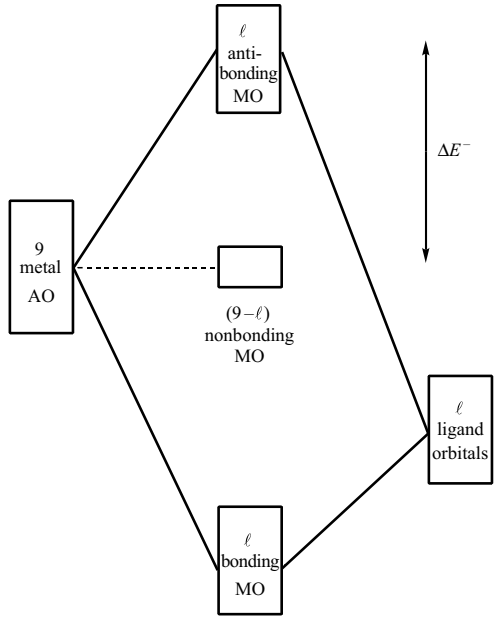

Figure 1.8. Simplified diagram for the interaction of the atomic orbitals on a metal centre and the ℓ ligands which surround it (σ interactions only).

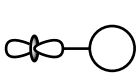

σ_{M-H} **1-39**

σ^*_{M-H} **1-40**

Given the relative energies for the participating orbitals (§ 1.3.2), we can make the following points:

1. The bonding MO, which describe the σ_{M-Lig} bonds, are mainly concentrated on the ligand orbitals. An example is given for an M-H bond involving the metal z^2 orbital (**1-39**).
2. The corresponding antibonding MO are mainly concentrated on the metal orbitals (**1-40**).
3. The nonbonding MO are orbitals that are localized on the metal centre. A more detailed analysis of the orbital structure of complexes (Chapter 2) will show that usually, but not always, these nonbonding MO are pure *d* orbitals, or orbitals in which the principal component is of *d* type.

1.6.2. Strong-field and weak-field complexes

The separation between the energy levels (ΔE^-, Figure 1.8) of the nonbonding and antibonding MO (σ^*_{M-Lig}) is directly linked to the strength of the interaction between the ligand orbitals and those on the metal. The stronger this interaction, the more the antibonding orbitals are destabilized, so the larger the energy gap ΔE^-. When the metal–ligand interaction is strong, ΔE^- is large and one refers to *strong-field complexes*; in contrast, when ΔE^- is small, one refers to *weak-field complexes*.

1.6.3. Electronic configuration and the 18-electron rule

In so far as the electronic occupation of the molecular orbitals is concerned, the stability of an ML_ℓ complex is generally maximized when the bonding MO, of which there are ℓ, together with the nonbonding MO, of which there are $(9 - \ell)$, are doubly occupied, but when the ℓ antibonding MO remain empty (Figure 1.8). The bonding MO describe the M-Lig bonds and the nonbonding MO represent lone pairs on the metal. In this situation, the total number of electrons is:

$$N_t = (2 \times \ell) + 2 \times (9 - \ell) = 18 \tag{1.13}$$

In this way, we rationalize the 18-electron rule that was previously discussed with reference to the valence electronic structure of the nearest noble gas (§ 1.1.2.1).

The electrons that occupy the nonbonding MO are not used to form metal–ligand bonds. They therefore correspond to the *n* electrons that 'remain' on the metal in the classical counting scheme (§ 1.1.2.3). The d^n notation for the electronic configuration of the metal assumes, however,

that all the occupied nonbonding orbitals on the metal are of *d* type (see Chapter 2).

Even if the 18-electron rule is often obeyed, we must not forget that there are many exceptions. There are some complexes that have *fewer than 18 electrons*. For example, the $[M(Lig)_4]$ complexes that adopt a 'square-planar' geometry (four ligands at the vertices of a square whose centre is occupied by the metal) with a d^8 electronic configuration (e.g.: $[Ir(CO)(Cl)(PPh_3)_2]$, § 1.1.2.1) are 16-electron complexes. Since the bonding MO that describe the bonds are doubly occupied, this analysis shows that one of the nonbonding orbitals in Figure 1.8 is empty, and a more detailed study of the electronic structure is necessary to understand this result (Chapter 2, §2.2). These 16-electron complexes are stable, but often reactive towards other molecules since they have a tendency to form 18-electron complexes, by binding other ligands. For example, Wilkinson's catalyst $[Rh(PPh_3)_3Cl]$ is used industrially for the catalytic hydrogenation of olefins (see Exercise 1.3).

There are also some complexes with *more than 18 electrons*, such as $[Ni(H_2O)_6]^{2+}$ which possesses 20 electrons (§ 1.1.2.1). Some antibonding MO must therefore be occupied, which can happen only if they are sufficiently low in energy, as is the case in weak-field complexes. *Organometallic* complexes, characterized by the presence of one or several metal–carbon bonds, are strong-field complexes. It is therefore rare for them to possess more than 18 electrons.

1.6.4. Analogy with the octet rule

In the same way, one can construct a simplified interaction diagram for AH_n (or AR_n) molecules in which A is an element from the second or third row of the periodic table (C, Si, N, P, O, S, etc.). There are thus four valence orbitals on the central atom: one *s* AO, and three *p* AO. The σ interactions with the orbitals on the atoms bound to A lead to the formation of n bonding MO, n antibonding MO and $(4-n)$ nonbonding MO. If the bonding and nonbonding MO are doubly occupied, the number of electrons N_t is equal to

$$N_t = (2 \times n) + 2 \times (4 - n) = 8 \tag{1.14}$$

We have therefore derived the octet rule. As examples, we can quote:

CH_4	$n = 4$	4 bonding MO, 4 antibonding MO, 0 nonbonding MO
NH_3	$n = 3$	3 bonding MO, 3 antibonding MO, 1 nonbonding MO
OH_2	$n = 2$	2 bonding MO, 2 antibonding MO, 2 nonbonding MO
FH	$n = 1$	1 bonding MO, 1 antibonding MO, 3 nonbonding MO

It is straightforward to verify that the number of bonding, nonbonding, and antibonding MO predicted by this simple model agree consistently with the detailed orbital structures of the NH_3, OH_2, and HF molecules (§ 1.1.4–1.1.6).

Exercises

1.1

What are the two coordination modes of the allyl ligand, $H_2C\text{-}CH\text{-}CH_2$, for which a Lewis structure is given below? In each case, categorize the ligand as $L_\ell X_x$.

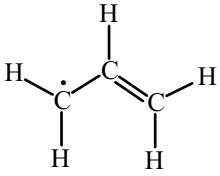

1.2

Write each of the following complexes as $[ML_\ell X_x]^q$, give the oxidation state of the metal *no*, the electronic configuration d^n, and the total number of electrons N_t. (1) $[Cr(CO)_6]$; (2) $[W(CO)_5]$; (3) $[Mn(CO)_5Cl]$; (4) $[TiCl_4]$; (5) $[Co(CO)_3(Et)]$; (6) $[Re(PR_3)(CO)_4Cl]$; (7) $[Fe(CO)_4(H)_2]$; (8) $[Fe(CO)_4(\eta^2\text{-}H_2)]$; (9) $[ReH_9]^{2-}$; (10) $[ReH_5(PR_3)_2(SiR_3)_2]$; (11) $[Ni(CO)_4]$; (12) $[Cu(SR)_3]^{2-}$; (13) $[Ni(CN)_5]^{3-}$; (14) $[RhI_3(CO)_2(Me)]^-$; (15) $[RhI_3(CO)(COMe)]^-$; (16) $[MoF_4(O)_2]^{2-}$; (17) $[Re(NR_3)_4(O)_2]^+$; (18) $[Mn(\eta^6\text{-}C_6H_6)(CO)_3]^+$; (19) $[Zr(\eta^5\text{-}C_5H_5)_2(H)(Cl)]$; (20) $[Nb(\eta^5\text{-}C_5H_5)_2(Me)_3]$; (21) $[Os(\eta^5\text{-}C_5H_5)(CO)_2Cl]$; (22) $[WCl_6]$; (23) $[Fe(CO)_4(\eta^2\text{-}C_2H_4)]$; (24) $[Zn(\eta^5\text{-}C_5H_5)(Me)]$.

1.3

Wilkinson's catalyst $[RhL_3Cl]$, where $L = PPh_3$, is used for the hydrogenation of alkenes. The reaction proceeds as follows:

$$[RhL_3Cl] \xrightarrow{H_2} [RhL_3Cl(H)_2] \longrightarrow [RhL_2Cl(H_2)] + L \xrightarrow{C_2H_4} [RhL_2Cl(H)_2(\eta^2\text{-}C_2H_4)] + L$$
$$[RhL_3Cl] + CH_3\text{-}CH_3 \longleftarrow [RhL_3Cl(H)(CH_2CH_3)] \longleftarrow [RhL_2Cl(H)(CH_2CH_3)] + L \quad (\downarrow)$$

For each step, give the oxidation state of the metal (*no*), the electronic configuration of the complex (d^n), and the total number of electrons (N_t).

1.4

1. Give the charge on the ligands CO, Cl, Et, PR_3, H, H_2, SiR_3, SR, CN, I, Me, COMe, F, O, NR_3, C_2H_4, C_6H_6, C_5H_5 if the ionic model is adopted (§ 1.2).

2. Formulate the complexes given in § 1.1.2.2 if this model is adopted, and hence deduce the oxidation state of the metal.

1.5

1. Give the oxidation state of the metal *no*, the electronic configuration d^n, and the total number of electrons N_t for the complexes $[Cr(\eta^6\text{-}C_6H_6)_2]$ and $[Ru(\eta^6\text{-}C_6H_6)(\eta^4\text{-}C_6H_6)]$.
2. How can one explain the change in the coordination mode $\eta^6 \rightarrow \eta^4$ of one of the ligands when chromium in the complex is replaced by ruthenium?
3. Using the same argument, predict the hapticity x for a cyclopentadienyl ligand in the following complexes: (*i*) $[Mn(CO)_3(\eta^x\text{-}C_5H_5)]$; (*ii*) $[W(CO)_2(\eta^5\text{-}C_5H_5)(\eta^x\text{-}C_5H_5)]$; (*iii*) $[Fe(CO)_2(\eta^5\text{-}C_5H_5)(\eta^x\text{-}C_5H_5)]$.

1.6

The borohydride ligand (BH_4^- in the ionic model) can bind in the η^1, η^2, or η^3 modes, depending on whether one, two, or three B-H bonds interact with the metal centre.

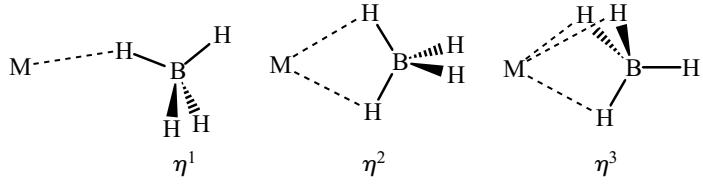

Rationalize the coordination mode in the following complexes: $[Cu(PR_3)_3(\eta^1\text{-}BH_4)]$, $[Cu(PR_3)_2(\eta^2\text{-}BH_4)]$, and $[Ti(CO)_4(\eta^3\text{-}BH_4)]^-$.

1.7

What is the oxidation state of the metal centres in the following binuclear complexes: (1) $[Re(CO)_5]_2$; (2) $[ReCl_4(H_2O)]_2^{2-}$; (3) $[MoCl_2(PR_3)_2]_2$; (4) $[Pd(\eta^3\text{-}C_3H_5)(\mu\text{-}Cl)]_2$; (5) $[Mo(\eta^5\text{-}C_5H_5)(CO)_2(\mu\text{-}SR)]_2$.

1.8

Consider the interaction between a metal atom and a ligand with an *s* orbital.

1. Show that there can always be an interaction between the ligand orbital and the *s* orbital of the metal. Sketch the shapes of the resulting bonding and antibonding MO.
2. What position must the ligand adopt to give (*i*) maximal and (*ii*) minimal overlap with the p_x orbital of the metal? What is its value in the latter case?
3. Repeat question 2 for the *xy* and z^2 metal orbitals.

This page intentionally left blank

Principal ligand fields: σ interactions

In this chapter, we shall construct the molecular orbitals (MO) of monometallic complexes ML_ℓ and thereby deduce their electronic structure by distributing the electrons in these orbitals. We shall study different types of 'ligand field', each one being characterized by the number of ligands and by their geometrical arrangement around the metal centre (octahedral complexes ML_6, tetrahedral, or square-planar ML_4, etc.).

We shall always begin the analysis by establishing the molecular orbitals of the *associated model complex*, in which all the ligands (*i*) are identical and (*ii*) only have σ-type interactions with the metal (Chapter 1, § 1.5.1). The resulting orbital scheme is characteristic of the ligand field being studied (octahedral, tetrahedral, square-planar, etc.). In a first approximation, it is applicable to all complexes of this type, even if the two conditions specified above are not met exactly. The main reason for this is that σ interactions exist in all complexes, and they are stronger than π interactions when the latter are present. Therefore, if π-type interactions are added in a 'real' complex to σ interactions, while the results are different from those obtained for the model complex, they are not completely transformed. The π effects will therefore be treated subsequently as *perturbations* to be added to the orbital scheme established for the model complex.[1] In the same way, different σ interactions associated with non-equivalent ligands produce changes compared to the model complex that can initially be neglected.

[1] Those ligands for which it is necessary to consider π-type interactions with the metal are studied in Chapter 3.

There are several ways of representing the ligand orbital that is involved in the σ interaction with the metal: as an *s* orbital (**2-1a**), as a *p* orbital (**2-1b**), or as a hybrid (*s*–*p*) orbital directed towards the metallic centre (**2-1c**). We shall use this last representation, since, except for hydride ligands which possess only a single valence orbital 1*s* and very electronegative monoatomic ligands such as F in which the contribution of the *p* orbital dominates, it is the most appropriate for all other ligands. The orbital on ligand L_i will be written σ_i, due to the nature of the bond which it can form with the metal.

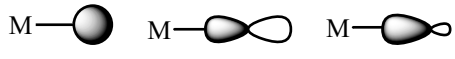

2-1a **2-1b** **2-1c**

To construct the molecular orbitals of a complex, we have to determine their shape, by which we mean the contributions of the metal and ligand orbitals to each one, as well as their relative energies. The 'fragment method' is widely used for the construction of the MO of a complex ML_ℓ; we allow the atomic orbitals (AO) of the central metal to interact with those on the ligands. Knowledge of the symmetry properties of these orbitals allows us to simplify the construction of these diagrams very considerably. If the two orbitals have the same symmetry properties, their overlap is non-zero and an interaction can occur. On the other hand, two orbitals of different symmetry have zero overlap ('by symmetry') and do not interact at all (Chapter 1, § 1.3.3). In this context, we shall sometimes use basic ideas from group theory, as well as several results established in Chapter 6 which the reader may consult when necessary.

2.1. Octahedral ML_6 complexes

Consider a complex in which the metal centre is surrounded by six identical ligands (L_1–L_6) placed at the vertices of an octahedron (**2-2**). The metal is placed at the origin, and the ligands on the axes x (L_2, L_4), y (L_1, L_3), and z (L_5, L_6). Each ligand L_i possesses an orbital σ_i directed towards the metal (**2-3**).

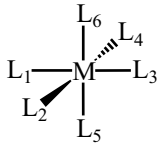

2-2

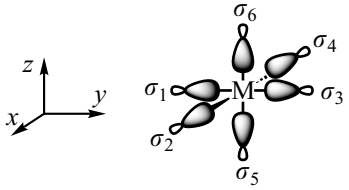

2-3

2.1.1. Initial analysis of the metal–ligand orbital interactions

Our first task is to examine how each of the orbitals on the ligands can interact with the *s*, *p*, and *d* orbitals on the metal centre.

As the *s* orbital has spherical symmetry, its overlap with any one of the σ_i orbitals is non-zero (σ_1 in **2-4**). And as the six ligands are equivalent, this overlap is the same no matter which orbital σ_i is considered, so the interactions between *s* orbital and each of the ligand orbitals are identical.

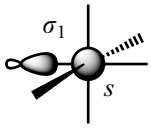

2-4 ($S \neq 0$)

We therefore find a bonding MO between the metal and the ligands (**2-5**) and a corresponding antibonding MO (**2-6**), where each

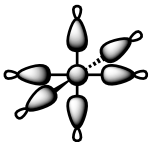

2-5 (bonding)

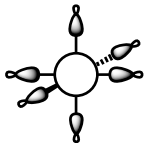

2-6 (antibonding)

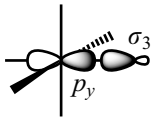

2-7 ($S \neq 0$)

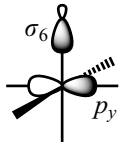

2-8 ($S = 0$)

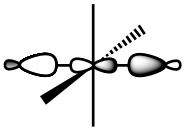

2-9 (bonding)

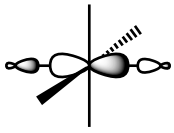

2-10 (antibonding)

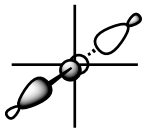

2-11 (bonding)

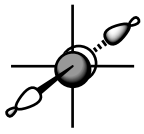

2-12 (antibonding)

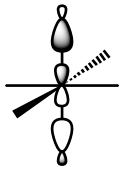

2-13 (bonding)

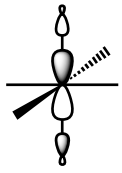

2-14 (antibonding)

σ_i contribution is equal in both orbitals. Since the ligands are more electronegative than the metal, the bonding orbital is mainly concentrated on the ligands but the antibonding orbital on the metal (Chapter 1, § 1.6.1).

We now turn to the *p*-type orbitals on the central atom. The p_y orbital overlaps with the orbitals on the ligands L_1 and L_3 located on the *y*-axis (σ_3 in **2-7**). But the four other ligands L_2, L_4–L_6, are placed in the nodal plane of p_y (*xz*), which is a symmetry element of the complex. The σ_i orbitals associated with these ligands are symmetric with respect to this plane, whereas the p_y orbital is antisymmetric: the overlaps between p_y and each of σ_2, σ_4–σ_6 are therefore zero 'by symmetry'. In the example shown in **2-8**, it is clear that the σ_6 orbital has a positive overlap with the grey lobe of the p_y orbital but an equivalent negative overlap with the white lobe, so the total overlap is equal to zero. Therefore, there cannot be any interaction between the p_y orbital and any of these four ligand orbitals.

The p_y orbital on the metal therefore combines with the σ_1 and σ_3 orbitals to form a bonding MO, mainly based on the ligands (**2-9**), and an antibonding MO mainly based on the metal (**2-10**).

This analysis is readily extended to the p_x and p_z orbitals, which can combine only with σ_2 and σ_4 for p_x (**2-11** and **2-12**) or σ_5 and σ_6 for p_z (**2-13** and **2-14**). The interactions involving the *p* orbitals of the metal therefore lead to the formation of three bonding and three antibonding MO. The three bonding orbitals differ from each other only by their orientations: they have the same energy, and are therefore degenerate. The same is clearly true for the antibonding orbitals.

We now turn to the interactions that involve the *d* orbitals of the metal centre. We consider first the three orbitals *xy*, *xz*, and *yz* that each contain two nodal planes, (*xz*, *yz*), (*xy*, *yz*), and (*xy*, *xz*), respectively. The six ligands, placed on the *x*-, *y*-, or *z*-axes (**2-2**), are all located in one of the two nodal planes of the *d* orbitals, and sometimes even at the intersection of these two planes. The overlap between any one of the σ_i orbitals and the *yz* (**2-15**), *xy* (**2-16**) or *xz* orbitals (**2-17**) is therefore equal to zero.

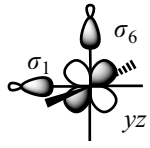

2-15 ($S = 0$)

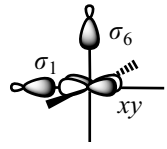

2-16 ($S = 0$)

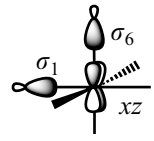

2-17 ($S = 0$)

Therefore, there cannot be any interaction between the three *xy*, *xz*, and *yz* orbitals and the σ_i orbitals on the ligands. In an octahedral complex, these three *d* orbitals therefore form a degenerate *nonbonding* set, located only on the metal (**2-18** to **2-20**).

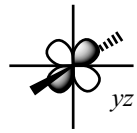

2-18 (nonbonding)

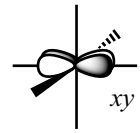

2-19 (nonbonding)

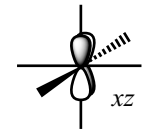

2-20 (nonbonding)

The situation is different for the two remaining *d* orbitals. The x^2-y^2 orbital points towards the ligands located on the *x*- and *y*-axes (L_1–L_4). The overlaps with the orbitals on these four ligands (σ_1 in **2-21**) are therefore non-zero and all equal (in absolute value), since the x^2-y^2 orbital has the same amplitude (in absolute value), at a given distance from the metal, in the direction of each of the ligands. But the ligands L_5 and L_6 are located on the *z*-axis, that is, the intersection of the two nodal planes of the x^2-y^2 orbital (the planes which bisect the *x*- and *y*-axes). No overlap is therefore possible between x^2-y^2 and the orbitals on these last two ligands (σ_6 in **2-22**).

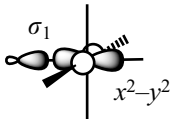

2-21 ($S \neq 0$)

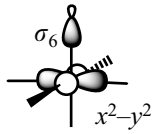

2-22 ($S = 0$)

The interaction of the x^2-y^2 orbital with the ligand orbitals therefore leads to a bonding MO, mainly concentrated on the ligands (**2-23**), and an antibonding MO, essentially the metal orbital (**2-24**). In each of these MO, the coefficients on the ligands L_1–L_4 are equal in absolute value, since the overlaps concerned are identical, but the coefficients on L_5 and L_6 are zero.

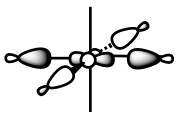

2-23
(bonding)

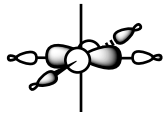

2-24
(antibonding)

The last orbital to be considered is the z^2 orbital. It is mainly oriented along the *z* axis, but also, to a lesser degree, in the *xy* plane; none of the ligands is located in its nodal cone (Chapter 1, Scheme **1-31**). It can therefore interact with the orbitals of all six ligands, though the overlap with a ligand placed on the *z*-axis (σ_6 in **2-25**) is larger than that with a ligand in the *xy* plane (σ_1 in **2-26**).

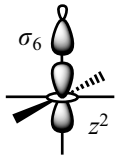

2-25 ($S \neq 0$)

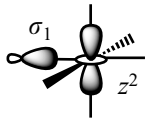

2-26 ($S \neq 0$)

The bonding (**2-27**) and antibonding (**2-28**) MO formed from the z^2 orbital therefore contain contributions from the six ligands, with the coefficients for L_5 and L_6, placed on the *z*-axis, being larger than those for L_1–L_4, in the *xy* plane (Chapter 6, § 6.6.5).

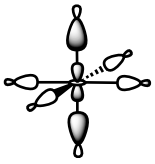

2-27
(bonding)

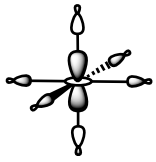

2-28
(antibonding)

This initial analysis of the orbital structure of octahedral complexes has relied simply on the existence, or the absence, of an overlap between the orbitals of the metal and those on the ligands, and on the difference in electronegativity between the metal and the ligands. It enables us to obtain several important results: (*i*) there are six bonding MO, mainly concentrated on the ligands, and six antibonding MO, mostly on the metal; (*ii*) there are three remaining orbitals located on the metal which take no part in the metal–ligand bonds (nonbonding orbitals). This description is consistent with the simplified scheme given in Chapter 1 (§ 1.6.1, Figure 1.8) which predicted the formation of ℓ bonding MO, ℓ antibonding MO, and $(9-\ell)$ nonbonding MO in ML_ℓ complexes. It also provides a qualitative description of the shape of

these MO, and shows that the three nonbonding orbitals are, in the particular case of an octahedral complex, pure *d* orbitals on the metallic centre.

2.1.2. Complete interaction diagram

The analysis presented above allows us to establish the main features of the orbital structure of octahedral complexes. It also shows that certain molecular orbitals are degenerate. This is the case, for example, for the three bonding MO constructed from the metal *p* orbitals (**2-9**, **2-11**, and **2-13**), or for the three nonbonding orbitals (**2-18** to **2-20**). However, other degeneracies exist which cannot readily be shown by the analysis above. To obtain a more complete description of the orbital structure, it is necessary to exploit *all* the symmetry properties of the octahedron and not simply this or that symmetry element as we have done so far.

There are four stages in the general procedure for constructing the MO of an ML_ℓ complex:

1. Find the appropriate point-group symmetry. In this case, it is the octahedral group, O_h.
2. Determine the symmetry properties of the orbitals on the central metal atom. They are given directly by the character table for the point group.
3. Do not consider the ligand orbitals *individually*, but use linear combinations of these orbitals which are 'adapted' to the symmetry of the complex.[2]
4. Allow the metal and ligand orbitals to interact (*fragment method*). Only orbitals of the same symmetry can interact, since their overlap is non-zero.

[2] In other words, the linear combinations of orbitals which are bases for an irreducible representation of the symmetry point group (see Chapter 6, § 6.4).

2.1.2.1. *The symmetry of metal orbitals*

Examination of the character table of the octahedral point group (O_h) gives us the symmetry of the metal orbitals directly, as this atom is located at the origin of the x, y, z frame (Table 2.1). The last two columns indicate the symmetry of several functions of x, y, and z which have a direct link with the analytical expressions, in Cartesian coordinates, of these orbitals (Chapter 1, § 1.4.1).

The *s* orbital, which has spherical symmetry, has the same symmetry properties as the function $x^2+y^2+z^2$. It is therefore a basis of the irreducible representation A_{1g} (the totally symmetric representation of the O_h group), or more simply 'it has A_{1g} symmetry'. The p_x, p_y, and p_z orbitals transform as x, y, and z, respectively. Their symmetry is therefore T_{1u} (a three-dimensional, or triply degenerate, representation).[3] Finally, the

[3] The dimension of the representation is given by the value of the character associated with the identity operation *E* (3 in the case of T_{1u}).

Table 2.1. Character table of the point group O_h

O_h	E	$8C_3$	$6C_2'$	$6C_4$	$3C_2$	i	$8S_6$	$6\sigma_d$	$6S_4$	$3\sigma_h$		
A_{1g}	1	1	1	1	1	1	1	1	1	1		$x^2+y^2+z^2$
A_{2g}	1	1	−1	−1	1	1	1	−1	−1	−1		
E_g	2	−1	0	0	2	2	−1	0	0	2		(z^2, x^2-y^2)
T_{1g}	3	0	−1	1	−1	3	0	−1	1	−1		
T_{2g}	3	0	1	−1	−1	3	0	1	−1	−1		(xy, xz, yz)
A_{1u}	1	1	1	1	1	−1	−1	−1	−1	−1		
A_{2u}	1	1	−1	−1	1	−1	−1	1	1	−1		
E_u	2	−1	0	0	2	−2	1	0	0	−2		
T_{1u}	3	0	−1	1	−1	−3	0	1	−1	1	(x, y, z)	
T_{2u}	3	0	1	−1	−1	−3	0	−1	1	1		

d orbitals have E_g symmetry for the z^2 and x^2—y^2 pair, but T_{2g} for the *xy*, *xz*, and *yz* set. It is thus important to realize that the five *d* orbitals, which clearly have the same energy for an isolated atom, are separated into two groups according to their symmetry properties: a doubly degenerate representation E_g and a triply degenerate set T_{2g}.

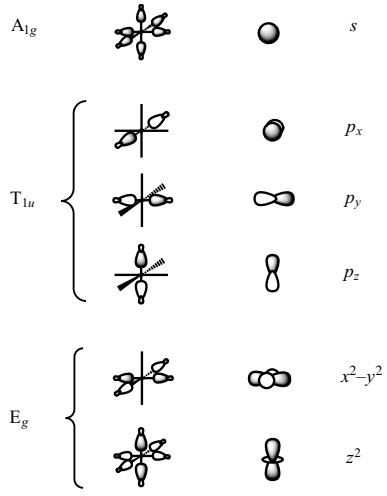

Figure 2.1. Symmetry-adapted σ orbitals for an octahedral complex ML_6, and orbitals of the same symmetry on the metal centre (consult Chapter 6, § 6.6.5 for the analytical expressions of these symmetry-adapted orbitals and the method for finding them).

2.1.2.2. *Symmetry-adapted orbitals on the ligands*

None of the ligand orbitals σ_i, considered individually, is a basis for the irreducible representations of the O_h group. For the construction of the orbital interaction diagram, it is therefore necessary to use linear combinations of these orbitals which are *adapted to the symmetry* of the octahedron. These are presented in Figure 2.1, next to the metal orbitals with the same symmetry.

In the orbital of A_{1g} symmetry, all the coefficients have the same value and sign. It is clearly a totally symmetric orbital, just like the *s* orbital on the central atom. Out-of-phase combinations on two ligands in *trans* positions appear in the three T_{1u} orbitals, along the *x*, *y*, or *z* axes. It is clear by inspection of the shape of these orbitals that they differ only in their orientations and that they have the same symmetry properties as the p_x, p_y, and p_z orbitals of the metal centre (Figure 2.1). These combinations of ligand orbitals are therefore degenerate by symmetry, just like the metal *p* orbitals (T_{1u} representation).

In the case of the first orbital of E_g symmetry, the coefficients for the four ligands in the *xy* plane are all of equal value, but of opposite sign, depending whether they are on the *x*- or the *y*-axis. The symmetry

properties of this orbital are therefore just the same as those of the metal $x^2 - y^2$ orbital, which also has E_g symmetry. The second E_g orbital contains contributions from all six ligands. The coefficients for the ligands located on the z-axis are twice as large as those for the ligands in the xy plane, and of opposite sign. The z^2 orbital, which also has E_g symmetry, shares these properties; its amplitude is proportional to $(2z^2 - x^2 - y^2)$ (Chapter 1, formula (1.11)). *It is important to realize that the two* E_g *orbitals that are degenerate by symmetry necessarily have the same energy* (Chapter 6). In contrast to the case of the three orbitals of T_{1u} symmetry, this result is not at all obvious just from the coefficients for the ligands in the two orbitals. This additional information, obtained after proper consideration of the octahedral symmetry of the complex, enables us to produce a complete description of their orbital structure.

Comment

In what follows, the symmetry of atomic or molecular orbitals will be represented with lower-case letters (a_{1g}, t_{1u}, e_g, t_{2g}, etc.), while upper-case letters will be reserved for the different irreducible representations in character tables, for the symmetry of electronic states and for spectroscopic terms.

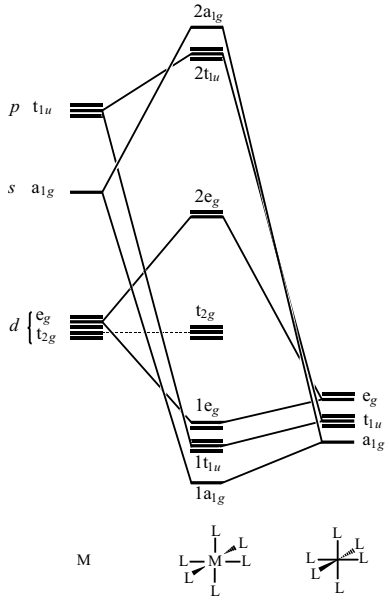

Figure 2.2. Interaction diagram (σ only) for an octahedral complex ML_6: the metal orbitals are on the left and the symmetry-adapted ligand orbitals on the right.

2.1.2.3. *Interaction diagram*

We can now construct all the MO of an octahedral complex, by allowing the metal orbitals (Figure 2.2, left-hand side) to interact with the symmetry-adapted combinations of orbitals on the six ligands (Figure 2.2, right-hand side).

The energetic ordering adopted for the metal orbitals follows the usual rule for the *d*-block transition metals: $\varepsilon(d) < \varepsilon(s) < \varepsilon(p)$ (Chapter 1, § 1.4.2). The six ligand-orbital combinations are not all at the same energy. To understand the energetic ordering in Figure 2.2, one must analyse the bonding or antibonding character of each for the ligand–ligand interactions (Figure 2.1). The a_{1g} orbital is the most stable, since all the interactions are bonding. In the t_{1u} orbitals, there is an antibonding interaction between two ligands that are *trans* to each other. Due to the large distance between these ligands, the orbitals may be considered to be practically nonbonding. For the two e_g orbitals (which necessarily have the same energy), it is easier to consider the first: the four interactions between the closer ligands (*cis*) are antibonding, but two weakly bonding interactions occur between the *trans* ligands. Overall, the e_g orbitals are therefore antibonding, leading to the energetic ordering: $\varepsilon(a_{1g})$ (bonding) $< \varepsilon(t_{1u})$ (nonbonding) $< \varepsilon(e_g)$ (antibonding). One must remember that the bonding or

antibonding interactions just described never involve atoms that are directly bonded to each other. The overlaps involved are therefore weak, due to the distance between the centres concerned (e.g. if the metal–ligand bond distances are 2.2 Å, the corresponding *cis*-ligand separation is 3.11 Å, and as much as 4.40 Å for the *trans* ligands). This explains why the energy separations between the different ligand orbitals are small (Figure 2.2, right-hand side). We conclude by noting that the ligand orbitals are placed lower in energy than those on the metal, since the ligands are in general more electronegative than the metal.

The molecular orbitals are obtained by allowing the orbitals of the M and L_6 fragments to interact (Figure 2.2). We note features that were established in § 2.1.1: the formation of six bonding MO ($1a_{1g}$, $1t_{1u}$, and $1e_g$), by bonding interactions involving the fragment orbitals whose symmetries are a_{1g}, t_{1u}, and e_g, and the formation of six corresponding antibonding MO ($2e_g$, $2a_{1g}$, and $2t_{1u}$). *The new feature concerns the degeneracy of the e_g orbitals (bonding or antibonding): it was not possible to establish this just from the shapes of the orbitals that were already determined* (**2-23** and **2-27** for the bonding MO, **2-24** and **2-28** for the antibonding MO). Three nonbonding MO of t_{2g} symmetry are found at an intermediate energy level. They are pure metal *d* orbitals (*xy*, *xz*, and *yz*), which remain nonbonding as there are no orbitals of the same symmetry on the L_6 fragment.

This general scheme, with six bonding MO, three nonbonding MO, and six antibonding MO is appropriate for all octahedral complexes, since it is based on the symmetry properties of the fragment orbitals. Moreover, the lowest antibonding MO (situated above the nonbonding t_{2g} orbitals) are always the two degenerate $2e_g$ orbitals, since they involve the metal *d* orbitals, which are lower in energy than the *s* and *p* orbitals which contribute to the antibonding MO $2a_{1g}$ and $2t_{1u}$, respectively. However, the energetic ordering given in Figure 2.2 for both the bonding and antibonding MO can depend on the nature of the metal and the ligands. For example, the bonding level $1e_g$ can be found between the bonding $1a_{1g}$ and $1t_{1u}$ levels, or the antibonding $2a_{1g}$ may be placed lower than the antibonding $2t_{1u}$ level.

Comment

There are *six valence atomic orbitals* on the metal which contribute to the formation of the *six metal–ligand bonds*: the *s* orbital, the three *p* orbitals, and two of the *d* orbitals. This result may be compared with that given by hybridization theory, where one forms six equivalent hybrids, directed towards the six vertices of an octahedron. One does indeed talk of d^2sp^3 hybridisation, each hybrid orbital being a suitable linear combination of two *d* orbitals, the *s* orbital, and the three *p* orbitals.

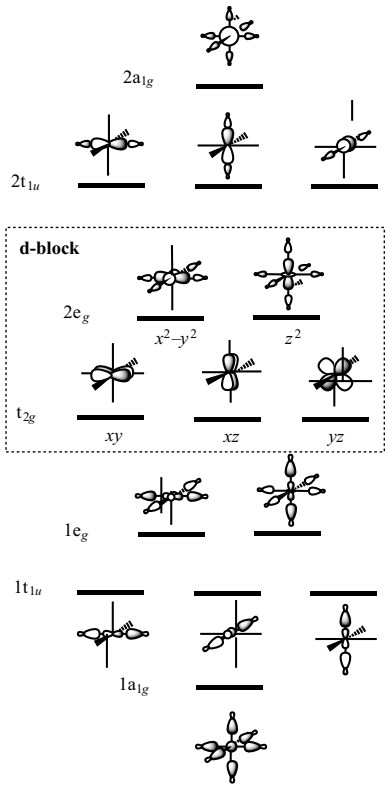

Figure 2.3. Molecular orbitals for an octahedral ML_6 complex in the orientation given in Scheme **2-2**.

2.1.2.4. *Molecular orbitals and the definition of the d block*

The shapes of the molecular orbitals may be obtained without difficulty from the shapes of the fragment orbitals (Figure 2.3). Given the greater electronegativity of the ligands, the bonding MO are more concentrated on them, whereas the antibonding MO are more concentrated on the metal. Among these MO, seven involve contributions from the metal *d* orbitals: the two bonding MO $1e_g$, the three nonbonding t_{2g} MO and the two antibonding MO $2e_g$. The term 'd block' of an octahedral complex (and also for other types of complex) is used to refer to the *five molecular orbitals that are mainly concentrated on the d orbitals of the metal*. The three nonbonding MO of t_{2g} symmetry clearly belong to the d block, since they are formed from pure *d* orbitals (*xy*, *xz*, and *yz*). For the MO of e_g symmetry, the bonding combinations ($1e_g$) are mainly concentrated on the ligands while the largest coefficient for the antibonding combinations ($2e_g$) is on the metal. It is these last two orbitals which are considered to belong to the d block. *The d block of an octahedral complex is therefore made up of three nonbonding degenerate* (t_{2g}) *MO and two antibonding MO which are also degenerate* ($2e_g$). These latter orbitals are often represented as $x^2—y^2$ and z^2, with the antibonding contributions on the ligands being implicitly taken into account in this simplified notation.

2.1.2.5. *Two other representations of the d block*

The orbitals of the d block, presented in the way we have just established, correspond to the arrangement of the ligands that is indicated in **2-2**: two ligands placed on each of the *x*-, *y*-, and *z*-axes. The three nonbonding orbitals are then *xy*, *xz*, and *yz*, and the two antibonding orbitals are $x^2—y^2$ and z^2. But other arrangements of the ligands with respect to the axes are of course possible. Two in particular will be useful to us in what follows: (*i*) where four metal–ligand bonds bisect the *x*- and *y*-axes (**2-29**); (*ii*) where the *z*-axis is a threefold symmetry axis (C_3) of the octahedron (**2-30**). It is clear that a change in the axis system cannot have any consequence for the structure of the d block, which consists of three degenerate nonbonding orbitals and two antibonding orbitals that are also degenerate. However, the expressions of some of these orbitals in the new axes systems do change.

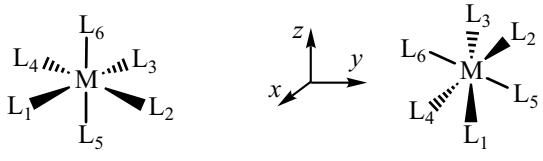

2-29 **2-30**

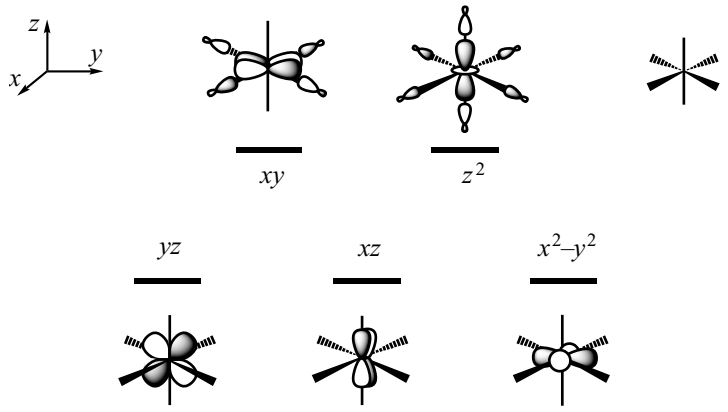

Figure 2.4. Representation of the orbitals of the d block for an octahedral complex ML_6 in the orientation shown in Scheme **2-29**.

We examine first the situation represented in **2-29**. The six ligands are still placed in one or other of the two nodal planes of the *xz* and *yz* orbitals. These two orbitals are therefore still nonbonding (Figure 2.4), as they were in the preceding case (Figure 2.3). Nor is there any change for the antibonding orbital z^2, since there are still two ligands on the *z*-axis and four in the *xy* plane. However, the *xy* orbital which was nonbonding now points towards all four ligands placed on the bisectors of the *x*- and *y*-axes: this orbital becomes one of the antibonding orbitals of the d block. On the other hand, these four ligands are now situated in the nodal planes of the x^2-y^2 orbital, which becomes, with *xz* and *yz*, the third nonbonding orbital of the d block. This new representation of the d block (Figure 2.4) may be distinguished from the preceding one (Figure 2.3) by 'exchange' of the *xy* and x^2-y^2 orbitals.

Analysis of the situation is more complex for the geometrical arrangement shown in **2-30**. The only orbital for which the result is obtained easily is z^2. The angle between the M–L bonds and the *z*-axis as it is now defined is exactly equal to 109.5°, which is the value of the angle of the nodal plane of the z^2 orbital (Chapter 1, Scheme **1-31**). As the six ligands are located on the nodal surface of this orbital, no interaction of σ type is possible, so z^2 is one of the three nonbonding orbitals. The difficulty in finding the two other nonbonding orbitals arises because none of the four ligands L_1–L_4 is now placed in one of the nodal planes of the *xy*, *xz*, *yz*, or x^2-y^2 orbitals. None of these orbitals is therefore nonbonding. Nor is any as antibonding as the $2e_g$ orbitals were in the preceding representations, since they do not point directly towards the ligands. An example is given in **2-31** for the *xz* orbital. The ligands L_5 and L_6 are in the nodal plane *yz* (coefficients zero). The orbitals on the ligands L_1–L_4 interact with *xz*, though they are not placed on the bisectors of the *x*- and *z*-axes where the amplitude of this orbital is greatest.

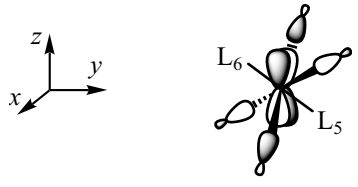

2-31

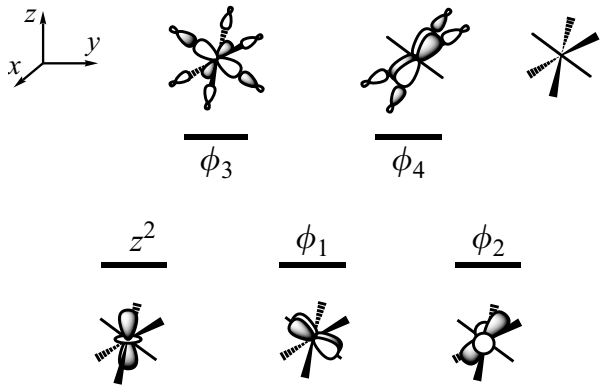

Figure 2.5. Representation of the orbitals of the d block of the octahedron when the *z*-axis coincides with a C_3 axis (Scheme **2-30**).

In fact, rather than considering the metal *d* orbitals individually, we must form new combinations that either 'avoid' the six ligands (nonbonding orbitals) or point towards them (antibonding orbitals). These linear combinations, which allow the original orbitals to be reoriented, are indicated below and shown graphically in Figure 2.5.

$$\phi_1 = \sqrt{\frac{2}{3}}(x^2 - y^2) - \sqrt{\frac{1}{3}}yz \tag{2.1}$$

$$\phi_2 = \sqrt{\frac{2}{3}}xy - \sqrt{\frac{1}{3}}xz \tag{2.2}$$

$$\phi_3 = \sqrt{\frac{1}{3}}(x^2 - y^2) + \sqrt{\frac{2}{3}}yz \tag{2.3}$$

$$\phi_4 = \sqrt{\frac{1}{3}}xy + \sqrt{\frac{2}{3}}xz \tag{2.4}$$

The first two combinations (ϕ_1 and ϕ_2) correspond to two orbitals which, with z^2, form the t_{2g} block. The last two (ϕ_3 and ϕ_4), on the other hand, have maximum overlap with the ligands and are the two antibonding e_g orbitals (Figure 2.5).

2.1.2.6. *Weak fields and strong fields*

In the absence of any ligand (isolated metal atom), the five *d* orbitals of course all have the same energy. One can therefore represent the effect of complexation on the *d* orbitals by Scheme **2-32**, where the d block of the complex is considered as defined earlier. The fivefold degeneracy of the *d* orbitals is lifted, to give three nonbonding orbitals (t_{2g}) and two antibonding orbitals (e_g).

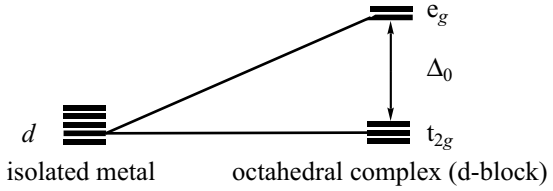

2-32

The energy separation (Δ_0) between the t_{2g} orbitals (nonbonding) and the e_g orbitals (antibonding) depends on the strength of the σ interactions between the metal and the ligands. The value of this energy gap allows us to distinguish, in the family of octahedral complexes, strong-field (large Δ_0) from weak-field complexes (small Δ_0) (see Chapter 1, § 1.6.2). Measurement of the energies of *d–d* transitions allows us to estimate the value of Δ_0 in a large number of complexes, and to establish a *spectrochemical series*, in which the ligands are ranked according to the strength of the field (value of Δ_0) that they create:

$$I^- < Br^- < Cl^- < F^- < OH^- < O^{2-} < H_2O < NH_3$$
$$< NO_2^- < CH_3^- < C_6H_5^- < CN^- < CO$$

Organometallic complexes, which contain one or several metal–carbon bonds, are thus strong-field complexes.

Comment

The value of Δ_0, and therefore the order of the ligands in the spectrochemical series, does not depend only on σ interactions. We shall see in Chapter 3 (§ 3.3.4.2) that the presence of π interactions can either decrease the value of Δ_0 ('π-donor' ligands such as I^- or Br^-) or increase it ('π-acceptor' ligands such as CN^- or CO).

2.1.3. Electronic structure

2.1.3.1. *d^6 diamagnetic complexes*

The notion that a complex is stable if all its bonding and nonbonding MO are doubly occupied is verified for many octahedral complexes. The six bonding MO, which form the six metal–ligand bonds, and the three nonbonding MO (t_{2g}) of the d block are thus doubly occupied, giving diamagnetic complexes (all the electrons are paired) with 18 electrons. As six electrons occupy the d block, the electronic configuration of these complexes is written as d^6 or $(t_{2g})^6$ (**2-33**).

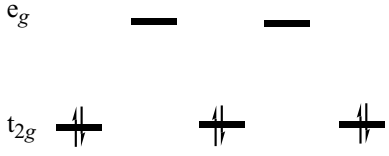

2-33

If we limit ourselves to octahedral complexes with six identical ligands that only have σ interactions with the metal (the model

studied in this chapter), examples include the complexes $[Fe(H_6)]^{4-}$, $[Ru(NH_3)_6]^{2+}$, $[Co(NH_3)_6]^{3+}$, $[Rh(NH_3)_6]^{3+}$, and $[Ir(NH_3)_6]^{3+}$ which are all 18-electron complexes, whose electronic configuration is d^6 (complexes of Fe(II), Ru(II), Co(III), Rh(III), and Ir(III), respectively). The presence of ligands that can have π-type interactions with the metal will of course modify the interaction scheme shown in Figure 2.2, but will not change it drastically. Thus, the complexes $[M(CO)_6]$ (M=Cr, Mo, W), $[Re(CO)_6]^+$, $[M(CN)_6]^{5-}$ (M=Mn, Re), $[M(CN)_6]^{4-}$ (M=Fe, Os), $[Co(CN)_6]^{3-}$, $[Mn(CNR)_6]^+$, $[Fe(CNR)_6]^{2+}$, $[M(H_2O)_6]^{3+}$ (M=Co, Rh, Ir), $[MCl_6]^{3-}$ (M=Rh, Ir) are also diamagnetic d^6 complexes. In other complexes, the presence of different ligands can, from the rigorous perspective of group theory, lower the symmetry of the complex considerably: the bond lengths are no longer all equal and the bond angles can deviate from the ideal value of 90°. However, the orbital scheme of the octahedron is essentially preserved (one may speak of 'pseudo-octahedral' symmetry), in particular as far as the main features of the d block are concerned: there are three energy levels below two, even if, within each of these groups, the strict degeneracy due to symmetry has disappeared. Complexes such as $[M(CO)_5I]^-$ (M=Cr, Mo), $[M(CO)_5Cl]$ (M=Mn, Re), $[Ru(CO)_4(Cl)(CH_3)]$, $[Ir(CO)_2(PR_3)(I)(Cl)(Me)]$, $[Mo(PR_3)_4(\eta^2\text{-}C_2H_4)_2]$, the molecular hydrogen complex $[W(PR_3)_2(CO)_3(\eta^2\text{-}H_2)]$ and even ferrocene $[Fe(\eta^5\text{-}C_5H_5)_2]$ (Chapter 1, Scheme **1-7**) are all pseudo-octahedral diamagnetic complexes, whose electronic configuration is d^6.

2.1.3.2. *Other cases*

There are octahedral complexes that have fewer than 18 electrons. d^0 complexes in which the d block is completely empty are an extreme case: examples include $[MF_6]$ complexes (M=Cr, Mo), $[WCl_6]$, $[MF_6]^-$ (M=V, Ta), $[MCl_6]^-$ (M=Ta, Nb), $[MF_6]^{2-}$ (M=Ti, Zr), $[ZrCl_6]^{2-}$, $[Mo(OMe)_6]$, and the organometallic Ti(IV) complex $[Ti(PR_3)_2(Cl)_3(CH_3)]$. These are very electron-deficient complexes, since formally there are only the *12 electrons* that form the 6 metal–ligand bonds. However, we note that the ligands usually have one or two lone pairs that are not involved in the metal–ligand bond (halide ligands, for example). These lone pairs play an important role in stabilizing complexes that apparently have too few electrons (Chapter 3, § 3.5). Another interesting case concerns complexes in which only three electrons occupy the d block (15-electron complexes whose electronic configuration is d^3). In the ground state, one electron occupies each of the orbitals in the t_{2g} group,[4] and the three electrons have parallel spin (Hund's rule). As typical examples, we mention $[Cr(NH_3)_6]^{3+}$, $[Mo(H_2O)_6]^{3+}$, $[V(H_2O)_6]^{2+}$, $[MF_6]$ (M=Rh, Ir), $[RuF_6]^-$, $[ReF_6]^{2-}$, $[MCl_6]^{2-}$

[4] Or orbitals 'derived' from the t_{2g} block when octahedral symmetry is broken by the presence of different ligands.

(M=Mn, Re), $[MoCl_6]^{3-}$ and the organometallic complexes $[V(CN)_6]^{4-}$, $[TaCl_2(dmpe)_2]$, $[MnMe_4(dmpe)]$ (dmpe=dimethylphosphino-ethane).

Two other striking aspects of the electronic structure of octahedral complexes may be noted for *weak-field* complexes (§ 2.1.2.6). In this case, the energy gap between the nonbonding (t_{2g}) and the antibonding (e_g) orbitals of the d block is small. When there are four, five, or six electrons to place in these orbitals we do *not* find them paired in the three orbitals of lowest energy. The ground state corresponds to the configuration in which as many orbitals of the d block as possible are occupied by a single electron, all with parallel spin. The exchange energy arising from this arrangement, together with the reduction of the interelectron repulsion, more than compensates the energy that is necessary to promote one or two electrons from the t_{2g} level to the e_g (Δ_0 is small). We thus obtain a 'high-spin' complex, which may be contrasted with a 'low-spin' complex in which as many electrons as possible are paired. Thus, the ground-state electronic configuration of high-spin d^5 complexes is that shown in **2-34**, with one electron in each of the five orbitals of the d block ($t_{2g}^3 e_g^2$), rather than that for the low-spin configuration shown in **2–35** (t_{2g}^5). This latter arrangement is found for strong-field d^5 complexes such as $[Mn(CN)_6]^{4-}$, $[Fe(CN)_6]^{3-}$, $[Mo(\eta^6\text{-}C_6H_6)]^{+}$, or $[Ir(Cl)_4(PR_3)_2]$. Many d^6 complexes are diamagnetic (electronic configuration $(t_{2g})^6$, § 2.1.3.1). But high-spin d^6 complexes also exist, such as $[Fe(H_2O)_6]^{2+}$ and $[CoF_6]^{3-}$, whose electronic configuration is ($t_{2g}^4 e_g^2$), with four unpaired electrons, two in the t_{2g} block and two in the e_g block. The fact that the destabilization of the antibonding levels in weak-field complexes is so small allows us to understand the existence of complexes with more than 6 electrons in the d block, that is, complexes with more than 18 electrons. As examples, we may mention the octahedral complexes $[Ni(NH_3)_6]^{2+}$ and $[Ni(H_2O)_6]^{2+}$, d^8 complexes that have 20 electrons. It is very rare to find more than 18 electrons in organometallic complexes, as these are strong-field complexes in which the antibonding orbitals are at high energy.

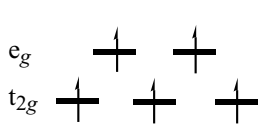

2-34 (d^5-high spin)

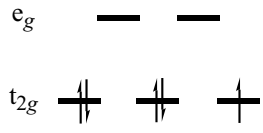

2-35 (d^5-low spin)

We shall now study other geometrical arrangements (ligand fields) that are frequently met in transition metal complexes. We shall generally limit ourselves to the characterization of the 'structure' of the d block, that is, the shape and the relative energy of the five orbitals

that make it up. Knowledge of this structure will enable us to anticipate the (or those) electronic configuration(s) that will be particularly favoured for a given family of complexes (e.g. d^6 for octahedral diamagnetic complexes). Moreover, the occupied *d* orbitals are in general the highest-energy occupied orbitals of the complex (nonbonding or weakly antibonding orbitals), and they therefore play an important role in problems linked to the geometrical structure and the reactivity of complexes (see Chapter 4).

2.2. Square-planar ML_4 complexes

In a square-planar ML_4 complex, the metal is placed in the centre of a square whose corners are occupied by the four ligands. One can therefore consider, at least formally, that a square-planar complex is formed by removing two ligands from an octahedral complex, for example, those situated on the *z*-axis (**2-36**). To establish the structure of the d block, it is convenient to start from the results already obtained for octahedral complexes.

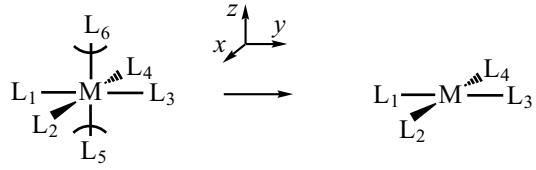

2-36

2.2.1. Characterization of the d block

We consider first the three nonbonding orbitals of the octahedron (*xy*, *xz*, and *yz*), where the representation chosen is given in Figure 2.3. These orbitals are nonbonding in the octahedron, as the coefficients for the six ligands are zero by symmetry. Removal of two of these ligands therefore has no effect on either the shape or the energy of these three orbitals, which stay pure nonbonding *d* orbitals in the square-planar complex (**2-37a–c**). The x^2-y^2 orbital is antibonding in the octahedron, because of its interactions with the four ligands in the *xy* plane. In contrast, the coefficients on the ligands located on the *z*-axis are zero by symmetry. Removal of these two ligands therefore has no influence on the shape and energy of this orbital, which remains antibonding in the square-planar complex (**2-37d**). The only *d* orbital which is modified on passing from the octahedron to the square plane is the antibonding z^2 orbital. Now the two main antibonding interactions in the octahedron concern the ligands placed on the *z*-axis. Removal of these ligands therefore leads

to a substantial stabilization of this orbital, though it remains weakly antibonding due to the small interactions with the four ligands placed in the *xy* plane (**2-37e**).

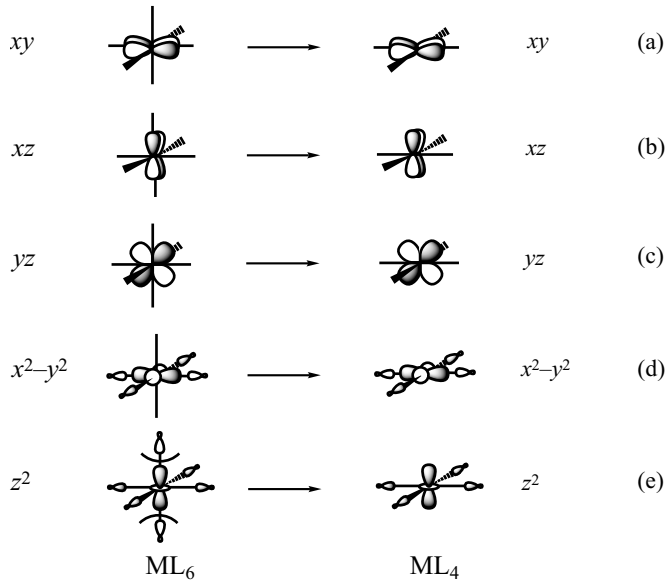

2-37

These changes in energy for the orbitals of the d block are illustrated in Figure 2.6, where the symmetry of the orbitals in the square-planar complex is also indicated (point-group symmetry D_{4h}). Notice that while the three nonbonding orbitals *xy*, *xz*, and *yz* are degenerate from the energetic point of view, only two of them (*xz* and *yz*) are degenerate by symmetry (e_g representation whose dimension is 2).

The main difference between the d blocks of octahedral and square-planar complexes concerns the number of nonbonding or weakly antibonding orbitals: there are three in the former but four in the latter.

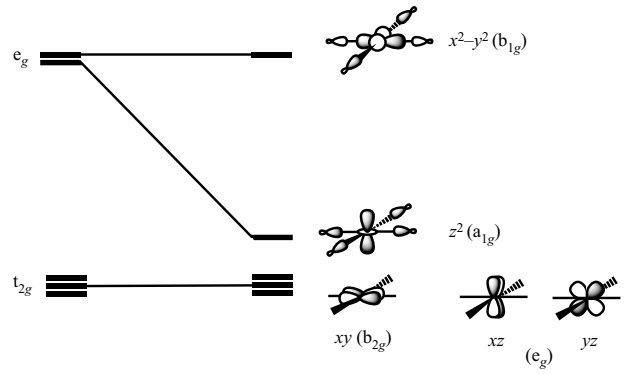

Figure 2.6. Derivation of the orbitals of the d block for a square-planar ML_4 complex from those of an octahedral ML_6 complex.

2.2.2. Electronic structure for 16-electron d^8 complexes

The favoured electronic configuration for a square-planar diamagnetic complex ML^4 involves the double occupation of the four low-energy orbitals of the d block (**2-38**). There are indeed many diamagnetic complexes with a d^8 electronic configuration, such as $[Pd(NH_3)_4]^{2+}$, $[M(CN)_4]^{2-}$ (M=Ni, Pd), $[PtCl_4]^{2-}$, $[PtHBr(PR_3)_2]$, $[AuBr_4]^-$, Vaska's complex $[Ir(CO)(Cl)(PPh_3)_2]$, and Wilkinson's hydrogenation catalyst $[Rh(Cl)(PPh_3)_3]$.

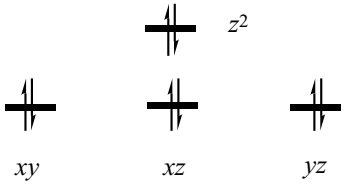

2-38

If we include the four doubly occupied MO that form the four metal–ligand bonds (these are not represented in Figure 2.6), we find that the total number of electrons in a d^8 complex is 16. But if we consult the qualitative analysis given in Chapter 1 (§ 1.6.1), it is at first sight surprising that the 18-electron rule is not respected in this family of complexes, since the bonding orbitals, the nonbonding, and the weakly antibonding orbital z^2 are all doubly occupied. This 'lack' of two electrons arises because, despite appearances, there is a nonbonding orbital on the metal that is empty. It is not an orbital from the d block, but the metal's p_z orbital whose nodal plane contains the four ligands (**2-39**). Although nonbonding, this orbital is never occupied: it is an $(n+1)p$ orbital whose energy is substantially higher (several eV) than that of an *nd* orbital.

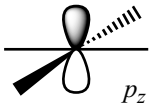

2-39

This aspect of their electronic structure means that these complexes are likely to undergo addition reactions, in which their 18-electron shell is completed by the arrival of new ligands. For example, the addition of a molecule of dihydrogen H_2 to Vaska's complex leads to the formation of an octahedral complex (**2-40**). In this addition product, the oxidation state of the metal is $+3$ (a d^6 complex), which, when the 12 electrons associated with the bonds are included, does indeed correspond to an 18-electron complex. We also note that this addition reaction is accompanied by a change in the metal's oxidation state, from $+1$ in the reactant (d^8) to $+3$ in the product (d^6). This is therefore called an *oxidative addition* reaction, since the oxidation state of the metal has increased. The reverse reaction is called *reductive elimination* (Ir(III) → Ir(I)).

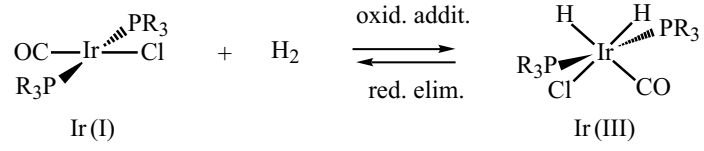

2-40

2.3. Square-based pyramidal ML_5 complexes

In an ML_5 complex which adopts a square-based pyramidal (SBP) geometry, four ligands (L_1–L_4) are located at the corners of a square which

is the base of the pyramid, while the fifth, or apical, ligand (L_5), is placed on the summit (or apex) of the pyramid (**2-41**). The metal centre may, depending on the complex, be either in the basal plane ($\theta = 90°$) (**2-41a**, § 2.3.1) or above this plane ($\theta > 90°$) (**2-41b**, § 2.3.2).

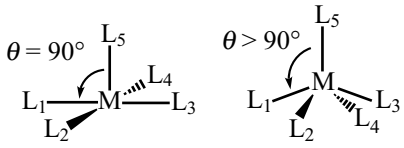

2-41a **2-41b**

2.3.1. Characterization of the d block (metal in the basal plane)

In the complex shown in **2-41a**, all the angles between the apical bond M–L_5 and the basal bonds M–$L_{1–4}$ are equal to 90°. This structure may formally be obtained by removing one of the ligands from an octahedral complex (L_6, **2-42**). We may therefore establish the MO of the d block for the SBP by starting from those that we already know for an octahedron, following the method previously used for square-planar complexes (§ 2.2.1).

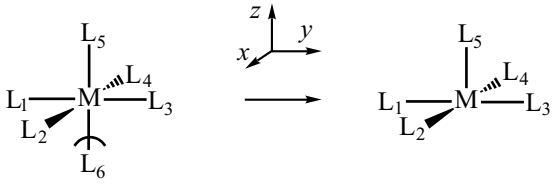

2-42

2.3.1.1. *Derivation of the d orbitals from those of the octahedron*

In the octahedral complex, the coefficients of the *xy*, *xz*, *yz*, and x^2-y^2 orbitals are zero for the ligands located on the *z*-axis (left-hand side of **2-37**). The removal of one of these ligands therefore makes no change to the shape or energy of these four orbitals: in the d block of the SBP ML5 complex, we therefore find that the three orbitals *xy*, *xz*, and *yz* are nonbonding, while x^2-y^2 is a strongly antibonding orbital. This result is just the same as that found when studying the square-planar geometry as a derivative of the octahedron (Figure 2.6). The z^2 orbital is stabilized by the elimination of one of the two antibonding interactions with the ligands placed on the *z*-axis (**2-43**). But this stabilization is not as large

as that observed when passing from an octahedral to a square-planar complex, since in this latter case, *both* the antibonding interactions along the *z*-axis are removed (Figure 2.6).

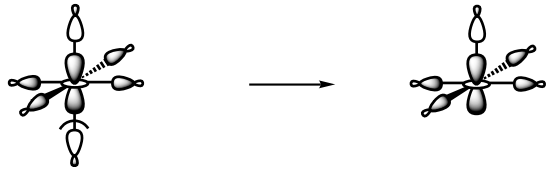

2-43

These results are shown in Figure 2.7, with the orbitals' symmetry (C_{4v} point group).

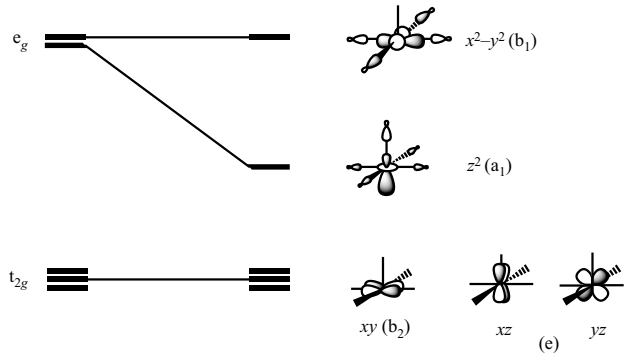

Figure 2.7. Derivation of the d-block orbitals for an ML_5 complex with an SBP geometry (the metal is in the basal plane) from those of an octahedral complex ML_6.

2.3.1.2. *Exact form of the z^2 orbital*

It appears that the shape of the z^2 orbital, as shown in Figure 2.7, is somewhat different from that indicated in **2-43**: the two lobes along the *z*-axis have different sizes, and the orbital is polarized towards the empty site of the original octahedron. The shape shown in **2-43** supposes that the only change from the original z^2 orbital of the octahedron is the removal of an antibonding interaction. But this is not the whole truth, as the symmetry is lowered from O_h to C_{4v}. The major change in fact involves the z^2 and p_z orbitals on the metal. In the octahedral complex, these two orbitals have different symmetries: for example, z^2 is symmetric with respect to the *xy* plane but p_z is antisymmetric (see **2-42** for the orientation of the axes). In the ML_5 complex, as there is only a single ligand on the *z*-axis, the xy plane is not a symmetry element for the complex. The z^2 and p_z orbitals therefore have the same symmetry (a_1, the totally symmetric representation of the C_{4v} group), with the result that they mix, giving a hybrid orbital belonging to the d block and called 'z^2'.

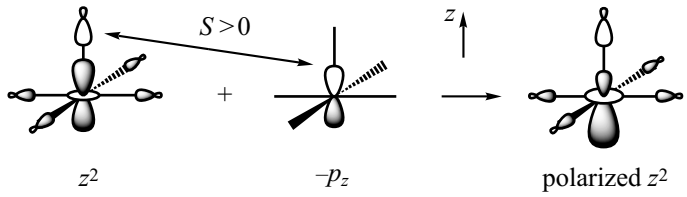

2-44

The orbital shown in **2-43** is in fact stabilized by a bonding interaction with the p_z orbital (see Appendix A). In Scheme **2-44** (left-hand side), the two orbitals are shown separated for greater clarity, but one must of course imagine that they are superposed. The way in which they must be combined to obtain a bonding mixture ($S > 0$) is not obvious, since one of the orbitals is delocalized over all the centres. We shall examine their overlap if the p_z orbital is oriented along negative z (**2-44**). It can be decomposed into three terms: (*i*) the overlap between the atomic orbitals z^2 and p_z: this term is zero since the two atomic orbitals involved are located on the same atom; (*ii*) the overlap between p_z and the orbitals on the ligands that define the base of the SBP complex: this term is also zero, since these ligands are placed in the nodal plane (xy) of p_z; (*iii*) the overlap between p_z and the orbital of the axial ligand (placed on the z-axis), which is the only non-zero term. It is clear that the choice adopted in **2-44** for the orientation of p_z leads to the overlap being positive. But how should this orbital be represented graphically? Where z is negative, the amplitudes of z^2 and p_z have the same sign, so they add. But where z is positive, they have the opposite sign, so they tend to cancel each other. The two lobes along the z-axis are therefore not equivalent, as the one along negative z is 'larger' (**2-44**, right-hand side). The participation of the p_z orbital therefore leads to a polarization of the z^2 orbital towards the vacant site of the octahedron. From the energetic point of view, this mixing stabilizes the orbital, since the polarization reduces the antibonding interaction with the axial ligand, by reducing the size of the lobe of the z^2 orbital that points towards that ligand.

2.3.2. Characterization of the d block (metal out of the basal plane)

In most SBP complexes, the metal is located above the base of the pyramid ($\theta > 90°$, **2-41b**). This geometrical deformation of the preceding structure leads to a displacement, of the same amplitude, of the ligands L_1 and L_3 in the yz plane, and of the ligands L_2 and L_4 in the xz plane (**2-45**). These movements change the shape and energy of some of the

orbitals of the d block represented in Figure 2.7. We shall consider each of these orbitals in turn.

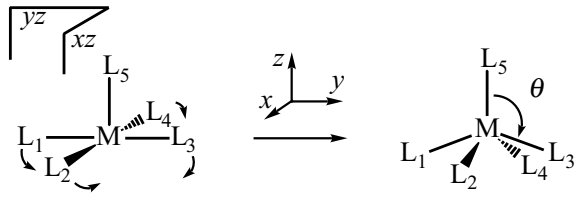

2-45

The *xy* orbital has its nodes in the *xz* and *yz* planes, the two planes in which the movements of the ligands occur. As the ligands remain located in the nodal planes, no interaction is possible with the *xy* orbital ($S = 0$), whose shape and energy are unchanged (a pure *d* orbital that is strictly nonbonding, **2-46**).

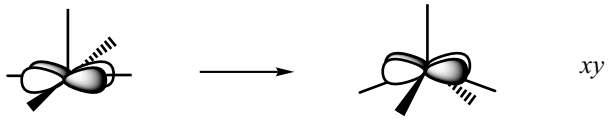

2-46

No interaction can take place between the *yz* orbital and the ligands L_2 and L_4 that stay in the nodal plane *xz* for all values of the angle θ. However, the ligands L_1 and L_3 leave the nodal plane *xy* and move into the *yz* plane in which that *d* orbital is mainly concentrated. As a result, the orbitals on the ligands L_1 and L_3 can interact with the *yz* orbital when θ is greater than 90°. The bonding combination is a low-energy orbital (an MO that represents a bond), but the antibonding combination is the new d-block orbital (**2-47**). The *yz* orbital, which is nonbonding if $\theta = 90°$, is therefore destabilized if θ is larger than 90°, its energy rising as the overlap with the ligand orbitals increases. The greatest destabilization occurs when $\theta = 135°$, the value for which the ligands L_1 and L_3 are in the region where the amplitude of the *yz* orbital is largest.

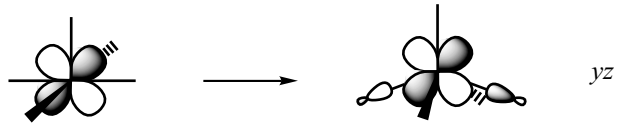

2-47

But this destabilization of the *yz* orbital is reduced by a bonding mixture with the p_y metal orbital, in a way that is exactly analogous to that described in § 2.3.1.2 for the z^2 orbital (see Appendix A). As the overlap between the *yz* and p_y orbitals on the metal is zero, a bonding interaction is obtained if the overlap between p_y and the orbitals on ligands L_1 and L_3 is positive. The appropriate combination is shown in **2-48**. If we imagine the superposition of the two orbitals represented in the left-hand part of this sketch, the grey lobe of p_y points towards the orbital on L_3 (grey lobe directed towards the metal) and the white lobe towards the orbital on L_1 (white lobe pointing towards the metal). This mixture with p_y leads to a change in the amplitude of the lobes of the *d* orbital (**2-48**). If we consider first the right-hand part of the *yz* orbital (grey lobe towards the top, white lobe towards the bottom), we must add the grey lobe p_y to it (**2-48**). As a result, the grey lobe of *yz* is enlarged (the amplitudes add) but the white lobe decreases in size (the amplitudes tend to cancel). On the left-hand side of the orbital, the opposite effect is observed: the amplitude of the white lobe increases in size, as it is added to that of the p_y orbital (white lobe pointing towards the left), while the amplitude of the grey lobe is diminished.

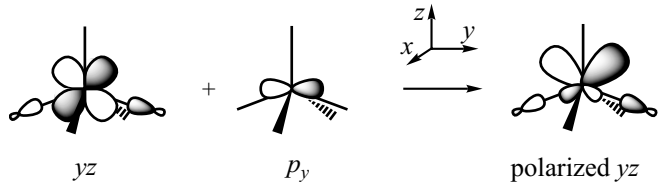

2-48

The polarization of the *yz* orbital by p_y therefore leads to a reduction in the size of the lobes pointing towards ligands L_1 and L_3, but an increase in the opposite direction (**2-48**). The antibonding character of the *yz* orbital is thereby reduced, so that in fact it becomes a *weakly antibonding* orbital which can be occupied in stable complexes.

The *xz* orbital behaves in just the same way as *yz*, but the roles of the ligands (L_1, L_3) and (L_2, L_4) are interchanged (**2-49**). It is now the mixture with the p_x orbital which polarizes *xz* in the direction opposed to the ligands L_2 and L_4. For any value of the angle θ, the *xz* and *yz* orbitals are related to each other by a rotation of 90° around the *z*-axis: they are degenerate by symmetry (e symmetry in the C_{4v} point group).

The z^2 orbital, which had antibonding interactions with all the ligands, is affected by the movement of the four basal ligands towards its nodal cone. If the angle θ is close to 125°, these ligands are even in this cone,[5] leading to zero overlap between the ligand orbitals and the z^2 orbital of the d block. For this latter orbital, the deformation that we are

[5] Since the angle of the nodal cone for z^2 is 109.5°, the corresponding value of θ is 125.25°. However, this is only an approximate value in the present situation, as the z^2 orbital is polarized by the p_z orbital.

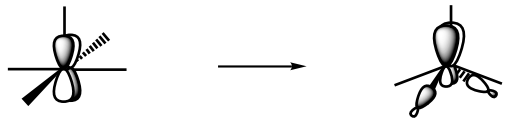

2-49

studying therefore produces a decrease, even perhaps an elimination, of the antibonding contributions on the basal ligands (**2-50**). The energy of this orbital is therefore lowered, though it remains higher than that of the nonbonding orbital xy, since there is still an antibonding interaction with the apical ligand L_5.

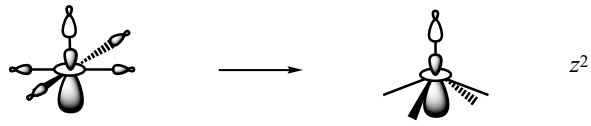

2-50

We turn last to the case of the antibonding orbital x^2-y^2 (**2-51**). An increase in the angle θ decreases the antibonding interactions with the orbitals on the four basal ligands, since these are no longer located in the regions where the amplitude of this orbital is greatest. As a result, the x^2-y^2 orbital is stabilized, by an amount which increases with the angle θ. However, this orbital remains the least stable of all the five in the d block.

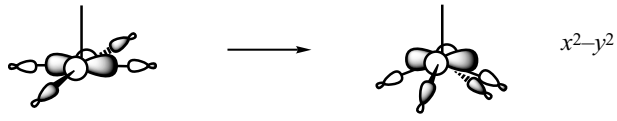

2-51

In Figure 2.8 we present a schematic correlation diagram, which shows the changes to the shape and the energy of the d-block orbitals during this geometrical deformation, as the angle θ varies from 90° to about 110°.

Comment

It must be noted that a crossing between the energy levels of the orbitals that are destabilized (xz and yz), and the z^2 orbital that is stabilized, can occur if θ becomes sufficiently large. Since these sets of orbitals have different symmetries (e and a_1, respectively), they cannot interact even if their energies are very similar or even equal (an 'allowed' energy-level crossing). The

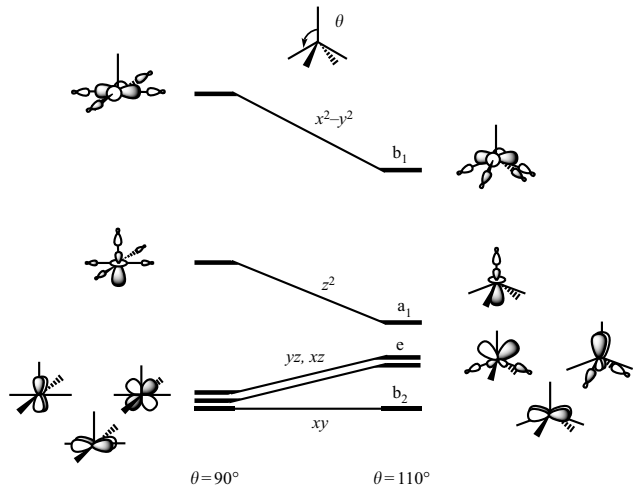

Figure 2.8. Correlation diagram for the d-block orbitals of an ML_5 complex with an SBP geometry where the angle between the apical and the basal bonds varies from 90° to about 110°.

value of the angle θ for which this crossing occurs depends on the exact nature of the metal and the ligands.

2.3.3. Electronic structure and geometry

2.3.3.1. *d^8 or d^6 diamagnetic complexes*

In the d block of ML_5 complexes which adopt an SBP geometry, there is only one strongly antibonding orbital, x^2-y^2 (Figure 2.8). The four nonbonding or weakly antibonding orbitals (xy, xz, yz, and z^2) are therefore likely to be doubly occupied, leading to diamagnetic complexes with a d^8 electronic configuration (e.g. $[Co(H)_5]^{4-}$, $[Ni(CN)_5]^{3-}$, $[Mn(CO)_5]^-$, $[Co(NCPh)_5]^+$, or $[PtI(PMe_3)_4]^+$). Including the ten electrons associated with the five bonds, these are 18-electron complexes. There are also diamagnetic complexes whose electronic configuration is d^6 (16-electron complexes), such as $[M(CO)_5]$ (M=Cr, Mo, W) or $[W(CO)_4(CS)]$. The presence of an empty low-energy orbital in the d block (the z^2 orbital, Figure 2.8) confers special properties on these complexes. They have only been isolated in rare-gas matrices, at very low temperatures, and they can easily bind a sixth ligand of the L type to give an octahedral 18-electron complex.

2.3.3.2. *Other cases*

Complexes with an intermediate electronic configuration, d^7, are also known, such as $[Mn(CO)_5]$, $[Re(CO)_5]$, $[Cr(CO)_5]^-$, and $[Co(CN)_5]^{3-}$. These are radical complexes with 17 electrons; the unpaired electron occupies the z^2 orbital. They can therefore dimerize, just like organic radicals, to form bimetallic complexes such as $[Mn_2(CO)_{10}]$, $[Re_2(CO)_{10}]$, or $[Re_2(CN)_{10}]^{6-}$, etc. For some electronic

counts, the presence of four orbitals with similar energies can favour the existence of high-spin complexes. For example, the ground-state electronic configuration of the complex $[MnCl_5]^{2-}$ (d^4) corresponds to the occupation of each of the orbitals (xy), (xz), (yz), and (z^2) by a single electron, with their spins parallel. High-spin complexes with a d^6 or d^8 electronic configuration are also known, which implies that the antibonding $x^2{-}y^2$ orbital is singly occupied. This can only happen for weak-field complexes. Deoxyhaemoglobin is a well-known example: it is a d^6 iron complex, whose electronic configuration is $(xy)^2(xz)^1(yz)^1(z^2)^1(x^2{-}y^2)^1$. We remark in closing this section that there are a few complexes, such as $[VOF_4]^-$ or $[Nb(NMe_2)_5]$, in which the d block is empty (d^0 configuration). As for the octahedral complexes, these very electron-deficient systems are only observed when the ligands possess lone pairs.

2.3.3.3. *Electronic count and geometry*

Correlation diagrams for the d-block orbitals, of the type shown in Figure 2.8, are often used to interpret the changes in the structures of complexes as a function of their electronic configuration d^n. In order to use them, one adopts the hypothesis, which in most cases is verified a posteriori, that the geometry of the complex is controlled by the *energy changes of the highest-occupied molecular orbital (the HOMO rule)*. ML_5 complexes with an SBP geometry provide an interesting illustration of this rule.

Comment

The structures observed for complexes whose electronic configuration is d^0 (d-block empty) are characterized by values of the angle θ greater than 90° (metal above the basal plane). This preference, which is caused by bonding orbitals in the complex, can, as we shall see, be either modified or maintained when there are electrons in the d block.

We consider first a diamagnetic d^6 complex. In the structure with $\theta = 90°$, three nonbonding orbitals (xy, xz, and yz) are doubly occupied (Figure 2.8). An increase in the value of θ above 90° leads to a destabilization of two of these orbitals (xz and yz), which is energetically unfavourable (Figure 2.8). We may therefore predict that these complexes will adopt a structure in which the metal stays in the basal plane ($\theta = 90°$). Experimental values for these complexes are indeed close to 90° (91–94° for the $[M(CO)_5]$ complexes if M=Cr, W). But in a d^8 diamagnetic complex, the two additional electrons occupy the z^2 orbital, which is stabilized when θ increases above 90° (Figure 2.8). Application of the HOMO rule leads to the prediction that in these complexes, the

metal will be located above the basal plane. This change in geometry due to the number of d electrons is indeed observed: the angle θ is 101.0° in $[Ni(CN)_5]^{3-}$ and 102.6° in $[Mn(CO)_5]^-$.

In the light of this analysis, we present the energy levels and orbital occupations for the d block of d^6 and d^8 diamagnetic complexes in Scheme **2-52**.

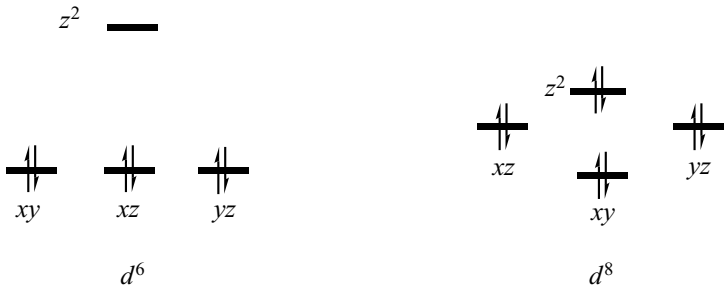

2-52

We can extend this analysis to other electron counts. In d^7 complexes, the z^2 orbital is singly occupied. We may therefore expect to find that θ is larger than 90°, but not as large as in the low-spin d^8 complexes in which this orbital is doubly occupied. The values of θ for d^7 complexes are indeed often intermediate between those found for low-spin d^6 and d^8 complexes: about 95° for $[Mn(CO)_5]$, $[Re(CO)_5]$, or $[Cr(CO)_5]^-$, 97.6° for $[Co(CN)_5]^{3-}$.

For a given number of electrons, the change from a low-spin to a high-spin complex can also lead to a change in geometry, since the HOMO is different. In a diamagnetic d^6 complex, whose electronic configuration is $(xy)^2(xz)^2(yz)^2$, we have seen that the angle θ is close to 90°. However, in a high-spin d^6 complex, whose electronic configuration is $(xy)^2(xz)^1(yz)^1(z^2)^1(x^2{-}y^2)^1$, the HOMO, $x^2{-}y^2$, is strongly stabilized by an increase in θ (Figure 2.8), thereby favouring a displacement of the metal out of the basal plane. This is exactly what is observed in deoxyhaemoglobin (a high-spin complex of Fe(II)), where the iron atom is placed well above the plane ($\theta = 110°$) defined by the porphyrin ring (a ligand of L_2X_2 type).

2.4. Tetrahedral ML_4 complexes

In a complex of this type, the metal is placed at the centre of a tetrahedron whose vertices are occupied by the four ligands. There are at least two ways to derive the d-block orbitals for a tetrahedral complex. In the 'direct' method, we allow the d orbitals of the metal to interact with the symmetry-adapted combination of ligand orbitals (Chapter 6, § 6.6.2.2

and Exercise 2.11), taking account of their symmetry properties in the T_d group. We may also start from the *d* orbitals of a square-planar complex and study their changes as the ligands are moved towards the tetrahedral geometry. We shall use the second approach here, as it not only gives us the d-block structure for a tetrahedral complex, but it also yields the orbital correlation diagram linking the two geometries most frequently found for ML_4 complexes.

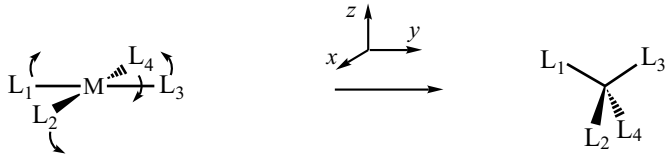

2-53

The change from one structure to the other is studied following the mechanism described in Scheme **2-53**, where the ligands L_1 and L_3 move upwards in the *yz* plane, and the ligands L_2 and L_4 downwards in the *xz* plane. In this way, we change from a square-planar (D_{4h} symmetry) to a tetrahedral complex (T_d symmetry), maintaining D_{2d} symmetry at intermediate points.

Comment

This is not the only way to move from one structure to the other. One can, for example, rotate one ML_2 unit by 90° with respect to the other, progressively adjusting the values of the bond angles (D_2 symmetry is conserved).

2.4.1. Characterization of the d block

We shall consider each of the five *d* orbitals of a square-planar complex as they are presented in Figure 2.6 (right-hand side). On moving to the tetrahedral structure, the *xy* orbital stays unchanged in both shape and energy (**2-54a**), as the four ligands move in one or other of the two nodal planes of this orbital (L_2 and L_4 in *xz*, L_1 and L_3 in *yz*). The *yz* and *xz* orbitals behave in just the same way as they do when the metal moves out of the basal plane in SBP ML_5 complexes (§ 2.3.2). On passing from the square plane to the tetrahedron, two ligands move in the plane where the amplitude of the orbital is greatest, but the other two ligands stay in one of the nodal planes. As a result, the *yz* orbital is destabilized by antibonding interactions with the ligands L_1 and L_3, but it has no interaction with L_2 and L_4 which are still located in the nodal plane *xz* (**2-54b**). In the same way, the *xz* orbital is destabilized by an interaction with the ligands L_2 and L_4 (**2-54c**). These two orbitals, *yz*

and xz, which were nonbonding in a square-planar complex, therefore become antibonding in a tetrahedral complex, while staying degenerate. However, just as in ML_5 complexes (§ 2.3.2), the antibonding interactions are reduced by mixing with a p orbital on the metal (p_y in the case of yz, p_x for xz) which polarizes the d orbital in the direction opposite to that of the two ligands with which it is interacting (**2-54b**) and see also Appendix A). The z^2 orbital becomes rigorously nonbonding (zero coefficients on the ligands, **2-54d**), and thus at the same energy as the xy orbital, since the four ligands in the tetrahedral structure are moved precisely on to its nodal cone (whose angle is exactly equal to 109.5°). The last orbital, x^2-y^2, is strongly stabilized since the four ligands leave the x- and y-axes on which they were located. The antibonding interactions are decreased but not eliminated, since in the tetrahedral structure, the ligands are not in the nodal planes of the x^2-y^2 orbital (**2-54e**).

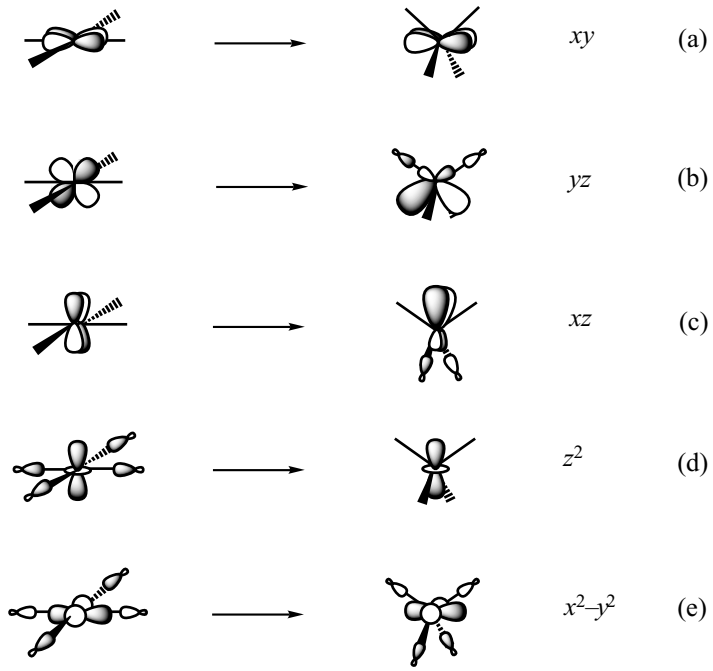

2-54

This analysis enables us to describe fully the structure of the d block of a tetrahedral complex: there are two degenerate nonbonding orbitals (xy and z^2), two degenerate antibonding orbitals (xz and yz), and a third antibonding orbital, x^2-y^2. The only remaining uncertainty concerns the relative energies of the (xz, yz) and x^2-y^2 antibonding orbitals. The answer to this question is found in the character table for the tetrahedral point group, T_d (Table 2.2).

Table 2.2. Character table for the T_d group (tetrahedral ML_4 complex)

T_d	E	$8C_3$	$3C_2$	$6S_4$	$6\sigma_d$		
A_1	1	1	1	1	1		$x^2+y^2+z^2$
A_2	1	1	1	−1	−1		
E	2	−1	2	0	0		$(2z^2-x^2-y^2, x^2-y^2)$
T_1	3	0	−1	1	−1		
T_2	3	0	−1	−1	1	(x,y,z)	(xy, xz, yz)

Inspection of the last column shows that the five *d* orbitals are found in two groups of degenerate orbitals, of e (doubly degenerate) and t_2 (triply degenerate) symmetry, respectively. As we have already shown that there are just two nonbonding orbitals, it is clear that they must have e symmetry. The antibonding orbitals therefore have t_2 symmetry, and all three are degenerate by symmetry. The d block of the tetrahedron therefore contains two nonbonding degenerate orbitals (e) and three antibonding orbitals that constitute another degenerate set (t_2).

Comment

We note that the roles of *xy* and x^2-y^2 orbitals are interchanged in a tetrahedral complex, depending on whether we adopt the analysis developed above (*xy* nonbonding (**2-54a**), x^2-y^2 antibonding (**2-54e**)), or the character table (x^2-y^2 degenerate with z^2, therefore nonbonding, *xy* degenerate with *xz* and *yz*, therefore antibonding). This arises simply from a different definition of the axes (a rotation of 45° around the *z*-axis) which interchanges the role of the *xy* and x^2-y^2 orbitals, as we have already seen in the case of the octahedron (Figures 2.3 and 2.4) or the square-planar complex plan (see Exercise 2.4).

We can now sketch the correlation diagram linking the d-block orbitals of a square-planar complex to those of a tetrahedron (Figure 2.9), following the deformation shown in **2-53**.

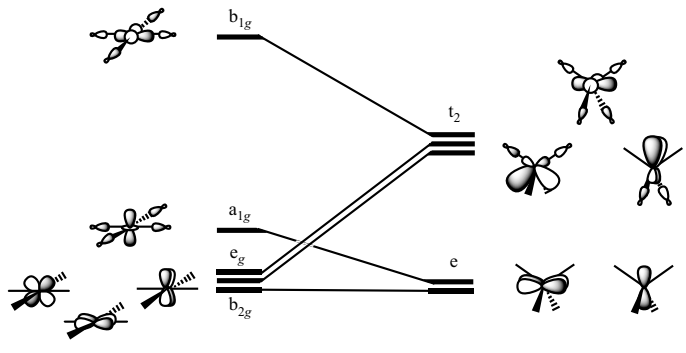

Figure 2.9. Correlation diagram linking the d-block orbitals of a square-planar ML_4 complex and those of a tetrahedral ML_4 complex, following the deformation shown in **2-53**.

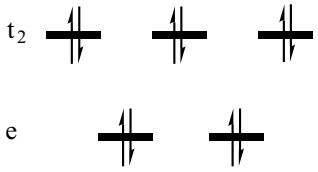

d^{10}

2-55

2.4.2. Electronic structure

2.4.2.1. *d^{10} diamagnetic complexes*

The separation between the e and t_2 levels of the d block is sufficiently small (the t_2 orbitals are only weakly antibonding) that all five orbitals can be occupied. Diamagnetic complexes with a d^{10} electronic configuration are thus obtained (**2-55**), such as $[Ni(H)_4]^{4-}$, $[Ni(CO)_4]$, $[M(PF_3)_4]$ (M=Ni, Pd), [Pt(dppe)2] (dppe=diphenylphosphinoethane), $[Ni(CN)_4]^{4-}$, $[Co(CO)_4]^{-}$, $[Fe(CO)_4]^{2-}$, $[Cu(CN)_4]^{3-}$, $[Cu(PMe_3)_4]^{+}$, $[Ag(PPh_3)_4]^{+}$, or $[Zn(Cl)_4]^{2-}$. These are 18-electron complexes, since eight additional electrons are associated with the four metal–ligand bonds.

2.4.2.2. *Other cases*

ML_4 complexes whose d block is empty (d^0 electronic configuration), such as $[TiCl_4]$ and $[MnO_4]^{-}$, also adopt a tetrahedral geometry. As in the examples of d^0 complexes already mentioned (§ 2.1.3.2 and 2.3.3.2), the ligands have lone pairs which play an important role in the stabilization of these species that apparently are strongly electron-deficient (formally, only eight electrons around the metal!). We may also mention tetrahedral d^8 complexes, such as $[NiCl_4]^{2-}$, $[Ni(PPh_2Et)_2Br_2]$, or $[CoBr(PR_3)_3]$. The structure of the d block, with the three t_2 degenerate orbitals, leads to a paramagnetic ground state ($e^4t_2^4$), with two unpaired electrons in the t_2 orbitals (a high-spin tetrahedral complex, right-hand side of **2-57**).

2.4.3. ML_4 complexes: square-planar or tetrahedral?

Not all ML_4 complexes have a square-planar or tetrahedral structure. 'Intermediate' geometries, of lower symmetry, can be observed (e.g. $[Fe(CO)_4]$ is a high-spin d^8 complex with C_{2v} symmetry, see § 2.8.3). However, a large number of ML_4 complexes adopt, either exactly or with only small deviations, one or other of these high-symmetry geometries. In this paragraph, we shall show how a knowledge of the d block for each type of structure (§ 2.2.1 and 2.4.1) enables us to establish a link between the d^n electronic configuration of the complex and the geometry that is observed experimentally. We shall concentrate our attention on the d^{10} and d^8 electronic configurations, which are the most common for ML_4 complexes.

It is straightforward to understand the structural preference for d^{10} complexes: in the tetrahedral geometry, all five d orbitals are low in energy and can thus receive ten electrons, whereas there are only four low-energy d orbitals in the square-planar geometry

(Figure 2.9). Complexes with a d^{10} electronic configuration therefore adopt a tetrahedral structure (§ 2.4.2.1).[6]

[6] The tetrahedral geometry is also favoured by the bonding MO, lower in energy than the d block, as shown by the experimental structures of d^0 complexes (§ 2.4.2.2) which have tetrahedral geometries.

In diamagnetic d^8 complexes (low-spin), four d orbitals must be doubly occupied. This count is ideal for the square-planar geometry, characterized by four low-energy d orbitals (three strictly nonbonding, one very weakly antibonding (**2-56**, left-hand side)), well separated from the fifth which is strongly antibonding. The situation is less favourable for the tetrahedral geometry: first, there are only four nonbonding electrons instead of six, and second, the distribution of four electrons in three orbitals (**2-56**, right-hand side) is energetically unfavourable since it does not obey Hund's rule (two electrons should occupy two different orbitals, with *parallel spins*). In summary, the d-block of a tetrahedral complex is not well suited to accomodate four pairs of electrons, and in fact diamagnetic d^8 complexes adopt a square-planar geometry ($[Ni(CN)_4]^{2-}$, $[Pd(NH_3)_4]^{2+}$, $[RhCl(PPh_3)_3]$, or $[Ir(CO)(Cl)(PPh_3)_2]$, for example).

Square-planar (d^8 low-spin) Tetrahedral (d^8 low-spin)

2-56

This leads us naturally to consider the case of paramagnetic d^8 complexes (high-spin), that have two unpaired electrons with parallel spin. The situation is now favourable for the tetrahedral geometry: Hund's rule is obeyed, and the occupied d orbitals are either nonbonding or only weakly antibonding (**2-57**, right-hand side). In contrast, in the square-planar geometry, an electron must be placed in the strongly antibonding orbital of the d block (**2-57**, left-hand side). The tetrahedral structure is therefore favoured for high-spin d^8 complexes (§ 2.4.2.2). As a consequence, the low-spin → high-spin change in d^8 ML_4 complexes is accompanied with a change in geometry, from square-planar to tetrahedral.

It is more difficult to predict whether a given complex with a d^8 electronic configuration will be low-spin, with a square-planar structure, or high-spin, with a tetrahedral structure. From a purely electronic point of view, the square-planar geometry seems to be favoured, with six nonbonding and two weakly antibonding electrons, instead of four nonbonding and four more strongly antibonding electrons in the tetrahedron (**2-58**). However, in this latter structure, the exchange energy due to the two unpaired electrons is a favourable factor. Steric factors

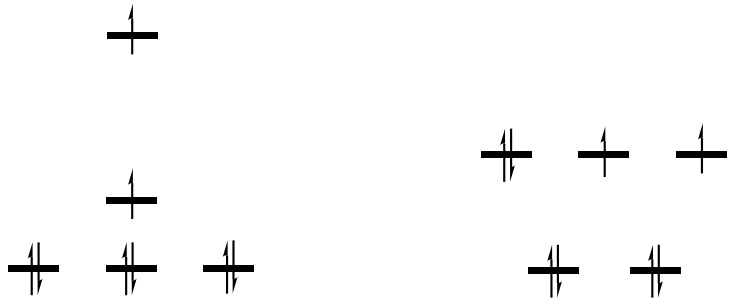

2-57 Square planar (d^8 high-spin) Tetrahedral (d^8 high-spin)

also play an important role, since they favour the tetrahedral structure, with bond angles of 109.5° rather than the square-planar arrangement with 90° bond angles. So complexes with very bulky ligands (triphenylphosphine, PPh_3, for example), are usually high-spin and tetrahedral. But the balance between all these factors seems to be quite subtle, since the complex $[Ni(PPh_2Et)_2Br_2]$ has been isolated in both forms, square-planar and tetrahedral; they are found to be in equilibrium in solution and are thus *very* close in energy.

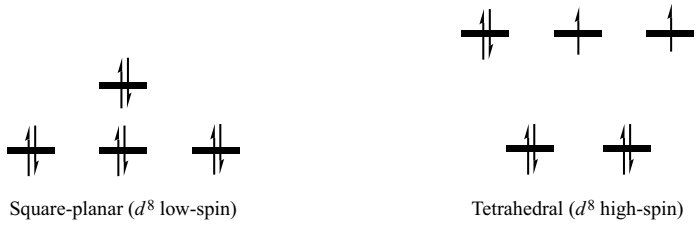

2-58 Square planar (d^8 low-spin) Tetrahedral (d^8 low-spin)

As we have already remarked at the beginning of this section, not all ML_4 complexes adopt such high-symmetry structures. In this context, d^9 complexes, whose electronic configuration is 'intermediate' between one which favours a square-planar geometry (diamagnetic d^8 complexes) and others which favour a tetrahedral geometry (paramagnetic d^8 or diamagnetic complexes d^{10}), are particularly interesting. The two structural types are indeed found in the family of d^9 ML_4 complexes: for example, square-planar for $[M(py)_4]^{2+}$ (M=Cu, Ag) (py=pyridine) but quasi-tetrahedral for $[Co(CN)_4]^{4-}$, $[Co(PMe_3)_4]$, and $[Ni(PR_3)_3X]$ (X=Cl, Br, I). A given complex can even adopt very different geometries depending on its environment. For example, 131 structures of the $[CuCl_4]^{2-}$ anion have been published,[7] which differ in the nature of the associated cation. The whole range of geometries has in fact been observed, from the square plane to an almost ideal tetrahedron!

[7] S. Keinan and D. Avnir *Inorg. Chem. 40*, 318 (2001).

2.5. Trigonal-bipyramidal ML_5 complexes

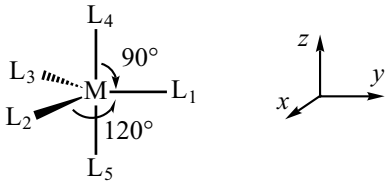

2-59

In an ML_5 complex which adopts a trigonal-bipyramidal (TBP) geometry, we distinguish the *equatorial* ligands (L_1, L_2, and L_3) from those in *axial* positions (L_4 and L_5, **2-59**). The former are located at the vertices of the triangular base of the bipyramid, and they define the equatorial plane of the complex (the *xy* plane in **2-59**), while the axial ligands are located at the vertices of the bipyramid. The angles between equatorial bonds are 120° (trigonal base), but those between an equatorial and an axial bond are 90°.

Comment

The equatorial and axial ligands are not equivalent by symmetry, since no symmetry operation of the complex's point group (D_{3h}) interchanges an equatorial ligand with an axial. Nor are they equivalent from a chemical point of view, and as a consequence, the M–L_{eq} and M–L_{ax} bond lengths can differ, even when all the ligands L are identical.[8]

[8] For this geometrical parameter, the difference appears to be so small that it can depend on the environment! For example, in the solid-state structure of $[Fe(CO)_5]$ determined by X-ray diffraction, the axial bonds are slightly longer than the equatiorial, by about 0.008 Å (D. Braga, F. Grepioni, and G. Orpen *Organometallics 12*, 1481 (1993)). But a study of the structure in the gas phase, by electron diffraction, gives the opposite result, with the equatorial bonds being longer by 0.01–0.03 Å (B. W. McClelland, A. G. Robiette, L. Hedberg, and K. Hedberg *Inorg. Chem. 40*, 1358 (2001)).

2.5.1. Characterization of the d block

With the orientation of the axes chosen in **2-59**, the equatorial ligands are located in the *xy* plane and the axial ligands on the *z*-axis, that is, at the intersection of the *xz* and *yz* planes.

The five ligands are thus placed in one or other of the nodal planes of the *xz* (nodal planes *xy* and *yz*) and *yz* (nodal planes *xy* and *xz*) orbitals. As a result, there cannot be any σ interaction between the ligands and these two orbitals which stay nonbonding in the d-block of a TBP complex (**2-60**). By consulting the character table for the D_{3h} point group, we find that these two degenerate orbitals have e″ symmetry.

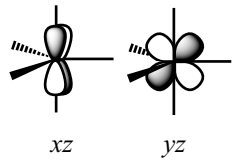

2-60

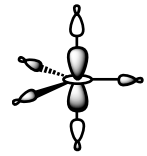

2-61

A third orbital in the d block may readily be characterized. The z^2 orbital is destabilized by antibonding interactions with all five ligands. This is the highest-energy orbital in the d block, with the strongest antibonding interactions involving the axial ligands along the *z*-axis (**2-61**).

The xy and x^2-y^2 orbitals have not yet been considered. The first is destabilized by antibonding interactions with the ligands L^2 and L^3 (**2-62**). No interaction is possible with the three other ligands which are located in the nodal plane yz. For the x^2-y^2 orbital, its two nodal planes bisect the x- and y-axes and they contain the z-axis. It therefore cannot interact with the axial ligands placed on this axis, but antibonding interactions will develop with the three equatorial ligands, as none of them is located in either of the nodal planes. Two representations can be given for this orbital (**2-63**). In the first (**2-63a**), the orientation of the axes is the same as that used previously, whereas in the second (**2-63b**), the plane of the page is chosen as the equatorial plane (xy). This second representation allows us to understand more easily the sign of the coefficients for the orbitals on the ligands L_2 and L_3 if the interaction with x^2-y^2 is to be antibonding (the sign for the orbital σ_1, on the ligand L_1, is obvious since it points along the y-axis). It is clear from **2-63b** that the overlap between the orbitals σ_2 and σ_3 and the part of the x^2-y^2 orbital concentrated along the horizontal axis (y) is positive, whereas with the part of the orbital concentrated along the vertical axis (x) it is negative. Now since the angle L_2–M–L_3 is 120°, the M–L_2 and M–L_3 bonds are closer to the x-axis than to the y-axis. The representation given in **2-63** therefore does indeed correspond to a negative value of the *total* overlap between the orbitals on the ligands L_2 and L_3 and the x^2-y^2 orbital on the metal centre, and thus to an antibonding interaction.

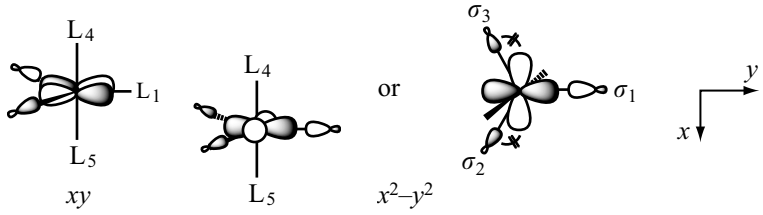

2-62 **2-63a** **2-63b**

It should be noted that the antibonding M–L_i character in this orbital is not equivalent for the three ligands. L_1 is situated on the y-axis and therefore has a larger axial overlap than do the ligands L_2 and L_3, which are placed between the x- and y-axes. Moreover, the coefficient for σ_1 is twice as large as those for σ_2 or σ_3 (Chapter 6, § 6.6.4.2). These two factors lead to the x^2-y^2 orbital being antibonding mainly with the ligand L_1, but xy is antibonding only with the ligands L_2 and L_3 (**2-62**). While this analysis enables us to deduce that the xy and x^2-y^2 orbitals are both antibonding in the d block, an important additional piece of information is provided by examination of the character table for the D_{3h} group (Table 2.3). From the last column, we learn that the xy and x^2-y^2 orbitals are *degenerate by symmetry* (e′ symmetry).[9]

[9] The linear combinations of the ligand orbitals with which they interact also have e′ symmetry, of course (see Chapter 6, § 6.6.4).

Table 2.3. Character table for the D_{3h} group

D_{3h}	E	$2C_3$	$3C_2$	σ_h	$2S_3$	$3\sigma_v$		
A_1'	1	1	1	1	1	1		x^2+y^2, z^2
A_2'	1	1	−1	1	1	−1		
E'	2	−1	0	2	−1	0	(x, y)	(x^2-y^2, xy)
A_1''	1	1	1	−1	−1	−1		
A_2''	1	1	−1	−1	−1	1	z	
E''	2	−1	0	−2	1	0		(xz, yz)

The orbitals shown in **2-62** and **2-63** therefore make up a set of two degenerate orbitals, of e′ symmetry. Their energy is of course higher than that of the e″ orbitals (xz and yz), since these latter are strictly nonbonding.

The character table also shows that the p_x and p_y orbitals on the central atom, like xy and x^2-y^2, have e′ symmetry (penultimate column). They can therefore lead to the formation of polarized degenerate e' orbitals in the d block, as their contribution *polarizes* the xy and x^2-y^2 orbitals. A more accurate shape of these orbitals can be obtained by adding a p_x contribution to xy (**2-64**) and p_y to x^2-y^2 (**2-65**), so that the overlap of the p orbital with the ligand orbitals is positive (see Appendix A, § 2.2). The addition of p_x to the xy orbital polarizes this orbital in the direction away from the ligands L_2 and L_3, thereby decreasing the antibonding interactions with these ligands (**2-64**). For x^2-y^2, the polarization by p_y decreases the amplitude of the orbital in the direction away from the ligand L_1 (**2-65**) with which the antibonding interaction was the strongest. As in the examples that we have already studied (see § 2.3.1.2 and 2.3.2 for SBP ML_5 complexes), the participation of the p orbitals leads to a reduction of the antibonding character of the d-block orbitals.

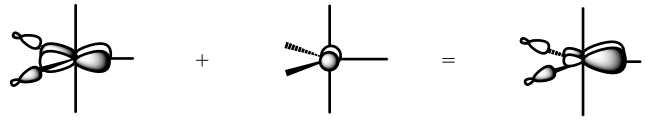

xy *px* polarized *xy*

2-64

x^2–y^2 $-p_y$ polarized x^2–y^2

2-65

The d block of an ML_5 complex with a TBP geometry is therefore made up of two degenerate nonbonding orbitals (*xz* and *yz*, with e″ symmetry), two degenerate orbitals that are fairly weakly antibonding (*xy* and x^2-y^2, with e′ symmetry) and one very strongly antibonding orbital (z^2, with a_1' symmetry).

These results are illustrated in Figure 2.10 for two different orientations of the bipyramid, the equatorial plane (*xy*) being either perpendicular to the plane of the page (left-hand side) or in this plane (right-hand side).

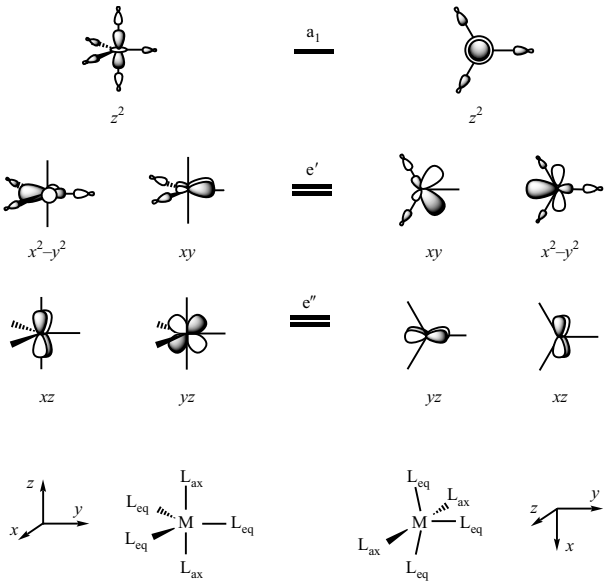

Figure 2.10. Representation of the d-block orbitals for an ML_5 complex with a TBP geometry, the equatorial plane (*xy*) being either perpendicular to the plane of the page (left-hand side), or in this plane (right-hand side). In this latter case, for greater clarity, the axial ligands are not shown.

2.5.2. Electronic structure

2.5.2.1. *Diamagnetic d^8 complexes*

The most common electron count for ML_5 complexes with a TBP geometry is d^8, which corresponds to the double occupation of the degenerate e″ and e′ orbitals (**2-66**). These are therefore 18-electron complexes, since there are 10 additional electrons associated with the five M–L bonds.

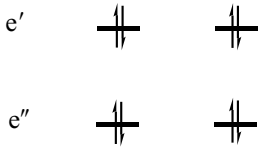

2-66

The species $[M(CO)_5]$ (M=Fe, Ru, and Os) are 'archetypal' TBP ML_5 complexes. We may also cite the complexes $[Mn(CO)_5]^-$, $[Fe(CO)_4(\eta^2\text{-}C_2H_4)]$, $[Fe(CO)_4(CN)]^-$, $[Co(C{=}N-CH_3)_5]^+$, $[Ir(PR_3)_3(CH_3)(\eta^2\text{-}C_2H_4)]$, and $[Ni(P(OEt)_3)_5]^{2+}$. It should be noted that the d^8 electron count has already been found to be favourable for ML_5 complexes that adopt an SBP geometry, with the metal above the basal plane (§ 2.3.3.1.). The two structural types have indeed been characterized in the d^8 — ML_5 family of complexes.[10] In the case of the

[10] For a review of the structures of ML_5 complexes, consult: S. Alvarez and M. Llunell *J. Chem. Soc. Dalton Trans.* 3288 (2000).

anion $[Ni(CN)_5]^{3-}$, the SBP structure can even coexist with a slightly distorted TBP structure when the associated cation is $[Cr(en)_3]^{3+}$ (en=ethylenediamine).[11]

[11] The transformation TBP(1) → SBP → TBP(2) is nothing more than the Berry pseudorotation which allows the exchange of axial and equatorial ligands to take place in a TBP complex.

2.5.2.2. *Other cases*

The complex $[Co(dpe)_2Cl]^{2+}$ (dpe=1,2-bis(diphenylphosphino) ethane) with a d^7 electronic configuration (a 17-electron low-spin complex) is also known in two structural forms: a red isomer with an SBP geometry (the chloride ligand is in the apical position), and a green isomer with a TBP geometry (the chloride ligand is in an equatorial position). TBP complexes with more than 18 electrons are also known. They are weak-field complexes (the z^2 orbital is occupied) with a d^9 electronic configuration (19 electrons), such as $[CuCl_5]^{3-}$, $[CuBr_5]^{3-}$, or $[Cu(imidazole)_3Cl_2]$, or d^{10} (20 electrons), such as $[CdCl_5]^{3-}$ or $[HgCl_5]^{3-}$.

2.6. Trigonal-planar ML_3 complexes

A trigonal-planar ML_3 complex can be formed by removing the two axial ligands from a TBP ML_5 complex (**2-67**). The d-block orbitals may therefore be readily deduced from those established in the preceding section.

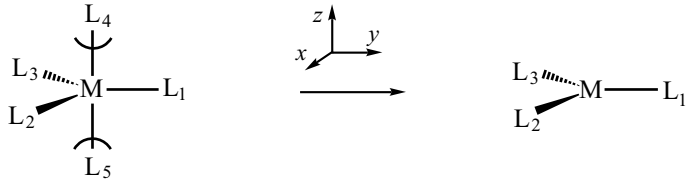

2-67

2.6.1. Characterization of the d block

The variations in energy for the five *d* orbitals are shown in Figure 2.11. The *xz* and *yz* orbitals (e″) of a TBP ML_5 complex have zero coefficients on the axial ligands, as do *xy* and x^2-y^2 (e′). The removal of these two ligands does therefore not change either the shapes or the energies of these four orbitals (Figure 2.11). But the z^2 orbital, which was strongly antibonding due to interactions with the axial ligands, is substantially stabilized by their removal, becoming almost nonbonding. Only three weak antibonding interactions with the ligands in the *xy* plane are left, and the amplitude of the z^2 orbital in this plane is small. Note that the orbital symmetries are the same in ML_5 (TBP) and ML_3 trigonal-planar complexes, as both have D_{3h} symmetry.

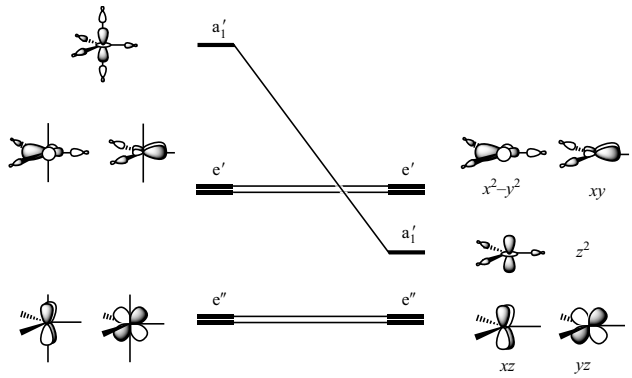

Figure 2.11. Derivation of the d-block orbitals for a trigonal-planar ML_3 complex from those of an ML_5 complex with a TBP geometry.

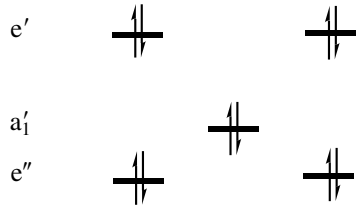

2-68

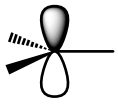

2-69

2.6.2. 16-electron d^{10} complexes

The d-block for ML_3 complexes with a trigonal-planar geometry thus contains two nonbonding degenerate orbitals (*xz* and *yz*), a very weakly antibonding orbital (z^2), and two weakly antibonding degenerate orbitals (*xy* and x^2-y^2). These five orbitals are sufficiently low in energy to be doubly occupied. As a result, the large majority of these complexes have a d^{10} electronic configuration (**2-68**), the simplest no doubt being $[PdH_3]^{3-}$. We may also cite the tricarbonyl complexes $[M(CO)_3]$ (M–Ni, Pd, or Pt), as well as $[Pt(Ph_3P)_3]$, $[Pt(\eta^2\text{-ethylene})(PR_3)_2]$, or $[Ni(\eta^2\text{-ethylene})_3]$, complexes in which the oxidation state of the metal is zero. There are also complexes of the metals from groups 11 (oxidation state I), such as $[Cu(CN)_3]^{2-}$, $[Cu(SR)_3]^{2-}$, or $[Au(PPh_3)_2Cl]$, and 12 (oxidation state II), such as $[HgI_3]^-$ and $[Hg(SR)_3]^-$.

These are all 16-electron complexes (six for the bonds and ten in the d block). The 'lack' of two electrons compared to the 18-electron rule arises because a nonbonding orbital on the metal remains empty. As in the case of square-planar ML_4 complexes, this is the *p* orbital perpendicular to the molecular plane (**2-69**), which, although nonbonding, is too high in energy to be occupied.

2.7. Linear ML_2 complexes

There are many ways in which a linear ML_2 complex may be obtained from the complexes already studied. For example, four coplanar ligands can be removed in an octahedral complex (**2-70**).

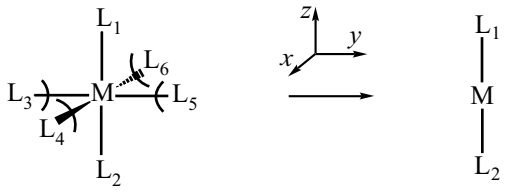

2-70

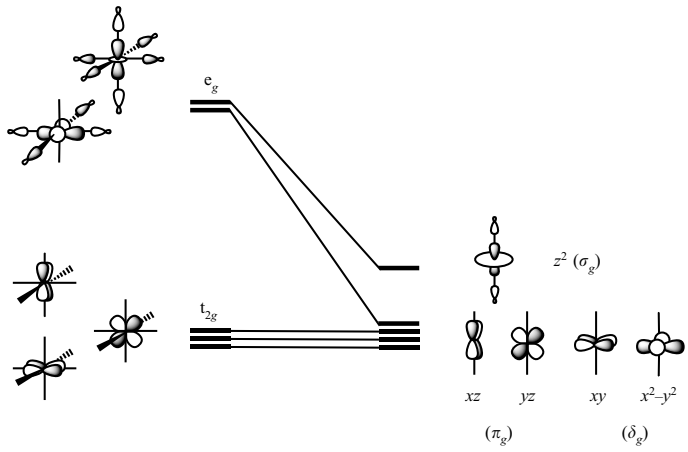

Figure 2.12. Derivation of the d-block orbitals for a linear ML_2 complex from the d orbitals of an octahedral ML_6 complex.

2.7.1. Characterization of the d block

Consider the orbitals in the d block of an octahedron (Figure 2.12, left-hand side). Removal of the four ligands L_3–L_6 has no effect on the three nonbonding t_{2g} orbitals which have zero coefficients on all the ligands. The antibonding x^2-y^2 orbital in the e_g block has antibonding interactions with the four ligands L_3–L_6, but zero coefficients on L_1 and L_2. After the removal of the ligands L_3–L_6, this orbital becomes strictly nonbonding (Figure 2.12). There are, therefore, four nonbonding orbitals in the d block of linear ML_2 complexes, whose symmetries are π_g (xz, yz) and δ_g (x^2-y^2, xy) in the $D_{\infty h}$ point group. These orbitals are therefore degenerate in pairs by symmetry, but in fact all four have the same energy (accidental degeneracy).

Comment

Notice that the π-type orbitals have just a single nodal plane that contains the internuclear axis, whereas the δ orbitals have two.

We have not yet considered the second orbital in the e_g block of the octahedron, z^2. It is stabilized by the elimination of the four weak antibonding interactions in the xy plane, but this stabilization should be rather small, as the two principal antibonding interactions, along the z-axis, are still present.

In fact, this fifth orbital is not very high in energy since it is polarized by mixing with the s orbital of the metal (s and z^2 have the same symmetry, σ_g, in the $D_{\infty h}$ point group). As in the previous examples which involved polarization by a p orbital (see also Appendix A, § 2.A3), the sign of the s orbital is such that its interaction with the ligand orbitals is bonding (**2-71**). The effect of this mixing is to increase the amplitude of the z^2 orbital in the xy plane, perpendicular to the internuclear axis, and to decrease it along this axis. The antibonding character of the polarized

z^2 orbital is therefore substantially reduced by the participation of the s orbital, so that its energy is not very high (Figure 2.12).

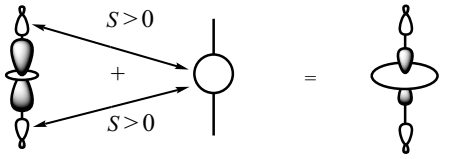

2-71

2.7.2. Electronic structure

In the very large majority of linear (or quasi-linear) ML_2 complexes, the five orbitals of the d block are doubly occupied (d^{10} electronic configuration, **2-72**). The most common examples involve the elements of group 11 (Cu, Ag, Au), where the metal is in the oxidation state I. Anions such as $[Cu(Me)_2]^-$, $[Cu(Ph)_2]^-$, $[Cu(Mes)_2]^-$ (Mes = 2, 4, 6−$Me_3C_6H_2$), $[Ag(CN)_2]^-$, $[Ag(C(SiMe_3)_3)_2]^-$, $[Au(C_6F_5)_2]^-$, or $[AuCl_2]^-$, cations such as $[Cu(NH_3)_2]^+$, $[Ag(NH_3)2]^+$, or $[Ag(CO)_2]^+$, and neutral complexes such as [AuMe(PMe_3)] or [AuCl(Mes)] are all known. There are also examples from group 12, such as $[Hg(CN)_2]$.

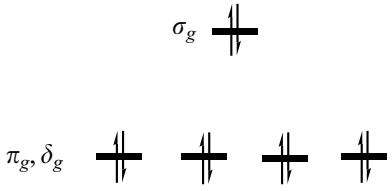

2-72

Although the d block is full, these complexes have only 14 electrons. This electronic deficiency is linked to the presence of two p orbitals on the metal (**2-73**) which remain empty, even though they are nonbonding, since they are too high in energy to be occupied. The small number of ligands, combined with this electron deficiency, makes these complexes very reactive. They can either bind other ligands, or exist as chains, in which the coordination number of the metal is higher than two, rather than as ML_2 monomers.

2-73

We should mention a few complexes in which the d block is not completely filled. For example, complexes with two borylamide ligands [N(Mes)(BR_2)] are known for M=Mn (d^5), Fe(d^6), Co (d^7), and Ni (d^8), and they adopt an almost linear geometry. These are all high-spin complexes, which is understandable given the small separation of the energy levels in the d block.

2.8. Other complexes or ML_n fragments

Other structures exist for ML_n complexes besides those considered so far, though they are less common for stable species. We shall study five

of them in this section: pyramidal ML_3 complexes (**2-74a**), 'T-shaped' ML_3 (**2-74b**), 'butterfly' ML_4 (**2-74c**), bent ML_2 (**2-74d**), and ML (**2-74e**).

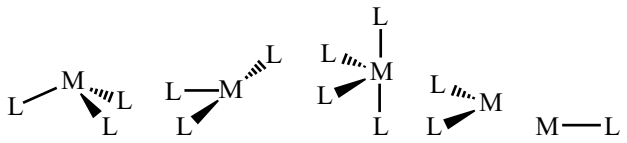

2-74a **2-74b** **2-74c** **2-74d** **2-74e**

These entities are interesting since they may be considered as 'fragments' of more important complexes, such as octahedral or square-planar. In this context, knowledge of their orbital structure is useful for two reasons:

1. They can be used as fragment orbitals in some complexes. For example, the main MO of the complex [(η^5-cyclopentadienyl)$Mn(CO)_3$] (**2-76**) can be constructed by interaction of the π MO of cyclopentadienyl with the *d* orbitals of the metallic fragment [$Mn(CO)_3$] in a pyramidal geometry.
2. The *d* orbitals of these species 'resemble' the orbitals of certain organic molecules or fragments, both in their shape and their electronic occupation. It is therefore important to be familiar with them if one wishes to establish a link between the electronic structures of transition metal complexes and of organic molecules (*the isolobal analogy*, see Chapter 5).

2.8.1. Pyramidal ML_3 complexes

The pyramidal ML_3 structure (**2-74a**), with C_{3v} symmetry, is not common for complexes with three ligands. But a few examples are known, such as the d^0 complexes [$M(HC(SiMe_3)_2)_3$] (M=Y or La), or the low-spin d^6 complexes [$M(Mes)_3$] (M=Rh or Ir) (**2-75**). Moreover, the pyramidal ML_3 entity can be considered as a *fragment* in 18-electron complexes of the type [(polyene)-ML_3], such as [(η^4-cyclobutadiene)$Fe(CO)_3$], [(η^5-Cp)$Mn(CO)_3$] (Cp=cyclopentadienyl) (**2-76**) or [(η^6-benzene)$Cr(CO)_3$].

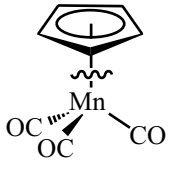

2-76

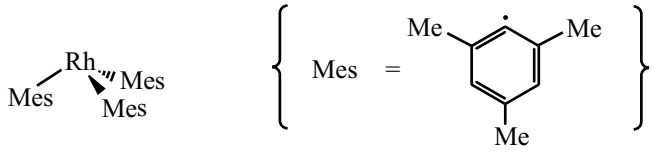

2-75

In one approach to the derivation of the d-block orbitals of this complex, we start from an octahedral complex with the geometry indicated in **2-77** and remove the three ligands L_4, L_5, and L_6. A pyramidal ML_3 fragment is thereby obtained, in which the angles between the M–L bonds are 90°. In the orientation that is chosen, the *z*-axis coincides with the C_3 axis of the resulting ML_3 complex.

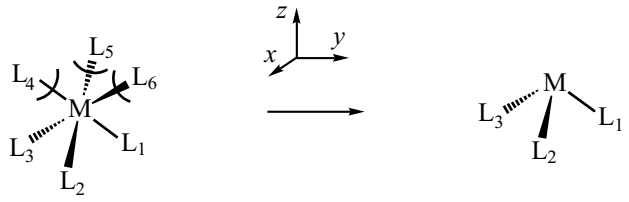

2-77

The t_{2g} (nonbonding) and e_g (antibonding) orbitals of an octahedral complex with this orientation of the axes have already been established (§ 2.1.2.5, Figure 2.5) and are presented on the left-hand side of Figure 2.13. The removal of three ligands does not change the three nonbonding orbitals, since the coefficients on these ligands were zero: they remain nonbonding and degenerate in the ML_3 fragment.

The z^2 orbital has a_1 symmetry (the totally symmetric representation of the C_{3v} point group), while the two other orbitals are degenerate by symmetry (1e). The e_g orbitals are stabilized by the elimination of half of the antibonding interactions that were present in the octahedron. However, they are still antibonding in the ML_3 fragment (Figure 2.13) and make up the degenerate orbital set 2e. As in several of the examples already treated, the antibonding character of these orbitals is reduced by mixing with the p_x (**2-78**) or p_y (**2-79**) orbitals, which polarizes them in the direction opposite to the ligands.

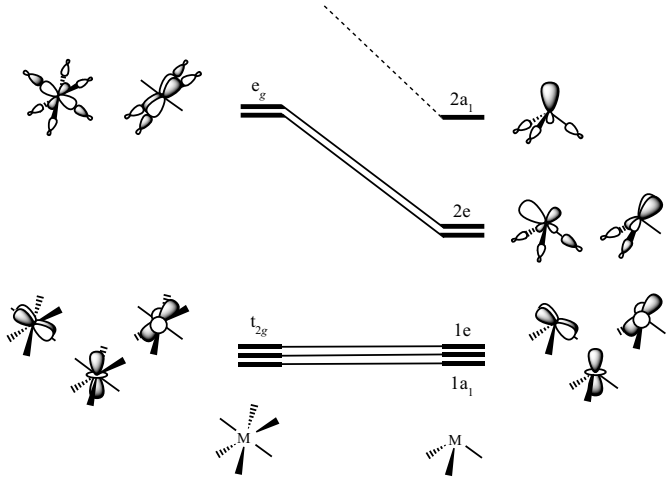

Figure 2.13. Derivation of the d-block orbitals for a pyramidal ML_3 complex from the *d* orbitals of an octahedral ML_6 complex. The hybrid *s*–*p* orbital lying above the d block is also shown.

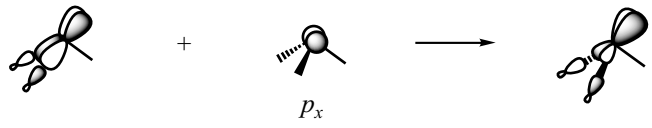

p_x

2-78

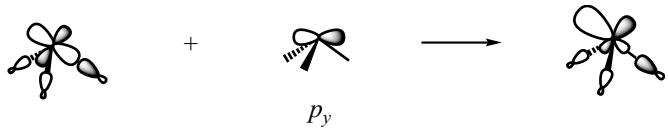

p_y

2-79

If the d block were completely filled, we would have a 16-electron complex. There would therefore be an empty nonbonding orbital on the metal centre. For a trigonal-planar ML_3 complex, that would be the p_z orbital perpendicular to the molecular plane (**2-69**). But in the present case, it is a hybrid orbital of a_1 symmetry, a linear combination of the *s* and *p* orbitals on the metal, which points in the direction opposite to the ligands (**2-80**). Due to the relative energies of the *nd*, $(n + 1)s$, and $(n + 1)p$ AO on the metal, it stays higher in energy than the 2e orbitals which are essentially of *d* character on the metal and weakly antibonding. This orbital lies lower than the pure *p* orbital of a trigonal-planar ML_3 complex, thanks to the contribution from the *s* orbital ($\varepsilon_s < \varepsilon_p$).

2-80

Notice that the structure of the d block, with three strictly nonbonding orbitals, enables us to understand why this geometry is observed for low-spin d^6 complexes, such as that represented in **2-75**.

2.8.2. 'T-shaped' ML_3 complexes

There are a few rare ML_3 complexes that adopt a non-trigonal planar geometry, in which one L–M–L angle is substantially larger than 120° (C_{2v} symmetry).[12] This type of structure is sketched in **2-81**, where the angle L_1–M–L_3 has the limiting value of 180°, justifying the name of a T-shaped structure. The diamagnetic d^8 complexes $[Rh(PPh_3)_3]^+$ (**2-82**) and $[Ni(Mes)_3]^-$ are typical examples. The T-shaped entity ML_3 is also interesting as it can be used as a fragment in monometallic complexes such as Zeise's salt, $[Pt(Cl)_3(\eta^2\text{-ethylene})]^-$ (**2-83**), or bimetallic complexes of the type $[Pd_2L_6]^{2+}$ (**2-84**).

[12] There are also a few planar complexes in which two of the three L–M–L angles are larger than 120° (Y-shaped structures). The preference for T- or Y-shaped structures will be analysed in greater detail in Chapter 4. For further information on the structures of ML_3 complexes, the reader may consult: S. Alvarez *Coord. Chem. Rev. 193–195*, 13 (1999).

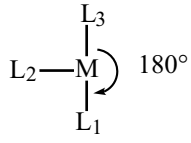

2-81

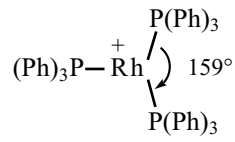

2-82

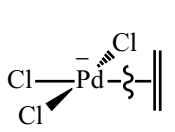

2-83

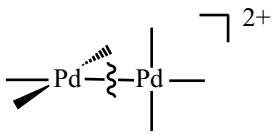

2-84

The orbitals of the d block may be derived from those of a square-planar complex (§ 2.2.1), by removing one of the ligands (**2-85**).

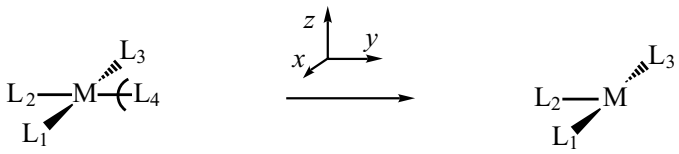

2-85

Changes to the shapes and energies of the orbitals are shown in Figure 2.14.

The three strictly nonbonding orbitals in the square-planar complex (with b_{2g} and e_g symmetries in the D_{4h} point group) are not affected by the removal of a ligand. They become the a_2, b_1, and b_2 nonbonding orbitals of the ML_3 fragment. The z^2 orbital (a_{1g}) is very weakly stabilized ($1a_1$), due to the disappearance of a small antibonding interaction, while the x^2-y^2 orbital, which is antibonding towards the four ligands in the square-planar complex (b_{1g}), is stabilized and becomes the $2a_1$ orbital in the ML_3 complex. This stabilization is enhanced by mixing with the p_y orbital which polarizes the orbital in the opposite direction to the ligand L_2 (**2-86**). But overall, this orbital stays fairly high in energy, due to the three antibonding interactions that are still present in the xy plane, along the directions of the lobes of x^2-y^2.

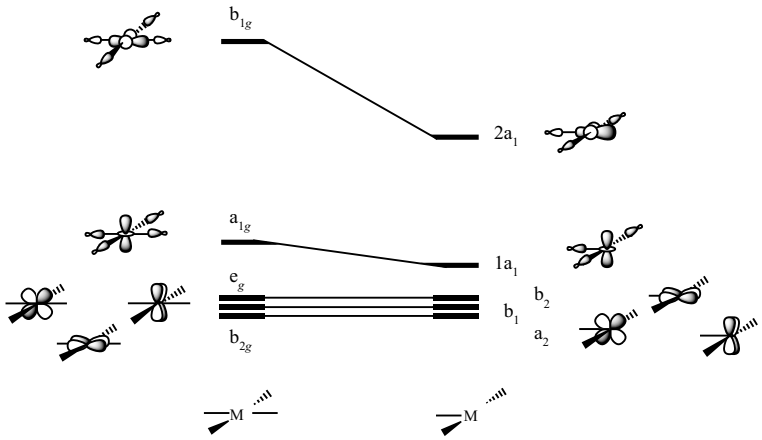

Figure 2.14. Derivation of the d-block orbitals of a T-shaped ML_3 complex from the *d* orbitals of a square-planar ML_4 complex.

2-86

The T-shaped ML_3 fragment is thus characterized by the presence of four low-energy *d* orbitals, instead of the five present in the trigonal-planar geometry (§ 2.6.1). As a result, the stable complexes mentioned at the beginning of this section, such as $[Rh(PPh_3)_3]^+$ (**2-82**), are diamagnetic and have a d^8 electronic configuration, whereas the d^{10} complexes, which are far more numerous, adopt a trigonal-planar geometry (§ 2.6.2).

2.8.3. 'Butterfly' ML_4 complexes

In the 'butterfly' ML_4 complex sketched in **2-74c**, one of the L–M–L angles is 180°, where the two bonds form the body of the butterfly. The angle between the other two bonds, which form the (folded) wings of the butterfly, is much smaller. More generally, ML_4 fragments are described as 'butterfly' when they have C_{2v} symmetry, which only implies the existence of two planes of symmetry and a C_2-axis (**2-87**). It is therefore possible for the two angles mentioned to have very variable values, so long as they are not equal (the symmetry would then be D_{2d}, as for the intermediate points along the deformation shown in **2-53**). This ML_4 structure, adopted by some complexes such as $[Fe(CO)_4]$ or $[Ir(H)_2(P(^tBu)_2Ph)]^+$ (**2-88**), can also be regarded as a fragment in the analysis of the electronic structure of other species, such as the carbene complex $[Fe(CO)_4(CR_2)]$ (**2-89**) or the bimetallic complex $[Fe_2(CO)_8]$ (**2-90**).

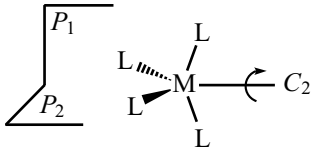

2-87

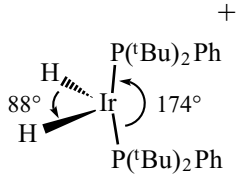

2-88

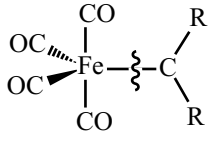

2-89

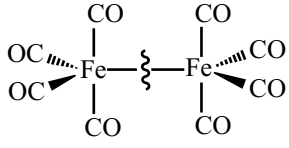

2-90

A butterfly ML_4 fragment can be obtained by the removal of two *cis* ligands in an octahedral complex (L_5 and L_6 in **2-91**). The L_1–M–L_2 and L_3–M–L_4 angles are then 90° and 180°, respectively. The *d* orbitals that we shall establish are adapted to this particular geometry, so some changes may be anticipated if these angles have different values (see, for example, Exercise 2.9).

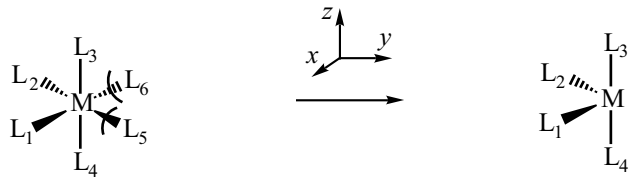

2-91

We have already established the *d* orbitals of an octahedral complex in the orientation chosen above, with four ligands placed along the bisectors of the *x*- and *y*-axes (§ 2.1.2.5, Figure 2.4); they are shown in the left-hand side of Figure 2.15.

Removal of the ligands L_5 and L_6 has no effect on either the shape or the energy of the three nonbonding t_{2g} orbitals of the octahedron (zero coefficients on these ligands). These orbitals ($a_2(xz)$, $b_1(yz)$, and $1a_1(x^2-y^2)$) therefore remain degenerate, not, as in the octahedron, by symmetry, but 'accidentally' in the lower-symmetry point group C_{2v}. In the e_g block, the z^2 orbital is only very slightly stabilized by the removal of the two weak antibonding interactions in the *xy* plane. It therefore stays as a strongly antibonding orbital ($3a_1$). In contrast, the *xy* orbital is strongly stabilized by the removal of two of the four antibonding interactions with the ligands located in the *xy* plane (b_2).[13] This stabilization is enhanced by mixing with the p_x orbital, which polarizes it in

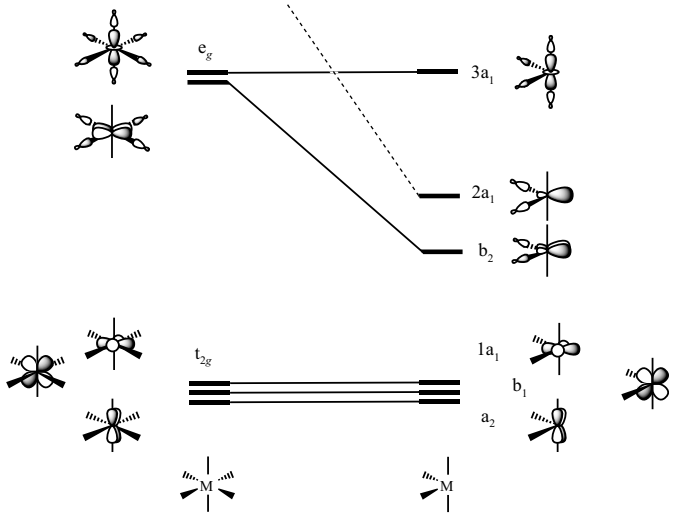

Figure 2.15. Derivation of the d-block orbitals for a 'butterfly' ML_4 complex from the *d* orbitals of an octahedral ML_6 complex. The hybrid *s*–*p* orbital ($2a_1$) placed between the b_2 and $3a_1$ orbitals of the d block is also indicated.

[13] In the character table for the C_{2v} group (Chapter 6, § 6.2.5.1), one does indeed find that the symmetries of the *xy*, *xz*, and *yz* orbitals are a_2, b_1, and b_2. However, the name of the orbital in a given symmetry is not the same as that we have just indicated. For example, *xy* is placed in the a_2 representation whereas we indicated that it has b_2 symmetry. These differences arise because the axis system previously used for the octahedron is not the one conventionally adopted for the C_{2v} group. For example, the C_2 axis should be the *z*-axis, rather than the *y*-axis. In other words, the orbitals sketched on the right-hand side of Figure 2.15 do indeed correspond to the symmetries indicated, and only their names would be changed if one adopted the axis system appropriate for the C_{2v} group.

the direction opposite to the ligands L_1 and L_2, in a way which we have already seen several times (**2-92**).

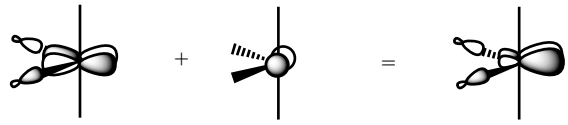

2-92

There are therefore four nonbonding or weakly antibonding *d* orbitals. If these orbitals are doubly occupied, the result, taking the four bonds into account, will be a 16-electron complex. As in the examples that we have already met, this result is linked to the existence of a nonbonding orbital on the metal which is not of *d* type. In the ML_4 butterfly complex, this is an *s–p* hybrid orbital of a_1 symmetry (**2-93**) which points along the C_2 symmetry axis of the complex, that is, between the two ligands which were removed in the original octahedral complex. Its energy, which is not very high due to the participation of the s orbital, is lower than that of the most antibonding orbital in the d block, as shown in Figure 2.15.

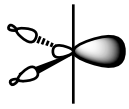

2-93

2.8.4. Bent ML_2 complexes

ML_2 complexes usually adopt a linear (or essentially linear) geometry (see § 2.7). Knowledge of the orbital structure for strongly bent ML_2 species is therefore useful mainly when one wishes to consider them as fragments in larger complexes. For example, the [(η^2-ethylene)Ni(PR_3)$_2$] complex (**2-94**) can be described in terms of a bent ML_2 entity interacting with a molecule of ethylene.

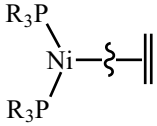

2-94

Starting from the butterfly ML_4 fragment previously studied, a bent ML_2 fragment may be obtained by removing the ligands L_3 and L_4 (**2-95**).

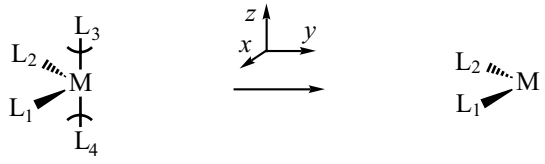

2-95

The *d* orbitals of this fragment are readily obtained from those of the ML_4 fragment (Figure 2.16). The shape and energy of the three nonbonding orbitals (a_2, b_1, and $1a_1$), and of the antibonding b_2 orbital, are all unchanged (zero coefficients on L_3 and L_4). However, the two main antibonding interactions in the z^2 orbital are eliminated, so that

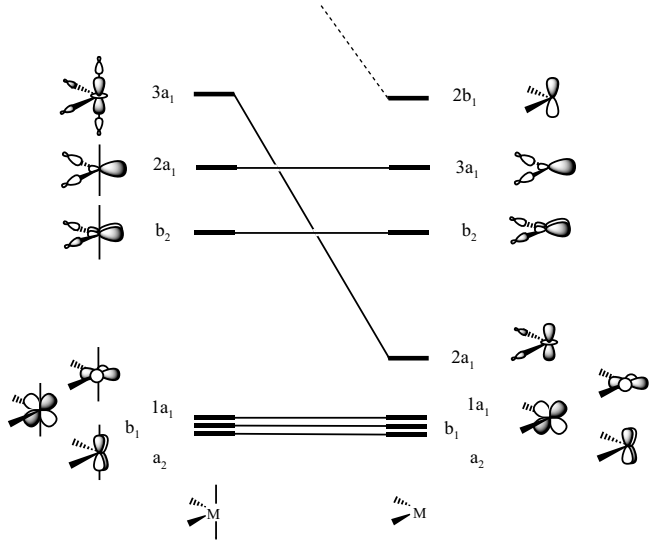

Figure 2.16. Derivation of the d-block orbitals for a bent ML_2 complex from the *d* orbitals of a 'butterfly' ML_4 complex. The hybrid *s*–*p* orbital ($2a_1$) and the metal *p* orbital (lying above the d block) are also indicated.

this orbital becomes nearly nonbonding ($2a_1$). The five orbitals in the d block are therefore nonbonding or weakly antibonding. Once the four electrons associated with the two M–L bonds are taken into account, a d^{10} electronic configuration leads to a 14-electron complex.

This lack of four electrons compared to the 18-electron rule arises because there are two nonbonding orbitals on the metal, which are not of *d*-type (**2-96**). The first is an *s*–*p* hybrid orbital ($3a_1$), identical to that found for the 'butterfly' ML_4 fragment (Figure 2.16, $2a_1 \rightarrow 3a_1$). The second is the *p* orbital perpendicular to the plane of the fragment ($2b_1$), which is strictly nonbonding. It is higher in energy than the $3a_1$ orbital, mainly because the *s* contribution in this latter hybrid orbital lowers its energy ($\varepsilon_s < \varepsilon_p$). Notice that these two orbitals have the same shape as the two nonbonding MO in bent AH_2 molecules, where A is a main-group element (Chapter 1, Figure 1.5), and that their energetic order is the same ($\varepsilon(a_1) < \varepsilon(b_1)$).

a_1 b_1

2-96

2.8.5. ML complexes

A coordination number of 1 is rare for stable complexes. The examples that are known involve a very bulky ligand such as the aryl radical, 2, 4, 6−$Ph_3C_6H_2$, which forms d^{10} ML complexes with copper and silver (**2-97**). The M–L unit can also be considered as a fragment in a complex with a higher coordination number, such as W–CO in the complex [(η^2-acetylene)$_3$W(CO)] (**2-98**).

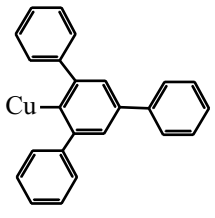

2-97

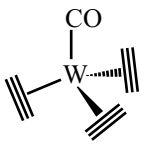

2-98

The orbitals of this fragment can be obtained in different ways, for example, by removing a ligand from a linear ML_2 complex (**2-99**) whose orbitals have already been derived (§ 2.7.1).

The four strictly nonbonding *d* orbitals of the ML_2 complex (π_g and δ_g) remain unchanged. The z^2 orbital is stabilized by the elimination of

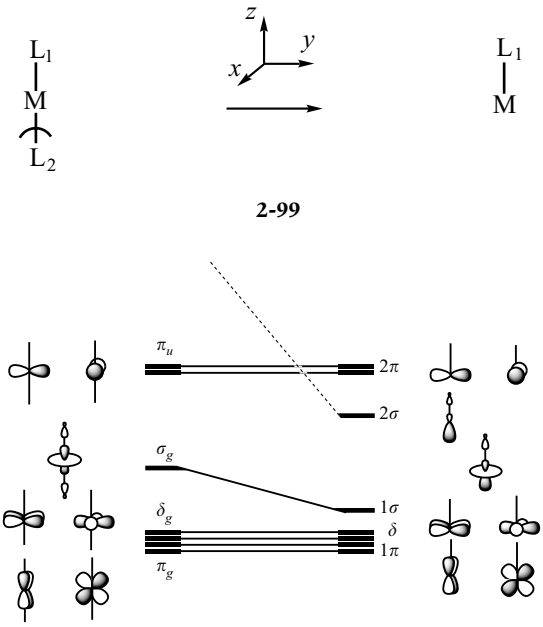

Figure 2.17. Derivation of the d-block orbitals for an ML complex from the *d* orbitals of a linear ML_2 complex. The nonbonding orbitals (*s*–*p* hybrid and pure *p*), located above the d block, are also shown (2σ and 2π).

an antibonding interaction (Figure 2.17). This stabilization is increased by mixing with the p_z orbital which polarizes z^2 in the direction opposite to the ligand (as happens for the z^2 orbital in an ML_5 complex (SBP), **2-44**). Notice that the removal of the inversion centre ($D_{\infty h} \rightarrow C_{\infty v}$) leads to the disappearance of the *g* and *u* subscripts in the symmetry labels (Chapter 6, § 6.2.5.2).

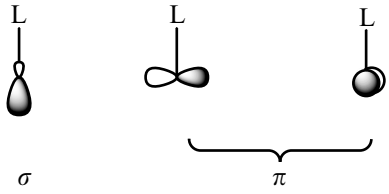

2-100

The d block of the M–L fragment therefore contains five low-energy orbitals that are all likely to be occupied. The rare stable complexes do indeed have a d^{10} electronic configuration (**2-97**). They are therefore 12-electron complexes with three empty nonbonding orbitals on the metal, an *s*–*p* hybrid orbital (σ symmetry) and two pure *p* orbitals of π symmetry that are higher in energy (**2-100**).

Exercises

2.1

1. Give the d^n electronic configuration of $[M(H_2O)_6]^{2+}$ octahedral complexes from the first transition series (M=Sc, Ti, V, Cr, Mn, Fe, Co, Ni, Cu, Zn).

2. If these are high-spin complexes, give their ground-state electronic configuration (just for the d block).
3. How many unpaired electrons are there in each case?

2.2

1. Give the d^n electronic configuration of the complex $[Cr(CO)_6]$.
2. Is this a high-spin or a low-spin complex? Deduce its ground-state electronic configuration (just for the d block).
3. Reduction of this complex leads to dissociation into $[Cr(CO)_5]^-$ and CO, rather than to the formation of $[Cr(CO)_6]^-$. Suggest an explanation.

2.3

Making use of the results given in Figure 2.3, give the approximate shapes and relative energies of the *bonding MO* for an octahedral complex whose ligands are located as shown in **2-29**.

2.4

Give the shapes and relative energies of the d-block MO for a square-planar ML_4 complex whose ligands are located on the bisectors of the x- and y-axes.

2.5

1. How many electrons are there around the metal in the $[Rh(PPh_3)_3]^+$ complex whose geometry is given in **2-82**?
2. Link this result to the existence of nonbonding MO, lying above the d block, in a 'T-shaped' ML_3 complex (see Figure 2.14, right-hand side, for this d block).
3. Give the shapes of these MO.

2.6

1. Construct the d-orbital correlation diagram linking a square-planar ($\theta = 90°$) to a pyramidal ML_4 complex ($\theta = 125.5°$, nodal cone angle for the z^2 orbital).

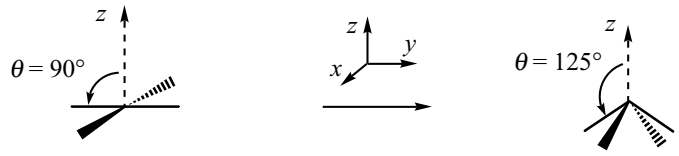

2. What happens to the shape and the energy of the nonbonding metal orbital that is not a d orbital?

Apical and basal bonds in ML_5 complexes (SBP)

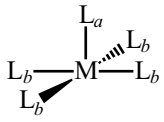

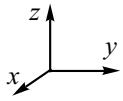

2.7

1. Give the shapes and relative energies of the five d-block orbitals for an ML_5 complex with an SBP geometry, if the metal is in the basal plane.

   In what follows, we shall only consider this geometry, even if the metal in some cases is above the basal plane.
2. In these complexes, we distinguish the basal ligands (L_b) from the apical one (L_a). Starting from the knowledge that the M–L_a bond is either a little shorter than or roughly equal in length to the M–L_b bonds for low-spin d^6 complexes, rationalize the following experimental results for the different electronic configurations:
   (a) In the *low-spin* complex $[Co(CN)_5]^{3-}$, on the other hand, we find Co–$(CN)_a$ = 2.01 Å but Co–$(CN)_b$ = 1.90 Å.
   (b) This trend is reinforced in the *low-spin* complex $[Ni(CN)_5]^{3-}$, where Ni–$(CN)_a$ = 2.17 Å but Ni–$(CN)_b$ = 1.85 Å.
3. Which is the longer bond (Mn–Cl_a or Mn–Cl_b) in the *high-spin* complex $[MnCl_5]^{2-}$?
4. What differences may be anticipated between a low-spin and a high-spin d^8 complex?

Bond lengths in d^8–ML_4 complexes

2.8

1. Indicate the splitting of the d block in an ML_4 complex whose geometry is
   (i) square-planar;
   (ii) tetrahedral.
2. What is the most stable electronic configuration for a d^8 complex in each geometry?
3. It is observed experimentally that typical metal–ligand bond lengths for d^8 complexes are larger in tetrahedral complexes (see table below: units are Å).

	Square-planar	Tetrahedral
Ni–P	2.14	2.28
Ni–S	2.15	2.28
Ni–Br	2.30	2.36

Suggest a rationalization.

2.9

1. Derive the d-block orbitals for a butterfly ML_4 complex from those of a TBP ML_5 complex.

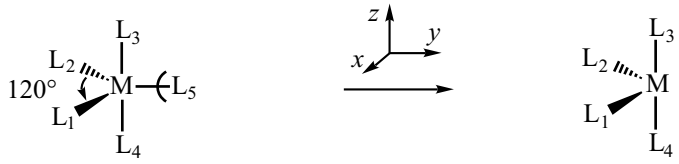

2. Are these different from the orbitals derived in § 2.8.3 starting from an octahedral complex (consider only the four lowest-energy *d* orbitals)?

2.10

Derive the *d* orbitals for the bent ML_2 fragment from those of a square-planar ML_4 complex. Compare them with those obtained in § 2.8.4.

Use of group theory

2.11

1. Construct all the MO of a tetrahedral complex, making use of symmetry-adapted combinations of ligand orbitals and the data in the character table for the T_d group (Chapter 6, § 6.6.2), following the procedure adopted in Figure 2.2 for an octahedral complex.
2. Indicate the orbitals associated with the σ bonds, the d-block orbitals, and the σ^* antibonding orbitals.

2.12

Repeat the questions in 2.11 for a trigonal-planar ML_3 complex (use the data in Chapter 6, § 6.6.3).

Orbital polarization (Appendix A)

2.13

1. In a square-planar ML_4 complex, which metal orbital of *s* or *p* type can polarize the z^2 orbital in the d block?
2. What are the consequences of this polarization for the shape of the orbital and for the metal–ligand interactions?

Appendix A: polarization of the *d* orbitals

In many complexes, some of the antibonding orbitals in the d block are *polarized* by mixing, either with a *p* orbital or with the *s* orbital of the metal (e.g. see **2-64** and **2-65** for *d*–*p* mixing and **2-71** for *d*–*s* mixing). The purpose of this appendix is to study the orbital interaction scheme that produces these polarizations in greater detail.

When an orbital in the d block results simply from the antibonding interaction between a metal *d* orbital and an orbital of the same symmetry located on the ligands (ℓ) (*two-orbital interaction scheme*, 2.A1), the *d* orbital is not polarized. However, polarization does occur if there is a *p* (or *s*) orbital on the metal that has the same symmetry as the *d* and *l* orbitals, which leads to a *three-orbital interaction scheme* (2.A2). In this case, while the *d* and *p* (or *s*) orbitals are of course orthogonal ($S = 0$), since they are located on the same atom, the overlaps between the *l* orbital on the ligands and each of the metal orbitals are non-zero (S_{l-d} and S_{l-p}, 2.A2).

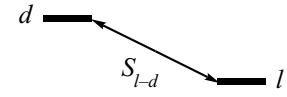

2.A1

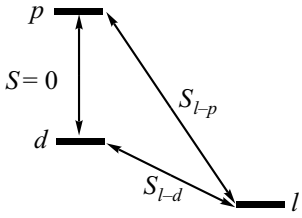

2.A2

2.A1. Three-orbital interaction diagram

We consider the case where two orbitals on the metal, for example, *d* and *p*, have the same symmetry as an orbital *l* on the ligands. In the interaction diagram (Figure 2.A1), the latter is placed at lower energy than the metal orbitals, due to the greater electronegativity of the ligands. The interaction between these three atomic orbitals leads to the formation of three MO (ϕ_1, ϕ_2, and ϕ_3). When we consider their energies, ϕ_1 is lower than *l* and ϕ_3 higher than *p*. The orbital ϕ_2 ends up at an intermediate energy level, a little higher than the *d* orbital with this combination of initial orbital energies.[14]

[14] Y. Jean and F. Volatron *'An Introduction to Molecular Orbitals'*, Oxford University Press, NY (1993), chapter 6.

Each MO is a linear combination of the three orbitals *l*, *d*, and *p*. When we examine their shapes, we find that the interactions between *l* and *d*, and between *l* and *p*, are both bonding in the lowest-energy MO ϕ_1 and both antibonding in the highest-energy MO ϕ_3. In the orbital ϕ_2, there is an antibonding overlap ($l - d$) but also a bonding overlap ($l - p$) (2.A3).

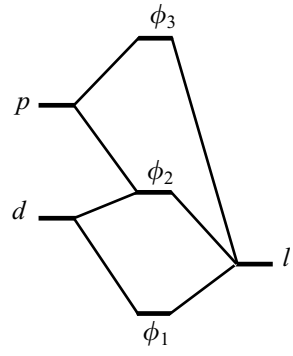

Figure 2.A1. Three-orbital interaction diagram, with two on the metal (*d* and *p*) and one on the ligands (*l*).

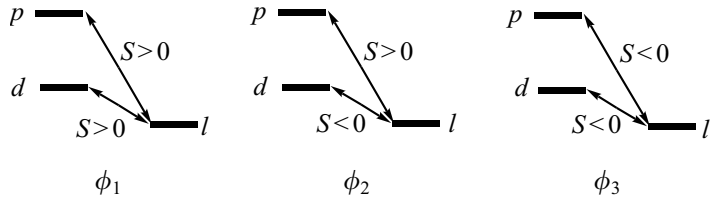

2.A3

2.A2. Polarization by a *p* orbital: TBP ML_5 complexes

The d block of an ML_5 complex with a TBP geometry contains two strictly nonbonding orbitals with e″ symmetry (*xz*, *yz*), one strongly antibonding orbital with a_1 symmetry (z^2), and two weakly antibonding orbitals with e′ symmetry (*xy*, x^2-y^2) (see § 2.5.1, Figure 2.10). We shall examine these last two in greater detail.

In the D_{3h} point group appropriate for this complex, the p_x and p_y orbitals have the same symmetry (e′) as *xy* and x^2-y^2 (see Table 2.3, § 2.5.1). Two combinations of orbitals on the equatorial ligands, l_x and l_y, also have this symmetry (Chapter 6, § 6.6.4.2). These six orbitals are shown in Figure 2.A2, where the plane of the page is the equatorial plane (*xy*).[15] Notice that it is possible to separate each pair of degenerate orbitals into an e'_x component, which is antisymmetric with respect to the *yz* plane, and an e'_y component which is symmetric with respect to this plane. The first group includes the *xy*, p_x, and l_x orbitals, while the x^2-y^2, p_y, and l_y orbitals belong to the second. No interaction is possible between orbitals that belong to different groups, since they have different symmetry properties with respect to the *yz* plane.

[15] The analysis that follows is also applicable to ML_3 complexes with a trigonal-planar geometry.

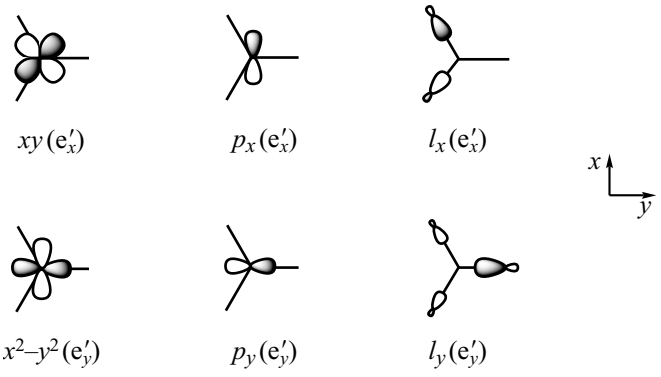

Figure 2.A2. Fragment orbitals (metal or ligands) with e′ symmetry in a TBP ML_5 complex. The equatorial ligands are in the plane of the page (*xy*), and the axial ligands are omitted for greater clarity.

The interactions between orbitals with e′ symmetry therefore give two equivalent blocks, one involving the three e'_x orbitals, the other the three e'_y orbitals (Figure 2.A3). The MO $1e'_x$, $2e'_x$, and $3e'_x$, are in the first, and $1e'_y$, $2e'_y$, and $3e'_y$ are in the second.

Application of the rules presented in § 2.A1 leads to the following orbital combinations in the $1e'_x$ (**2.A4**), $2e'_x$ (**2.A5**), and $3e'_x$ (**2.A6**) MO.

The $1e'_x$ orbital (**2.A4**) belongs to the group of *bonding* MO in the ML_5 complex, characterized by (*i*) bonding metal–ligand interactions, reinforced here by the polarization of the *d* orbital; (*ii*) a lower energy than that of the ligand orbitals; and (*iii*) larger coefficients on the ligands than on the metal. This orbital does not belong to the d block of the complex. The $3e'_x$ orbital (**2.A6**) is one of the *antibonding* MO in

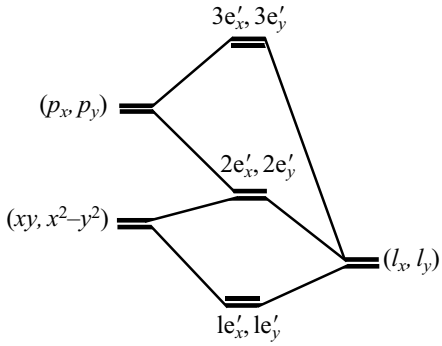

Figure 2.A3. Interaction diagram for orbitals with e′ symmetry in a TBP ML_5 complex.

the complex, and the *d*–*p* mixing in the metal reinforces its antibonding character. This is the highest-energy MO (Figure 2.A3); it is more concentrated on the p_x metal orbital than on *xy* and is also not part of the d block. Among the three MO that we are considering, the one that belongs to the d block is therefore the one with intermediate energy, $2e'_x$ (**2.A5**), since it is mainly concentrated on the initial orbital with intermediate energy, *xy*. The contribution of the p_x orbital to this MO leads to its overlap with the ligand l_x orbital being bonding (a result that we had always assumed in Chapter 2). As a result, the *xy* orbital is polarized in the direction opposite to the ligands, and its antibonding character is reduced. A similar analysis of the interactions of the e'_y orbitals shows that the second d-block orbital with e′ symmetry is the $2e'_y$ orbital, which is degenerate with $2e'_x$, and in which the l_y ligand orbital mixes in an antibonding way with x^2-y^2, but in a bonding way with p_y (**2.A7**).

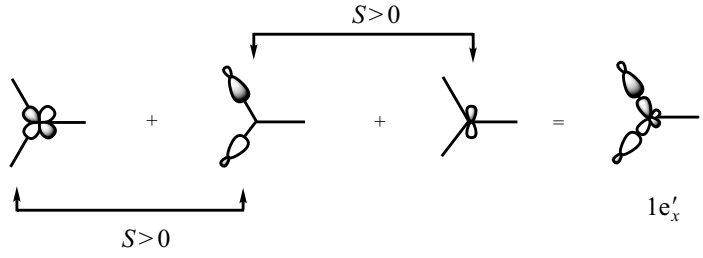

2.A4

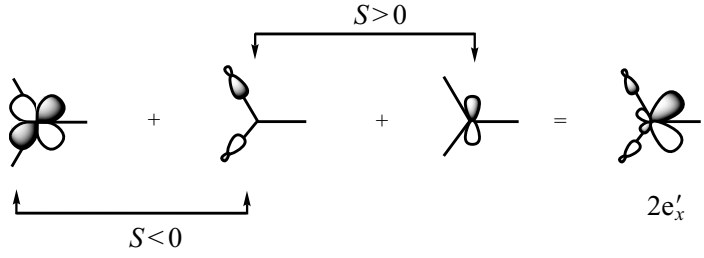

2.A5

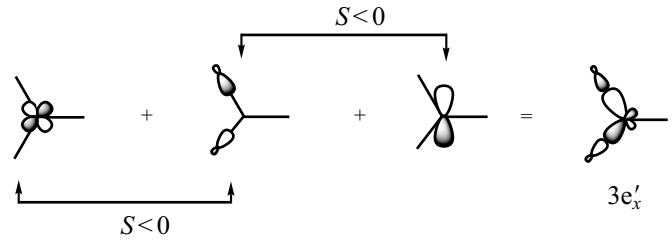

2.A6

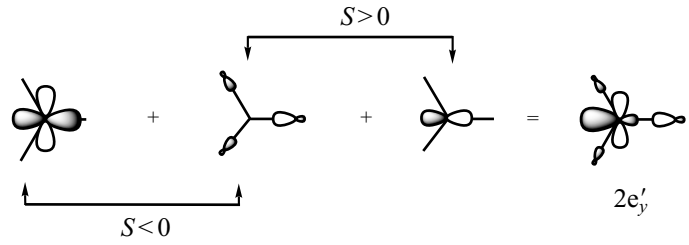

2.A7

2.A3. Polarization by the *s* orbital: linear ML_2 complexes

It is possible for a *d* orbital to have the same symmetry as the metal *s* orbital. In particular, this happens for linear ML_2 complexes, in which both the z^2 and the (higher-energy) *s* orbitals have σ_g symmetry. A three-orbital interaction scheme is therefore appropriate for these two orbitals and the ligand orbital *l* with the same symmetry (Figure 2.A4), giving three MO, $1\sigma_g$, $2\sigma_g$, and $3\sigma_g$.

As in the preceding example, mixing between z^2 and *s* reinforces the bonding character of the $1\sigma_g$ MO and the antibonding character of the $3\sigma_g$ MO. The orbital with intermediate energy, $2\sigma_g$, is the only one of these three that belongs to the d block. In this orbital, there is antibonding mixing between z^2 and *l*, but mixing of bonding type between *s* and *l* (**2.A8**). The *s* contribution decreases the amplitude of z^2 along the *z*-axis but increases it in the *xy* plane. The polarization of the z^2 orbital therefore reduces the antibonding metal–ligand interactions.

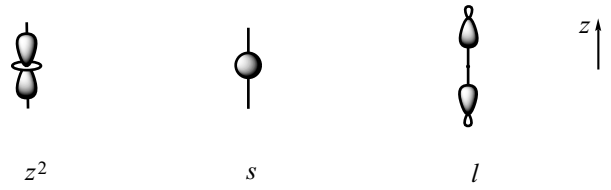

Figure 2.A4. Fragment orbitals (metal and ligands) with σ_g symmetry in a linear ML_2 complex.

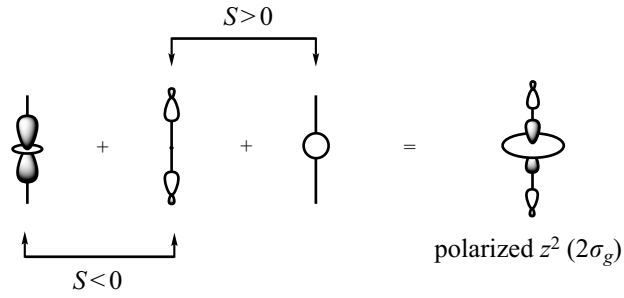

2.A8

Without this polarization, the energy of a z^2 orbital that is antibonding with the ligands located on the *z*-axis is very high. Polarization of the orbital in the *xy* plane, which does not contain any ligands, lowers its energy sufficiently for it to be occupied in stable linear ML_2 complexes (d^{10} complexes, § 2.7.2).

2.A4. Polarization by the *s* orbital and by a *p* orbital: SBP ML_5 complexes

In some cases, it is possible for a *d* orbital to be polarized by the *s* orbital and simultaneously by a *p* orbital. This happens, for example, to the z^2 orbital in ML_5 complexes with an SBP geometry (§ 2.3.1.2). This orbital does indeed have the same symmetry as the *s* and p_z orbitals (a_1 in the C_{4v} point group). The z^2 orbital of the d block has antibonding interactions with the ligands ($z^2 - l$, **2.A9**); the *s* and *p* contributions mix in so that:

(1) the contribution from p_z is bonding with the apical ligand (located on the *z*-axis);.
(2) the contribution from *s* is bonding with the basal ligands (located in a plane perpendicular to the *z*-axis) (**2.A9**).

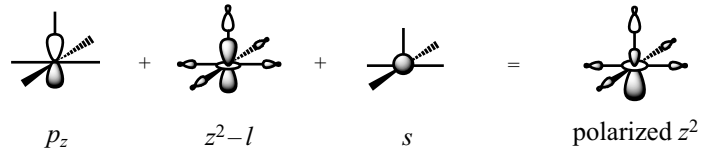

2.A9

Notice that we had simplified the problem in § 2.3.1.2, by only considering mixing with the p_z orbital. It is indeed this latter which is

responsible for the polarization towards the vacant site of the octahedron that is the most important feature of the z^2 orbital in SBP ML_5 complexes.

Appendix B: orbital energies

When deriving the d block associated with different ligand fields, we obtained nonbonding, 'weakly' antibonding, or 'strongly' antibonding orbitals. These ideas can be made more precise by undertaking calculations which yield numerical values for orbital energies. We have used the extended Hückel method for model complexes of the MH_n type, the MH_n distance being fixed at 1.7 Å. The values obtained are given in eV; while they should only be considered as indications, they can help to give an idea of the energy-level splittings with respect to the initial nonbonding level (ε_d) in the main ligand fields. Information on the shapes of the orbitals may be obtained from the figures indicated in Chapter 2.

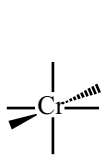

e_g –6.02

t_{2g} –11.22

Octahedral complex CrH_6
$\varepsilon_d(\mathrm{Cr}) = -11.22$ eV
(see Figure 2.3)

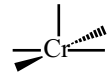

b_1 –6.02

a_1 –9.41

(b_2, e) –11.22

SBP complex CrH_5
(metal in the basal plane)
$\varepsilon_d(\mathrm{Cr}) = -11.22$ eV
(see Figure 2.7)

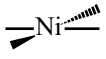

b_{1g} –8.60

a_{1g} –12.62

(b_{2g}, e_g) –12.99

Square-planar complex NiH_4
$\varepsilon_d(\mathrm{Ni}) = -12.99$ eV
(see Figure 2.6)

t_2 –11.48

e –12.99

Tetrahedral complex NiH_4
$\varepsilon_d(\mathrm{Ni}) = -12.99$ eV
(see Figure 2.9)

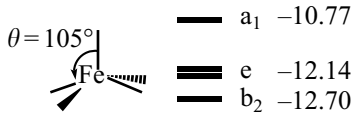

SBP complex FeH_5
(metal out of the basal plane)
ε_d(Fe) = −12.70 eV
(see Figure 2.8)

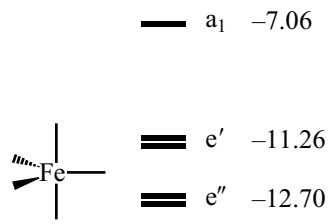

TBP complex FeH_5
ε_d(Fe) = −12.70 eV
(see Figure 2.10)

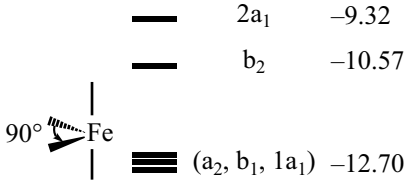

'Butterfly' complex FeH_4
ε_d(Fe) = −12.70 eV
(see Figure 2.15)

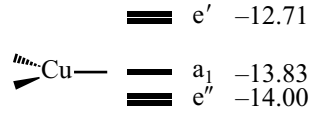

Trigonal-planar complex CuH_3
ε_d(Cu) = −14.00 eV
(see Figure 2.11)

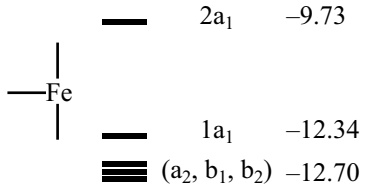

'T-shaped' complex FeH_3
ε_d(Fe) = −12.70 eV
(see Figure 2.14)

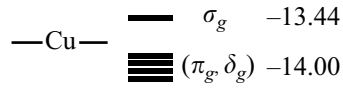

Linear complex CuH_2
ε_d(Cu) = −14.00 eV
(see Figure 2.12)

This page intentionally left blank

π-type interactions

In the preceding chapter, we derived the structure of the d block for several different ML_n complexes in which the ligands were assumed to use only a single orbital to form the metal–ligand bond. This orbital was either nonbonding or essentially so, and oriented towards the metal centre. Since the overlap between this ligand orbital and a *d* orbital on the metal is of the *axial* type, their interaction leads to the formation of a molecular orbital (MO) which characterizes a σ bond. As we have already seen in Chapter 1 (§ 1.5.2), some ligands have another orbital (or even two) that can in principle contribute to the bonding with the metal. The orientation of this orbital is usually perpendicular to the axis defined by the σ bond, so the resulting overlap with a *d* orbital on the metal is *lateral*, and the interaction of π type. Two examples are shown below (**3-1**), in which the ligand orbitals are pure *p* atomic orbitals.

3-1

Among the ligands that can in principle have a π interaction with a metal centre, it is important to distinguish two types, depending on the electronic occupation of the orbital that is concerned on the ligand:

- if it is doubly occupied, the ligand is said to be a π-donor
- if it is empty, then the ligand is a π-acceptor.

This nomenclature is of course linked to the capacity of the ligand to give or receive electrons through the π interaction with the metal.

Comment

The notation 'π' that is used here is almost never strictly correct according to group theory, where it reserved for doubly degenerate orbitals in linear molecules (Chapter 6). It is, however, widely used to refer to *local* symmetry; the expression 'π interaction' is used when the two orbitals share a common nodal plane and have lateral overlap (**3-1**).

The examples treated in this chapter involve octahedral complexes. However, the procedure we have used is general and can be applied to all ligand fields. Several illustrations may be found in the exercises at the end of the chapter.

3.1. π-donor ligands: general properties

3.1.1. The nature of the π orbital on the ligand

A π-type orbital on a ligand can be doubly occupied only if it is sufficiently low in energy. We may therefore be concerned with:

1. A *nonbonding p* orbital on a very electronegative atom. Although nonbonding, this orbital is very low in energy and characterizes a lone pair on the atom linked to the metal. For example, consider the *p* lone pair on the nitrogen atom of an amido group that can interact with one of the metal *d* orbitals (Scheme **3-2** where the geometry around nitrogen is assumed to be planar).

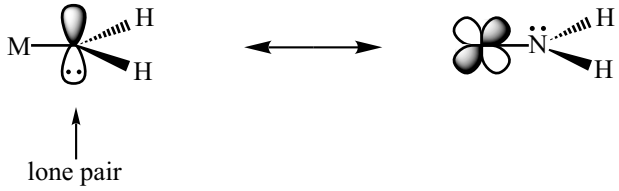

3-2

2. A *bonding orbital* that characterizes a π bond between two atoms of the ligand, as in the case of the imino ligand (**3-3**) with the doubly occupied π_{NC} orbital. Notice that a π-bonding orbital on the ligand is automatically accompanied by the corresponding π^*-antibonding orbital. A ligand of this type can therefore act simultaneously as a π-donor, with its bonding orbital, and as a π-acceptor, thanks to its empty π^* orbital. It is categorized as a π-donor if the former interaction is dominant. A heteronuclear bond provides a favourable case, if, as in the imino ligand (**3-3**), the more electronegative atom is bonded to the metal. The π orbital in such cases is mainly concentrated on the atom bonded to the metal (large overlap), whereas the π^* orbital is mainly concentrated on the more distant centre (small overlap, see Chapter 1, § 1.3.2).

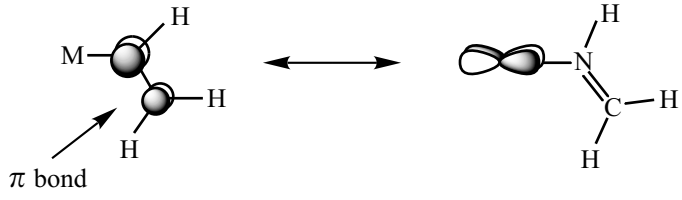

3-3

3.1.2. 'Single-face' and 'double-face' π-donors

Some ligands possess a single nonbonding doubly occupied *p* orbital, such as the amino ligand (**3-2**), or a single π-bonding orbital near to the metal centre, such as the imino ligand (**3-3**). These are said to be 'single-face' π-donors.

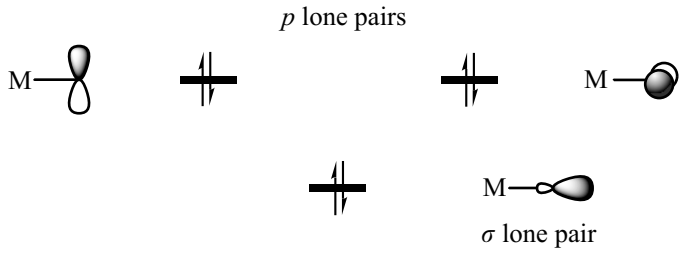

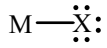

3-4

Other ligands, however, possess *two orbitals* of this type, in perpendicular planes: these are 'double-face' π-donors. The halogens are the most common example (F, Cl, Br, I). These are X-type ligands, with seven valence electrons. Formation of the σ bond involves the unpaired electron on the halogen and a metal electron; as a result, the oxidation state of the metal is increased by one (Chapter 1, § 1.1.1.2). There are therefore three lone pairs which remain on the halogen bonded to the metal (Chapter 1, § 1.5.2.3): a σ-type lone pair for which the M–X internuclear axis is a symmetry axis, and two lone pairs characterized by nonbonding *p* orbitals which 'point' perpendicular to the internuclear axis (more strictly, their axes of revolution are perpendicular to this axis, **3-4**). Due to its symmetry, the σ lone pair cannot participate in a π-type interaction.[1] However, the *p* lone pairs interact with the metal *d* orbitals through two π-type interactions which take place in perpendicular planes (**3-5**). Thus, a halogen linked to a metal centre is a 'double-face' π-donor.

[1] The polarization of this orbital, in the direction opposite to the metal, significantly weakens its σ-type overlap with the orbitals of the same symmetry on the metal. This orbital therefore has a negligible influence on the shapes and energies of the MO of the complex, as it remains localized on the ligand.

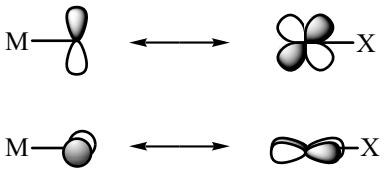

3-5

Analogous interactions occur when the *p* orbitals are replaced by two π-bonding orbitals. This is the case when a ligand with a triple bond (one σ and two π) binds to the metal in the η^1 mode, as shown in **3-6** for the nitrile ligand. As we have already noted for 'single-face' π donors, the π-donor character of the ligand increases as the orbital coefficient becomes larger on the atom bound to the metal. This therefore

requires the more electronegative atom to be bound to the metal in the η^1 mode.

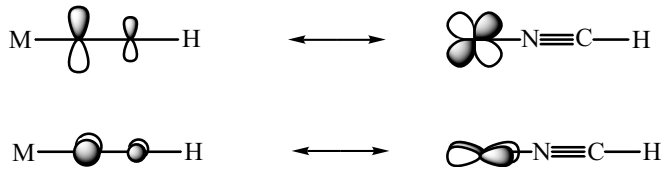

3-6

3.1.3. Perturbation of the *d* orbitals: the general interaction diagram

We now wish to discover how the orbitals of the d block that we have previously obtained, by analysing only the σ interactions (Chapter 2), are modified by the presence of a π donor. These MO, either nonbonding or antibonding, are mainly concentrated on the *d* orbitals of the metal, as this is a rather electropositive element. The orbital involved on a π-donor ligand characterizes either a lone pair located on a very electronegative centre, or a π bond. In all cases, *the p or π orbitals of a π-donor ligand are lower in energy than the d-block orbitals* obtained by considering only the σ interactions.

This relative position of the orbital energies has important consequences for the way in which the d block is perturbed by interaction with a π donor. We shall consider the simplest case, where a nonbonding doubly occupied ligand *p* orbital interacts with a nonbonding metal *d* orbital that is assumed to be empty (Figure 3.1). Due to the relative energies of the interacting orbitals, their bonding combination is mainly concentrated on the ligand, whereas the largest coefficient in the antibonding combination is on the metal. Which of these two orbitals is the one that we shall consider a member of the d block? To make our choice, we use the same criterion as that previously adopted when examining σ-type interactions (see, for example, Chapter 2,

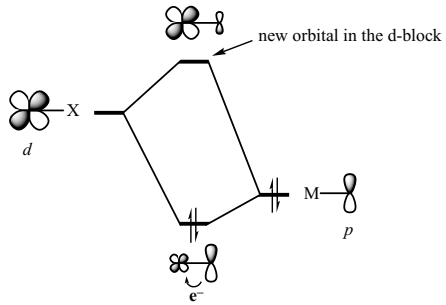

Figure 3.1. Sketch of the interaction between the doubly occupied orbital on a π-donor ligand (X) and an empty *d* orbital on the metal centre.

§ 2.1.2.4): it is the molecular orbital that is mainly concentrated on the metal *d* orbital, that is, the *antibonding combination* of the interacting orbitals. The bonding molecular orbital, as we have seen, is mainly concentrated on the ligand.

> Rule: the π interaction between a d-block orbital and the orbital of a π donor leads to a *destabilization* of the d-block orbital, by mixing with the ligand orbital *in an antibonding sense*.

Figure 3.1 also enables us to obtain further insight into the concept of a π-donor ligand. Before the interaction, the *d* orbital on the metal is empty but the *p* orbital localized on the π donor contains two electrons. After the interaction, these electrons occupy the bonding molecular orbital which is partially delocalized onto the metal. This delocalization of the occupied MO on to the two centres results in a partial electron transfer from the ligand to the metal centre, a result which is quite consistent with the label of π donor attached to the ligand. The interaction is stabilizing, since it involves two electrons (Chapter 1 § 1.3.2).

However, the *d* orbital on the metal centre is not necessarily always empty. In fact, the occupation of this orbital depends on the d^n electronic configuration of the complex, and it is quite possible for it to be doubly occupied. In that case, the π interaction is destabilizing on balance, since it involves four electrons, and moreover the electron transfer from the ligand to the metal in the bonding MO is now compensated by electron transfer from the metal to the ligand in the antibonding MO (**3-7**): overall, there is no longer any electron transfer between the two centres.

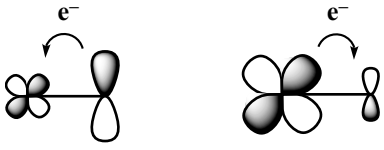

3-7

In this case, therefore, the ligand can no longer play the role of a π donor, since there is now no empty *d* orbital on the metal into which some of its electron density can be transferred. However, this ligand is still described as a π donor, to indicate that it possesses at least one π-type orbital that is capable of electron transfer to a metal centre, so long as the latter can act as an acceptor. Notice that the rule given above about the consequences of the interaction with a π-donor ligand on the d block is valid for any d^n electronic configuration of the complex: since the ligand orbital is at lower energy than the *d* orbital with which it interacts, the new *d* orbital, whether it is empty or occupied, is always destabilized by an antibonding interaction with the ligand π orbital.

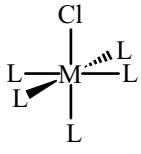

3-8

3.1.4. A first example: the octahedral complex $[ML_5Cl]$

Consider an octahedral complex with one Cl ligand (or any other halogen) which is a double-face π-donor (§ 3.1.2) (**3-8**); the five other ligands only have σ interactions with the metal.

In order to construct the d block of this complex, we start from the orbitals that were obtained by only considering σ interactions, then we perturb them by introducing the π interactions. The d block derived from these σ interactions will be assumed identical to that already established for a fully octahedral complex (ML_6), that is, split into two degenerate groups (t_{2g} and e_g, Chapter 2, § 2.1.2.4). This is of course a simplification, since in an $[ML_5Cl]$ complex, the σ interaction created by one of the L ligands is different from that involving the Cl.[2]

[2] In particular, the orbitals derived from the e_g block of the regular octahedron, where we find the antibonding σ-type interactions with the ligands, are no longer degenerate in the lower-symmetry complex $[ML_5Cl]$.

3.1.4.1. *Perturbation of the d block*

By examining the symmetry properties of the *d* orbitals of the regular octahedron as well as those of the π donor, we can predict which ones will be perturbed by the π interactions. In the case of the $[ML_5Cl]$ complex (**3-8**), it is convenient to use the symmetry planes *xz* (P_1) and *yz* (P_2) (**3-9**).

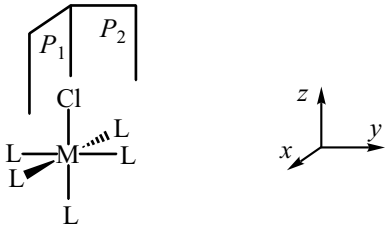

3-9

The *xy* orbital is antisymmetric with respect to the two planes (**AA**), *xz* is symmetric with respect to P_1 but antisymmetric with respect to P_2 (**SA**), while *yz* is antisymmetric with respect to P_1 but symmetric with respect to P_2 (**AS**). The antibonding orbitals, x^2-y^2 and z^2, are symmetric with respect to both planes (**SS**). On the chlorine atom, the lone pairs (p_x and p_y) have **SA** and **AS** symmetries, respectively (**3-10**).

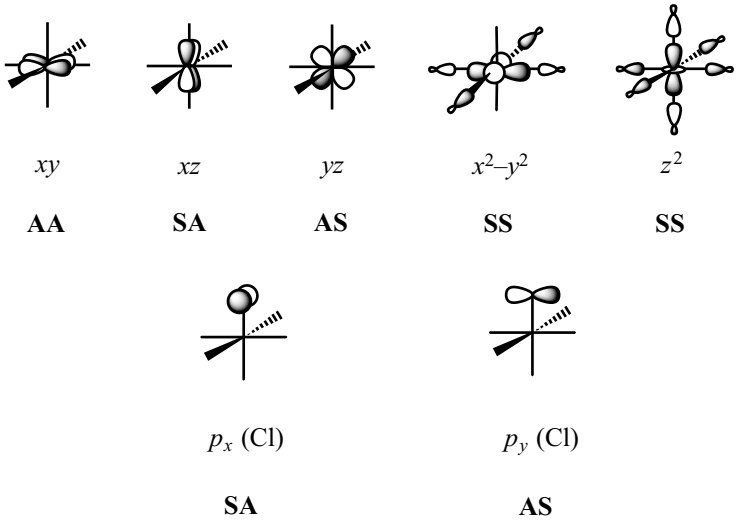

3-10

We can now construct the interaction diagram between the orbitals of the d block and those of the π-donor ligand (Figure 3.2), by combining orbitals with the same symmetry, p_x with *xz*, and p_y with *yz*.

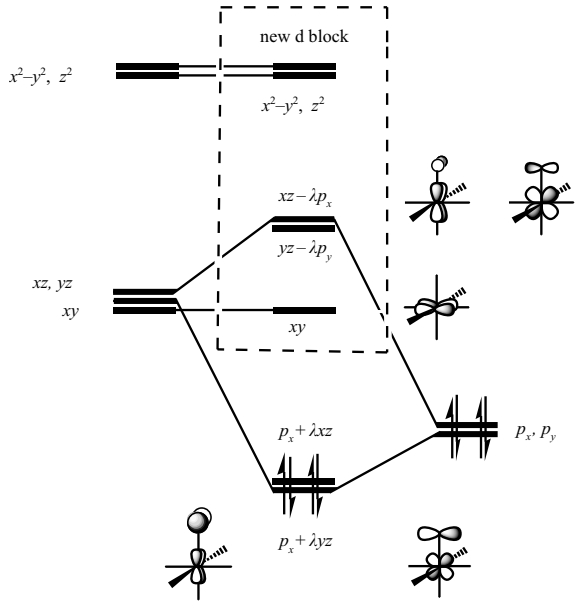

Figure 3.2. Interaction diagram showing the perturbation of the d block of an octahedral complex (σ interactions only, left-hand side) by the two orbitals of a double-face π-donor ligand (Cl, for example, right-hand side). The electronic occupation shown corresponds to a d^0 electronic configuration.

These two interactions are equivalent in the sense that they involve orbitals that are related by a rotation of 90°: xz and yz on the one hand, p_x and p_y on the other. They therefore lead to the formation of two degenerate bonding MO and two antibonding MO that are also degenerate. As we showed in § 3.1.3, the antibonding MO ($xz - \lambda p_x$ and $yz - \lambda p_y$, mainly concentrated on the metal ($\lambda < 1$)),[3] are the ones which belong to the d block of the [ML_5Cl] complex. The presence of a chloride ligand therefore lifts the degeneracy of the three initial orbitals in the t_{2g} block of the octahedron, destabilizing two of them while leaving the third unchanged.

[3] These expressions are not normalized.

The two remaining orbitals in the d block (x^2-y^2 and z^2) are identical to the initial MO derived by considering only the σ interactions, since, by symmetry, they are not involved in the π interactions.[4] The two lowest-energy MO ($p_x + \lambda xz$ and $p_y + \lambda yz$) are mainly localized on the chlorine and characterize the two p lone pairs that are stabilized by a bonding interaction with the d orbitals of the same symmetry. The occupation of the d block naturally depends on the exact nature of the [ML_5Cl] complex; Figure 3.2 corresponds to a complex with a d^0 electronic configuration.

[4] Notice that in the point group of this complex (C_{4v}), the degenerate MO have e symmetry, while xy, x^2-y^2, and z^2 have b_2, b_1, and a_1 symmetries, respectively.

3.1.4.2. *The influence of the electronic configuration on the π-donor character of the Cl ligand*

The interaction scheme given in Figure 3.2 does not depend on the d^n electronic configuration of the [ML_5Cl] complex: starting from the d block of the octahedron, two of the three nonbonding orbitals will always be destabilized while the three other orbitals are unaffected. However, the electron transfer resulting from the π interactions does depend on the electronic occupation of the d block.

In a d^0 complex (Figure 3.2), the two lone pairs p_x and p_y are partially delocalized on to the metal after the interaction (bonding MO $p_x + \lambda xz$ and $p_y + \lambda yz$), and each interaction results in some electron transfer from the ligand to the metal. Since all the other orbitals are empty, there is no transfer in the opposite sense: in an $[ML_5Cl]$ complex with a d^0 electronic configuration, the chloride does indeed play the role of a double-face π-donor. A d^2 complex behaves in the same way: the two electrons in the d block occupy the nonbonding xy orbital after the interaction, and therefore remain completely localized on the metal.

For the d^3–d^6 electronic configurations, the xz and yz orbitals, which were nonbonding before the interaction, are progressively filled, leading to some electron transfer in the opposite direction, from the metal to the ligand. So these orbitals, which were localized on the metal, become partially delocalized onto the chloride ligand after the π interaction (antibonding MO $xz - \lambda p_x$ and $yz - \lambda p_y$). In the limiting case of a low-spin d^6 complex, in which the three lowest d levels are all doubly occupied, the π interactions no longer lead to any electron transfer from the chloride ligand to the metal. The Cl $\rightarrow$ metal transfers in the bonding MO $p_x + \lambda xz$ and $p_y + \lambda yz$ are balanced by the metal $\rightarrow$ Cl transfers in the antibonding MO $xz - \lambda p_x$ and $yz - \lambda p_y$. In other words, the metal in the d^6 electronic configuration has no *empty* orbital available to accept the π electrons of the chloride ligand. Thus, the only consequence of the presence of a double-face π-donor ligand is the destabilization of two of the three nonbonding levels in the octahedron.

3.2. π-acceptor ligands: general properties

3.2.1. The nature of the π orbital on the ligand

π-acceptor ligands are characterized by the existence of at least one empty orbital that can have a π interaction with a d orbital on the metal. If this orbital is empty, it must be fairly high in energy. It may be:

1. A p orbital on a fairly electropositive atom, such as the boron p orbital in boryl complexes or the carbon p orbital in carbene complexes[5] (**3-11**).

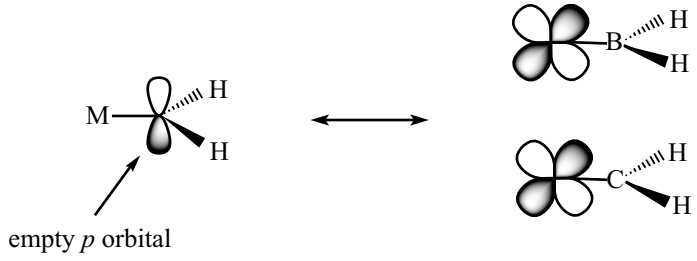

3-11

[5] In this description, the carbene is considered as an L ligand, with two electrons in the $2a_1$ orbital but where the p orbital of b_1 symmetry is empty (see Figure 1.5, Chapter 1, for the MO of a bent AH_2 species). In some cases, it can also be described as an X_2 ligand, with one electron in each of the a_1 and b_1 orbitals (see Chapter 4, § 4.3).

2. A π^* antibonding orbital associated with a π bond between two atoms of the ligand. This orbital is therefore delocalized onto two centres, but its overlap with the metal *d* orbital is large if it is mainly concentrated on the atom that is bonded to the metal. This is what happens when the metal is less electronegative than the second centre involved in the double bond (Chapter 1, § 1.2.2), as is the case, for example, for the formyl ligand HC=O (**3-12**).

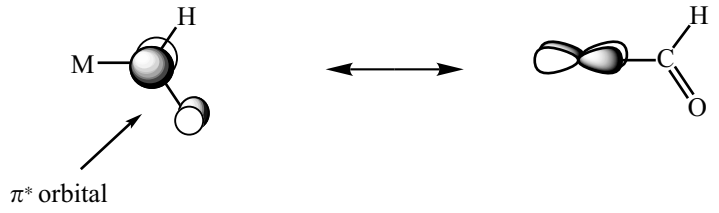

3-12

3.2.2. 'Single-face' and 'double-face' π-acceptors

As for π-donor ligands, we distinguish π-acceptor ligands which possess a single empty *p* or π^* orbital (single-face acceptors) from those which have two, pointing in two perpendicular directions (double-face acceptors). The boryl, carbene (**3-11**), and formyl (**3-12**) ligands, for example, are all in the first category.

Among double-face π-acceptors, we may cite the B—H ligand, with its two nonbonding empty *p* orbitals (Chapter 1, § 1.5.2.2). There is another which is particularly important in organometallic chemistry, the carbonyl ligand, C≡O, which we shall study in this section. The principal molecular orbitals of CO that are involved in the interaction with a metal centre are shown in Figure 3.3 (see Chapter 1, § 1.5.2.4). They are the three highest-energy occupied MO, the π_{CO} bonding orbitals and the nonbonding σ_C orbital that essentially characterizes the lone pair on the carbon atom, and the two lowest-energy empty MO, the π^*_{CO} antibonding orbitals. The π_{CO} orbitals are mainly concentrated on the oxygen, which is the more electronegative centre, and the π^*_{CO} orbitals

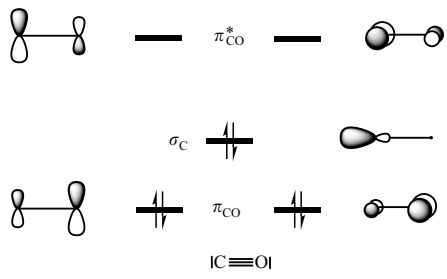

Figure 3.3. Electronic structure of the carbonyl ligand (C≡O): the three highest occupied and the two lowest unoccupied orbitals.

on the carbon. The nonbonding σ_C orbital, which is the highest occupied molecular orbital (HOMO) on the ligand, forms a σ bond with the metal. As a result, the carbonyl ligand usually binds to a transition metal in the η^1 mode, with a linear M−C≡O arrangement that maximizes the σ overlap. The π interactions, that involve both the π_{CO} bonding MO and the π^*_{CO} antibonding MO, are added to this σ interaction. This example illustrates a problem posed by all the ligands with a double or triple bond that are coordinated to the metal in the η^1 mode (i.e. through one of the atoms involved in the multiple bond): using their occupied π orbital(s), they can act as a π donor, whereas their empty π^* orbitals can allow them to act as a π acceptor. Depending on the relative strength of these two interactions, the ligand can act overall either as a π donor or as a π acceptor.

To analyse this probem in the case of the carbonyl ligand (see Appendix C for more details), we consider a linear M−C≡O arrangement and one of the *d* orbitals on M (*yz*, **3-13**) that can interact with the π system of the carbonyl ligand. It is easy to see that this *d* orbital has a non-zero overlap with a pair of π and π^* orbitals on CO, those that are oriented parallel to the *z*-axis, leading to a three-orbital interaction. The $d \leftrightarrow \pi$ and $d \leftrightarrow \pi^*$ interactions (**3-13**), which involve orbitals with different energies, are proportional to $S^2/\Delta\varepsilon$ (Chapter 1, § 1.3.2). They are

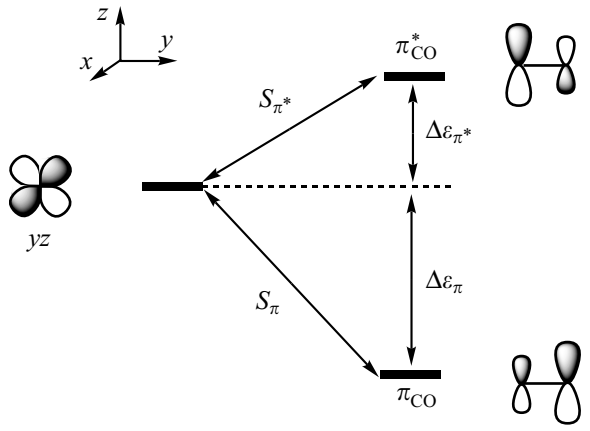

M—C≡O

3-13

therefore strengthened by a small orbital energy difference ($\Delta\varepsilon$) and by a large overlap (*S*). The overlap term clearly favours the interaction with π^*_{CO} ($S^*_\pi > S_\pi$, due to the relative sizes of the coefficients on carbon in the π^*_{CO} and π_{CO} MO). Moreover, it can be shown (see appendix) that the *d* orbital is closer in energy to the antibonding orbital than to the bonding

orbital ($\Delta\varepsilon_\pi^* < \Delta\varepsilon_\pi$, **3-13**) for almost all the transition elements. In the three-orbital interaction scheme shown in **3-13**, both factors, overlap and energy difference, therefore favour the $d \leftrightarrow \pi^*$ interaction. We may therefore simplify the diagram, *by neglecting the relatively weak interaction ($d \leftrightarrow \pi$) and retaining only the dominant interaction ($d \leftrightarrow \pi^*$)*. This latter interaction, which involves an empty orbital on the carbonyl ligand, therefore gives it π-acceptor character.

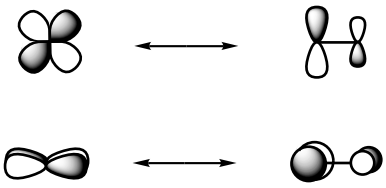

3-14

In this simplified model, we therefore consider that the π interactions with the carbonyl ligand involve only the two π^*_{CO} orbitals; it is thus a *double-face* π-acceptor (**3-14**).

3.2.3. Perturbation of the *d* orbitals: the general interaction diagram

When the unoccupied orbital on the acceptor ligand is a π^* antibonding MO, its energy level is almost always higher than that of the nonbonding or weakly antibonding orbitals in the d block.[6] The same remark may be made about a nonbonding *p* orbital on a very electropositive centre, such as boron in boryl complexes (**3-11**). But the relative orbital energies are less clear when the centre bearing the empty *p* orbital is moderately electronegative, such as carbon in the carbene complexes $[L_nM{-}CR_2]$ (**3-11**). They then depend on the nature of the metal and of the substituents on the carbene ligand (see Chapter 4, § 4.3). At this stage of our analysis, we shall only consider the more common case where the energy level of the *p* or π^* orbitals on the π-acceptor ligand is higher than that of the nonbonding or weakly antibonding orbitals in the *d* block.

As an example, we consider a π-acceptor ligand whose nonbonding *p* orbital interacts with a doubly occupied *d* orbital (Figure 3.4). Due to the relative energies of the initial orbitals, the bonding combination is mainly concentrated on the metal and the antibonding combination on the ligand. As in the preceding examples, the new d-block orbital is mainly concentrated on the metal, that is, in this case, the *bonding* combination of the initial orbitals.

> Rule: the π interaction between a d-block orbital and the orbital of a π-acceptor ligand leads to a *stabilization* of the d-block orbital, by mixing with the ligand orbital *in a bonding sense*.

Figure 3.4 shows the resulting π electron transfer involving the ligand and the metal. Before the interaction, the two electrons were localized in the metal *d* orbital. After the interaction, these electrons occupy the bonding molecular orbital which is partially located on

[6] This point is treated in detail in the appendix for the carbonyl ligand.

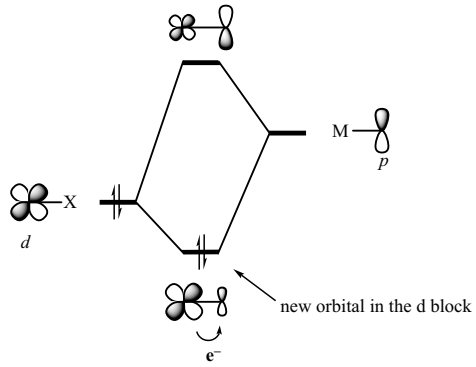

Figure 3.4. Sketch of the interaction between a doubly occupied *d* orbital and the unoccupied orbital of a π acceptor (X).

the ligand. This delocalization is thus accompanied by some electron transfer from the metal to the π-acceptor ligand.

3.2.4. A first example: the octahedral complex [ML_5CO]

3.2.4.1. *Interaction diagram*

We consider an octahedral complex with one carbonyl ligand, a double-face π-acceptor, and five other ligands that only have σ interactions with the metal (**3-15**).

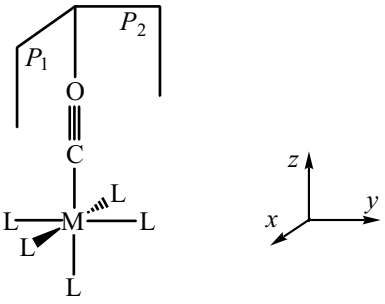

3-15

To construct the d block of this complex, we shall follow the same procedure as that used for a complex with a π donor (§ 3.1.4): we start from the orbitals for an ideal octahedral ML_6 complex in which there are only σ interactions, then we perturb these orbitals by 'switching on' the π interactions with the carbonyl ligand.

We have already established (see **3-10**) the symmetries of the metal *d* orbitals with respect to the planes of symmetry P_1 and P_2 (**3-15**): *xy* (**AA**), *xz* (**SA**), *yz* (**AS**), x^2-y^2 and z^2 (**SS**). Following the analysis developed in § 3.2.2, only the empty antibonding π^*_{CO} orbitals are treated. They are oriented parallel to the *x*- and *y*-axes, and have **SA** and **AS** symmetries, respectively (**3-16**).

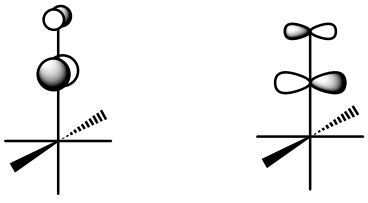

3-16

We can now construct the diagram for the interaction between the orbitals of the *d* block and the π_{CO} orbitals on the carbonyl ligand (Figure 3.5), by combining the π^*_x and *xz* orbitals, with **SA** symmetry, and the π^*_y and *yz* orbitals, with **AS** symmetry. These are two equivalent interactions, since they involve orbitals which are related by a rotation of 90°: (*xz*, *yz*) on the one hand and (π^*_x, π^*_y) on the other. They therefore lead to the formation of two degenerate bonding MO and two antibonding MO that are also degenerate. As shown in § 3.2.3, the bonding MO ($xz+\lambda\pi^*_x$ and $yz+\lambda\pi^*_y$), which are mainly concentrated on the metal, are the orbitals which belong to the d block of the [ML_5CO] complex. The presence of a CO ligand therefore lifts the degeneracy of

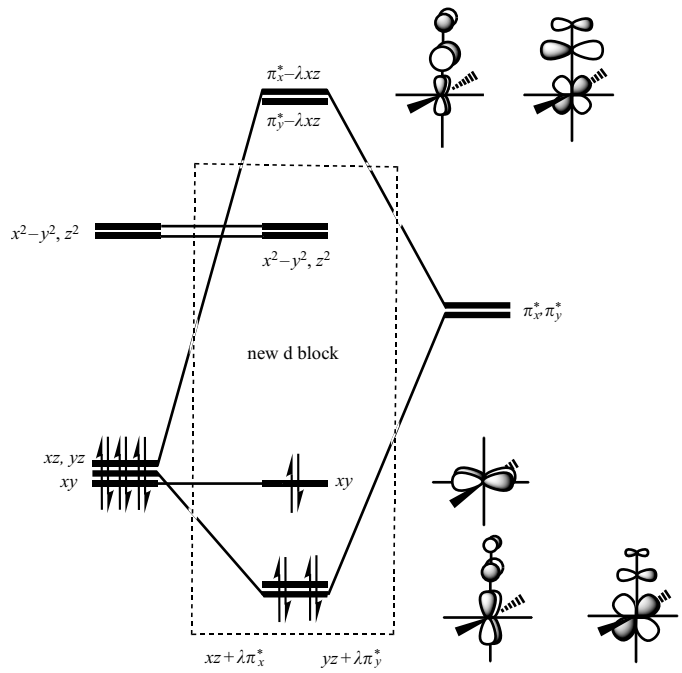

Figure 3.5. Interaction diagram showing the perturbation of the d block of an octahedral complex (left-hand side, σ interactions only) by the two π^*_{CO} orbitals of a carbonyl ligand (right-hand side). The electronic occupation shown corresponds to a complex with a d^6 electronic configuration.

the three orbitals in the original t_{2g} block of the octahedron, stabilizing two of them but leaving the third (xy) unchanged. The two remaining orbitals in the d block (x^2-y^2 and z^2) are identical to the original MO derived for σ interactions only, since they are not affected by the π interactions. Finally, the two highest-energy MO ($\pi_x^*-\lambda xz$ and $\pi_y^*-\lambda yz$) are mainly concentrated on the carbonyl ligand. The occupation of the d block clearly depends on the exact nature of the [ML_5CO] complex; Figure 3.5 corresponds to a complex with a d^6 electronic configuration. Before the interaction, the four electrons stabilized by the π interactions occupied pure metal d orbitals (xz and yz). After the interaction, these orbitals are partially delocalized onto the carbonyl ligand, showing the π-acceptor character of this species.

Comment

The relative position of the σ-antibonding (x^2-y^2, z^2) and the π-antibonding ($\pi_x^* - \lambda xz$ and $\pi_y^* - \lambda yz$) orbitals may be inverted with respect to that shown in Figure 3.5. It depends among other things on the energy gap between the nonbonding (xy, xz, and yz) and the antibonding (x^2-y^2, z^2) orbitals created by the σ interactions.

3.2.4.2. *The metal–carbonyl bond: donation and back-donation interactions*

The σ bond between the carbonyl ligand and the metal centre is formed by the σ_C orbital that characterizes the lone pair on the carbon atom (Figure 3.3) and by a d orbital on the metal (z^2 in the orientation shown

in **3-15**). This interaction, which leads to a transfer of electrons from the ligand to the metal, is called the *donation interaction* (**3-17a**). The π interactions described in Figure 3.5 produce a transfer of electrons in the opposite direction, from the metal to the ligand. These are *back-donation interactions* (**3-17b**). The carbonyl ligand is therefore simultaneously a σ-donor and a π-acceptor.

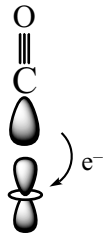

3-17a Donation

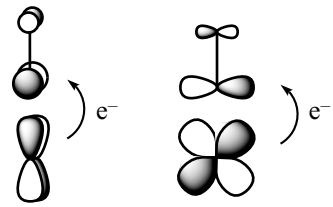

3-17b Back donation

The π interactions reinforce the metal–carbon bond (bonding interactions M—C) but weaken the CO bond (antibonding interactions C—O) (**3-17b**). This electronic reorganization can be represented by the Lewis structures shown in **3-18**.

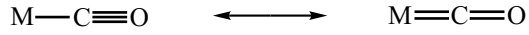

3-18

Experimentally, the metal–carbon bond is observed to be substantially shorter than the value that would be expected for a σ-only bond, by some 0.2–0.3 Å. The result for the CO bond is less clear, as the distances measured for carbonyl complexes fall in the very narrow range of 1.14–1.15 Å. These values are only slightly longer than that found for the free ligand (1.13 Å). The equilibrium CO distance is therefore almost insensitive to the transfer of electrons, an observation that can at least partially be explained by the fact that the difference in length between a triple and a double bond is also relatively small (1.13 and 1.23 Å, respectively). Infrared spectroscopy (IR) provides a far better probe, from the value of the IR absorption frequency associated with the stretching of the CO bond (ν_{CO}). This frequency is related to the strength of the bond and is very sensitive to the electronic population in the π^*_{CO} orbitals. For example, for the isolated ligand it decreases from 2143 to 1489 cm^{-1} on passing from the ground state to the excited electronic state in which an electron has been excited from the nonbonding σ_C orbital to the antibonding π^*_{CO} orbital (Figure 3.3). This is therefore a very sensitive indicator which enables the transfer of metal π electrons to one or several carbonyl ligands to be demonstrated. Thus, ν_{CO} decreases from 2143 cm^{-1} in isolated CO to 2000 cm^{-1} in $[Cr(CO)_6]$, a complex with a d^6 electronic configuration, and even to 1860 cm^{-1} in $[V(CO)_6]^-$, another d^6 complex which, due to its anionic nature, is

particularly effective for the transfer of electron density to π-acceptor ligands.

3.3. Complexes with several π-donor or π-acceptor ligands

In the first example that we considered, there was only a single ligand able to perturb the d block of the complex through π interactions. When several ligands of this type are present, their individual effects are added, destabilizing the *d* orbitals in the case of π-donors (antibonding mixing in the d block) or stabilizing them in the case of π-acceptors (mixing of a bonding type in the d block). However, as we shall see in the following examples, the effect produced by *n* ligands of a given type is not necessarily *n* times larger than that produced by a single ligand. The symmetry properties of the complex may prevent some orbitals, either occupied for π donors or empty for π acceptors, from interacting with the d-block orbitals.

3.3.1. The *trans*-$[ML_4Cl_2]$ octahedral complex

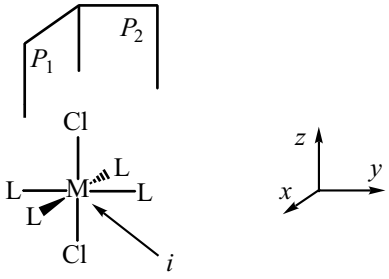

3-19

Consider an octahedral complex of the type $[ML_4Cl_2]$, with two double-face π-donor ligands (Cl) in *trans* positions and four other ligands which only have σ interactions with the metal. Three of the symmetry elements in the complex are shown in **3-19**: the planes P_1 (*xz*) and P_2 (*yz*) and the inversion centre *i*, located on the central atom.

3.3.1.1. *π-type orbitals on the ligands*

Four lone pairs of π-type are available, described by the p_x and p_y orbitals on each chlorine atom. It must be noticed that the *two Cl ligands are equivalent by symmetry*, that is, they are interchanged by at least one symmetry element (e.g. the horizontal plane *xy* or the inversion centre *i*).

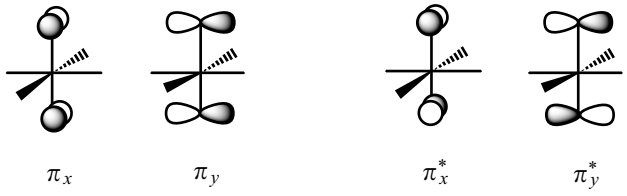

3-20

Rather than consider each of the p_x and p_y orbitals individually, it is therefore preferable to use linear combinations of these orbitals that properly

reflect the symmetry of the complex (Chapter 6, § 6.4). In the case of two equivalent atoms, these are simply 'bonding' and 'antibonding'[7] combinations of the initial orbitals. These are usually indicated by (π_x, π_y) and (π_x^*, π_y^*), respectively (**3-20**), making reference to the nature of the overlap (π) and the orientation of the orbitals (x- or y-axes).

Electronically speaking, these four orbitals are doubly occupied, since they are formed from atomic orbitals that describe π-type lone pairs on each of the chloride ligands. They therefore provide a *delocalized description* of these lone pairs, which is adapted to the symmetry of the complex.

Before constructing the diagram for the interaction between the π orbitals on the ligands and the *d* orbitals on the metal centre, we must analyse the symmetry properties of these orbitals. We shall describe two methods, in which we use either some selected symmetry elements, or the full set of these elements and the machinery of group theory.

[7] The bonding or antibonding character is weak, due to the large separation between the two chlorine atoms. It is perhaps better to replace 'bonding/antibonding' by 'in-phase/out-of-phase', to emphasize only the way in which the initial atomic orbitals are combined.

3.3.1.2. *Taking symmetry into account: initial analysis*

To characterize orbital symmetry, we may, as in the examples already treated (§ 3.1.4 and 3.2.4), use the planes P_1 and P_2 (**3-19**). But we must add a third element to enable us to distinguish the symmetry of the bonding and antibonding combinations that we have constructed above. This additional element might be the xy plane, or it might be the inversion centre i. With respect to this latter element, the $\pi_{x,y}$ orbitals are antisymmetric (**A**) but the $\pi_{x,y}^*$ orbitals are symmetric (**S**) (see **3-21** for the π_y and π_y^* orbitals).

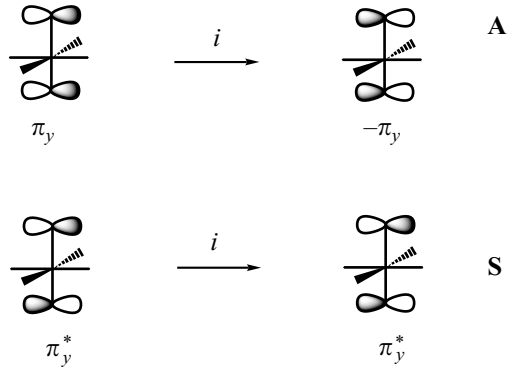

3-21

When we take all three of these elements into account (P_1, P_2, and i), the symmetry labels are **SAA** for π_x, **ASA** for π_y, **SAS** for π_x^*, and **ASS**

for π_y^*; on the metal, they are **AAS** for *xy*, **SAS** for *xz*, **ASS** for *yz*, and **SSS** for both x^2–y^2 and z^2 (**3-22**).

This initial analysis of the symmetry properties shows us that *two of the four lone pair*s of the chloride ligands, those described by the bonding combinations π_x and π_y, *cannot interact with the d-block orbitals*, due to their different symmetry properties ($S = 0$). In the same way, the *xy*, x^2–y^2, and z^2 orbitals on the metal cannot, *by symmetry*, interact with the ligand orbitals. The only interactions that are possible ($S \neq 0$) occur between π_x^* and *xz* on the one hand (symmetry **SAS**), and between π_y^* and *yz* on the other (symmetry **ASS**).

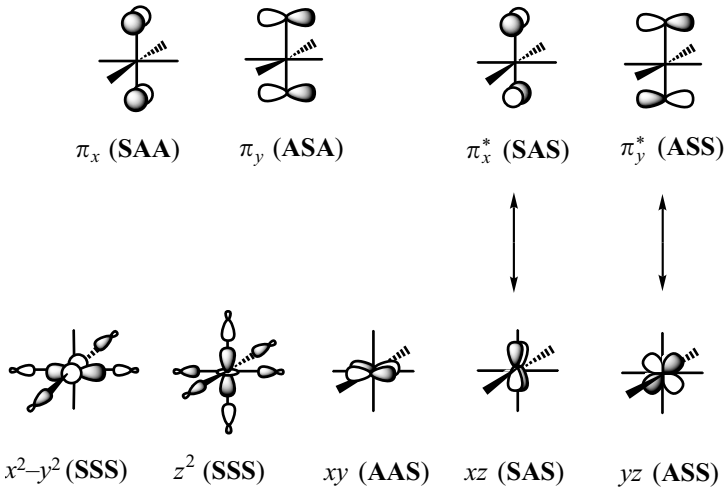

3-22

3.3.1.3. *Taking symmetry into account: the use of group theory*

Rather than select only some symmetry elements present in the system being studied, one can consider all of them by using group theory. This is the most rigorous method—there is no danger of forgetting a symmetry element that might be important for a particular interaction—and it allows us, particularly in high-symmetry systems, to anticipate certain special properties such as the existence of orbitals *that are degenerate by symmetry*. The symmetry elements of the complex studied here are characteristic of the D_{4h} point group (Chapter 6, § 6.2.2 and 6.6.1).

If we consider the two π^* antibonding combinations of the lone pairs, we notice that they are related by a rotation of 90° about the *z*-axis, which is a symmetry element of the system (a C_4-axis). The same applies for the two π-bonding combinations, and also for the *xz* and *yz* orbitals on the metal. These are pairs of orbitals that are degenerate by symmetry in the D_{4h} point group. If we consult the character table for

Table 3.1. Character table for the D_{4h} point group

D_{4h}	E	$2C_4$	C_2	$2C_2'$	$2C_2''$	i	$2S_4$	σ_h	$2\sigma_v$	$2\sigma_d$		
A_{1g}	1	1	1	1	1	1	1	1	1	1		x^2+y^2, z^2
A_{2g}	1	1	1	−1	−1	1	1	1	−1	−1		
B_{1g}	1	−1	1	1	−1	1	−1	1	1	−1		x^2-y^2
B_{2g}	1	−1	1	−1	1	1	−1	1	−1	1		xy
E_g	2	0	−2	0	0	2	0	−2	0	0		(xz, yz)
A_{1u}	1	1	1	1	1	−1	−1	−1	−1	−1		
A_{2u}	1	1	1	−1	−1	−1	−1	−1	1	1	z	
B_{1u}	1	−1	1	1	−1	−1	1	−1	−1	1		
B_{2u}	1	−1	1	−1	1	−1	1	−1	1	−1		
E_u	2	0	−2	0	0	−2	0	2	0	0	(x, y)	

this group (Table 3.1), we notice that it contains two two-dimensional representations, referred to as E_u and E_g, which differ by their behaviour with respect to the inversion centre of the complex (i, located on the central metal): E_g is symmetric (its character in the i column is positive), but E_u is antisymmetric (a negative character). The bonding combinations (π_x, π_y), which are antisymmetric with respect to the inversion centre (**3-21**), have e_u symmetry, but the antibonding combinations (π_x^*, π_y^*), which are symmetric with respect to the inversion centre, have e_g symmetry. The character table also gives us the symmetries of the d orbitals on the metal centre, in the last column: a_{1g} for z^2, b_{1g} for x^2—y^2, b_{2g} for xy, and e_g for (xz, yz).

In the case being examined, we therefore come to the same conclusion as that established in the preceding section from a limited number of symmetry elements: the only interactions that occur concern the (π_x^*, π_y^*) orbitals on the ligands, and (xz, yz) on the metal centre, which constitute two degenerate pairs of orbitals with e_g symmetry in the D_{4h} point group.

3.3.1.4. *The interaction diagram*

We are now in a position to construct the diagram which describes the π interactions in a *trans*-[ML_4Cl_2] complex (Figure 3.6). We shall adopt the notations of group theory to represent the orbitals' symmetries. As in the preceding examples (§ 3.1.4 and 3.2.4), we suppose that the d block of the complex, before the interaction, is similar to that of a regular octahedral complex, with three nonbonding degenerate orbitals (xy, xz, and yz with the axes defined in **3-19**) and two degenerate antibonding orbitals, x^2—y^2 and z^2 (left-hand side of Figure 3.6). The first three orbitals, which formed the t_{2g} block in the regular octahedron, have b_{2g} (xy) and e_g (xz, yz) symmetries in the D_{4h} point group. The symmetries of the antibonding orbitals derived from the e_g block in the octahedron become

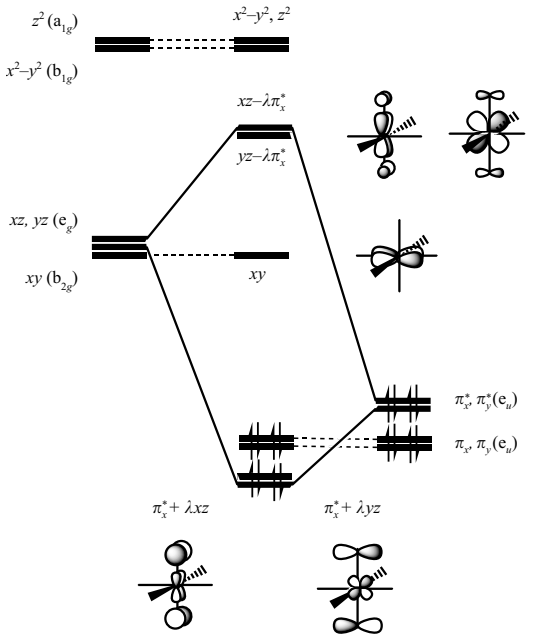

Figure 3.6. Interaction diagram showing the perturbation of the d block of an octahedral complex (σ interactions only, left-hand side) by the lone pairs of two double-face π-donor ligands (Cl, for example, right-hand side) in *trans* positions. The electronic occupation shown corresponds to a complex with a d^0 electronic configuration.

a_{1g} for z^2 and b_{1g} for x^2—y^2. The occupation of these orbitals depends on the d^n electronic configuration of the complex, the example given in Figure 3.6 corresponding to a d^0 complex whose d block is empty. We find the π-type orbitals of the chlorine atoms on the right-hand side of the figure (**3-20**). The e_u bonding combinations are placed slightly lower in energy than the e_g antibonding combinations, though the energy difference is only slight, due to the large separation between the two centres. The energies of these four orbitals are therefore close to that of a pure *p* orbital on chlorine. As a result, they are placed at a lower energy level than the nonbonding *d* orbitals on the metal. Notice that these π and π^* orbitals are all doubly occupied, and that they offer a delocalized description of the four π-type lone pairs on the chloride ligands (two per ligand).

For symmetry reasons, as we have already established, the two lone pairs described by the orbitals with e_u symmetry (**3-20**) cannot interact with the d-block orbitals. The only interactions that are possible ($S \neq 0$) occur between the lone pairs with e_g symmetry and the (*xz*, *yz*) orbitals on the metal (Figure 3.6). This interaction stabilizes four electrons from the lone pairs (the $\pi_x^* + \lambda xz$ and $\pi_y^* + \lambda yz$ orbitals, mainly concentrated on the Cl ligands) but destabilizes two of the three octahedral nonbonding orbitals ($xz - \lambda\pi_x^*$ and $yz - \lambda\pi_y^*$, mainly concentrated on the metal). This destabilisation is larger than that produced by a single chloride ligand ([ML_5Cl] complex, Figure 3.2) since there are now *two* π*-type antibonding interactions* for each of these orbitals. Two of the lone pairs, and therefore four electrons, are not affected by these interactions.

The new d block of the complex, as always, contains five orbitals that are mainly composed of the *d* orbitals on the metal: *xy*, nonbonding, $xz - \lambda\pi_x^*$ and $yz - \lambda\pi_y^*$, π antibonding, and $x^2 - y^2$ and z^2, σ antibonding.

This example shows us that for symmetry reasons, the π interactions are not simply additive when the number of ligands is increased. Two lone pairs are involved in both the monochloro octahedral complex (Figure 3.2) and the *trans* dichloro complex, although four lone pairs are a priori available in the latter case. The difference between the two complexes concerns the magnitudes of the destabilization of the *xz* and *yz* orbitals of the d block and the stabilization of the lone pairs that take part in the interactions, both of which are larger in the dichloro compound. It must also be noted that for a given type of complex (octahedral, for example) and a given number of π-donor (or -acceptor) ligands, the symmetry properties of the complex, and therefore the metal–ligand interactions which occur, also depend on the arrangement of these ligands. This point is illustrated in Exercise 3.4, which concerns an octahedral $[ML_4Cl_2]$ complex in which the two chloride ligands are now in *cis* positions.

3.3.2. The *trans*-$[ML_4(CO)_2]$ octahedral complex

This complex has the same symmetry as the preceding one (the D_{4h} point group). Since the carbonyl groups are π-acceptors, we consider the two empty π_x^* and π_y^* orbitals on each, and these are combined in pairs to form the symmetry-adapted orbitals for the complex (**3-23**). The bonding combinations, ($\pi_x^{*(+)}$ and $\pi_y^{*(+)}$), which are antisymmetric with respect to the inversion centre, have e_u symmetry, whereas the antibonding combinations, ($\pi_x^{*(-)}$ and $\pi_y^{*(-)}$), which are symmetric with respect to this operation, have e_g symmetry.

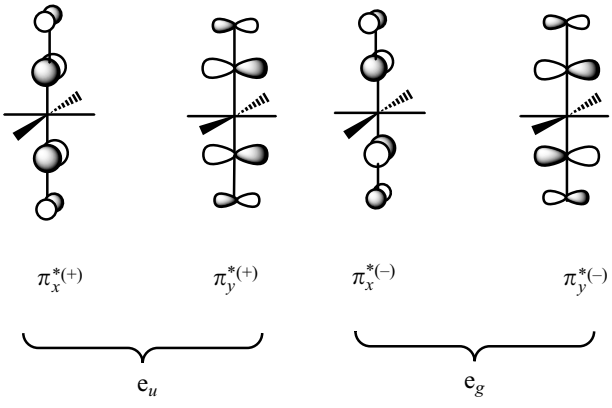

3-23

Since the overlaps between the π_x^* (or π_y^*) orbitals are very small, due to the large distance between the ligands, the energies of the bonding

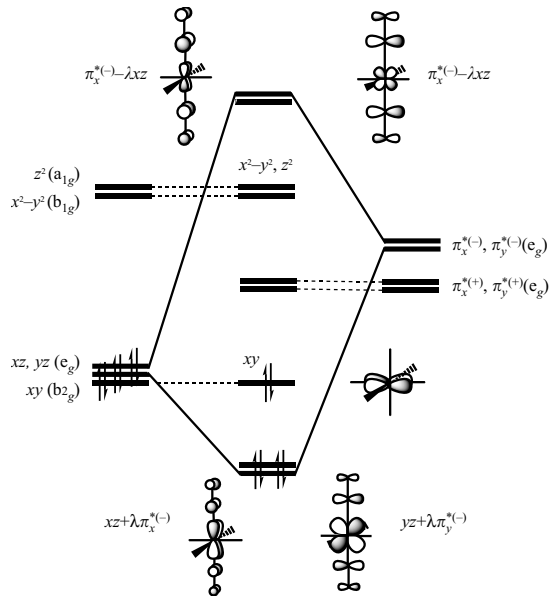

Figure 3.7. Interaction diagram showing the perturbation of the d block of an octahedral complex (σ interactions only, left-hand side) by the π^* orbitals of two double-face π-acceptor carbonyl ligands (right-hand side) in *trans* positions. The electronic occupation shown corresponds to a complex with a d^6 electronic configuration.

(e_u) and antibonding (e_g) combinations are close to that of a π^* orbital in an isolated carbonyl ligand. As a result, they are higher in energy than the nonbonding *d* orbitals on the metal, with the e_u orbitals being very slightly more stable than the e_g (Figure 3.7, right-hand side). These four orbitals are, of course, empty. On the left-hand side of the figure, we find the *d*-block orbitals, assumed to be those of a regular octahedron without any π interactions. The occupation of these orbitals depends on the electronic configuration of the complex that is considered. In Figure 3.7, we are concerned with a d^6 complex. As in the preceding complex, only two of the four π-type orbitals on the ligands—the e_g orbitals—and two nonbonding orbitals on the metal (*xz* and *yz*, which also have e_g symmetry) can interact. This interaction therefore stabilizes those two d-block orbitals ($xz + \lambda\pi_x^{*(-)}$ and $yz + \lambda\pi_y^{*(-)}$, mainly concentrated on the metal), whereas the antibonding combinations are mainly concentrated on the ligands ($\pi_x^{*(-)} - \lambda xz$ and $\pi_y^{*(-)} - \lambda yz$). The new d block therefore consists of the following orbitals: $xz + \lambda\pi_x^{*(-)}$ and $yz + \lambda\pi_y^{*(-)}$, which are π-bonding, *xy* (nonbonding), and x^2–y^2 and z^2, which are σ-antibonding.

In the case of a d^6 complex, four electrons from the d block are stabilized. The stabilization is larger than that produced in the complex with just one carbonyl ligand (Figure 3.5), since there are two π-bonding interactions in each orbital stabilized instead of only one.

3.3.3. Construction of the d-block orbitals 'by hand'

The relative energies of the π-type ligand orbitals and the metal *d* orbitals control the nature of the two interactions that occur in the d block: (*i*) an

antibonding interaction with the occupied orbital of a π-donor, which destabilizes the *d* orbital; (*ii*) a bonding interaction with the empty orbital of a π-acceptor which stabilizes the *d* orbital. The shape of the perturbed *d* orbitals can easily be obtained when there is a single ligand with a π system: one only needs to combine the *d* orbital and the π-type orbital with which it can overlap, in a bonding manner for an acceptor but in an antibonding sense for a donor. When there are two ligands of this type, we need first to construct the symmetry-adapted π MO for the complex, and then decide which of these could interact with the d orbitals. Once this is done, the same rules are applied for the perturbation of the *d* orbitals by the symmetry-adapted orbitals on the ligands: an antibonding mixing with destabilization for π-donors, but a bonding mixture with stabilization for π-acceptors (Figures 3.6 and 3.7). In the two complexes we have studied, the shapes of the symmetry-adapted orbitals are obvious (§ 3.3.1 and 3.3.2), but it can be much more difficult to obtain them in other cases (see, for example, Chapter 6, § 6.6.6 and Exercise 6.13). We now consider whether it is always necessary, for each type of complex (octahedral, TBP, square-planar, etc.) and for each type of substitution, to determine the symmetry-adapted combinations of ligand orbitals before being able to discover the shapes of the perturbed *d* orbitals. In principle, it is indeed necessary to work in stages, along those lines, but we are now going to show, starting from the two preceding examples, how the main thrust of the information can be obtained more quickly.

3.3.3.1. *The* trans-$[ML_4Cl_2]$ *and* trans-$[ML_4(CO)_2]$ *complexes revisited*

The $d \leftrightarrow \pi$ interactions due to a single Cl ligand were studied in the monochloro complex ($[ML_5Cl]$, Figure 3.2). If we now re-examine the d-block orbitals of the dichloro complex *trans*-$[ML_4Cl_2]$ (Figure 3.6), we notice, but after the event, that we could have obtained them directly by considering successively the contributions expected for each of the two ligands, that is, by proceeding in two stages, as shown in **3-24**.

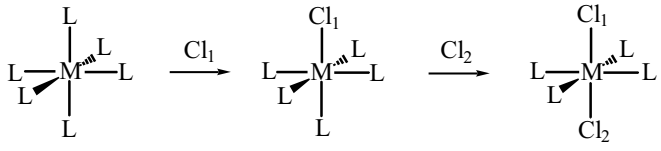

3-24

The interactions of the lone pairs $p_x^{(1)}$ and $p_y^{(1)}$ of the first substituent Cl_1 leave the *xy*, x^2-y^2, and z^2 orbitals unchanged (zero overlaps),

whereas *xz* and *yz* are destabilized by antibonding interactions with $p_x^{(1)}$ and $p_y^{(1)}$, respectively (non-zero overlaps). Analogous observations can be made for the second substitution by Cl_2, since the same overlaps are involved when we consider the $p_x^{(2)}$ and $p_y^{(2)}$ lone pairs. This two-stage decomposition of the construction of the d-block orbitals for the *trans*-$[ML_4Cl_2]$ complex is illustrated in **3-25** for the three initially nonbonding orbitals of the octahedron. The *xy* orbital which cannot interact with any of the lone pairs is unchanged, whereas the *xz* and *yz* orbitals are destabilized in the same way (two equivalent antibonding interactions).

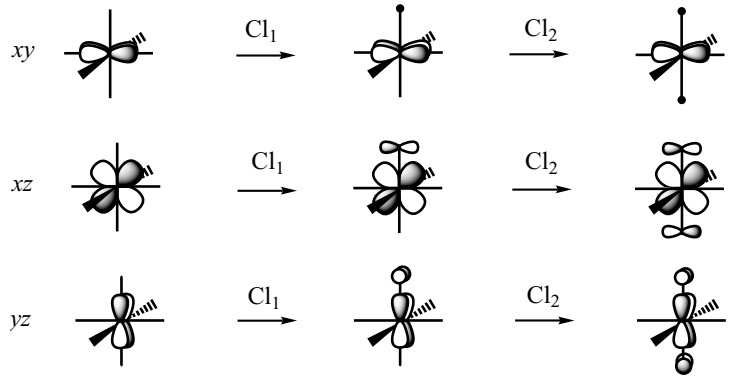

3-25

On can proceed in the same way for the *trans*-$ML_4(CO)_2$ complex, the only difference being that the mixing with the π^*_{CO} orbitals occurs in a bonding sense (π acceptor) (**3-26**).

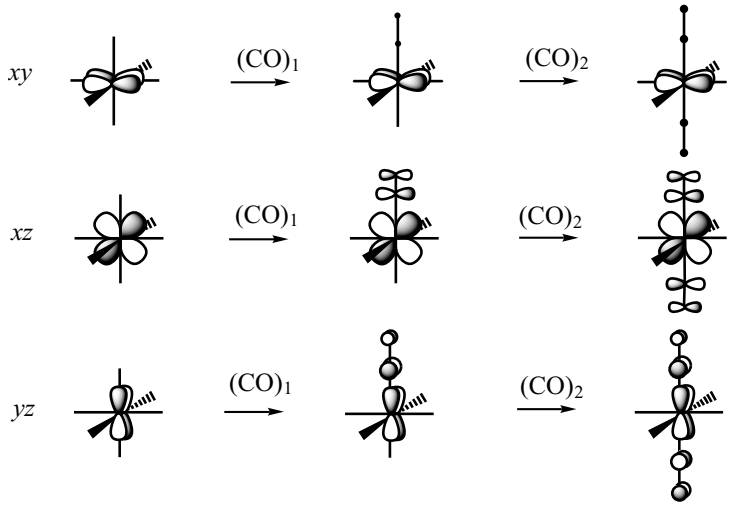

3-26

3.3.3.2. mer-[$ML_3(CO)_3$] *complexes*

We shall now apply this method 'by stages' to a new octahedral complex with three carbonyl ligands and three other ligands that only have σ interactions with the metal. The arrangement chosen for the ligands is indicated in **3-27**. Of the two possible isomers for an [$ML_3(CO)_3$] complex, this one is the *mer* isomer, in contrast to the *fac* isomer in which the carbonyl ligands are placed at the three vertices that make up a face of the octahedron. On the C_1O_1 and C_3O_3, carbonyl ligands, the π^* orbitals point parallel to the *x*- and *z*-axes, whereas on the central ligand C_2O_2 they are parallel to the *x*- and *y*-axes (**3-27**). We now examine how each of the octahedral orbitals can overlap with the π^* orbitals on the carbonyl ligands.

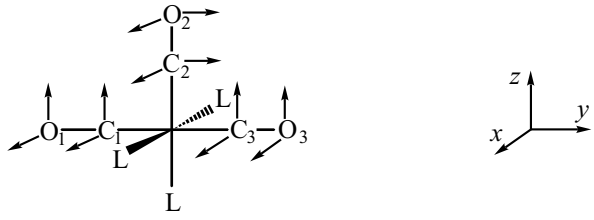

3-27

The x^2-y^2 and z^2 orbitals have zero overlap with all the π^* orbitals, as in the preceding complexes. These orbitals (σ antibonding) are therefore not perturbed by the π interactions. It is only the nonbonding *xy*, *xz*, and *yz* orbitals, derived from the t_{2g} block of the regular octahedron, that will be perturbed.

We consider first the *xy* orbital (**3-28**). Its overlap with $\pi_x^{*(1)}$ is nonzero, but it is zero with $\pi_z^{*(1)}$, located in a nodal plane of *xy*. As a result, *xy* is stabilized by a bonding interaction with $\pi_x^{*(1)}$. This analysis allows us to anticipate an equivalent interaction with the $\pi_x^{*(3)}$ orbital on the symmetry-related ligand C_3O_3. But the two orbitals $\pi_x^{*(2)}$ and $\pi_y^{*(2)}$ on the central ligand C_2O_2 are both located in the nodal planes of *xy* (*xz* and *yz*, respectively), and their overlap with *xy* is zero (**3-28**). We conclude that *xy* is *stabilized by two bonding interactions*, with $\pi_x^{*(1)}$ and $\pi_x^{*(3)}$ (**3-31a**).

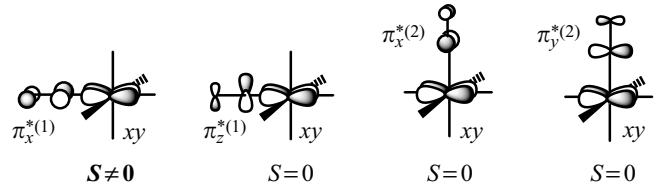

3-28

The *yz* orbital can interact with $\pi_z^{*(1)}$ on C_1O_1, but not with $\pi_x^{*(1)}$ which is located in one of its nodal planes (*xy*) (**3-29**). The same remarks may be made about the group C_3O_3. On the central carbonyl C_2O_2, $\pi_y^{*(2)}$ is the only orbital whose overlap with *yz* is non-zero. The *yz* orbital is therefore stabilized by *three bonding interactions*, with $\pi_z^{*(1)}$, $\pi_y^{*(2)}$, and $\pi_z^{*(3)}$ (**3-31b**). Notice that the contributions of $\pi_z^{*(1)}$ and $\pi_z^{*(3)}$ are equal in magnitude, by symmetry, but the contribution of $\pi_y^{*(2)}$ on the central carbonyl C_2O_2 may be different, since it is not exchanged with the two other groups by any symmetry element in the complex.

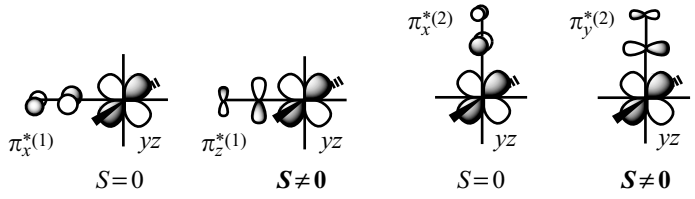

3-29

The *xz* orbital cannot interact with any of the orbitals on the C_1O_1 and C_3O_3 groups, and can combine only with the $\pi_x^{*(2)}$ orbital on the central group C_2O_2 (**3-30**). Therefore, the *xz* orbital is *stabilized by a single bonding interaction*, with $\pi_x^{*(2)}$ (**3-31c**).

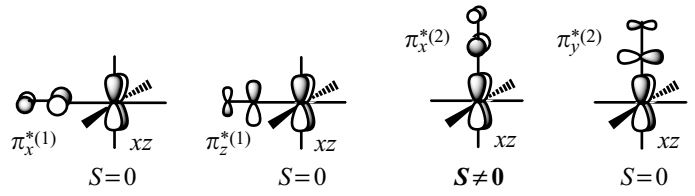

3-30

We see, therefore, that the three nonbonding orbitals derived from the t_{2g} block of the regular octahedron are perturbed in different ways in the substitution pattern that we have studied (**3-31**). All the $d \leftrightarrow \pi^*$ interactions concern the same lateral overlap between a pure *d* orbital and a π^*_{CO} orbital, but the number of interactions changes from one orbital to another.

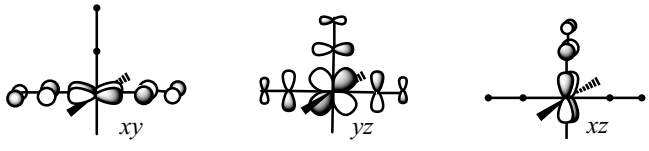

3-31a **3-31b** **3-31c**

As a consequence, the degeneracy of the three orbitals is lifted in this substitution pattern. We can anticipate that *yz*, stabilized by three bonding interactions with the π^*_{CO} orbitals, is lower in energy than *xy* (two bonding interactions), which in turn is lower than *xz* (only a single bonding interaction) (**3-32**). Part of the complete diagram for the interaction of these three *d* orbitals and the π^*_{CO} orbitals has therefore been obtained. Moreover, it is the most important part, since it gives us the three new *d* orbitals that may be occupied in this strong-field octahedral complex. It is straightforward to derive the missing parts of this diagram. Three antibonding combinations, mainly concentrated on the carbonyl groups, correspond to the three bonding combinations described in **3-31**. We note that three linear combinations of the π^*_{CO} orbitals have been used in these interactions. Since initially there were six π^*_{CO} orbitals, two per ligand, three other combinations have not interacted; they remain entirely localized on the ligands, at an energy level close to that of an isolated π^*_{CO} orbital.

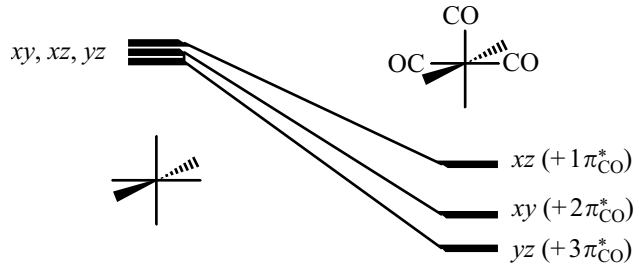

3-32

3.3.3.3. *A rigorous or an approximate method?*

The method we have used has consisted in analysing successively the possible interactions for each of the ligands with a π system. This method, which can be applied in the same way to any type of complex with any substitution pattern (see Exercises 3.1–3.5), enables us to obtain rather quickly the shapes of the *d* orbitals as perturbed by the π interactions, as well as their relative energies. The use of group theory, which requires us in each case to construct the symmetry-adapted orbitals on the ligands, is more time-consuming. But is there really a fundamental difference between the two methods? The application of group theory is based on the symmetry elements of the complex as a whole; this is the rigorous way to proceed. However, the construction 'by hand' that has been proposed in the two preceding sections uses local symmetry elements shared by a *d* orbital and a particular π^* orbital, to deduce whether interaction is possible between them (Schemes **3-28**–**3-30**). The two methods fuse when the symmetry elements of the complex and the local

symmetry elements used are identical. This is the case, for example, for the *trans*-$[ML_4Cl_2]$ and *trans*-$[ML_4(CO)_2]$ complexes (§ 3.3.3.1) and for the *xy* and *yz* orbitals of the *mer*-$[ML_3(CO)_3]$ complex. However, in this latter case, we used a local symmetry element that is not a symmetry element of the complex. Use of the horizontal plane *xy* allows us to show that the overlap between $\pi_x^{*(1)}$ and *xz* is zero (**3-30**, left-hand side), and we concluded that $\pi_x^{*(1)}$ makes no contribution to the *xz* orbital (**3-31c**). This conclusion is not rigorous, since the *xy* plane is not a symmetry element for the complex as a whole. Fortunately, calculations show that the participation of $\pi_x^{*(1)}$ in this orbital is very small (as is that of $\pi_x^{*(3)}$, by symmetry), precisely because the local overlap between $\pi_x^{*(1)}$ and *xz* is zero. The approximate description of the *d* orbitals given in **3-31** is thus essentially correct.

3.3.4. $[MCl_6]$ and $[M(CO)_6]$ octahedral complexes

When the six double-face π-donor or π-acceptor ligands are identical, octahedral symmetry is preserved. We therefore find the usual splitting pattern in the d block, into two groups of degenerate orbitals, whose symmetries are t_{2g} and e_g. We shall now use the method set out in the preceding section to determine the shapes of the MO and the energetic consequences of the π interactions.

3.3.4.1. *The d block in* $[MCl_6]$ *and* $[M(CO)_6]$ *complexes*

In the $[MCl_6]$ complex, each orbital in the t_{2g} group (*xy*, *xz*, and *yz*) can interact with four of the *p* orbitals that characterize lone pairs on the ligands (**3-33**). All the interactions are antibonding (π-donor ligands); they destabilize the three orbitals in an equivalent way, so these remain degenerate.

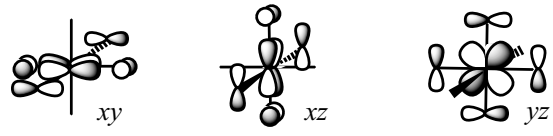

3-33

It is easy to verify that the orbitals in the e_g group (z^2 and x^2-y^2) have zero overlap with all the nonbonding *p* orbitals on the ligands, so their energy and shape remain unchanged. The symmetry properties of the octahedral complexes $[MCl_6]$ therefore allow only three linear combinations of the nonbonding *p* orbitals on the chloride ligands, those shown in **3-33**, to interact with the d-block orbitals. In other words,

only three lone pairs out of the twelve (two per ligand) can transfer electron density to the metal centre; we shall return to this point in § 3.5, Figure 3.10.

By an exactly analogous analysis, it can be shown that in the case of six carbonyl ligands, the three orbitals in the t_{2g} block are stabilized to the same extent by four bonding interactions with the π^*_{CO} orbitals (**3-34**), though the two e_g orbitals are not affected.

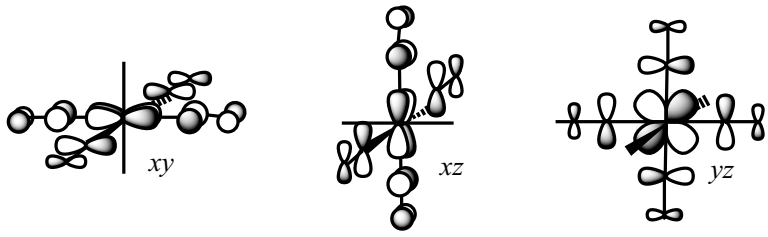

3-34

3.3.4.2. *Strong-field and weak-field complexes*

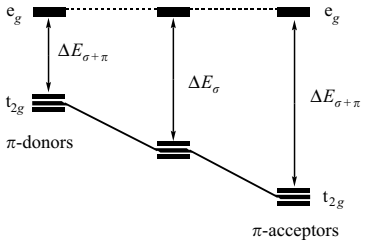

Figure 3.8. Perturbation of the d block (in the centre, σ interactions only) of an octahedral complex ML_6 by the π interactions with double-face π-donor ligands (L = Cl, for example) on the left, and double-face π-acceptor ligands (L = CO, for example) on the right.

The energetic consequences of the π interactions for the d-block orbitals in the $[MCl_6]$ and $[M(CO)_6]$ complexes are shown in Figure 3.8. If everything else is equal, the σ interactions in particular, the presence of π-donor ligands decreases the energy separation (ΔE) between the t_{2g} and e_g orbitals (weak field), whereas π-acceptor ligands increase this separation (strong field). This trend is consistent with the spectrochemical series presented below, which, from measurements of the *d–d* transition energies ($t_{2g} \rightarrow e_g$), ranks ligands according to the strength of the field that they create (Chapter 2, § 2.1.2.6). It is clear that π-donor ligands, such as the halogens, are found at the beginning of the series (weak field), whereas π-acceptor ligands, such as carbonyl or cyanide, are at the end (strong field). For example, ΔE decreases from 26,600 to 15,060 cm^{-1} passing from $[Cr(CN)_6]^{3-}$ (six π-acceptor ligands) to $[CrF_6]^{3-}$ (six π-donor ligands), even though these two complexes have the same d^3 electronic configuration.

$$I^- < Br^- < Cl^- < F^- < OH^- < O^{2-} < H_2O < NH_3 < NO_2^- < CH_3^- < C_6H_5^- < CN^- < PR_3 < CO \qquad (3.1)$$

Notice, however, that the π interactions are not the only factor which influences the $t_{2g} - e_g$ energy separation. We must remember that the σ interactions create the primary *d*-orbital splittings, and that as these interactions become stronger (phosphine ligands PR_3, metal–carbon bonds in organometallic complexes, for example), the antibonding e_g levels are pushed to ever higher energy.

3.4. π complexes: the example of ethylene

In all of the preceding examples, the ligands that possess a π system are bound to the metal centre by a single atom (coordination mode η^1). The situation is different when several ligand atoms are bound in an equivalent way to the metal centre. In particular, this is the case for π complexes (Chapter 1, § 1.1.1.3), in which the π system of the ligand 'points' in the direction of the metal, rather than being perpendicular to the metal–ligand bond. The description of the metal–ligand bonds now requires us to take all the π orbitals of the ligand into account, both occupied and empty, as well as the orbitals of appropriate symmetry on the metal. As an example, we shall first consider the simplest complex from this family, that in which a molecule of ethylene is bound to the metal in the η^2 mode.

3.4.1. Orbital interactions: the Dewar–Chatt–Duncanson model[8]

[8] J. Chatt, L. A. Duncanson *J. Chem. Soc.* 2939 (1953); M.J.S. Dewar *Bull. Soc. Chim. Fr.* 18, C79 (1951).

3.4.1.1. *σ or π interactions?*

We consider first the π-bonding orbital on ethylene. It can interact with a metal orbital, for example, z^2 (**3-35**). The resulting overlap is intermediate between an axial overlap, normally associated with a σ interaction, and a lateral overlap which corresponds to a π interaction. Notice that there is no nodal surface that is common to the two orbitals, and that their overlap is not changed by a rotation of the ligand around the *z*-axis. As a consequence, even though the ligand orbital is of π type, the metal–ligand interaction in which it is involved has the characteristics of an ordinary σ interaction (see **3-17a**, for example). The π^* orbital can also interact with a metal *d* orbital, for example, *xz* (**3-36**). As in the 'traditional' π interactions described in preceding sections, the two orbitals have a common nodal plane (*yz*), and a rotation of the ligand around the *z*-axis decreases their overlap, to the extent that it is completely eliminated for a rotation of 90°. The interaction that involves the π^* orbital can therefore be described as a π interaction.

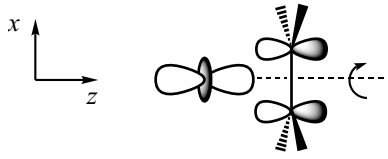

3-35

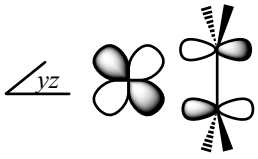

3-36

3.4.1.2. *The Dewar–Chatt–Duncanson model*

Ethylene behaves as an L-type ligand thanks to its doubly occupied π orbital. It can transfer electron density to the metal (a *donation* interaction) by interaction with an empty orbital on the metal centre, whose symmetry is suitable (z^2, for example, **3-37a**). This is a stabilizing two-electron interaction, which stabilizes the π level of the ligand. Due to the relative energies of the two initial orbitals, the occupied MO is mainly concentrated on the ligand (a bonding orbital).

There is a second interaction that involves the empty antibonding π^* orbital and the metal *d* orbital with the same symmetry (*xz*), which is lower in energy than the π^* orbital (**3-37b**). If this latter orbital is doubly occupied, this interaction is stabilizing, and it leads to a transfer of electron density from the metal to the ligand. This is therefore a *back-donation* interaction, where ethylene plays the role of a π acceptor, using its empty π^* orbital. The doubly occupied orbital, mainly concentrated on the metal, is part of the d block of the complex; it can be described as a metal *d* orbital that is stabilized by a bonding interaction with the π^* orbital on ethylene.

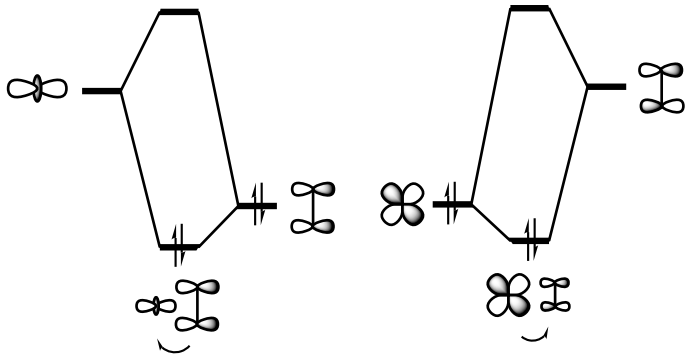

3-37a **3-37b**

These two stabilizing interactions taken together constitute the Dewar–Chatt–Duncanson model of the bond between an olefin and a metal centre.

3.4.2. Electronic structure of a d^6 complex $[ML_5(\eta^2\text{-}C_2H_4)]$

3.4.2.1. *The complete interaction diagram*

Consider a pseudo-octahedral d^6 complex of the type $[ML_5(\eta^2\text{-}C_2H_4)]$ (**3-38**), where the five L ligands are supposed to have only σ interactions with the metal centre. If this complex is decomposed into a d^6 fragment ML_5, with a square-base pyramidal (SBP) geometry, and an ethylene fragment, the interaction between the orbitals on the two fragments enables us to analyse the electronic factors that are at the origin of the ethylene–metal bond.

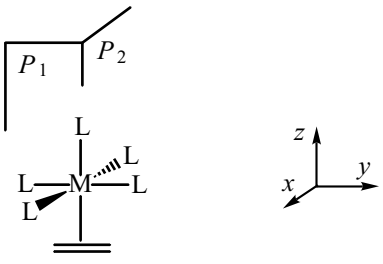

3-38

On the metallic fragment ML_5, we consider the four low-energy *d* orbitals in this type of structure (Chapter 2, § 2.3.1), together with the π and π^* orbitals on the ethylene ligand. The π orbital is doubly occupied, as are the three strictly nonbonding *d* orbitals of the d^6 fragment ML_5.

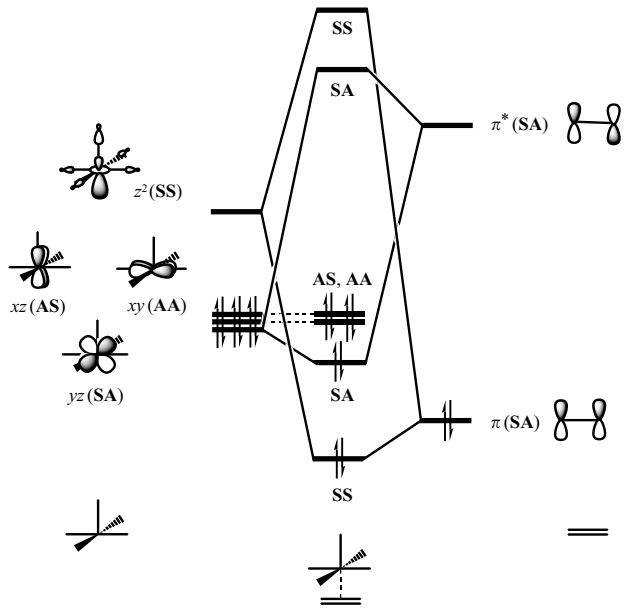

Figure 3.9. Diagram for the interaction between the d orbitals of a d^6ML_5 fragment and the π and π^* orbitals on an ethylene ligand (the Dewar–Chatt–Duncanson model).

Given the orbitals' symmetry properties with respect to the planes P_1 and P_2 that are defined in **3-38**, we obtain the interaction diagram shown in Figure 3.9. The π orbital (**SS**) is stabilized by a bonding interaction with the polarized z^2 orbital (**SS**) on the metallic fragment. The doubly occupied yz orbital (**SA**) is stabilized by a bonding interaction with the π^* orbital (**SA**). The two other d orbitals (xy (**AA**) and xz (**AS**)) are not affected by the interaction.[9] The two stabilizing interactions, donation ($\pi \rightarrow z^2$) and back-donation ($yz \rightarrow \pi^*$), are thus indeed those that were described in a general way in the preceding section.

[9] In the C_{2v} point group of the complex, the symmetry labels are a_1 (**SS**), a_2 (**AA**), b_1 (**AS**), and b_2 (**SA**).

The MO of the complex that are shown in Figure 3.9 can therefore be described in the following ways: (*i*) the **SS** bonding MO is a bond orbital; (*ii*) the **SA** weakly bonding MO and the **AS** and **AA** nonbonding MO are the three orbitals that are derived from the t_{2g} block of a regular octahedron. If they are doubly occupied, the electronic configuration is d^6; (*iii*) the **SA** antibonding MO is essentially antibonding on the ethylene ligand; (*iv*) lastly, the **SS** antibonding MO, largely composed of the z^2 orbital, is mainly antibonding for the ethylene ligand and the *trans* ligand L. In fact, it is one of the orbitals that are derived from the antibonding e_g block of a regular octahedron. The other orbital, x^2-y^2, does not appear on this diagram since we did not consider it on the initial ML_5 fragment, as its energy is too high.

3.4.2.2. *A molecular ethylene complex or a metallacyclopropane?*

The donation interaction ($\pi \rightarrow z^2$) reduces the electron density in the π-bonding orbital of the ethylene ligand. The carbon–carbon

bond is therefore weakened (**3-39**). Now the back-donation interaction ($yz \rightarrow \pi^*$) transfers electron density into the π^* antibonding orbital, which also weakens this bond (**3-40**). However, these two interactions are both bonding between the carbon atoms and the metal centre, so they contribute to the formation of metal-carbon bonds.

The question is thus open: is it appropriate to speak of an ethylene complex, in which the ligand is clearly identified as molecular ethylene (**3-41a**), or is it better to describe it as a metallacyclopropane, with a C—C single bond and two M—C bonds (**3-41b**)? These are in fact two mesomeric forms of the same complex; the metal oxidation state, in particular, is different in these two forms, being higher by two in the metallacycle. The change from one limiting form to the other represents the *oxidative addition* reaction of ethylene, which leads to the metallacyclopropane. The real complex is usually intermediate between these two limiting forms. Typically, the carbon–carbon bond length is around 1.43 Å (instead of 1.32 or 1.54 Å for a standard double or single bond, respectively), and the ethylene ligand becomes non-planar: the CH_2 groups become pyramidal, in the direction opposite to the metal centre, though not as extensively as in a real three-membered ring.

From the electronic structure point of view, there are similarities between the two **SS** and **SA** bonding molecular orbitals of the π complex (**3-42** and **3-43**, left-hand side) and the corresponding orbitals of the metallacyclopropane. The latter can be represented schematically by considering the in-phase and out-of-phase combinations of two localized orbitals, each of which characterizes a σ_{MC} bond (**3-42** and **3-43**, right-hand side).[10] The first combination corresponds to the orbital $\pi + z^2$ of the molecular ethylene complex, the second to the orbital $yz + \pi^*$.

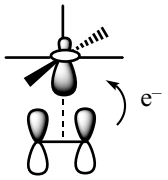

3-39

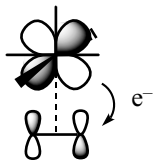

3-40

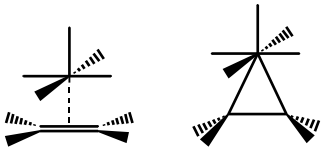

3-41a **3-41b**

[10] There is, however, a difference in the relative magnitudes of the coefficients on the metal and on the ligand in the orbital whose symmetry is written **SA**. In the molecular ethylene complex, this orbital is concentrated mostly on the metal, whereas in the metallacyclopropane, it is mainly on the ligand. We shall return to this point in § 4.5 of Chapter 4, which is devoted to the mechanism of oxidative addition.

SS

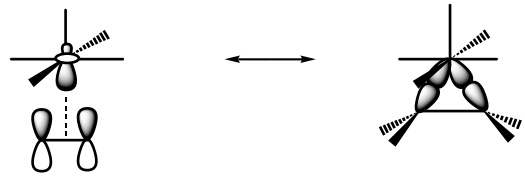

3-42

SA

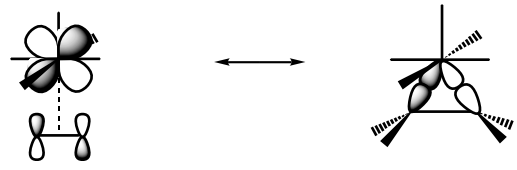

3-43

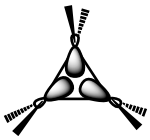

3-44 (**SS**)

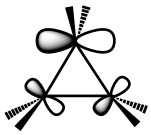

3-45 (**SA**)

Similarly, there is a resemblance between these orbitals and two of the three orbitals that characterize the C−C bonds in cyclopropane itself (**3-44**, symmetry **SS** and **3-45**, symmetry **SA**).

In fact, depending on the nature of the metallic fragment ML_n which interacts with the ethylene ligand and on the substituents on this ligand, a whole range of interactions can be observed, ranging from weak interactions, which correspond to a complex of molecular ethylene, to strong interactions which lead to a structure close to a metallacyclopropane. So the best answer to the general question posed at the beginning of this section 'a π complex of molecular ethylene or a metallacyclopropane?' seems in fact to be . . . both!

3.4.3. Metallocenes Cp_2M

3.4.3.1. *The π system of the cyclopentadienyl ligand*

The shapes and the relative energies of the five π orbitals in cyclopentadiene (Cp) are presented in Figure 3.10, where the electronic occupation corresponds to the anion Cp^- (the ionic model). A symbolic representation of the orbitals, which shows only the nodal positions between the carbon atoms, is given on the right of the figure. As a consequence of the three occupied π MO, Cp^- can be characterized as an L_3 ligand.

The donation and back-donation interactions of the Dewar–Chatt–Duncanson model can occur, thanks to the three occupied and the two empty MO, respectively.

3.4.3.2. Cp_2M *complexes: the ferrocene example*

The three occupied MO on each Cp^- ligand combine in-phase ($\pi^{(+)}$) and out-of-phase ($\pi^{(-)}$), leading to the formation of six occupied MO that are delocalized onto the two ligands. It is easy to verify that $\pi_1^{(+)}$

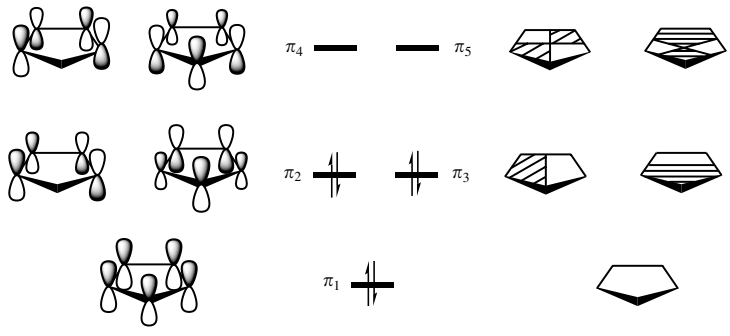

Figure 3.10. The π system of the cyclopentadienyl ligand (Cp^-).

has the proper symmetry to interact with the *s* orbital on the metallic centre (**3-46a**). Similarly, $\pi_1^{(-)}$ can interact with p_z (**3-46b**), $\pi_2^{(+)}$ with p_y (**3-46c**), $\pi_3^{(+)}$ with p_x (**3-46d**), $\pi_2^{(-)}$ with yz (**3-46e**) and $\pi_3^{(-)}$ with xz (**3-46(f)**). In this way, six occupied bonding MO are formed that characterize six bonds, as in an octahedral complex.

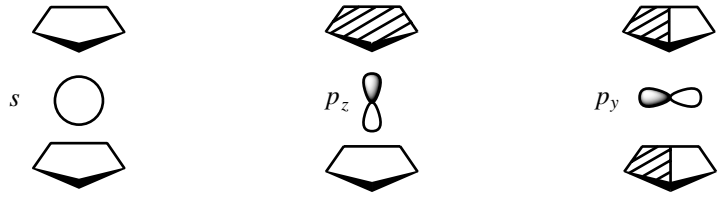

3-46a **3-46b** **3-46c**

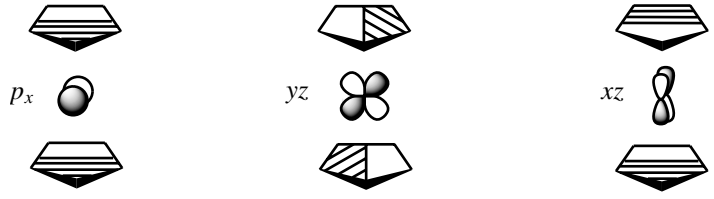

3-46d **3-46(e)** **3-46(f)**

The participation of two *d* orbitals in the MO that describe the bonds leads to the presence of two antibonding orbitals in the d block (yz and xz), while the other *d* orbitals ($z^2, x^2{-}y^2$, and xy) make up a block of three nonbonding or nearly nonbonding orbitals. In fact, $x^2{-}y^2$ and xy are stabilized by bonding interactions with the π^* orbitals of appropriate symmetry on the Cp rings (Figure 3.11).

The d block of a Cp_2M complex therefore has the same characteristics as that of an octahedral complex. In ferrocene, $[Cp_2Fe]$, whose electronic configuration is (d^6), the three nonbonding *d* orbitals are occupied and this complex can be described as pseudo-octahedral, with 18 electrons.

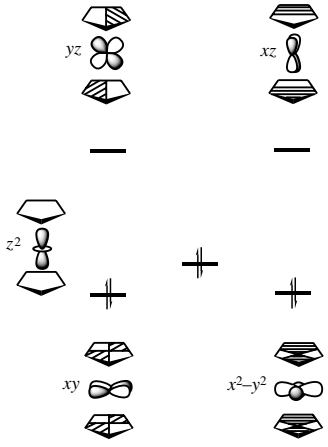

Figure 3.11. The d block of a Cp_2M complex, where the electronic occupation (d^6) corresponds, for example, to ferrocene $[Cp_2Fe]$.

3.4.4. Cp_2ML_n complexes

There are many complexes of the type $[Cp_2ML_n]$ ($n = 1, 3$), where M is a transition metal towards the left of the periodic classification (M = Ti, V, Zr, Hf, Mo, for example). In these complexes, the Cp_2M fragment is bent, rather than linear as in the metallocenes. The other ligands are all located in the plane that is perpendicular to that defined by the M atom and the centres of the two Cp rings (**3-47** and **3-48**). If $n = 3$, this arrangement imposes very small L−M−L angles (about

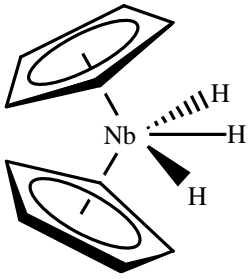

3-47

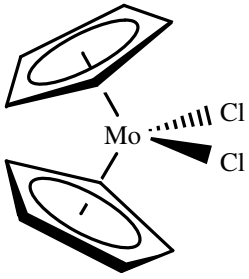

3-48

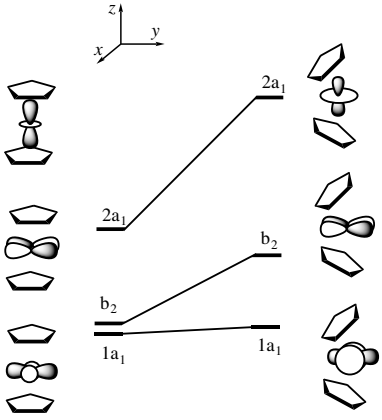

Figure 3.12. Energy changes for the three lowest-energy orbitals of the d block for a Cp_2M complex passing from a linear to a bent arrangement of the Cp ligands.

60° in $Cp_2Nb(H)_3$, **3-47**). Since each Cp ligand forms three bonds with the metal, the coordination number of these complexes is seen to be between 7($n = 1$) and 9($n = 3$), which is quite rare for the metals of the first three transition series.

3.4.4.1. *The bent* Cp_2M *fragment*

Consider the three low-energy *d* orbitals previously established for a linear Cp_2M complex (Figure 3.11, the z^2, x^2-y^2, and xy orbitals). In the C_{2v} point group, these orbitals have a_1 (z^2 and x^2-y^2) and b_2 (xy) symmetries. When the Cp_2M fragment is bent (Figure 3.12), the b_2 orbital is destabilized, since the stabilizing interactions with the π^* orbitals on the Cp rings decrease and the repulsive interactions between the M—Cp bonds increase. The same behaviour could be expected for the $1a_1$ orbital (x^2-y^2), but it mixes with the $2a_1$ orbital (z^2), with the result that its energy stays roughly constant, whereas the $2a_1$ orbital is strongly destabilized (an interaction between two orbitals of the same symmetry). This mixing between z^2 and x^2-y^2 which accompanies the bending of the fragment leads to a polarization of x^2-y^2 along the *x*-axis, and of z^2 in the *xy* plane, as shown to the right of Figure 3.12.

It will be useful to consider another representation of these orbitals, which shows their amplitudes and nodal properties in the symmetry plane *xy* which interchanges the two Cp ligands (**3-49**). The other ligands (L) in $[Cp_2ML_n]$ complexes lie in this plane.

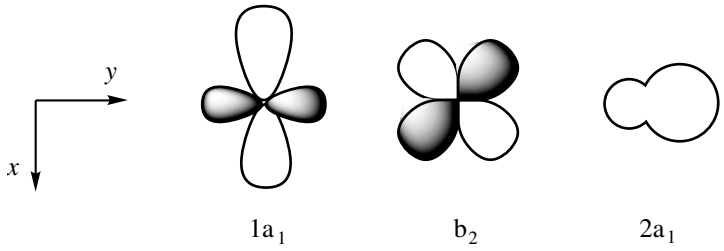

3-49

3.4.4.2. Cp_2ML_n *complexes* ($n = 2, 3$)

We consider first the complex $[Cp_2MoCl_2]$ (**3-48**). It can be decomposed into a metallic fragment, $[Cp_2Mo]^{2+}$, and two chloride ligands, Cl^- (the ionic model). The metallic fragment has a d^2 electronic configuration: the $1a_1$ orbital described above is occupied and the two other *d* orbitals (b_2 and $2a_1$) are empty (Figure 3.13, left-hand side). The two Cl^- ligands

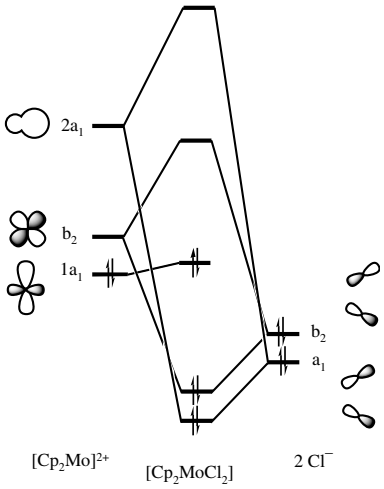

Figure 3.13. Construction of the MO of the complex $[Cp_2MoCl_2]$ from those on the $[Cp_2Mo]^{2+}$ and 2 Cl^- fragments.

supply four electrons that occupy two MO, which are in-phase (a_1) and out-of-phase (b_2) combinations of two *p* orbitals (Figure 3.13, right-hand side). The formation of the MO of the complex from those on the fragments therefore involves an interaction between b_2 and a_1 pairs of orbitals. For the latter, the dominant interaction involves the $2a_1$ orbital on the metallic fragment. In fact, the a_1 orbital on the chlorides is concentrated in the nodal planes of the $1a_1$ orbital on the metallic fragment, so the overlap between these two orbitals is very weak.

There is thus only one approximately nonbonding orbital in the d block, and it is doubly occupied. With a d^2 electronic configuration, and taking account of the eight metal–ligand bonds, $[Cp_2MoCl_2]$ is therefore an 18-electron complex. 16-electron d^0 complexes are also known in this family ($n = 2$), such as $[Cp_2ZrCl_2]$; the nonbonding *d* orbital is empty in them.

We now turn to a complex from the Cp_2ML_3 family, such as Cp_2NbH_3 (**3-47**). This can be decomposed into a metallic fragment, Cp_2Nb^{3+}, whose electronic configuration is d^0, and a fragment that groups together the three hydrides, H_3^{3-} (the ionic model), with six electrons in three orbitals. The symmetries of these three orbitals are well adapted to interact with the three *d* orbitals of the metallic fragment (**3-50**). In particular, there is a large overlap between the $1a_1$ orbital on the metallic fragment and the $2a_1$ orbital of H_3^{3-}.

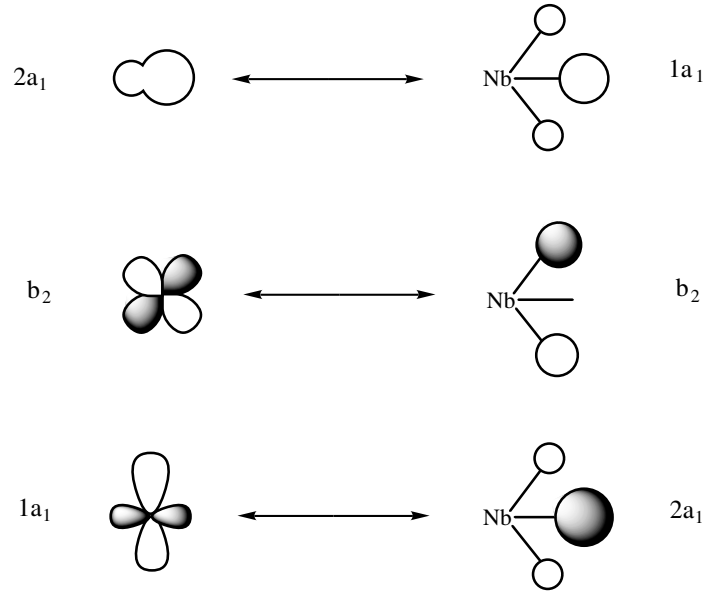

3-50

After the interaction, three doubly occupied bonding MO are formed that are mainly concentrated on the hydrides (**3-51a**). They characterize the three Nb—H bonds. The three antibonding combinations, (**3–51b**) which belong to the d block, are empty.

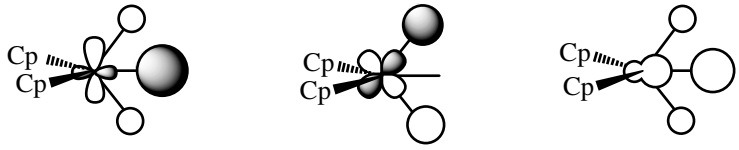

3-51a

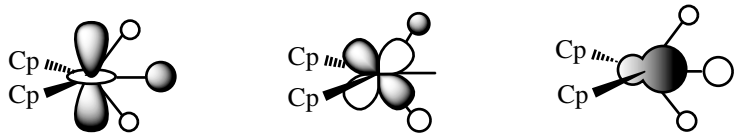

3-51b

There are therefore no nonbonding *d* orbitals in this complex. With its d^0 electronic configuration and nine bonds around the metal, $[Cp_2NbH_3]$ is an 18-electron complex.

3.5. π interactions and electron counting

The formal electron count, as it is usually performed for transition metal complexes, (Chapter 1, § 1.1), takes account of the electrons involved in the σ interactions and the n nonbonding electrons on the metal which do not participate in these interactions (d^n electronic configuration). But it ignores the consequences of the π interactions, even though these are accompanied by transfers of electron density involving some d-block orbitals.

As a first illustration of this point, consider $[W(PR_3)_6]$ and $[W(CO)_6]$; both are described as octahedral complexes whose electronic configuration is d^6, with six electrons in the three t_{2g} orbitals of the d block of the octahedron. A phosphine ligand, PR_3, may, in a first approximation, be considered as a simple σ-donor.[11] From this viewpoint, the occupied t_{2g} orbitals of the $[W(PR_3)_6]$ complex are therefore pure atomic *d* orbitals, entirely localized on the metal. However, since the carbonyl ligand is a π acceptor, the t_{2g} orbitals of the $[W(CO)_6]$ complex are partially delocalized on to the ligands (**3-34**), leading to a substantial transfer of electron density from the metal to the ligands. Although both formally have a d^6 electronic configuration, the shape of

[11] Notice, however, that when the substituents R are very electronegative, the σ^* orbitals associated with the P—R bonds are substantially lowered in energy, and the phosphine PR_3 can behave as a double-face π-acceptor. In extreme cases, such as PF_3, its π-acceptor strength is even close to that of a carbonyl ligand.

the orbitals reflects the fact that the electron density at the metal centre is higher in the $[W(PR_3)_6]$ complex than in $[W(CO)_6]$.

Complexes with π-donor ligands that can transfer electron density to the metal centre are even more interesting. Consider the octahedral complex $[W(Cl)_6]$, for example: according to the standard counting procedure, its electronic configuration is d^0 [W(VI)], and therefore it is a 12-electron complex. But this description is substantially modified if we take account of the π interactions. We have already seen that the three orbitals of the t_{2g} block are destabilized by antibonding interactions with the *p* lone pairs on the chloride ligands (***3-33***). In this complex, therefore, *all the orbitals of the d block are antibonding*, those destabilized by the σ interactions (the e_g block) being higher in energy than those destabilized by the π interactions (Figure 3.14). This antibonding character of all the d-block orbitals enables us to understand the stability of this d^0 complex rather more easily.[12] Moreover, though the π interactions destabilize three orbitals in the d block, they also stabilize the three orbitals mainly concentrated on the lone pairs of the chloride ligands (Figure 3.14). The t_{2g} orbitals of the metal therefore contribute partially to the occupied MO. As a consequence, though it is accurate, following the normal definition of the d block, to describe $[W(Cl)_6]$ as a d^0 complex, the t_{2g} orbitals of the metal are in fact partially occupied, and the metal is much less poor in electrons than it appears at first sight.

In view of this analysis, it might seem legitimate for the π electrons that are transferred, at least partially, to the *d* orbitals of the metal centre to be included in the electron count. The complex $[W(Cl)_6]$, previously described as a 12-electron complex (σ electrons only), thus becomes an . . . 18-electron complex if one takes account of the six π electrons

[12] We noted, in Chapter 2, that complexes with a d^0 electronic configuration can exist if the ligands possess lone pairs (see § 2.1.3.2, 2.3.3.2, and 2.4.2.2)

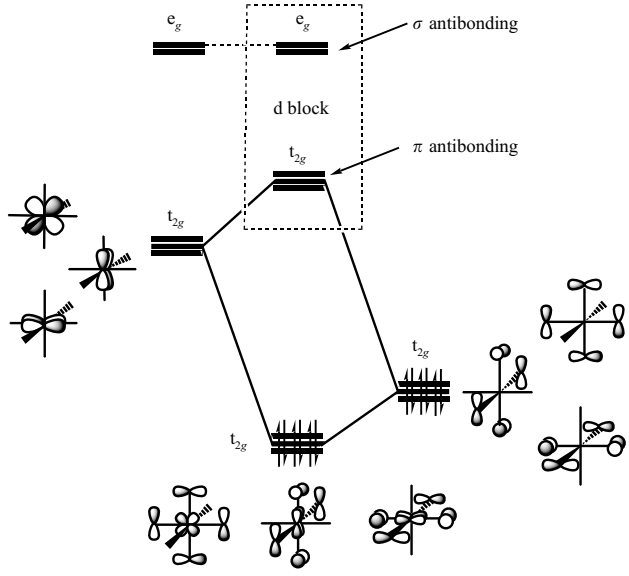

Figure 3.14. Interaction diagram showing the perturbation of the d block for an octahedral $[M(Cl)_6]$ complex (σ interactions only, left-hand side) by the symmetry-adapted π orbitals (t_{2g}) on the six double-face π-donor ligands. The electronic occupation shown corresponds to a complex with a d^0 electronic configuration ($[W(Cl)_6]$, for example).

'transferred' to the metal (Figure 3.14). It is not a coincidence if the '18-electron rule' is now verified with this new counting procedure: once the π interactions are considered, there are no empty nonbonding MO on the metal. To attain the normal count of 18 electrons around the metal, it is therefore sufficient for *all* the bonding MO (σ *and* π) to be doubly occupied; this electron count allows us to understand the stability of a complex which at first sight is very electron-deficient.[13] The stability of the complex $[W(Cl)_6]$ in an octahedral geometry contrasts strikingly with the instability of $[W(Me)_6]$ in this same geometry. The latter is also a d^0 complex, but one for which the π interactions are negligible. It therefore possesses three MO based on *d* orbitals that are nonbonding and unoccupied, and it can be described as a 'true' 12-electron complex. In fact, it adopts a different geometry, which is trigonal-biprismatic; we may conclude that the octahedral geometry of $[W(Cl)_6]$ is controlled by π interactions.

This analysis can be extended to other ligand fields, and is not limited to complexes whose d block is completely empty. In the presence of π-donor ligands, the apparent electron deficiency is compensated by interactions with the lone pairs on the ligands. Consider tetrahedral complexes such as $[Ti(Cl)_4]$ or $[Zr(Cl)_4]$, which are d^0 complexes of Ti(IV) or Zr(IV), and therefore complexes with only eight electrons! However, it can readily be shown that five of the eight orbitals that characterize the lone pairs on the four chloride ligands are able, by symmetry, to interact with the d-block orbitals (Chapter 2, § 2.4.1): two have e symmetry and three have t_2 symmetry. In this way, 10 π electrons are 'transferred' to the metal, so the complexes may be considered to have 18 electrons.

[13] To understand this stability another way, notice that as a result of the π interactions, there is a fairly large energy gap between the highest occupied (π bonding) and the lowest unoccupied MO (π^* antibonding).

Exercises

π interactions in an ML_4 complex

3.1

1. Indicate the shapes and the relative energies of the four lowest-energy d-block orbitals for a square-planar ML_4 complex (σ interactions only).
2. How are these shapes and energies modified in the complexes?
   (a) $[PtCl_4]^{2-}$
   (b) $[Ni(CN)_4]^{2-}$
3. Repeat the question for Wilkinson's catalyst, $[Rh(PPh_3)_3Cl]$; for simplicity, the triphenylphosphine ligands may be considered to be pure σ donors.

π interactions in an ML_5 complex (TBP)

3.2

1. Indicate the shapes and the relative energies of the four lowest-energy d-block orbitals for an ML_5 complex in a TBP geometry (σ interactions only).
2. How are the shapes and energies of these orbitals modified if a carbonyl group is in an axial position (**1a**), or an equatorial position (**1b**)? (for the first structure, show that certain overlaps that are non-zero by symmetry are in fact very small, so they may be neglected).

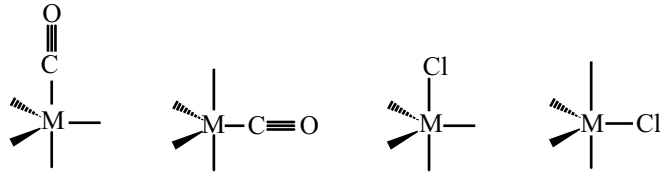

1a **1b** **2a** **2b**

3. Deduce the more favourable substitution site for π interactions in diamagnetic d^4 and d^8 complexes.
4. Repeat question 2 for complexes substituted by a chloride ligand in an axial (**2a**) or equatorial position (**2b**).
5. Deduce the more favourable substitution site for π interactions in diamagnetic d^4 and d^8 complexes **2a** and **2b**.

π interactions in an octahedral ML_6 complex

3.3

1. By writing a Lewis structure, show that C≡N is an X-type ligand.
2. Assuming that the order of increasing energy for the MO is the same in CN as in C≡O,
   (a) indicate the nature of the MO that has a σ interaction with a metal centre;
   (b) give the shape and the occupation of the π-type MO;
   (c) indicate whether this ligand is a π acceptor or a π donor;
   (d) indicate whether the CN ligand binds to the metal through carbon or nitrogen in the η^1 coordination mode.
3. Give the shapes and relative energies of the three lowest-energy *d* orbitals in an octahedral complex of the type $[M(CN)_6]$.
4. In which of the two complexes $[Fe(CN)_6]^{4-}$ and $[Fe(CN)_6]^{3-}$ are the Fe—CN bonds shorter?
5. Is this result predictable just from the oxidation state of the metal in the two complexes?

3.4

Consider an octahedral complex $[ML_4Cl_2]$ in which the Cl ligands are in *cis* positions: the *x*-axis bisects the Cl—M—Cl angle, as shown below.

1. Identify the two planes of symmetry in the complex (P_1 and P_2).
2. Give the shapes of the three nonbonding orbitals for a regular octahedral complex in which the ligands only have σ interactions with the metal. Indicate their symmetry properties with respect to P_1 and P_2.
3. Construct the four symmetry-adapted orbitals that characterize the π-type lone pairs on the Cl ligands, and give their symmetries with respect to P_1 and P_2.
4. How many lone pairs on the ligands are involved in π interactions?
5. Place these seven orbitals (three *d* orbitals on the metal and four lone-pair orbitals) on an energy-level diagram, and justify the relative positions:
   (a) of the ligand and metal orbitals;
   (b) of the four different ligand orbitals.
6. Construct the interaction diagram, and indicate which of the resulting MO belong to the d block.
7. How many electrons are there around the metal according to the traditional count in the case of a d^0 complex?
8. How many electrons are there once the π transfers are taken into account?

Pentagonal bipyramidal ML_7 *complex*

3.5

Among the different geometries that can be adopted by an ML_7 complex, the pentagonal-bipyramid (PBP), with two axial ligands (L_1 and L_7, on the *z*-axis) and five equatorial ligands (L_2–L_6, in the *xy* plane), is one of the most common.

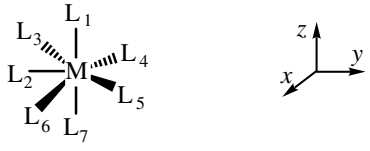

1. How many of the d orbitals are strictly nonbonding? Give the shapes of these orbitals.
2. Consider PBP complexes with a d^4 electronic configuration in which there is one carbonyl ligand, in either an axial (L_1) or an equatorial position (choose the position L_2).
   (a) analyse the π-type interactions in each isomer;
   (b) deduce the favoured site for a carbonyl ligand.

The use of group theory

3.6

Solve Exercise 3.1 (question 2) by making use of the results of Exercise 6.13 (Chapter 6) on the symmetry-adapted orbitals for ML_4 complexes with a π system on the ligands, and the character table for the D_{4h} point group (Table 6.18).

3.7

1. Give the shapes and relative energies of the five d-block orbitals for a trigonal-planar ML_3 complex (σ interactions only).
2. Consider the complex $[Ni(CO)_3]$ in this geometry. By making use of the results established in Chapter 6 (§ 6.6.6.2), give the symmetry-adapted linear combinations of the π^*_{CO} orbitals (the point group is D_{3h}, whose character table is given in Table 6.21).
3. Construct the diagram for the interaction of these orbitals with those in the d block of question 1. Deduce the shapes and relative energies of the d-block MO in $[Ni(CO)_3]$.
4. Try to find these orbitals without using group theory (construction 'by hand', § 3.3). Show that some of the information provided by group theory cannot be readily obtained without its use.

Appendix C: the carbonyl ligand, a double-face π-acceptor

In an octahedral complex with a carbonyl ligand (see § 3.2.2), two metal d orbitals (xz and yz, **3C.1**) can interact with the π-bonding and π^*-antibonding MO on the CO ligand: π_x and π^*_x with xy, π_z and π^*_z with yz, following two equivalent three-orbital interaction diagrams (see Appendix A, Chapter 2). By comparing the strength of the $d \leftrightarrow \pi$ and $d \leftrightarrow \pi^*$ interactions, we may deduce whether the carbonyl ligand is a π donor or a π acceptor. These interactions, which involve orbitals of different energy, are proportional to $S^2/\Delta\varepsilon$ (Chapter 1, § 1.3.2); they therefore increase in strength with a decrease in the orbital energy difference, but with an increase in the overlap.

Table 3C.1. *d*-orbital energies for the metals of the first transition series, and the energy differences $d - \pi_{CO}(\Delta\varepsilon_\pi)$ and $\pi^*_{CO} - d(\Delta\varepsilon_{\pi^*})$ calculated by the extended Hückel method (eV)

	Sc	*Ti*	*V*	*Cr*	*Mn*	*Fe*	*Co*	*Ni*	*Cu*
ε_d	−8.5	−10.8	−11.0	−11.2	−11.7	−12.6	−13.2	−13.5	−14.0
$\Delta\varepsilon_\pi$	7.2	4.9	4.7	4.5	4.0	3.1	2.5	2.2	1.7
$\Delta\varepsilon_{\pi^*}$	−0.6	1.7	1.9	2.1	2.6	3.5	4.1	4.4	4.9

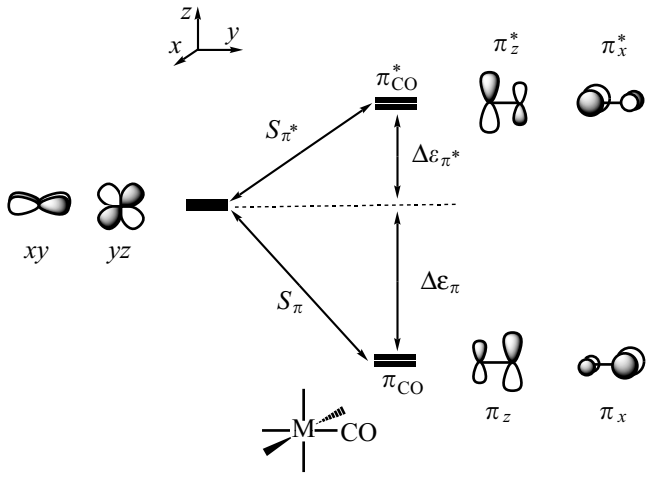

3.C1

The comparison of $\Delta\varepsilon_\pi$ with $\Delta\varepsilon_{\pi^*}$ is not straightforward, since the *d*-orbital energy depends on the nature of the metal: these metal orbitals become considerably more stable as one moves from left to right in the periodic classification (Chapter 1, Table 1.3). One can obtain at least a qualitative indication of the relative values of $\Delta\varepsilon_\pi$ and $\Delta\varepsilon_{\pi^*}$ by using the extended Hückel method,[14] for example, for the metals of the first transition series (Table 3C.1). The energy of the *d* orbitals lies between −8.5 eV (Sc) and −14.0 eV (Cu),[15] and the energies calculated for the π_{CO} and π^*_{CO} MO are −15.7 and −9.1 eV, respectively, for a C—O distance of 1.14 Å(the average value in metal carbonyl complexes).

If we consider only the energetic criterion, the interaction with the π^*_{CO} orbitals is stronger than with π_{CO} for all the metals on the left of the table, up to and including manganese ($\Delta\varepsilon_{\pi^*} < \Delta\varepsilon_\pi$), suggesting that the carbonyl ligand should behave as a π acceptor. On the other hand, for the metals furthest to the right, and particularly for Co, Ni, and Cu, the energy separation involving the π_{CO} orbitals is smaller.

The second criterion that needs to be examined involves the overlap. The analysis here is simpler, since the S_π and S_{π^*} overlaps, for a given metal, are proportional to the magnitudes of the coefficients on carbon

[14] R. Hoffmann *J. Chem, Phys.* 1963, *39*, 1397. One may also consult Y. Jean and F. Volatron *Structure électronique des molécules*, volume 2, 3rd edn., chapter 14, Dunod (2003).

[15] These values differ only slightly from those in Table 1.4 (Chapter 1) that were obtained from spectroscopic data: $\varepsilon_{3d}(\text{Sc}) = -7.92$ eV and $\varepsilon_{3d}(\text{Cu}) = -13.46$ eV.

in the π_{CO} and π^*_{CO} MO, respectively (we are neglecting here the overlap with that part of the MO located on the oxygen atom, since this is so much further from the metal centre). As a result of the polarization of the π orbitals, the coefficient on carbon is far larger in the antibonding orbital (0.66) than in the bonding (0.37). The ratio of the overlaps S_{π^*}/S_{π} is therefore 1.78. Since the interaction depends on the square of the overlap, we may conclude that the overlap term favours the π-acceptor character of the carbonyl ligand by a factor of about 3.2. For the metals located towards the left of the periodic table, the combination of a smaller energy difference and a much larger overlap ensures that the $d \leftrightarrow \pi^*_{CO}$ interactions are far stronger than the $d \leftrightarrow \pi_{CO}$ interactions, so the carbonyl ligand behaves as a double-face π-acceptor. For the metals located towards the right, the energy difference favours the π-donor character of the carbonyl ligand, but the overlap favours a π-acceptor behaviour. If we examine the extreme case of copper, (Table 3.C1), the overlap factor (about 3.2 in favour of the $d \leftrightarrow \pi^*_{CO}$ interaction) is only slightly different from the energetic factor (about 2.9 in favour of the $d \leftrightarrow \pi_{CO}$ interaction). This is the only case where the π-donor and π-acceptor characters are roughly balanced, and this arises because the d orbitals on copper are very low in energy, compared to those on the other transition metals.

To conclude, an accurate treatment of the π interactions that involve the carbonyl ligand requires both the occupied π_{CO} and empty π^*_{CO} MO to be taken into account (a three-orbital interaction scheme, **3.C1**). If one notes that the interactions involving the antibonding MO are dominant, *one can simplify the description, by considering only the π^*_{CO} orbitals on the carbonyl ligand*. In this simplified model, three MO are considered for this ligand: the occupied orbital σ_C, that characterizes the lone pair on carbon (Chapter 3, Figure 3.3), giving the ligand a σ-donor character, and the two empty π^*_{CO} orbitals, which confer a double-face π-acceptor character.

Applications

A detailed knowledge of the electronic structure of transition metal complexes, and in particular of the shape and electronic occupation of the d-block orbitals, enables several problems related to their structure and reactivity to be studied. The examples discussed in this chapter illustrate a method for analysing these problems that usually relies on a study of orbital interactions between the ligand and the metal centre, and/or on a correlation diagram that links the orbitals of two different structures. The answers that one may hope to obtain from this type of analysis are *qualitative* rather than quantitative. For example, one can often determine which of two possible conformations of a complex is the more stable, *and why*, without being able to deduce the energy difference between them. Once the electronic factors that favour a particular structure are established, it may well also be possible to predict the type of changes that will follow from, for example, a change in the nature of the ligands. A qualitative interpretation of the structure and reactivity of complexes is exceedingly interesting for chemists, even if studies of a different type, that depend on accurate calculations, are necessary to provide theoretical data that may usefully be compared, quantitatively, with experimental results.

4.1. Conformational problems

Several conformations may sometimes be envisaged for a particular complex, depending on the orientation of a ligand with respect to the rest of the molecule. In such circumstances, the analysis for each conformation of the interactions between the ligand orbitals and those on the remaining fragment containing the metal often enables us to understand why one particular conformation is energetically favoured. We shall consider four examples in this section, using this 'fragment method', which involve mono- and bis-ethylene complexes and a molecular hydrogen complex; several other examples are presented at the end of the chapter in the form of exercises.

4.1.1. d^8-[$ML_4(\eta^2$-$C_2H_4)$] complexes

Consider a trigonal-bipyramidal (TBP) complex in which an ethylene ligand occupies an equatorial site. The d^8 electronic configuration, which

leads to an 18-electron complex, is the most common for this class of compounds (Chapter 2, § 2.5.2) and the complex $[Fe(CO)_4(\eta^2\text{-}C_2H_4)]$ is a well-known example.

Two limiting orientations may be envisaged for the ethylene ligand, depending on whether the carbon–carbon bond is perpendicular to the equatorial plane (**4-1a**) or in that plane (**4-1b**). Both structures have C_{2v} symmetry and we shall use the planes of symmetry P_1 and P_2 (**4-1**) to analyse the symmetry of the most important orbitals.

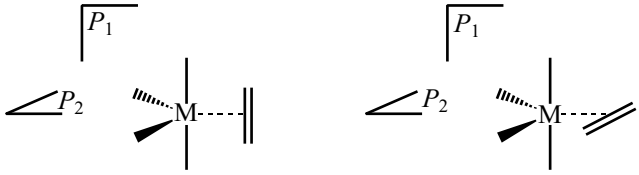

4-1a (perpendicular) **4-1b** (coplanar)

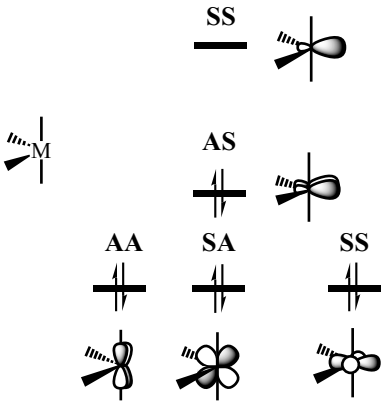

4-2

The orbital structure of each conformation may be analysed as the result of the interaction between the occupied π orbitals and the empty π^* orbitals on ethylene on one hand, and the orbitals of a d^8 ML_4 fragment with a 'butterfly' geometry (Chapter 2, § 2.8.3) on the other. For this latter, we shall consider the four occupied orbitals of the d block (three nonbonding, one weakly antibonding) and the lowest-energy empty orbital, which is an *s–p* hybrid orbital pointing towards the empty site of the TBP. The shapes of these orbitals are presented below (**4-2**) in the simplest case, where the four ligands are identical and only have σ interactions with the metal. To simplify matters, the small contributions from the ligands to the two highest orbitals are not shown. The symmetries of the orbitals with respect to the planes P_1 and P_2 are also indicated in **4-2**.

On passing from the perpendicular structure to the coplanar one (**4-1**), the orientation of the ML_4 fragment does not change. However, there is a rotation of the ethylene ligand by 90°, and therefore also of the associated π and π^* orbitals. These are shown in **4-3a** and **b**, and their symmetries with respect to the planes P_1 and P_2 are given for each

4-3a (perpendicular) **4-3b** (coplanar)

conformation.[1] We note already that the symmetry of the π^* orbital changes from one conformation to the other, and this will prove to be crucial for the conformational preference for the complex.

The π orbital on the ethylene ligand, whose symmetry is **SS** in both conformations, can interact with (*i*) the empty orbital and (*ii*) the occupied nonbonding orbital of the same symmetry on the ML_4 fragment (**4-2**). The first of these interactions involves two electrons; it constitutes the donation interaction of the Dewar–Chatt–Duncanson model (Chapter 3, § 3.4.1.2) for the metal–olefin bond in this complex. It is easy to see that the overlap between these orbitals does not depend on the orientation of the olefin, due to the cylindrical symmetry of the empty orbital on the metal centre (**4-4a** and **b**). Things are essentially the same for the second interaction: the overlap occurs mainly with the lobe of the *d* orbital that points towards the π orbital, and this lobe also has cylindrical symmetry with respect to the metal–olefin axis (**4-5a** and **b**). We may conclude that since the interactions which involve the π orbital of the ethylene ligand are identical in the two conformations, they cannot contribute to a pronounced energetic preference for one of them.

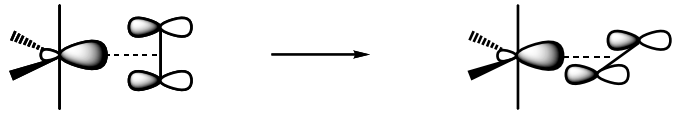

4-4a **4-4b**

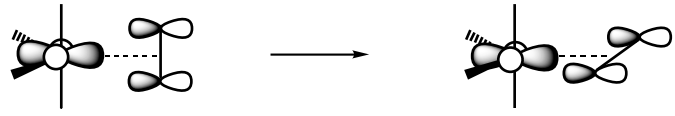

4-5a **4-5b**

We now consider the interaction of the empty π^* orbital with the orbital of the same symmetry on the metal fragment. In the perpendicular conformation, the nonbonding orbital with **SA** symmetry is involved, but the antibonding **AS** orbital is concerned in the coplanar conformation (**4-2**). In both cases, this is a two-electron stabilizing interaction that leads to a transfer of electron density from the metal to the ligand. This is therefore the back-donation interaction in the Dewar–Chatt–Duncanson model (Chapter 3, § 3.4.1.2). As the orbital involved on the metallic fragment is not the same in the two conformations, *the strength of this interaction depends on the conformation considered*. Now the energetic stabilization created by an interaction is proportional to the square of the overlap and inversely proportional to the energy difference between the orbitals (Chapter 1, § 1.3.2). The antibonding π^*

[1] If the symmetry labels of the C_{2v} group are used, the symmetries **SS**, **SA**, **AS**, and **AA** correspond to a_1, b_1, b_2, and a_2, respectively.

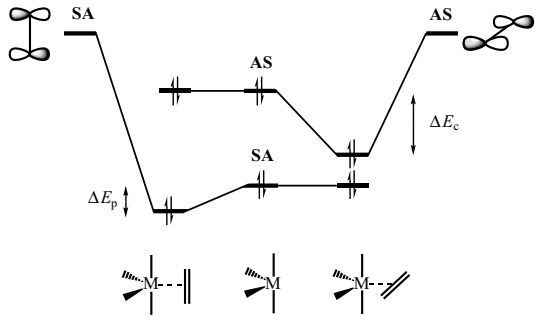

Figure 4.1. Comparison of the back-donation interactions ($d \rightarrow \pi^*$) in the perpendicular (on the left) and coplanar (on the right) conformations of a d^8-[$ML_4(\eta^2$-ethylene)] complex (**4-1**). The energy levels and symmetries of the d orbitals involved in the two cases are given in the centre of the diagram.

orbital is higher in energy than the d-block orbitals, which are non-bonding or, in one case, weakly antibonding (**4-2** and Figure 4.1). The energy separation between the interacting orbitals is therefore smaller in the coplanar conformation, since, in this case, it is the highest-energy occupied orbital on the metallic fragment that is involved. Moreover, the overlap involves a d orbital that is polarized towards the π^* orbital in the coplanar conformation (S_c), but a pure d orbital in the perpendicular case (S_p). Therefore, $S_c > S_p$, (**4-6**). In summary, a smaller energy separation and a larger overlap favour the back-donation interaction in the planar structure.

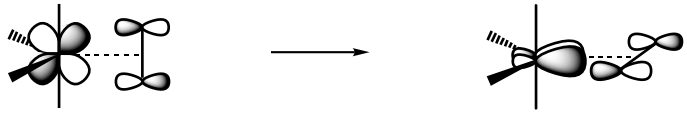

4-6a (S_p) **4-6b** (S_c)

The greater electronic stabilization which follows ($\Delta E_c > \Delta E_p$, Figure 4.1) leads to a preference for this conformation, which is indeed adopted in all known complexes of the type d^8-[$ML_4(\eta^2$-olefin)]. The barrier to olefin rotation measured by nuclear magnetic resonance (NMR) is of the order of 10–15 kcal mol^{-1}.

4.1.2. d^6-[$ML_5(\eta^2$-$C_2H_4)$] complexes: staggered or eclipsed conformation?

An octahedral complex with an ethylene ligand may adopt either the conformation in which the carbon–carbon bond eclipses the neighbouring M—L bonds (**4-7a**), or the staggered conformation shown in **4-7b**. This latter should be more stable on steric grounds. But experimentally, the *eclipsed* conformation is observed for complexes with a d^6 electronic configuration, such as [$Mo(PR_3)_5(\eta^2$-$C_2H_4)$]—hence the interest in this conformational problem.

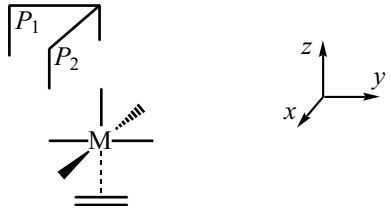

4-7a (eclipsed) **4-7b** (staggered)

The two conformations have C_{2v} symmetry, and as in the preceding example, we shall use the two planes of symmetry $P_1(yz)$ and $P_2(xz)$ to analyse the symmetries of the orbitals on the ethylene fragment (π and π^*) and of those on the d^6 metallic fragment ML_5. For the latter, we shall consider the four lowest-energy d orbitals (three doubly occupied nonbonding and the empty polarized z^2 orbital, see Chapter 2, § 2.3.1).

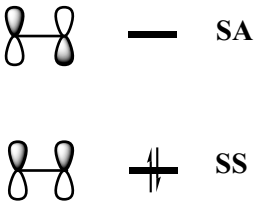

4-8

To pass from the eclipsed conformation (**4-7a**) to the staggered (**4-7b**), the orientation of the ethylene molecule has been fixed and a rotation of 45° applied to the ML_5 fragment. The orbitals of the ethylene fragment are therefore as shown in **4-8** for both conformations, whereas the reorientation of the metallic fragment leads to a change in the name and the symmetry of one of the its nonbonding orbitals (**4-9a** and **b**): xy (**AA**) becomes x^2-y^2 (**SS**) (Chapter 2, § 2.1.2.4 and 2.1.2.5).

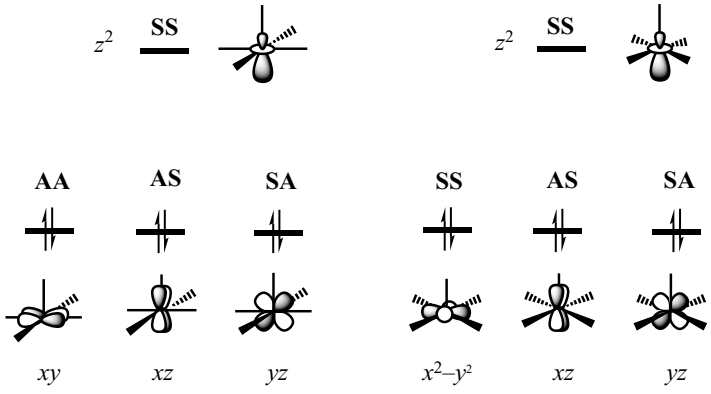

4-9a (eclipsed) **4-9b** (staggered)

In this system, the donation interaction of the Dewar–Chatt–Duncanson model involves the occupied π orbital and the empty z^2 orbital, both with **SS** symmetry, in the two conformations. As the z^2 orbital has cylindrical symmetry, the overlap between π and z^2 does not depend on the orientation of the ethylene ligand, so this interaction cannot lead to any conformational preference. The back-donation interaction involves the empty π^* orbital and the occupied yz orbital, both with symmetry **SA**, in the two conformations. This second

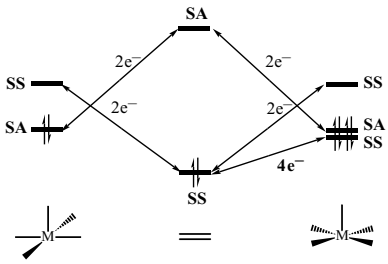

Figure 4.2. Interactions between the π and π^* orbitals on ethylene (in the centre) and the orbitals of the same symmetry on the d^6-ML_5 fragment in eclipsed (left) and staggered (right) conformations.

interaction is therefore also identical in the two conformations. So in this system, the conformational preference does not arise from *either* of the stabilizing interactions that have been invoked to describe the metal–ligand bond. If we consider the symmetries of the various orbitals in the eclipsed conformation, no additional interaction is possible, other than those we have already described. However, in the staggered structure, there is an interaction between the occupied π orbitals and $x^2 - y^2$, as both have **SS** symmetry. This destabilizing four-electron interaction, between the π orbital on the olefin and one of the nonbonding *d* orbitals on the metal (Figure 4.2), exists only in the staggered conformation; it is therefore the origin of the observed preference for the eclipsed conformation. The experimental barrier to olefin rotation is of the order of 10 kcal mol^{-1}.

The electronic structure of the two conformations can be described more completely by constructing the MO that result from the interaction of the fragment orbitals. Those on ethylene are placed in the middle of Figure 4.3, while those of the metallic fragment are on the left (eclipsed) or on the right (staggered conformation). In the interests of clarity, only the doubly occupied MO of the full complex are shown. The back-donation interaction between the **SA** orbitals produces the same stabilization in both conformations. There is a stabilizing interaction (donation) that involves the **SS** orbitals in the eclipsed conformation (left-hand side). For the staggered conformation, the two-electron stabilizing interaction and the four-electron destabilizing interaction described above (Figure 4.2) are represented by a three-orbital interaction scheme (**SS** symmetry) that involves four electrons.

The lowest-energy orbital in each conformation of the complex is mainly concentrated on the π orbital of ethylene. This is a bonding metal–ligand orbital that does not belong to the d block. The three other occupied MO are mainly or entirely concentrated on the metal *d* orbitals. They are the MO derived from the t_{2g} block of a regular octahedral

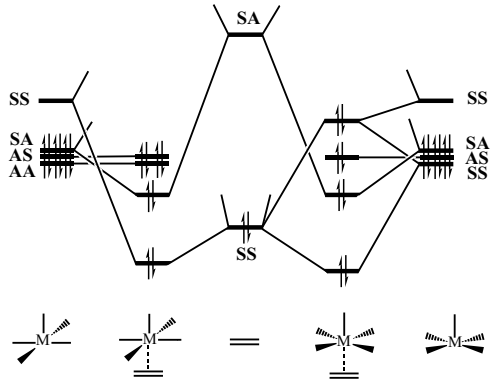

Figure 4.3. Construction of the MO for the eclipsed and staggered conformations of the d^6-[$ML_5(\eta^2$-ethylene)] complex, by interaction between the π and π^* orbitals on ethylene (centre) and the orbitals of the d^6-ML_5 fragment (on the left for the eclipsed conformation, on the right for the staggered).

complex, the degeneracy being partially or completely lifted by the presence of the ethylene ligand. These three MO are all doubly occupied, since we are considering a complex with a d^6 electronic configuration. For each conformation, there is a d-block orbital that is stabilized by a bonding interaction with the π^* orbital on ethylene and a nonbonding orbital. The preference for the eclipsed conformation arises from the third occupied orbital, which is nonbonding in the eclipsed structure but destabilized in the staggered case (**SS**). This destabilization should be linked to the analysis illustrated in Figure 4.2, which shows a repulsive interaction between **SS** orbitals in the staggered conformation.

In conclusion, we note that the highest-occupied molecular orbital (HOMO) 'rule', according to which the more stable of two structures of a given species is the one whose HOMO is at lower energy, is perfectly applicable to this conformational problem, and to the one treated in the preceding section (see Figure 4.1).

4.1.3. d^6-[$ML_4(\eta^2$-$C_2H_4)_2$] complexes: coupling of two π-acceptor ligands

A new conformational problem arises when there are two ligands for which several orientations are possible, instead of just one: does the orientation of one of them have an influence on the other? Steric repulsions may, of course, be significant, but here we shall be interested in purely electronic factors that may induce a coupling between the orientations of the two ligands.

Octahedral complexes of the type d^6-[$ML_4(\eta^2$-$C_2H_4)_2$], in which there are two ethylene ligands in *trans* positions, provide a characteristic example to illustrate this point. The problem of the orientation of each C═C bond with respect to the rest of the complex has been treated in the preceding section, where it was shown that in the most stable conformation, these bonds eclipse the neighbouring M—L bonds. If this result is accepted, there is still the question of the relative orientation of the two ethylene ligands. Two limiting structures can be imagined: the coplanar conformation (**4-10a**), which has D_{2h} symmetry, in which the two C═C bonds are located in the same plane (yz); and the perpendicular conformation (**4-10b**), with D_{2d} symmetry, in which one of the ethylene molecules has turned by 90° to be in the xz plane. Experimentally, this second orientation is observed in this class of compounds, for example, in the complexes *trans*-[$Mo(PMe_3)_4(C_2H_4)_2$] and *trans*-[$Mo(diphos)_2(C_2H_4)_2$] (diphos = $Ph_2PCH_2CH_2PPh_2$). The barrier to rotation about the metal–olefin bond has been estimated to be about 15 kcal/mol in this latter compound. Since the two ethylene molecules are well separated, by about 4 Å, it seems unlikely that steric factors are the origin of this conformational preference. It is therefore natural to

look for an electronic factor, by analysing the interactions between the ligands and the residual metallic fragment.

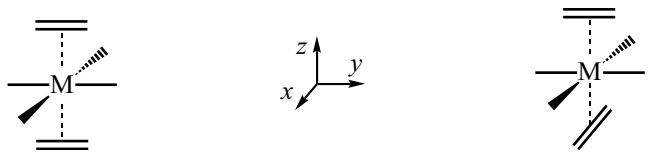

4-10a (coplanar) **4-10b** (perpendicular)

We shall consider the π and π^* orbitals on the ethylene ligands in each conformation, as they interact with the orbitals of the square-planar d^6-ML_4 fragment in which the three nonbonding d orbitals, xy, xz, and yz (Chapter 2, § 2.2.1) are doubly occupied. Two other orbitals will also be considered in the following analysis, since they point towards the two ethylene molecules (**4-11**): the empty z^2 orbital which is weakly antibonding, and p_z which is nonbonding but higher in energy (Chapter 2, § 2.2.2).

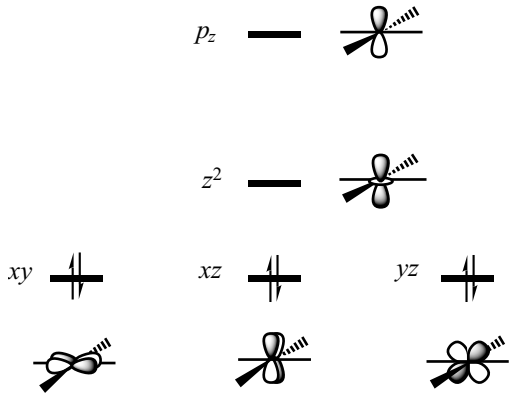

4-11

We consider first the interactions of the occupied π orbitals. The situation is identical to that described in the preceding section for the eclipsed confirmation of a d^6 $[ML_5(\eta^2\text{-}C_2H_4)]$ complex: the overlap between a π orbital and any of the occupied nonbonding orbitals on the metallic fragment is zero. However, there are two interactions with the empty z^2 and p_z orbitals, as shown in **4-12** for the coplanar conformation. The in-phase combination of the π_1 and π_2 orbitals ($\pi^{(+)}$) interacts with z^2 (**4-12a**), and the out-of-phase combination ($\pi^{(-)}$) with p_z (**4-12b**). These are two-electron interactions (ligand $\rightarrow$ metal donation), and after the interaction, only the bonding MO, mainly concentrated on the ligands, are doubly occupied. Due to the cylindrical symmetry of the z^2 and p_z orbitals, there is no change to the overlaps involved if one of

the two ethylene molecules is rotated by 90° to give the perpendicular conformation. The interaction between the two π orbitals is changed, but the distance between the ligands is too large for this change to give any energetically significant consequences. The donation interactions do not, therefore, give rise to any pronounced conformational preference.

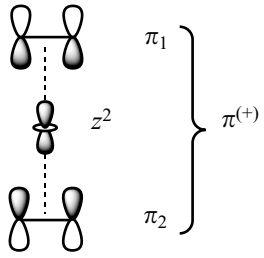

4-12a

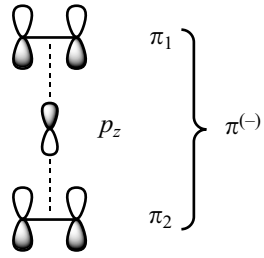

4-12b

We now turn our attention to the interactions that involve the empty π^* orbitals. As in the monoethylene complex (§ 4.1.2), the overlap for each of the π^* orbitals with z^2 is zero by symmetry. The same is true for the p_z orbital, which, like z^2, has cylindrical symmetry with respect to the z-axis. We must still consider the interactions with the nonbonding and doubly occupied d orbitals (**4-11**), that is, the metal → ligands back-donation interactions. Following the method developed in § 3.3 of the preceding chapter, we shall examine the overlap of the π^* orbitals with each of the three nonbonding d orbitals, remembering that a nonzero overlap leads to a bonding interaction $d \leftrightarrow \pi^*$ that stabilizes the d orbital (π-acceptor character of the ligand). In the planar conformation, the two π^* orbitals, concentrated in the yz plane, overlap with the yz orbital which is therefore stabilized by two bonding interactions (**4-13a**). In other words, yz is stabilized by the out-of-phase combination ($\pi^{*(-)}$) of the orbitals π_1^* and π_2^*. But the xz and xy orbitals, which are antisymmetric with respect to the yz plane, have zero overlap with the π^* orbitals, which are symmetric with respect to this plane. Their shapes and energies therefore stay unchanged (**4-13b** and **c**).

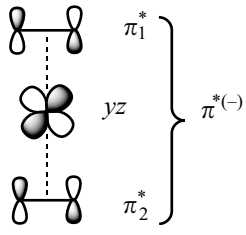

4-13a ($yz + 2\pi^*$)

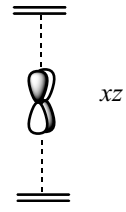

4-13b (xz)

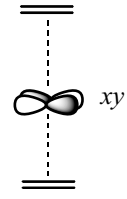

4-13c (xy)

In the perpendicular conformation, the π_1^* orbital still interacts with the orbital *yz* (**4-14a**), but π_2^* now overlaps with the orbital *xz* (**4-14b**), and *xy* remains as a pure *d* orbital (**4-14c**). In this conformation, two *d* orbitals are therefore stabilized to an equivalent extent (bonding interactions), but the third is unchanged.

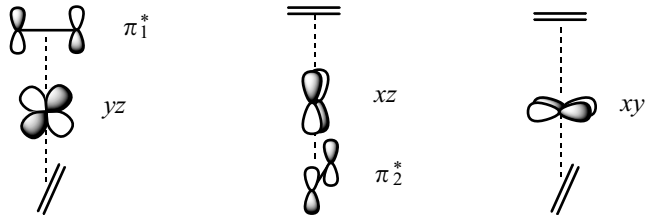

4-14a ($yz + \pi^*$) **4-14b** ($xz + \pi^*$) **4-14c** (xy)

These results are given as an interaction diagram in Figure 4.4; symmetry labels from the D_{2h} point group are used for the coplanar conformation (on the left), and from the D_{2d} point group for the perpendicular conformation (on the right). The $\pi^{*(+)}$ and $\pi^{*(-)}$ combinations in the coplanar structure have b_{2u} and b_{3g} symmetry, respectively, whereas the π^* orbitals in the perpendicular structure form a degenerate pair of orbitals of e symmetry. Due to the large spatial separation between the ethylene ligands, the energies of the $\pi^{*(+)}$ and $\pi^{*(-)}$ combinations are very similar, and only slightly different from the energy of the degenerate π^* orbitals in the perpendicular conformation. The three nonbonding *d* orbitals on the metal, whose symmetries are b_{3g} (*yz*), b_{2g} (*xz*), and b_{1g} (*xy*) in the D_{2h} point group, and e (*yz*, *xz*) and b_2 (*xy*) in the D_{2d} point group, respectively, are placed in the centre of the figure. Interaction between orbitals of the same symmetry leads, as we have shown above, to the stabilization of one *d* orbital in the coplanar conformation (**4-13a**), whereas *two* of them are stabilized in the perpendicular conformation (**4-14a** and **b**).

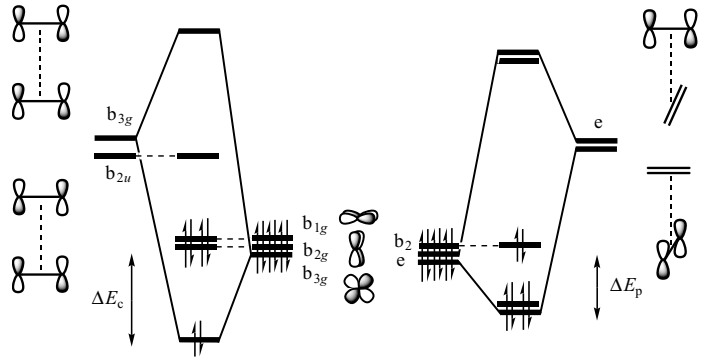

Figure 4.4. Diagram for the interaction between the nonbonding *d* orbitals (in the centre) and the π^* orbitals on the ethylene ligands in the coplanar (D_{2h}, on the left) and perpendicular (D_{2d}, on the right) conformations of an octahedral *trans* $[ML_4(\eta^2\text{-}C_2H_4)_2]$ complex with a d^6 electronic configuration.

Comment

In each conformation, the three doubly occupied MO are the orbitals derived from the t_{2g} block of a regular octahedral complex with a d^6 electronic configuration.

From the energetic point of view, four electrons are stabilized in the perpendicular conformation, but only two in the coplanar case. However, the stabilization of the orbital is larger for the coplanar conformation ($\Delta E_c > \Delta E_p$), since there are two bonding interactions (**4-13a**), as compared to only one for the degenerate orbitals (**4-14a** and **b**). In order to deduce the conformational preference, it is therefore necessary to know whether ΔE_c is smaller than, equal to, or more than twice as large as ΔE_p.

Since these are interactions between orbitals with different energies, the stabilizations ΔE are proportional to $S^2/\Delta\varepsilon$, where S is the overlap between the orbitals and $\Delta\varepsilon$ the energy difference between them (Chapter 1, § 1.3.2). The term $\Delta\varepsilon$ is essentially the same for the conformations, since the energies of the $\pi^{*(-)}$ (coplanar conformation) and π^* (perpendicular conformation) orbitals are almost identical. What can be said about the S^2 term? If $S_{d\pi^*}$ is the *bonding* overlap between a d orbital and a π^* orbital, the overlap between the fragment orbitals in the perpendicular conformation is $S_p = S_{d\pi^*}$, and the total stabilization due to the *four* electrons (Figure 4.4, right-hand side) is proportional to $4S^2_{d\pi^*}$. In the coplanar conformation, the overlap takes place between a d orbital and the $\pi^{*(-)}$ orbital, which is written as $(1/\sqrt{2})(\pi^*_1 - \pi^*_2)$ in normalised form. The overlap involved, S_c, is therefore $(1/\sqrt{2})(S_{d\pi^*} + S_{d\pi^*}) = \sqrt{2}S_{d\pi^*}$, and the stabilization of the *two* electrons (Figure 4.4, left-hand side) is proportional to $2(\sqrt{2}S_{d\pi^*})^2 = 4S^2_{d\pi^*}$. We therefore come to exactly the same result for the two conformations, so we can apparently deduce that there will be essentially free rotation for an ethylene ligand, but this conclusion is contradicted by the experimental results that were presented briefly at the beginning of this section, which indicate a barrier to rotation of about 15 kcal mol^{-1}.

However, we must remember that the expression showing that the energetic stabilization is proportional to $S^2/\Delta\varepsilon$ holds only when there is a large energy difference $\Delta\varepsilon$ between the two interacting orbitals. If the energy gap is not large, then the stabilization is proportional to S (Chapter 1, § 1.3.2, Note 8). In the case under discussion, the energy separation $d - \pi^*$ may be as little as about 2 eV for a molybdenum complex (an estimate obtained from calculations that use the extended Hückel method). It is therefore worthwhile to examine the other limiting case (small $\Delta\varepsilon$, stabilization proportional to S) to compare the two conformations. If we reuse the overlaps calculated above, we find that the stabilization is proportional to $2\sqrt{2}S_{d\pi^*}$ in the coplanar

conformation, but to $4S_{d\pi^*}$ in the perpendicular conformation. The latter is now clearly favoured. This analysis shows us that we can anticipate a marked conformational preference for the perpendicular structure if the $d - \pi^*$ energy separation is not too large. As this gap increases, the energy difference between the two conformations should progressively decrease.

This preference for the perpendicular structure, which is more or less pronounced depending on the orbital energies, is an important result that can be generalized as follows: when two π-acceptor ligands are present, it is preferable for each to interact with a different occupied d orbital, as happens in the perpendicular conformation, rather than for both to interact with the same d orbital, as happens in the planar conformation.

4.1.4. Orientation of H_2 in the 'Kubas complex' $[W(CO)_3(PR_3)_2(\eta^2\text{-}H_2)]$

The preferential orientation of a ligand may also be caused by the presence of non-equivalent ligands on the metallic fragment. In this section, we shall treat what is known as a 'molecular hydrogen complex', that is, a complex in which a *molecule of dihydrogen* is bound to a metal centre in the η^2 mode. This molecule behaves as an L-type ligand, thanks to the two electrons in its $\sigma_{H—H}$ bond. The first example of this type of complex was characterized in 1984, by Kubas and co-workers.[2] It is the d^6 octahedral complex $[W(CO)_3(PR_3)_2(\eta^2\text{-}H_2)]$ (**4-15a**), where R = ^{i}Pr, in which the length of the H—H bond as measured by neutron diffraction (0.82 Å) is only slightly greater than that in an isolated H_2 molecule (0.74 Å).

[2] G. J. Kubas, R. R. Ryan, B. I. Swanson, P. J. Vergamini, H. J. Wassermann *J. Am. Chem. Soc. 106*, 451 (1984). In the following 17 years, about 800 research articles appeared that are devoted to studies of the structures and reactivities of molecular hydrogen complexes.

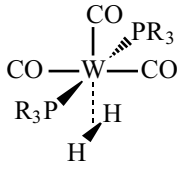

4-15a (exp)

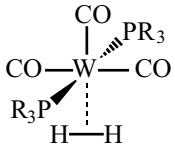

4-15b

One of the remarkable aspects of the structure of this complex is linked to the non-equivalence of the ligands other than H_2 (PR_3 or CO). The dihydrogen molecule is oriented parallel to the W—PR_3 bonds, even though at least one other conformation, that with H—H parallel to the W—CO bonds (**4-15b**), could be imagined. Is there an electronic factor that causes this conformation preference? Before we can answer this question, we have to analyse the orbital interactions that lead to the metal-H_2 bond.

4.1.4.1. *Orbital interactions in a d^6-$[ML_5(\eta^2\text{-}H_2)]$ complex*

We consider first a model d^6 complex $[ML_5(\eta^2\text{-}H_2)]$ in which the five non-H_2 ligands are identical and only have σ interactions with the metal centre. We shall limit ourselves to the conformation in which the H—H bond eclipses two neighbouring M—L bonds (**4-16**).

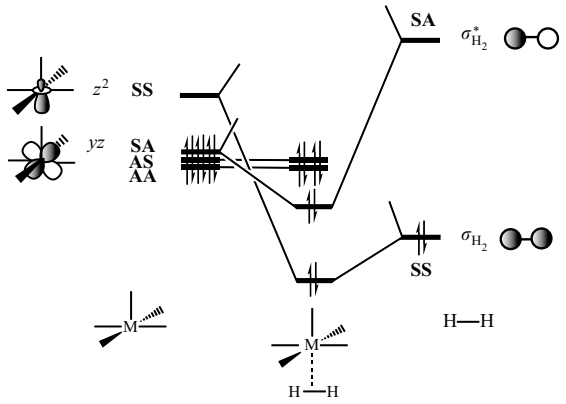

Figure 4.5. Diagram of the interaction between the four lowest-energy d orbitals for a d^6 ML_5 fragment (SBP) and the σ_{H_2} and $\sigma^*_{H_2}$ orbitals of H_2, that enables the MO of the d^6 model complex $[ML_5(\eta^2\text{-}H_2)]$ (**4-16**) to be constructed.

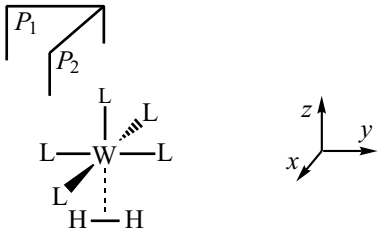

4-16

The complex can be described as the result of interaction of an H_2 molecule with a d^6 square-based pyramidal (SBP) ML_5 metallic fragment. For the latter, we consider, as in § 4.1.2, the four lowest-energy d orbitals (three of which are doubly occupied and nonbonding, the fourth being the polarized, empty z^2 orbital), and the σ_{H_2} and $\sigma^*_{H_2}$ orbitals on H_2 associated with the H—H bond. Given the orbital symmetries with respect to the planes P_1 and P_2 (**4-16**), the interaction diagram shows two two-electron stabilizing interactions (Figure 4.5), between occupied σ_{H_2} and empty z^2 on the one hand (**SS** symmetry), and between occupied yz and empty $\sigma^*_{H_2}$ on the other (**SA** symmetry).

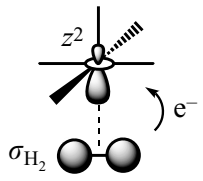

4-17a ($H_2 \rightarrow M$)

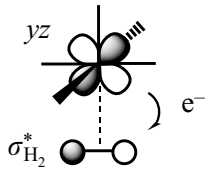

4-17b ($M \rightarrow H_2$)

The first interaction, which leads to a transfer of electron density from dihydrogen to the metal, is of the donation type (**4-17a**), whereas the second, which involves the empty orbital on H_2, is a metal → dihydrogen back-donation interaction (**4-17b**).

Comment

This bonding scheme is completely analogous to the Dewar–Chatt–Duncanson model for the interaction of an ethylene molecule with a metallic centre (Chapter 3, § 3.4), the π_{CC} and π^*_{CC} MO being replaced here by the σ_{H_2} and $\sigma^*_{H_2}$ MO.

Notice that *both* interactions weaken the H—H bond: donation reduces the population of the bonding orbital σ_{H_2}, and back-donation increases the population of the antibonding orbital $\sigma^*_{H_2}$. An increase of

the H—H distance is indeed observed, to a greater or lesser extent, in *all* molecular hydrogen complexes. At the same time, both the occupied **SS** and **SA** MO are bonding between the metal and the hydrogen atoms (**4-17**), so M—H bonds are being formed. This complex may therefore be viewed as a 'frozen structure' along the reaction pathway that leads to the rupture of the H—H bond and the formation of two M—H bonds (an oxidative addition reaction with the formation of a dihydride complex).[3]

[3] In solution, an equilibrium is established for the Kubas complex between the dihydrogen and dihydride forms, confirming that the molecular hydrogen complex is an intermediate in the oxidative addition reaction of H_2.

4.1.4.2. *Orientation of H_2 in the Kubas complex*

We shall consider two orientations for the H_2molecule. The H—H bond is either parallel to the W—CO bonds (**4-18a**), or parallel to the W—PR_3 bonds (**4-18b**), the latter conformation being found experimentally.

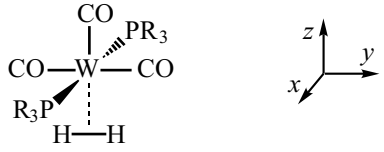

4-18a **4-18b**

As in the preceding examples (§ 4.1.2 and 4.1.3), the donation interaction does not depend on the orientation of the dihydrogen molecule, due to the cylindrical symmetry of the z^2 orbital (**4-19a**). The back-donation interaction involves either the *yz* or the *xz* orbital on the metallic fragment, in the first or second confirmations, respectively (**4-19b** and **c**), and the $\sigma^*_{H_2}$ MO on dihydrogen. If all the ligands other than H_2 are identical, the *xz* and *yz* orbitals are degenerate and there is therefore no difference between the two back-bonding interactions represented in **4-19b** and **c**. Both sketches therefore represent the eclipsed conformation of a $d^6[ML_5(\eta^2\text{-}H_2)]$ complex.

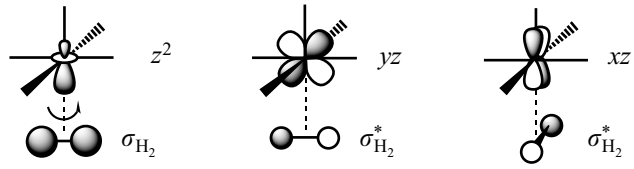

4-19a **4-19b** **4-19c**

In the Kubas complex, the presence of carbonyl ligands (π acceptors) and phosphines (which may, in a first approximation, be considered as

pure σ-donors), lifts the degeneracy of the nonbonding *d* orbitals. As we have shown in Chapter 3 (§ 3.3.3.2), *yz* is stabilized by three bonding interactions with π^*_{CO}, *xy* by two but *xz* by only one (**4-20**); as a result, the energies of these orbitals follow the order $\varepsilon_{yz} < \varepsilon_{xy} < \varepsilon_{xz}$.

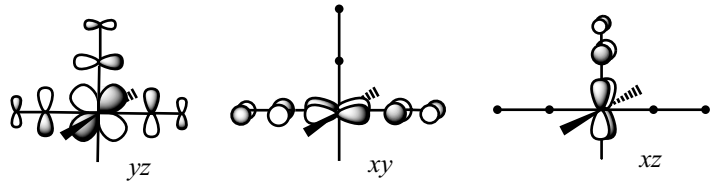

4-20

There is an important consequence of this energetic non-equivalence: in this complex, the back-donation interaction depends on the conformation that is adopted. In structure **4-18a**, $\sigma^*_{H_2}$ interacts with the lowest of the three *d* orbitals (*yz*), but with the highest (*xz*) in **4-18b**. Since the $\sigma^*_{H_2}$ orbital is strongly antibonding, the energy gap ($\Delta\varepsilon$) between it and any of the three *d* orbitals is large. We may therefore assume that the stabilization created by the interaction is proportional to $S^2/\Delta\varepsilon$. The energetic factor ($\Delta\varepsilon$) favours conformation **4-18b**, since the energy gap between the interacting orbitals is smaller (Figure 4.6). When we consider the overlap, it is important to realize that *yz* is delocalized into three carbonyl groups, but *xz* into only one (**4-20**). Since MO are always normalized, the coefficient of the *d* orbital is larger for $xz(+1\pi^*_{CO})$ than for $yz(+3\pi^*_{CO})$, thereby favouring structure **4-18b** ($S_{\sigma^*-xz} > S_{\sigma^*-yz}$, Figure 4.6). So both factors, energy gap and overlap, favour the conformation in which H—H is parallel to the W—PR_3 bonds.

We note, in conclusion, that the conformation adopted by H_2 in the Kubas complex is controlled by the back-donation interaction (**4-15**).

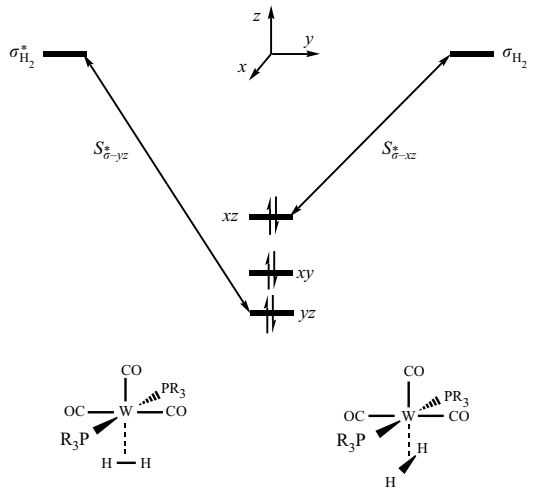

Figure 4.6. The back-donation interaction in conformations **4-18a** (on the left, H—H parallel to the W—CO bonds) and **4-18b** (on the right, H—H parallel to the W—PR_3 bonds) of the complex $[W(CO)_3(PR_3)_2(\eta^2\text{-}H_2)]$.

But since there is a large energy gap between the orbitals involved in this interaction, the conformational preference is rather weak, and the barrier to rotation of the H_2 molecule is only about 2–3 kcal mol^{-1}.

4.2. 'Abnormal' bond angles

The geometry of some complexes may be very different from one's initial thoughts, particularly for bond angles. We shall study two examples, to see which electronic factors may cause what appears to be a large distortion from an 'ideal' structure.

4.2.1. Agostic interactions

4.2.1.1. *Introduction*

In carbene complexes [$L_nM{=}CHR$], the most common geometry is trigonal-planar about the carbon, with M—C—H_α and M—C—R angles close to 120° (**4-21a**). But a large structural change occurs in some complexes: the M—C—H_α angle decreases to about 80°, whereas the M—C—R angle increases very considerably, to 160–170° (**4-21b**). The deformation that is observed can therefore be described as a pivoting of the alkylidene ligand, which brings the C—H_α bond closer to the metal centre.

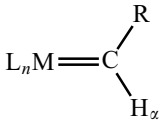

4-21a

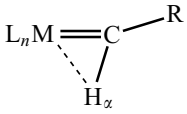

4-21b

The same phenomenon can be observed with an alkyl ligand. For example, the methyl group can pivot, decreasing the M—C—H_1 angle from the expected value of 109° (**4-22a**) to about 90° (**4-22b**).

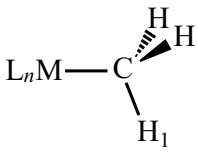

4-22a

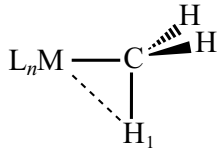

4-22b

All these complexes are electron-deficient ($N_t < 18$). The deformation that is observed has therefore often been interpreted as the consequence of the pressure to complete the valence shell of the metal, even if a substantial geometrical distortion is necessary, by introducing an additional interaction with a C—H bond.

The group which brings the C—H bond with its two electrons into the vicinity of the metal centre has been called 'agostic' by Brookhart and Green.[4] These complexes can be considered as 'frozen' structures on the pathway for the insertion of a metal into a C—H bond, in the same way that molecular hydrogen complexes were treated on the oxidative addition pathway that leads to a dihydride (§ 4.1.4).

[4] M. Brookhart, M. L. H. Green *J. Organomet. Chem. 250*, 395 (1983).

4.2.1.2. *An agostic methyl group: the complex* $[Ti(Cl)_3(Me_2P{-}(CH_2)_2{-}PMe_2)(CH_3)]$

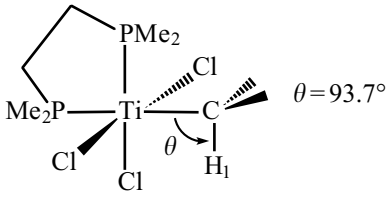

4-23

The structure of the complex $[Ti(Cl)_3(Me_2P{-}(CH_2)_2{-}PMe_2)(CH_3)]$ obtained by neutron diffraction reveals an agostic methyl group, as the Ti—C—H_1 angle is only 93.7° (**4-23**). It is an essentially octahedral complex, in which the oxidation state of titanium is +4. The electronic configuration is thus d^0, so the d block is completely empty! This complex is therefore severely electron-deficient, as $N_t = 12$ (the electrons associated with the six metal–ligand bonds).

To simplify the problem, we shall analyse the model octahedral complex $[Ti(H)_5(CH_3)]^{2-}$, in which all the ligands except CH_3 have been replaced by hydrogen atoms. The two negative charges are necessary to obtain a d^0 electronic configuration. Although this simplified complex has no experimental reality, it does possess the essential characteristics of the real complex **4-23**: the same number of ligands, the same electronic configuration, and the presence of a methyl ligand that may be subject to an agostic distortion.[5]

We shall consider two structures in turn: the non-agostic case (**4-24a**) in which the Ti—C—H_1 angle is 109°, and an agostic version (**4-24b**) where the Ti—C—H_1 angle is close to 90°. To pass from one structure to the other, the methyl group is pivoted about the carbon atom, as in the experimental structure **4-23**.

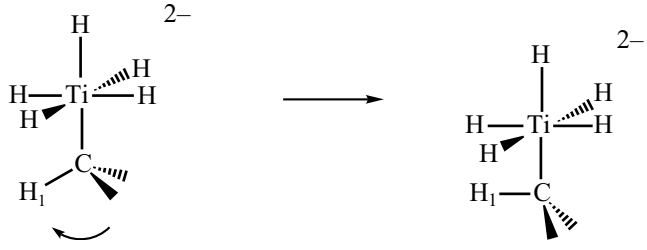

4-24a (non-agostic) **4-24b** (agostic)

We shall analyse the interactions between the methyl group and the metallic centre by decomposing the complex $[Ti(H)_5(CH_3)]^{2-}$ into two fragments, CH_3^- and $[TiH_5]^-$. In the first, which is a pyramidal AH_3 system, the lone pair on carbon is described by a hybrid orbital that is essentially nonbonding (see Chapter 1, Figure 1.4). This MO is the highest-energy occupied orbital; we shall refer to it as n_{CH_3}, and at least initially, it is the only orbital that we shall consider on this fragment (Figure 4.7, right-hand side). The metallic fragment is of the ML_5 type (SBP), where the metal is located in the base of the pyramid. As in the examples treated in § 4.1.2 and 4.1.4, we shall consider only the four lowest-energy *d* orbitals on this fragment, three of which are nonbonding (*xy*, *xz*,

[5] This is an acceptable model for a *qualitative* analysis based on changes in overlaps, on the occupation of different orbitals, etc. But if more accurate calculations were to be undertaken for a *quantitative* study, then it would be necessary to study either the real complex, or a much less simplified model, such as $[Ti(Cl)_3(PH_3)_2(CH_3)]$.

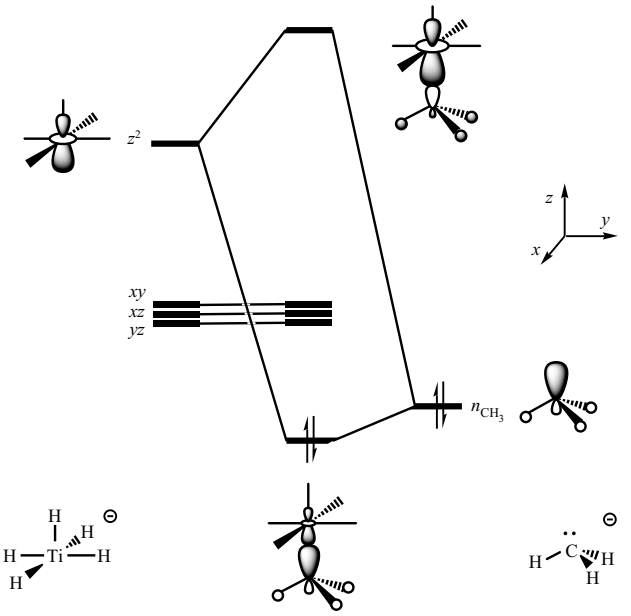

Figure 4.7. Orbital interaction diagram for the CH_3^- and $[TiH_5]^-$ fragments in the non-agostic structure **4-24a**.

and *yz*) and one antibonding (z^2). Since the electronic configuration of $[TiH_5]^-$ is d^0, these four orbitals are empty (Figure 4.7, left-hand side).

We consider first the non-agostic structure **4-24a**, in which the local C_3 axis of the methyl group coincides with the Ti—C bond. The orbital interaction diagram is presented in Figure 4.7. The orbital n_{CH_3} cannot interact with any of the nonbonding orbitals on the metallic fragment, since it is of σ-type and located in one of the nodal planes of the *xy*, *xz*, and *yz* orbitals. However, its overlap with z^2 is very large, since these two orbitals both point along the *z*-axis and they are polarized towards each other. Their interaction produces a bonding MO, which is doubly occupied and mainly concentrated on the ligand; it characterizes the $\sigma_{Ti—C}$ bond. The antibonding combination makes up one of the antibonding MO of the d block in this octahedral complex (the z^2 orbital).

The pivoting of the methyl group (**4-24b**) moves its local C_3 axis, so that the n_{CH_3} orbital is no longer oriented along the *z*-axis (**4-25**). The overlap between n_{CH_3} and z^2 therefore decreases, as does the electronic stabilization associated with this interaction. If this were the only factor to consider, this motion would therefore be energetically unfavourable, and no agostic distortion would be expected.

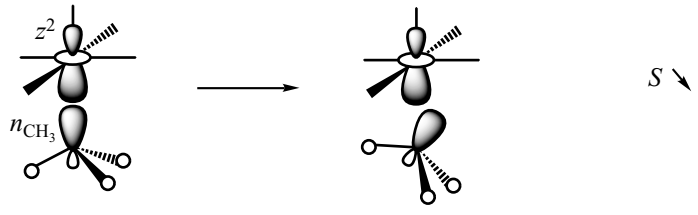

4-25

However, there is another significant change in the orbital interactions: the overlap between n_{CH_3} and *yz*, which was zero in the non-distorted structure, becomes substantial in the agostic structure (**4-26**). Since the *yz* orbital is empty (a d^0 fragment), a new stabilizing interaction is created which now favours the agostic structure. Note that no interaction can take place between n_{CH_3} and *xy* or *xz* ($S = 0$), whatever the geometry.

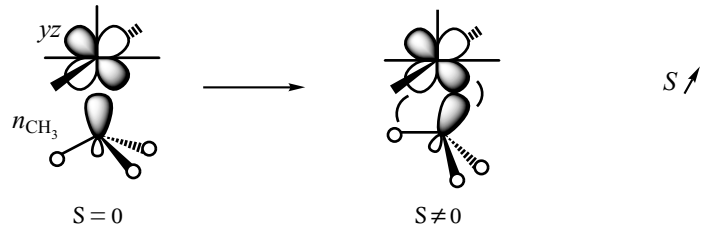

4-26

Two factors have therefore been revealed; one is unfavourable for the distortion, but the other favours it. How, then, can we explain why the second factor dominates the first? We need to consider the relative energies of the orbitals concerned. The energy gap $\Delta\varepsilon$ between n_{CH_3} and *yz* (nonbonding) is much smaller than that between n_{CH_3} and z^2 (antibonding; see Figure 4.7). Now the electronic stabilization increases if the difference in energy between the interacting orbitals decreases. The agostic distortion therefore progressively replaces the ($n_{CH_3} \leftrightarrow z^2$) interaction by a stronger one ($n_{CH_3} \leftrightarrow yz$). Despite what might have been expected, this distortion reinforces the Ti—C bond.

At this point in our analysis, we must note that the interpretation of the agostic distortion we have suggested does not really match the notion that it is due to an additional interaction between a hydrogen atom, or a C—H bond, and the metal centre. Notice, however, that a weak M. . . H bonding interaction does appear in the MOs represented in **4-26** for the agostic structure (right-hand side). Moreover, one of the bonding MO of CH_3 (often referred to as π_{CH_3}), that mainly characterizes the C—H_1 bond, does have an increased interaction with the empty *yz* orbital, due to the substantial overlap between $1s_{H_1}$ and *yz* (**4-27**). This interaction

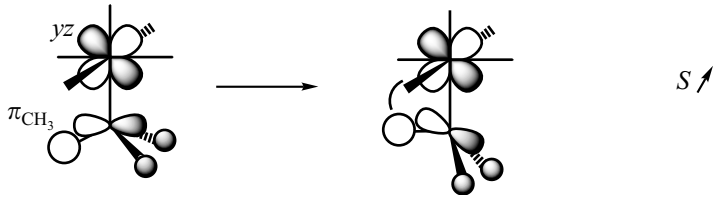

4-27

leads to a transfer of electron density from the ligand to the metal, weakening the C—H_1 bond (loss of bonding electrons) but creating an incipient Ti—H bond (gain of bonding electrons). This factor adds to the one previously discussed, further stabilizing the agostic structure.

To conclude, the important point is that the agostic distortion occurs because there is a *low-energy, empty orbital* (*yz* in our example) in the non-distorted complex that can be used to make the distortion favourable. Both characteristics are important: (*i*) *empty*, because if it were occupied, the two-electron stabilizing interactions shown in **4-26** and **4-27** (right-hand sides) would become repulsive four-electron interactions, which would therefore oppose the distortion. We are reminded of the need for an electron-deficient metal, that was noted at the beginning of this section; (*ii*) *low in energy*, so that the favourable factor described in **4-26** dominates the unfavourable factor described in **4-25**. This aspect is also very important, since no agostic distortion of the methyl group is observed, for example, in the complex [$Ti(Cl)_3(CH_3)$], even though it is extremely electron-deficient (formally, only eight electrons!). It can be shown that the empty orbital that could be used in an agostic distortion is in fact too high in energy in this complex to be useful; the three Ti—C—H angles remain equal.

4.2.2. d^6 ML_5 complexes: a 'T-shaped' or 'Y-shaped' geometry?

d^6 ML_5 complexes are electron-deficient species (16e) that often appear as reaction intermediates. They are indeed obtained from octahedral d^6 ML_6 complexes (18e) by the loss of a ligand, which is the first stage in many organometallic reactions. Despite this high reactivity, many of them have been isolated and geometrically characterized.

For a long time, the only coordination mode known for these complexes was the SBP. The group VI (Cr, Mo, W) pentacarbonyl complexes were the first to be observed, and many others with this geometry were later characterized with different metals (Ru(II), Rh(III), Ir(III), etc) and very varied ligands (alkyl, silyl, phosphine, halide, etc.). In all these complexes, the angle between two basal transoid ligands lies between 160° and 180°; three examples are shown in **4-28**.

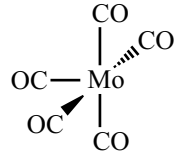

4-28a

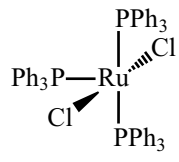

4-28b

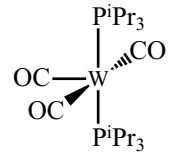

4-28c

There is nothing surprising about this coordination mode for *diamagnetic* d^6 ML_5 systems. The d block of an SBP complex, with the metal either in the basal plane of the pyramid or close to it, contains three nonbonding orbitals that are derived from the t_{2g} block of the octahedron (see Chapter 2, § 2.3.1). This environment is therefore ideal to accommodate three pairs of electrons. Subsequently, however, far more surprising structures were observed.[6] These complexes adopt the geometry of a distorted trigonal bipyramid, where one of the equatorial angles is only some 75-80°. Three examples are shown in **4-29**.

[6] The first two structures of this type were discovered in 1986: H. Werner, A. Hohn, M. Dziallas *Angew. Chem. Int. Ed. Engl. 25*, 1090 (1986); M. D. Fryzuk, P. A. McNeil, R. G. Ball *J. Am. Chem. Soc. 108*, 6414 (1986).

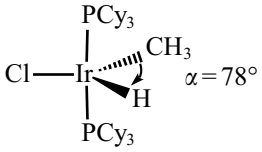

4-29a

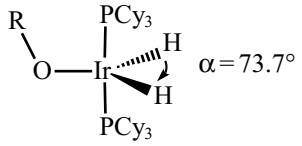

4-29b

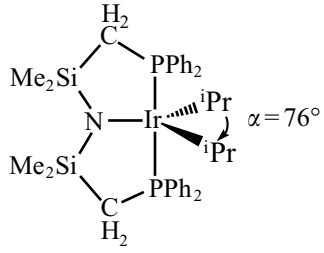

4-29c

Notice that the movement from an SBP structure to a distorted TBP geometry can be described by the change of one bond angle (α) from ~180° to ~75°, the intermediate value of 120° corresponding to a regular TBP geometry (**4-30**). Referring to the relative positions of the ligands L_1, L_2, and L_3, the SBP structure is said to be 'T-shaped', and the distorted TBP to be 'Y-shaped'.

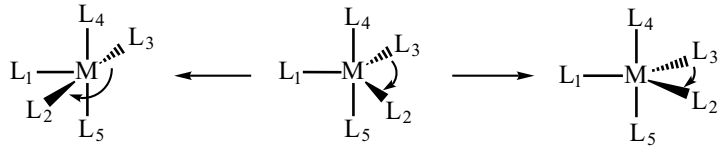

4-30

Three questions arise:

1. Why do the diamagnetic d^6 ML_5 complexes not adopt a regular TBP geometry ($\alpha = 120°$)?
2. Why are two different structures observed, 'T-shaped' and 'Y-shaped'?
3. What are the electronic factors that favour one or other of these structures?

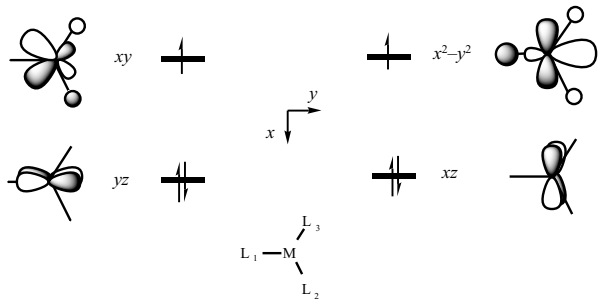

Figure 4.8. d-block of a TBP complex (the strongly antibonding orbital z^2 is not shown). In the interests of clarity, the axial ligands located on the *z*-axis are omitted. The electronic occupation is given for a d^6 paramagnetic ML_5 complex (a triplet state).

The answer to the first question is straightforward, if we analyse the structure of the d block of a TBP complex (Figure 4.8, where the equatorial plane *xy* is the plane of the page); two orbitals are nonbonding (*xz* and *yz*) and two are weakly antibonding (*xy* and x^2-y^2).

Six electrons must be placed in these orbitals. It is clear that the splitting pattern of the d block favours a paramagnetic ground state, with one electron in each of the antibonding orbitals (a triplet state, Figure 4.8). However, this orbital arrangement is not favourable for diamagnetic complexes (all electrons paired), and all those we have mentioned are of this type. That is why none of them adopts the regular TBP structure.

4.2.2.1. *Correlation diagram Y ← TBP → T (σ interactions only)*

The geometries that are observed experimentally suggest that we should study the correlation diagram for the d-block orbitals as the TBP structure ($\alpha = 120°$) is changed either to the T-shaped ($\alpha = 180°$) or to the Y-shaped geometry (α close to 80°). We shall suppose initially that the ligands only have σ-type interactions with the metal.

During this deformation, the ligands L_2 and L_3 move in the equatorial plane of the initial TBP (**4-30**). They therefore remain in one of the nodal planes (*xy*) of the nonbonding *xz* and *yz* orbitals (Figure 4.7), so the shapes and energies of these two stay constant. But substantial changes do occur for the two other orbitals on leaving the regular TBP structure. In the T-shaped structure, the ligands L_2 and L_3 are situated

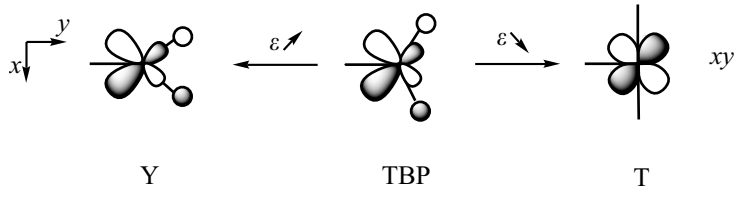

4-31

in a nodal plane of the *xy* orbital, which therefore becomes nonbonding (**4-31**, right-hand side). On the other hand, the antibonding interaction with L_2 and L_3 increases in the Y-shaped structure, leading to a destabilization of the *xy* orbital (**4-31**, left-hand side).

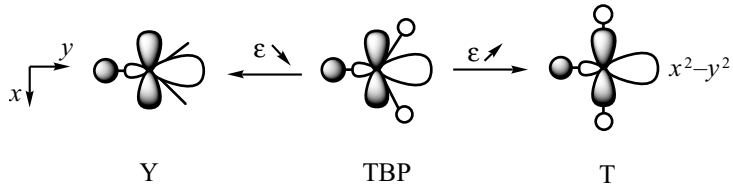

4-32

Turning to the x^2-y^2 orbital, movement to the T-shaped structure increases its antibonding interactions with L_2 and L_3 located on the *x*-axis, producing a destabilization (**4-32**, right-hand side). In contrast, these interactions are decreased, if not eliminated, in the Y-shaped structure, as these ligands are placed approximately on the nodal surfaces of the x^2-y^2 orbital (**4-32**, left-hand side). This orbital is therefore stabilized, but not to the point of becoming nonbonding, as there is still an antibonding interaction with ligand L_1.

The correlation diagram shown in Figure 4.9 groups all these results. It is striking that the deformation of the TBP to the T- or Y-shaped structures stabilizes one of the two antibonding orbitals (*xy* for T, x^2-y^2 for Y) but destabilizes the other. As a consequence of this lifting of the orbital degeneracy, associated with a deformation of the complex which lowers its symmetry ($D_{3h} \rightarrow C_{2v}$), the diamagnetic state in which the two electrons are paired is stabilized. This is an example of what is known as a Jahn–Teller distortion.

We are now able to understand why diamagnetic d^6 ML_5 complexes can adopt either the T- or Y-shaped structure, as there are three

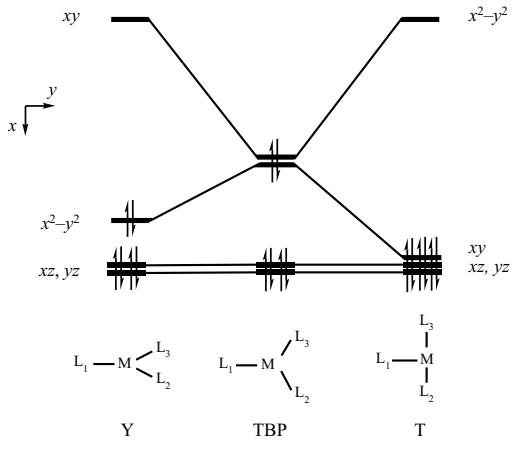

Figure 4.9. Schematic correlation diagram for the four lowest-energy *d* orbitals, linking the central TBP structure to the Y- or T-shaped geometries (left- and right-hand sides, respectively).

low-energy *d* orbitals in each of them. In the first, the ground-state electronic configuration is $((xz)^2, (yz)^2, (xy)^2)$, whereas in the second it is $((xz)^2, (yz)^2, (x^2-y^2)^2)$. The T-shaped structure does appear a little more favourable from the diagram, since the three occupied orbitals are nonbonding.

4.2.2.2. *The role of π-type interactions*

The crucial electronic factor turns out to be the π-donor or π-acceptor properties of the ligand L_1 that is *trans* to the angle α. We consider first a π-acceptor ligand such as CO. It is easy to show that the *xz* and *yz* orbitals, both of which are occupied, are influenced by the π^*_{CO} orbitals to the same extent in the T- and Y-shaped structures: *xz* stays unchanged (the overlap is zero by symmetry), whereas *yz* is stabilized by a bonding interaction with the π^*_{CO} orbital that is parallel to the *z*-axis. It is the third occupied orbital that makes the difference: *xy* (T-shaped structure) is *stabilized* by a bonding interaction, but x^2-y^2 (Y-shaped structure) stays unchanged, since its overlap with the π^*_{CO} orbitals is zero by symmetry (**4-33**). The preference for the T-shaped structure due to the σ interactions is therefore reinforced by the presence of a π-acceptor ligand in the position L_1.

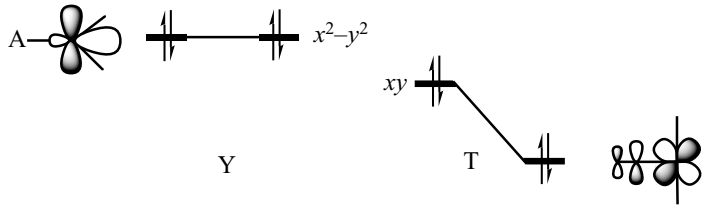

4-33 ($L_1 = \pi$ acceptor (A))

We now consider a π donor such as Cl. The same analysis is applied, but we now find that the *xy* orbital of the T-shaped structure is *destabilized* by an antibonding interaction with a lone pair on chlorine (**4-34**).

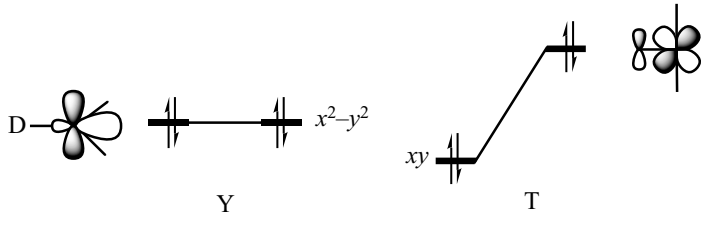

4-34 ($L_1 = \pi$ donor (D))

The presence of a π-donor therefore destabilizes the T-shaped structure with respect to the Y-shaped one. Looking at the structures shown in **4-29**, we do indeed notice that they all have a π-donor ligand (chloride, alkoxy, amino) *trans* to the acute angle α. In the case of a single-face π-donor ligand (amino, for example), the destabilizing effect for the T-shaped structure shown in **4-34**, which therefore favours the Y-shaped structure, can only occur if the lone pair on the donor lies in the equatorial plane, so that it can interact with the *xy* orbital. That is just what happens in the complex shown in **4-29c**.

4.3. Carbene complexes

4.3.1. Ambiguity in the electron count for carbene complexes

Carbene complexes, whose general formula is $[L_nM{=}CR_2]$ and which formally contain an M=C double bond, create a real problem for the calculation of the metal's oxidation state. This problem arises because the bent CR_2 ligand possesses two nonbonding orbitals, close in energy, in which two electrons must be placed (see Chapter 1, Figure 1.5). The lower of these is a hybrid orbital n_σ (**4-35a**), whereas the higher is a pure *p* orbital (if we consider the simplest example, methylene, CH_2), n_p (**4-35b**).

4-35a (n_σ)

4-35b (n_p)

In the covalent model, the two electrons are placed in the lower-energy orbital (configuration $(n_\sigma)^2$), so that the carbene is considered as an L-type ligand which does not oxidize the metal (**4-36a**). However, due to the small difference in energy between the n_σ and n_p nonbonding MO, the ground electronic state of several carbenes (CH_2, for example) is in fact the triplet $^3[(n_\sigma)^1(n_p)^1]$. In this situation, with two unpaired electrons, it seems more logical to consider the carbene as an X_2 ligand (**4-36b**) which oxidizes the metal by two units.

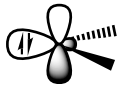

4-36a (L)

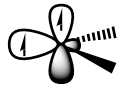

4-36b (X_2)

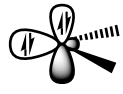

4-36c (dianion)

If we now consider the ionic model, the electronic octet of the carbon must be completed, which means that we must consider the dianionic form $(CR_2)^{2-}$ (**4-36c**). Since the two extra electrons were supplied by the metal, we obtain the same oxidation state as that yielded by the covalent model with an X_2 ligand. In the ionic description, the dianion $(CR_2)^{2-}$ is a strong π-donor, due to its doubly occupied *p* orbital.

It is important to be aware of these different possible points of departure, since the ambiguity in the calculation of the oxidation

state appears very frequently in experimental articles about these complexes. An example is given in **4-37**, where we see that the complex $[Cp_2Ta(CH_3)(CH_2)]$ can be described as a d^2 Ta(III) complex, if CH_2 is considered as an L-type ligand in the covalent model, or as a d^0 Ta(V) complex if we use either the X_2 description of the covalent model or the ionic description. It may well seem disconcerting not to know if the electronic configuration of this complex is d^2 or d^0, since that appears to imply that one does not know how many electrons must be placed in the d block! Note, however, that the total number of electrons does not depend on the model chosen ($N_t = 18$).

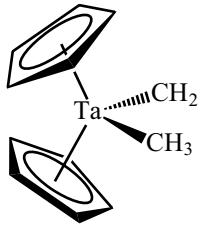

$CH_2 = L \Rightarrow [Ta(L_2X)_2(L)(X)] \Rightarrow Ta(III): \quad d^2$

$CH_2 = X_2 \Rightarrow [Ta(L_2X)_2(X_2)(X)] \Rightarrow Ta(V): \quad d^0$

} covalent

$(CH_2)^{2-}; 2Cp^-; (CH_3)^- \Rightarrow Ta^{5+}: \; d^0$ ionic

4-37

This apparently complicated situation (which is at least fairly complicated in reality) arises from the different possible choices for the electron distribution within the CR_2 ligand (L or X_2?) or between the ligand and the metallic fragment (a neutral or a dianionic ligand?). The initial distribution is in fact somewhat arbitrary no matter which choice is made, and the situation becomes clearer if one considers the electronic structure *of the complex as a whole*, rather than that of the separate fragments.

4.3.2. Two limiting cases: Fischer carbenes and Schrock carbenes

To clarify these points, we shall consider the carbene as an L-type ligand (**4-36a**). It therefore acts as a σ donor, using its lone pair described by the n_σ orbital, which interacts with an empty orbital on the metal (e.g. z^2, **4-38a**). In this model, the n_p orbital is empty, so the carbene acquires a π-acceptor character (single face) (**4-38b**). The interaction scheme is similar to that in the Dewar–Chatt–Duncanson model (Chapter 3, § 3.4.1) used, for example, to describe ethylene complexes or molecular hydrogen complexes (§ 4.1.4).

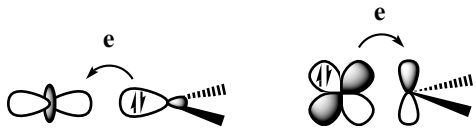

4-38a **4-38b**

However, an important difference arises, since the empty *p* orbital on the carbene can be strictly nonbonding (as in CH_2), and therefore at low energy, rather than antibonding (π^*_{CC}, $\sigma^*_{H_2}$) as in the preceding examples. Depending on the nature of the metal, the ligands and the substituents on the carbene, this orbital can therefore be *either higher or lower in energy* than the *d* orbitals on the metal. To prove this point, one need only consider the energy of the *d* orbitals for the first transition series, which ranges from −8.5 (Sc) to −14 eV (Cu), whereas the energy of a *p* orbital on carbon is −11.4 eV (parameters of the extended Hückel method).

4.3.2.1. *Two interaction schemes for back-donation*

When the *p* orbital is higher in energy than the *d* orbital, we obtain a typical back-donation scheme, with the formation of a bonding MO mainly located on the metal (**4-39**): formally, we may consider that the π interaction does not oxidize the metal, since the two electrons stay mainly localized on this centre. In this case, the description of the carbene as an L-type ligand is therefore quite appropriate. However, if the *p* orbital is *lower* in energy than the *d* orbital, the occupied bonding MO is mainly concentrated on the carbene (**4-40**), so that in a formal

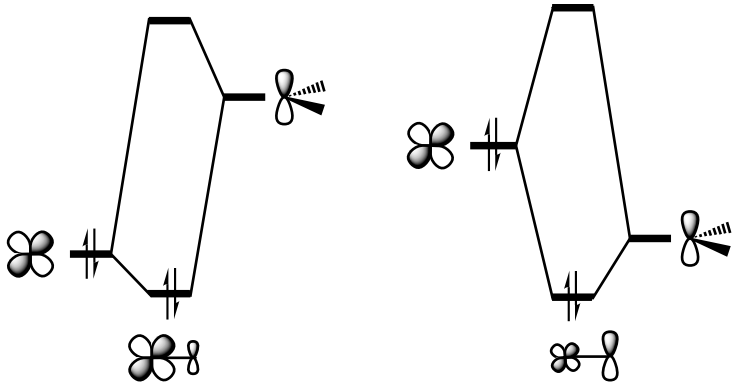

4-39 **4-40**

sense, two electrons have been transferred from the metal to this ligand. In other words, the *d* orbital that was occupied before the interaction is

transformed to an MO of the complex that is mainly concentrated on the ligand: the d block therefore 'loses' two electrons. In this case, the description of the carbene as an X_2-type ligand or as a dianionic ligand $(CR_2)^{2-}$, which leads to an increase of the metal's oxidation state by two units, corresponds more closely to reality.

The ambiguity that we noticed previously for the electron count in carbene complexes in fact corresponds to chemical reality: the L and X_2 (or dianion) formulations are appropriate for the situations described in **4-39** and **4-40**, respectively.

We shall now examine how the nature of the metal, the ligands, and the substituents on the carbene can favour one or other of these two possibilities.

4.3.2.2. *Fischer carbenes and Schrock carbenes*

How can the situation described in **4-39** be favoured, with an acceptor orbital on the carbene that is clearly higher in energy than the metal *d* orbital? We require that the *d* orbital is low in energy and at the same time that the *p* orbital is high. The *d* orbital factor therefore leads us to consider metals *towards the right-hand side* of the periodic classification, or at the limit in the centre, since the energy of the metal orbitals is lowered on passing from left to right in a transition series (see Chapter 1, Table 1.4). In addition, the presence of *π-acceptor ligands* also leads to a lowering of the level of the *d* orbitals. As far as the carbene is concerned, the energy of the empty *p* orbital is raised *if the substituents are π donors*, that is, if they have lone pairs (halogens, O—R, NR_2, etc.). An example is shown in **4-41** for the carbene CCl_2. The in-phase combination of the *p* lone pairs on the chlorine atoms

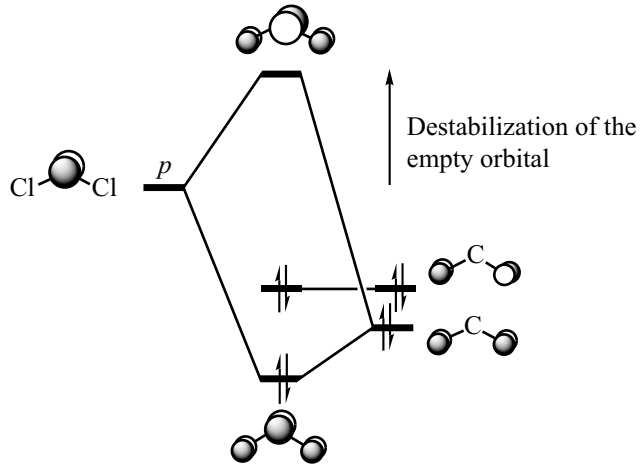

4-41

destabilizes the empty orbital on carbon and therefore favours the situation depicted in **4-39**. Carbene complexes that possess these characteristics are called *Fischer carbenes*. As examples, we may consider complexes such as $[(CO)_5W{=}C(Ph)(OMe)]$, $[(CO)_4Fe{=}C(Ph)(OMe)]$, $[(CO)_5Cr{=}C(N^iPr_2)(OEt)]$, or $[Cp(CO)(PPh_3)Fe{=}CF_2]^+$. Since the carbene is usually considered to be an L-type ligand for the calculation of the oxidation state of the metal, these are described as complexes of W(0), Fe(0), Cr(0), and Fe(II), respectively.

In this group of compounds, the carbene acts as a σ donor and a rather weak π acceptor, due to the relative energies of the *d* and *p* orbitals. Overall, the electron density around the carbon of the carbene is decreased, leading to a metal–carbon bond that is polarized $M(\delta^-) = C(\delta^+)$, with an *electrophilic* character for the carbon centre: it is therefore likely to be attacked by nucleophiles, and it is possible, for example, to interconvert two carbene complexes (**4-42**).

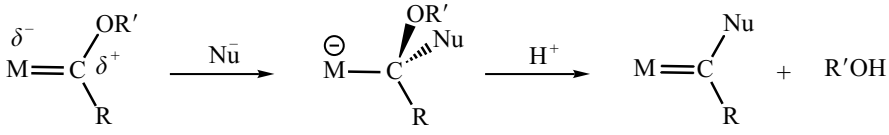

$Nu^- = H^-, R^-, R_2N^-, RS^-$

4-42

In order to obtain the situation shown in **4-40**, where the *p* orbital on carbon is at lower energy than the *d* orbital, the conditions previously suggested for the Fischer carbenes must be reversed: the metal must come from the left of the periodic table, and must have π-donor ligands to destabilize the *d* orbital, instead of π-acceptors. Moreover, to ensure that the *p* orbital on the carbene is as low in energy as possible, its substituents cannot be π donors: CH_2 itself is a good candidate, and, more generally, alkyl substituents are suitable (the term 'alkylidene' is often used for a carbene substituted by alkyl groups). The complexes $[Cp_2(CH_3)Ta{=}CH_2]$ and $[CpCl_2Ta{=}C(H)(CMe_3)]$ are typical examples. As we have already noted, the metal in this group of complexes is usually considered to be oxidized by two units by the alkylidene ligand, so the two examples mentioned above contain Ta(V).

Carbene complexes that possess these properties are called *Schrock carbenes*. The π interaction shown in **4-40** is accompanied by a substantial transfer of electron density from the metal to the carbon atom. This transfer more than outweighs the σ donation (ligand $\rightarrow$ metal), so that the metal–carbon bond is polarized in the sense $M(\delta^+){=}C(\delta^-)$. Schrock carbenes therefore possess a *nucleophilic carbon*, and give, for example, addition products with Lewis acids such as $AlMe_3$ (**4-43**).

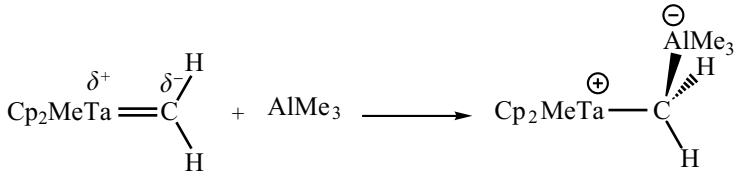

4-43

In summary, Fischer carbenes (electrophiles) and Schrock carbenes (nucleophiles) correspond to two different possibilities for the orbitals that participate in the π interaction (**4-39** and **4-40**). We often distinguish between them for the calculation of the metal's oxidation state: the carbene ligand is considered to be of L-type for the first category, but as an X_2 ligand (or CR_2^{2-}) for the second. The characteristics that we have suggested for each category are, of course, only general indications. Some complexes may be found on the border between the two groups. For example, the complex $[Cp_2(CH_3)Ta{=}CH_2]$ is, as expected, a nucleophilic carbene (Schrock-type), but the tungsten complex $[Cp_2(CH_3)W{=}CH_2]^+$, which has exactly the same ligands, is electrophilic (Fischer-type). The presence of a positive charge on the metallic fragment, which stabilizes the metal's *d* orbitals and thereby favours the situation shown in **4-39**, provides a plausible explanation of this difference in behaviour, despite the low energy of the nonbonding *p* orbital on the carbon atom.

4.4. Bimetallic complexes: from a single to a quadruple bond

In organic chemistry, we know that two carbon atoms can be linked by a single bond (σ), a double ($\sigma + \pi$), or a triple bond ($\sigma + 2\pi$). The increase in bond order is accompanied by a decrease in interatomic distance, from 1.54 Å (C—C), through 1.34 (C=C) to 1.20 Å (C≡C). From the orbital point of view, these different bond orders correspond to the occupation of one, two, or three bonding MO between the two carbon atoms (**4-44**), it being clear that the corresponding antibonding MO are empty. The orbital that characterizes the σ bond has cylindrical symmetry about the internuclear axis in each case, whereas the orbitals that characterize the π bond(s) have a nodal plane (**4-44**).

It is natural to wonder how many bonds, of what type, can exist between the two metal centres in bimetallic complexes. The characteristics presented above will reappear in the description of metal–metal bonds, but the presence of *d*-type orbitals introduces a significant new feature.

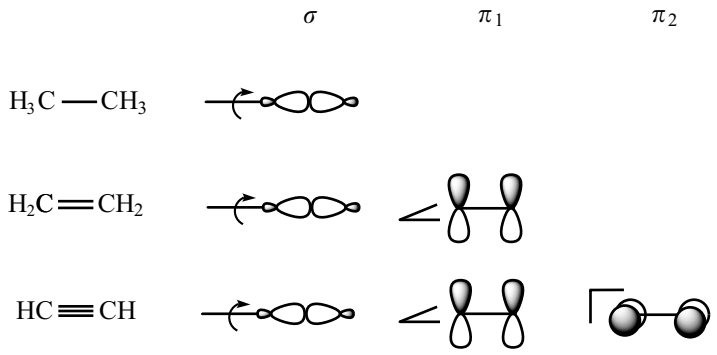

4-44

4.4.1. σ, π, and δ interactions

We shall consider the interactions between the *d* orbitals on two metallic centres, *initially ignoring any influence of the ligands on these orbitals*. Each interaction leads to the formation of a bonding and an antibonding MO, but only the first of these, written $^{(+)}$, is shown in **4-45**. The interaction between the z^2 orbitals (**4-45a**) is of σ type; the axial overlap between the two orbitals has cylindrical symmetry around the internuclear axis (z). The MO $xz^{(+)}$ and $yz^{(+)}$ (**4-45b**) have the same characteristics as the π orbitals of acetylene (**4-44**); they are bonding, and they possess a nodal plane that passes through the nuclei.

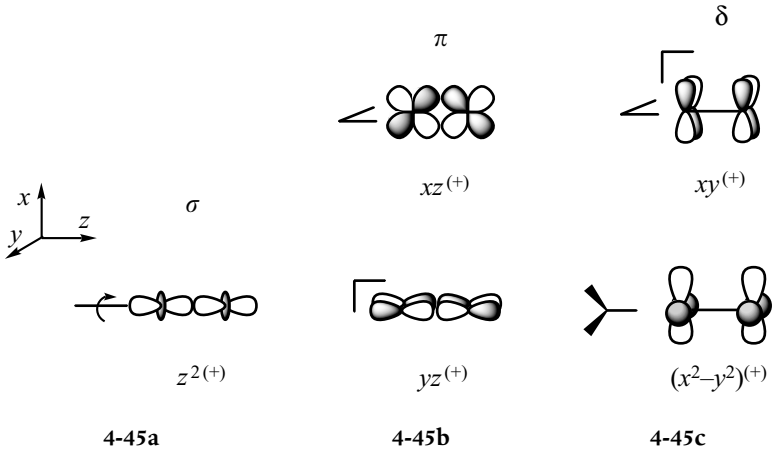

4-45a **4-45b** **4-45c**

The novel feature compared to organic systems arises in the interactions between the pairs of orbitals xy and x^2-y^2. In each case, the bonding MO that are formed have *two nodal planes*, instead of just one for the π MO: these are the xz and yz planes for the $xy^{(+)}$ orbital, and the planes that bisect the x-and y-axes for the $(x^2-y^2)^{(+)}$ orbital (**4-45c**). These are described as δ interactions.

The overlaps involved depend on the type of interaction. The axial overlap S_σ is larger than or comparable to the lateral overlaps S_π. However, the S_δ overlap is much smaller than these, only about a third or a quarter of S_π.

4.4.2. M_2L_{10} complexes

Consider a bimetallic complex of the type M_2L_{10} (**4-46**), whose MO may be constructed by the interaction of two monometallic fragments ML_5 with an SBP geometry.

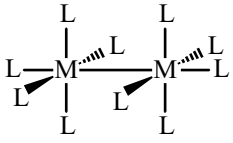

4-46

On each fragment, we shall consider the four lowest-energy *d* orbitals, as in the preceding examples that concerned this fragment (§ 4.1.2, 4.1.4, and 4.2.1.2): three are nonbonding (*xy*, *xz*, and *yz*) and one is weakly antibonding (z^2). These orbitals are not involved in the description of the M—L bonds in each fragment, and are therefore available to form bonding and antibonding MO between the two metallic centres.

There is a very strong σ interaction between the z^2 orbitals, since the two fragment orbitals are polarized towards each other, two π-type interactions between the *xz* and *yz* orbitals, and a weaker δ-type interaction between the *xy* orbitals (**4-47**).

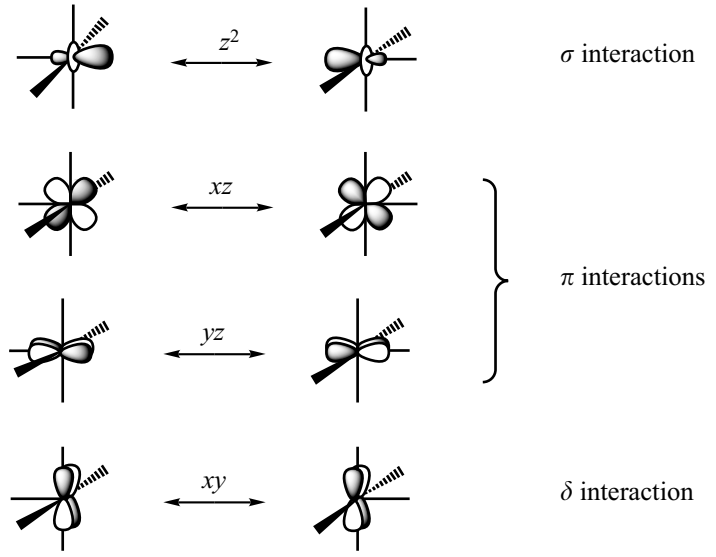

4-47

The interaction diagram for these fragment orbitals is shown in Figure 4.10, where it is clear that the σ interaction is stronger than the π interactions, which in turn are larger than the δ interaction.

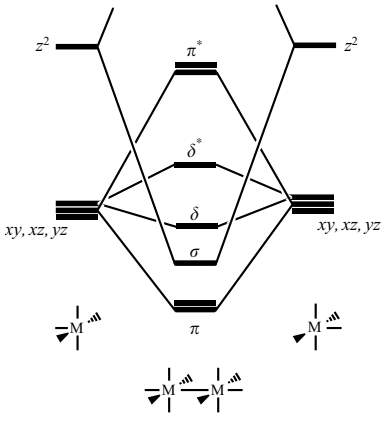

Figure 4.10. Interaction scheme for the *d* orbitals on two ML_5 fragments (SBP) to form the MO of a bimetallic complex M_2L_{10}.

Since the *xy*, *xz*, and *yz* orbitals are initially at the same energy, there is no ambiguity in the energetic order of the π and δ MO: $\varepsilon_\pi < \varepsilon_\delta < \varepsilon_{\delta^*} < \varepsilon_{\pi^*}$. Moreover, the highest-energy MO (not shown) is σ^*. However, it is less easy to be sure of the position of the σ bonding MO. Although the interaction is the strongest of those concerned, the orbitals involved are the highest in energy (z^2). The energy separation between the nonbonding and antibonding levels in each fragment, which is variable from one complex to another, is thus an important parameter. The ordering shown in Figure 4.10, where the σ orbital is placed between the π and δ levels, corresponds to a fairly small energy separation in the fragments. The number and the nature of the metal–metal bonds clearly depend on the electronic occupation of these orbitals.

We shall examine first the complex $[Re_2(CO)_{10}]$. It may be considered to be formed from two $[Re(CO)_5]$ fragments, whose electronic configuration is d^7 (Re(0)). There are therefore 14 electrons in all to be placed in these MO, which leads to the electronic configuration $(\pi)^4(\sigma)^2(\delta)^2(\delta^*)^2(\pi^*)^4$ (**4-48a**). The interactions of π and δ type therefore do not contribute to bonding between the metallic centres, since *both* the bonding and antibonding MO are occupied. However, the σ orbital is occupied, whereas its antibonding σ^* counterpart is empty. We can therefore conclude that there is a single bond between the two metallic centres, of σ type, in the complex $[Re_2(CO)_{10}]$.

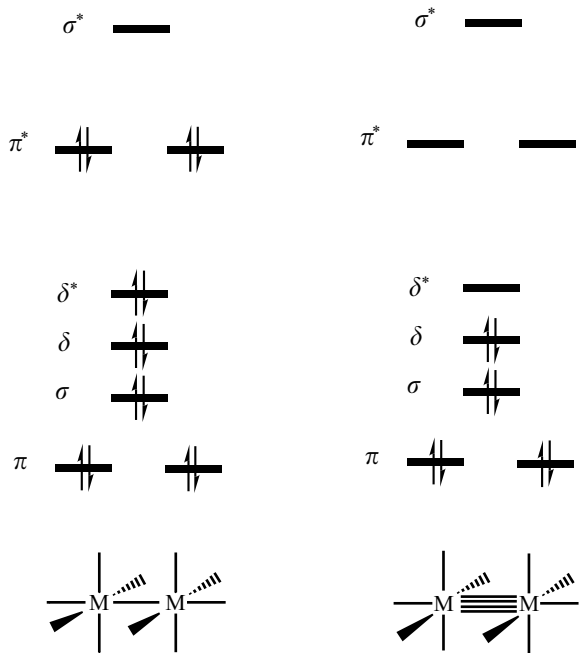

4-48a **4-48b**

It is clear that to increase the bond order, *the number of electrons must be reduced*, so that fewer antibonding MO are occupied. In the complex $[Re_2(Cl)_8(H_2O)_2]^{2-}$, each monometallic fragment $[Re(Cl)_4(H_2O)]^-$ has a d^4 electronic configuration (Re(III)). There are therefore eight electrons to be placed in the MO of this complex, which leads to the electronic configuration $(\pi)^4(\sigma)^2(\delta)^2$ (**4-48b**). As only the bonding orbitals are occupied, there is a *quadruple bond* between the two metal centres. There are two π bonds, one σ bond, and a new entity that does not exist organic chemistry: *a δ bond*.

The change from a single to a quadruple bond is accompanied by a very substantial shortening of the Re–Re bond, whose length decreases from 3.04 Å in $[Re_2(CO)_{10}]$ to 2.22 Å in $[Re_2(Cl)_8(H_2O)_2]^{2-}$.

4.4.3. The $[Re_2(Cl)_8]^{2-}$ complex: a staggered or an eclipsed conformation?

The most famous example of a quadruply bound bimetallic complex is $[Re_2(Cl)_8]^{2-}$, whose structure inspired Cotton to propose, for the first time, the existence of a δ bond, in addition to σ and π bonds, between two metallic centres.[7] The Re–Re distance is very short (2.24 Å), a value close to that found in the complex $[Re_2(Cl)_8(H_2O)_2]^{2-}$ already studied above; most strikingly, the complex is observed to have an *eclipsed* structure (**4-49a**) rather than the staggered conformation (**4-49b**) that would have been expected. It is also important to note that this complex is diamagnetic.

[7] F. A Cotton *Inorg. Chem.* *4*, 334 (1965)

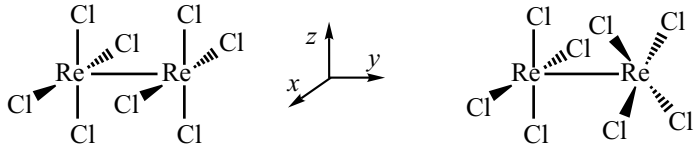

4-49a (exp) **4-49b**

As a first approximation, we can construct the MO for this complex by considering the interaction of two monometallic $[ReCl_4]^-$ fragments with a square-planar geometry (in fact, the Re—Re—Cl angles are 103.7°).

We consider first the eclipsed conformation (**4-49a**). The interaction scheme for the fragment orbitals is similar to that shown in Figure 4.10 for two SBP ML_5 fragments which also have an eclipsed conformation. The only change in the *d* orbitals of the fragments is the lowering in energy of the z^2 orbital, which is almost nonbonding in a square-planar ML_4 complex (see Scheme **4-11**), whereas it is antibonding in an SBP ML_5 complex (Figure 4.10). As a consequence, the strong interaction

between the z^2 orbitals leads to a σ MO that is now lower in energy than the π orbitals. The energetic ordering of the MO is therefore: $\varepsilon_\sigma < \varepsilon_\pi < \varepsilon_\delta < \varepsilon_{\delta^*} < \varepsilon_{\pi^*} < \varepsilon_{\sigma^*}$. Since each fragment has a d^4 electronic configuration (Re(III)), there are eight electrons to be placed in these MO. In this diamagnetic complex, the ground-state electronic configuration $(\sigma)^2(\pi)^4(\delta)^2$ is thus characteristic of a quadruple bond between the two metallic centres (**4-50a**).

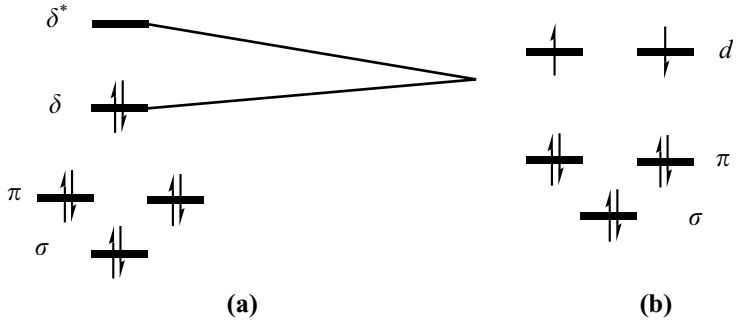

4-50a (eclipsed) **4-50b** (staggered)

We now turn to the staggered conformation. One monometallic unit has thus been rotated by 45° around the *z*-axis with respect to the other (**4-49b**). This has no consequence for the σ interaction, due to the cylindrical symmetry of the orbitals concerned (z^2). The π interactions involve two degenerate orbitals on each centre that are concentrated in two perpendicular planes, (as in the ML_5 fragments, **4-47**). The sum of the two π interactions is not changed by the rotation of one fragment, as the reduction of the overlap with one of the degenerate orbitals is compensated by the increase in overlap with the other. But an important change does occur for the δ interaction: the overlap between the *xy* orbitals in the eclipsed conformation disappears in the staggered form, since the two orbitals that are now concerned ($xy^{(1)}$ and $(x^2-y^2)^{(2)}$) have different symmetries (with respect to the plane of the paper, for example) (**4-51**). There are therefore *two nonbonding d levels* in this conformation (**4-50b**).

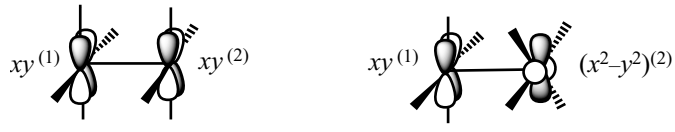

S ≠ 0 S = 0

4-51

In the diamagnetic ground state, movement from the eclipsed to the staggered confirmation therefore leads to the rupture of the δ bond, which explains why the first structure (quadruply bound) is more stable than the second ('only' a triple bond). However, if we consider the triplet state $^3\delta\delta^*$, the staggered conformation with two nonbonding d electrons is more stable than the eclipsed (one electron in a δ bonding orbital, one in an antibonding δ^*). As a result, the movement from the diamagnetic ground state to the first excited triplet state is accompanied by a change in conformation for the complex (eclipsed $\rightarrow$ staggered).

4.5. The reductive elimination reaction

In this last example, we shall study a chemical reaction. In general, problems concerning reactivity are more difficult to treat than structural problems. A reaction is accompanied by a complete electronic reorganization, involving the breaking and making of bonds, and several vital factors, such as the relative stabilities of the reactants and products, are not easy to obtain from qualitative analyses of electronic structure. However, some worthwhile information can be obtained, usually from a correlation diagram that relates the MO in the reactants to those in the products. We thus obtain a description of the electronic reorganization that is associated with the reaction under study, in terms of molecular orbitals.

4.5.1. Definition

The elimination of the molecule R—R′ (R and R′ are X-type ligands such as H, alkyl, halogen, etc.) is a decomposition mode that is frequently found for organometallic complexes [L_nMRR′] (**4-52**).

$$[L_n\,MRR'] \xrightarrow[\text{elimination}]{\text{reductive}} [L_n\,M] + R\text{–}R'$$

4-52

The removal of two X-type ligands leads to a decrease of two units in the metal's oxidation state; the electronic configuration changes from d^n to d^{n+2}. The metal is therefore reduced, which explains the name 'reductive elimination'. The opposite reaction is called 'oxidative addition'.

4.5.2. Simplified model for the reaction $[L_nMR_2] \rightarrow [L_nM] + R{-}R$

Four electrons are intimately involved in the reorganization of the bonds. In the reactant, these are the electrons associated with the two M—R

bonds that will be broken. In the products, they are the two electrons in the new R—R bond and the two electrons that remain on the reduced metal. In the simplest description of this reaction by MO theory, we shall consider only the orbitals associated with these electrons, that is:

1. In the reactant, two (occupied) bonding MO that describe the bonds that are to be broken, and the two corresponding (empty) antibonding MO.
2. In the products, the (occupied) bonding and (empty) antibonding MO associated with the new bond that is formed (R—R), and the two nonbonding MO that remain on the metal (with two electrons in total) after the departure of the two ligands.

A typical correlation diagram for these MO is shown in Figure 4.11. The MO of the reactant are placed on the left. The bonding orbitals, $\sigma^{(+)}$ and $\sigma^{(-)}$, are mainly concentrated on the ligands, whereas the antibonding orbitals, $\sigma^{*(+)}$ and $\sigma^{*(-)}$, are mainly on the metal (Chapter 1, § 6.1). We shall not try to discover the exact shape of these MO, in particular the contribution from the different atomic orbitals (AO) on the metal (*s*, *p*, *d*, or mixture?). The representation shown here is *schematic*, since in reality the MO spread over the whole complex, rather than being limited to the two bonds. The important point is that there is a symmetric bonding MO ($\sigma^{(+)}$) and an antisymmetric bonding MO ($\sigma^{(-)}$), just as there is a 'symmetric' (a_1) and an 'antisymmetric' (b_2) MO that describe the two A—H bonds in a bent AH_2 molecule (Chapter 1, Figure 1.5). The same remark may be made about the antibonding $\sigma^{*(+)}$ and $\sigma^{*(-)}$. In the products, the MO that are R—R bonding ($\sigma_{R—R}$) and antibonding ($\sigma^*_{R—R}$) are the lowest and highest in energy of the four orbitals, respectively. The relative energies of $\sigma_{R—R}$ and $\sigma^{(+)}$ indicate that the

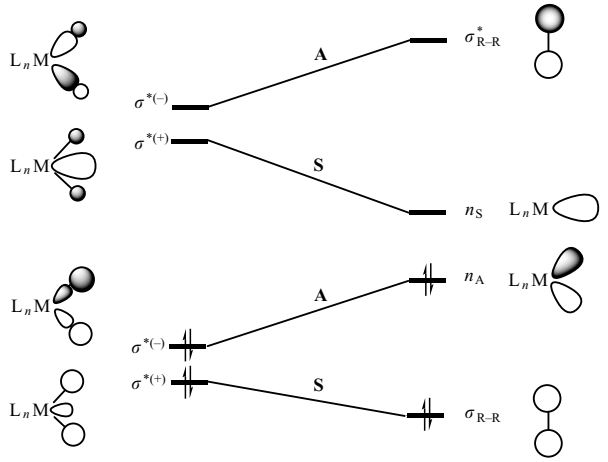

Figure 4.11. Schematic correlation diagram for the reductive elimination reaction $[L_nMR_2] \rightarrow [L_nM] + R—R$. Only the four most strongly perturbed orbitals are shown.

R—R bond is assumed to be stronger than the M—R bond. Among the two nonbonding orbitals (n_A and n_S), the antisymmetric orbital n_A has been placed lower in energy than the symmetric n_S. This is the case when the first is a polarized *d* orbital and the second a hybrid orbital of *s*–*p* type.[8]

[8] If the opposite holds, the ground-state electronic configuration of the reactant correlates with a doubly excited configuration of the product. This would be a *symmetry-forbidden reaction*, according to Woodward and Hoffmann.

The diagram in Figure 4.11 shows us that the antisymmetric orbital $\sigma^{(-)}$ is strongly destabilized, as the two metal–ligand bonding interactions are removed. The activation energy for the reaction is linked to the change in energy for this orbital. In contrast, the symmetrical orbital $\sigma^{*(+)}$ is strongly stabilized, as the two antibonding interactions disappear. The final point to note is the reduction of the metal centre. The $\sigma^{(-)}$ orbital, which is mainly concentrated on the ligands, correlates with the n_A orbital that is localized on the metal: in a formal sense, the metal has gained two electrons.

4.5.3. An example: d^8-$[L_2MR_2] \rightarrow d^{10}$-$[L_2M] + R—R$.

We shall consider a square-planar ML_4 complex with a d^8 electronic configuration which possesses two alkyl ligands (R) in *cis* positions. The reductive elimination of R_2 leads to the formation of a d^{10} $[ML_2]$ complex. An example is shown in **4-53**, that involves the elimination of ethane from a complex that contains a chelating diphosphine ligand.

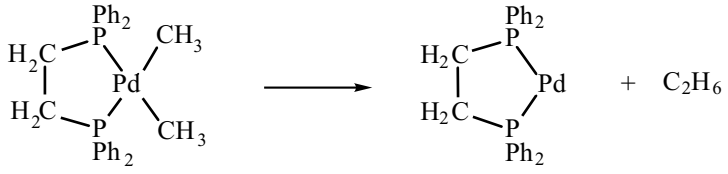

4-53

4.5.3.1. *Correlation diagram for the highest-symmetry mechanism* (C_{2v})

Several different mechanisms can be considered for this reaction, depending on the way in which R_2 is eliminated. We shall study here the pathway with the highest symmetry possible; the orientation of the R_2 unit with respect to the rest of the complex stays unchanged (**4-54**). C_{2v} symmetry is maintained along this reaction pathway, and the symmetry labels used for the orbitals will be appropriate.

In the correlation diagram, we shall represent not only the four MO described in the preceding section, but also the nonbonding or weakly antibonding orbitals in the d block and the other nonbonding orbitals on the metal. In this way, we shall obtain a more complete description

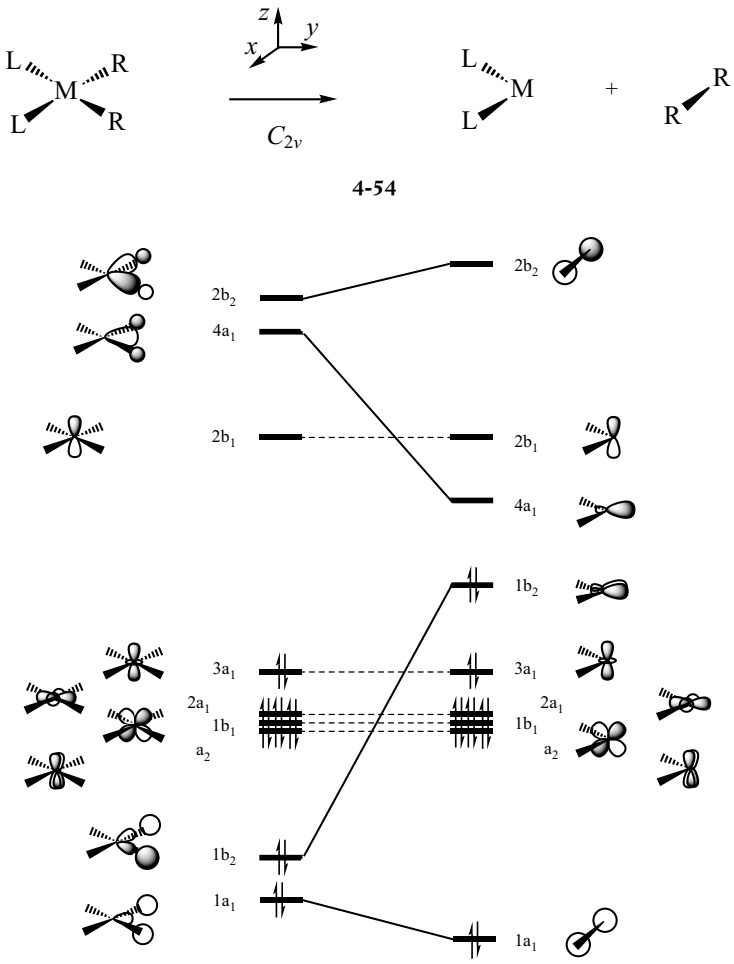

Figure 4.12. Correlation diagram for the MO involved in the reductive elimination reaction d^8-$[L_2MR_2] \rightarrow d^{10}$-$[L_2M]$ (bent) + R_2 in the mechanism where C_{2v} symmetry is conserved.

of the electronic reorganization that is associated with this elimination reaction.

For the reactant (left-hand side of Figure 4.12), there are therefore the $\sigma_{M—R}$ bonding ($1a_1$ and $1b_2$) and $\sigma^*_{M—R}$ antibonding ($4a_1$ and $2b_2$) MO and, at an intermediate energy, the three nonbonding d orbitals (x^2-y^2, xz, and yz), together with the slightly antibonding z^2 orbital and the nonbonding p_z orbital (Chapter 2, § 2.2). The bonding MO are doubly occupied, as are the four d orbitals (d^8). For the products (right-hand side of Figure 4.12), we consider the $\sigma_{R—R}$ and $\sigma^*_{R—R}$ MO ($1a_1$ and $2b_2$), the five nonbonding (x^2-y^2, xz, and yz), or weakly antibonding (z^2 and, at slightly higher energy, xy) d orbitals as well as the two nonbonding orbitals p_z and $s-p_y$ ($2b_1$ and $4a_1$) (Chapter 2, § 2.8.4). In the ground-state electronic configuration, the $\sigma_{R—R}$ MO and the five d orbitals are doubly occupied (d^{10}). C_{2v} labels are used for the symmetries of these orbitals.

The first conclusion that we may draw from this correlation diagram is that the elimination reaction is symmetry-allowed according to this mechanism: the ground-state electronic configuration of the reactant correlates with the ground state of the products. Moreover, the energy changes of the four 'principal' MO (solid lines) are the same as those given in the simplified diagram of the previous section (Figure 4.11). In particular, notice the destabilization of the $1b_2$ orbital and its transformation from a ligand orbital in the initial complex into a d-block orbital of the ML_2 complex.

4.5.3.2. *Use of the correlation diagram: influence of the nature of the metal*

Experimentally, it has been shown that the reductive elimination of R_2 is easier for a nickel complex than for the isoelectronic palladium-containing species. This result may be readily understood from the correlation diagram in Figure 4.12.

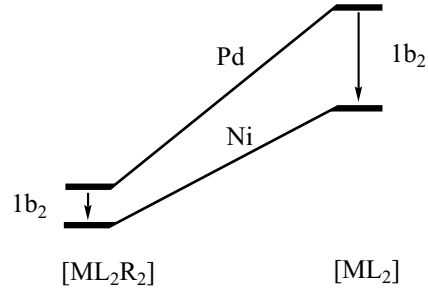

4-55

As we have already noted, the activation energy of this reaction is mainly caused by the destabilization of the $1b_2$ orbital. In the reactant, this MO is mainly concentrated on the ligands, but in the products it is a metal-based orbital, since it is part of the d block of the $[ML_2]$ complex. On moving from palladium to nickel, the energy of the *d* orbitals is lowered appreciably, from −9.58 to −12.92 eV (see Table 1.4, Chapter 1). This lowering in energy stabilizes the $1b_2$ orbital, only weakly in the reactant (small coefficient on the metal) but strongly in the product (a *d* orbital). This analysis shows us that the destabilization of the $1b_2$ orbital is smaller for a nickel complex than for one containing palladium (**4-55**). The activation energies follow the same trend, and the greater tendency for a nickel complex to undergo reductive elimination is thereby explained.

4.6. Principal references used for each section (§) of this chapter

References

T. A. Albright, J. K. Burdett, M.-H. Whangbo, *Orbital Interactions in Chemistry*, John Wiley & Sons, New York (1985), chapter 19.5 (§ 4.5).

T. A. Albright, R. Hoffmann, J. C. Thibeault, D. L. Thorn *J. Am. Chem. Soc. 101*, 3801 (1979) (§ 4.1.1, 4.1.2, and 4.1.3).

C. Bachmann, J. Demuynck, A. Veillard *J. Am. Chem. Soc. 100*, 2366 (1978) (§ 4.1.3).

M. Bénard. *J. Am. Chem. Soc. 100*, 2354 (1978) (§ 4.4).

J. K. Burdett, T. A. Albright *Inorg. Chem. 18*, 2112 (1978) (§ 4.1.3).

F. A. Cotton, R. A. Walton, *Multiple Bonds Between Metal Atoms*, Wiley, New York (1982) (§ 4.4).

R. H. Crabtree, *The Organometallic Chemistry of Transition Metals*, John Wiley & Sons (1988), chapter 11 (§ 4.3).

O. Eisenstein, Y. Jean *J. Am. Chem. Soc. 107*, 1177 (1985) (§ 4.2.1).

R. J. Goddard, R. Hoffmann, E. D. Jemmis *J. Am. Chem. Soc. 102*, 7667 (1980) (§ 4.2.1 and 4.3).

P. J. Hay *J. Am. Chem. Soc. 104*, 7007 (1982) (§ 4.4).

Y. Jean, O. Eisenstein, F. Volatron, B. Maouche, F. Sefta *J. Am. Chem. Soc. 108*, 6587 (1986) (§ 4.1.4).

F. Mathey and A. Sevin, *Chimie Moléculaire des Eléments de Transition*, Les Editions de l'Ecole Polytechnique (2000), chapter 3 (§ 4.3).

I. E.-I. Rachidi, O. Eisenstein, Y. Jean *New J. Chem. 14*, 671 (1990) (§ 4.2.2).

J.-F. Riehl, Y. Jean, O. Eisenstein, M. Pélissier *Organometallics 11*, 729 (1992) (§ 4.2.2).

J.-Y. Saillard, R. Hoffmann *J. Am. Chem. Soc. 106*, 2006 (1984) (§ 4.1.4).

S. Shaik, R. Hoffmann, C. R. Fisel, R. H. Summerville *J. Am. Chem. Soc. 102*, 1194 (1980) (§ 4.4).

D. C. Smith, W. A. Goddard III *J. Am. Chem. Soc. 109*, 5580 (1987) (§ 4.4).

K. Tatsumi, R. Hoffmann, A. Yamamoto, J. K. Stille *Bull. Soc. Chim. Japan 54*, 1857 (1981) (§ 4.5)

Exercises

Conformation of d^{10}-[(η^2-C_2H_4)ML_2] complexes

4.1

1. Which is the more stable conformation for an [(η^2-C_2H_4)ML_2] complex with a d^{10} electronic configuration, **1** or **2**?

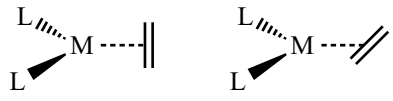

1 **2**

2. How does the barrier to olefin rotation change when the substituents R are varied: R═CN (tetracyanoethylene), R═H (ethylene), R═Cl (tetrachloroethylene)?
3. Repeat question 2, replacing the two non-ethylene ligands on the metal by a bidentate ligand that constrains the L—M—L angle to be much larger than 120°.

ML_3 *complexes*

4.2

1. Starting from the *d* orbitals of an octahedron, construct the *d* orbitals (shapes and relative energies) for a 'T-shaped' ML_3 fragment (L_2—M—L_3 = 180°, L_1—M—L_2 = L_1—M—L_3 = 90°).

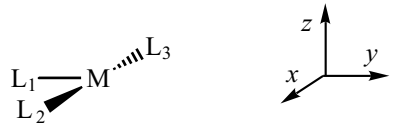

2. How do the orbital energies of this fragment change on moving from the T-shape to a trigonal geometry (120° bond angles)?

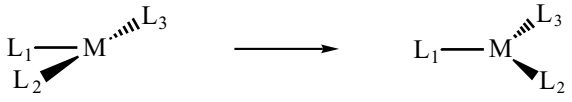

3. From the results you obtain in 2 above, predict the geometries adopted by the complexes $[Rh(PPh_3)_3]^+$ and $[Pt(PPh_3)_3]$.

Octahedral dioxo complexes

4.3

We wish to compare the relative stabilities of the *cis* and *trans* isomers of d^0 and d^2 octahedral dioxo complexes; remember that the oxo group is an X_2-type ligand.

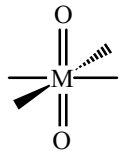

Trans

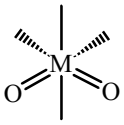

Cis

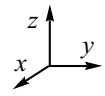

1. Give the shapes and relative energies of the *d* orbitals for an octahedral complex in the absence of any π-type interactions, in the two orientations shown above. *In what follows, we shall only consider the nonbonding d orbitals*.
2. We now turn to dioxo complexes. If the four non-oxo ligands are pure σ donors, give the interaction schemes *d* (metal) $\leftrightarrow$ *p* (oxo) for each isomer.
3. Which isomer is the more stable for a d^0 complex? For a d^2 complex?
4. Deduce the structures of the complexes $[OsO_2F_4]^{2-}$ and $[MoO_2Cl_4]^{2-}$.

Carbene–dihydrogen coupling in an octahedral complex

4.4

In the molecular hydrogen complex $[Os(NH_3)_4(CR_2)(H_2)]^{2+}$, a Fischer carbene and a dihydrogen molecule are in *cis* positions. We shall consider four limiting structures (0, 0), (0, 90), (90, 0), and (90, 90) that are characterized by the orientations of the carbene (first angle) and of the dihydrogen molecule (second angle).

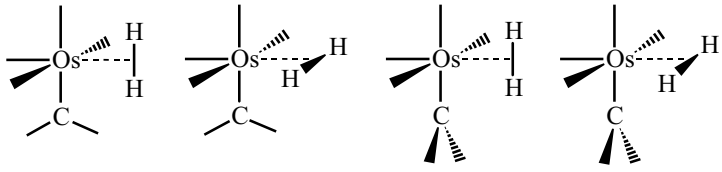

(0, 0) (0, 90) (90, 0) (90, 90)

1. What is the electronic configuration d^n for this complex?
2. For each of the four conformations above, analyse the back-donation interactions towards the carbene and towards the dihydrogen.
3. From the results of this analysis, suggest the favoured structure(s) for this complex.
4. Which limiting conformations are possible for the *trans* isomer? Which should be the most stable a priori?

Coupling of two trans carbenes in an octahedral complex

4.5

Consider the conformations 1 and 2 of octahedral complexes in which two Fischer carbenes are in *trans* positions. The non-carbene ligands are pure σ donors.

1. Give the shapes and relative energies of the three lowest-energy d-block MOs for the two conformations.

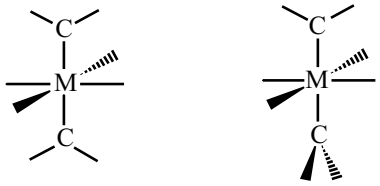

1 2

2. Deduce the conformations for a d^2, d^4, or d^6 diamagnetic complex.
3. How is the barrier to rotation modified if the non-carbene ligands are π acceptors?

The reductive elimination reaction

4.6

We wish to study the reductive elimination of H_2 from an octahedral complex with a d^6 electronic configuration, following the mechanism shown in **4-56**, which leads to a square-planar d^8 ML_4 complex.

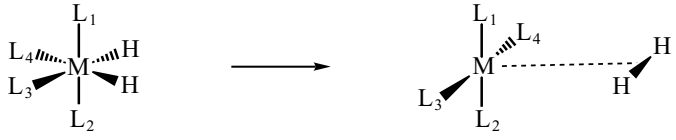

4-56

1. Sketch the correlation diagram for the MO associated with this reaction. For the reactant, consider the nonbonding *d* MO and the MO that characterize the two M—H bonds which will be broken; for the products, the MO of H_2, the occupied *d* orbitals, and the nonbonding *p* orbital of the ML_4 complex. Two planes should be used to characterize the symmetries of the MO.
2. Is this reaction allowed by symmetry?
3. How does the correlation diagram show the reduction of the metal?

The isolobal analogy

In Chapter 2, the *d* orbitals (and, in some cases, the *s*, *p*, or *s–p* hybrid orbitals on the metal) were constructed for many types of ML_n complexes in which the ligands have σ-type interactions with the metal. The shapes and relative energies of these orbitals depend on the number of ligands and their geometrical arrangement around the metal. Naturally, any π-type interactions that are present also play a role. Thus, the *d* orbitals in the octahedral complex $[WCl_6]$ (six π-donor ligands) are different from those in the octahedral complex $[W(CO)_6]$ (six π-acceptor ligands). But *'there is a time for detail and there is a time for generality'*[1]: in both cases, the *d* orbitals are split $3 + 2$, with three degenerate orbitals (the t_{2g} block) lower in energy than the two degenerate orbitals of the e_g block, and this result is characteristic of *all* octahedral ML_6 complexes. In the same way, the orbital structure of AH_n molecules or fragments (or more generally AR_n), in which A is a main-group element, depends essentially on the number and geometrical arrangement of the substituents on the central atom. But beyond the obvious difference created by the presence of *d* orbitals in organometallic complexes, there are resemblances between the molecular orbitals (MO) of ML_n complexes and those of AH_n molecules. These similarities can lead to related properties: thus J. Halpern had noted in 1968 the similarity in behaviour of organic radicals and of d^7 ML_5 complexes.[2] But it is chiefly R. Hoffmann who developed this concept and showed its remarkable fruitfulness.[1]

[1] R. Hoffmann 'Building bridges between inorganic and organic chemistry (Nobel lecture)', *Angew. Chem. Int. Ed. 21*, 711 (1982).

[2] J. Halpern in *Advances in Chemistry; Homogeneous Catalysis*, No 70, American Chemical Society, Washington, DC (1968) pp. 1–24.

5.1. The analogy between fragments of octahedral ML_6 and of tetrahedral CH_4

In many cases, we established the orbitals of ML_n fragments earlier in this book by starting from a complex in which one or several ligands were removed. For example, the orbitals of ML_5 complexes (SBP, C_{4v}), ML_4 ('butterfly', C_{2v}), and ML_3 (pyramidal, C_{3v}) were obtained from those of an octahedral ML_6 complex, by removing one, two, or three ligands, respectively (Chapter 2, § 2.3.1, 2.8.1, and 2.8.3). In certain respects, each of these complexes was therefore considered as a fragment of an octahedron (**5-1**).

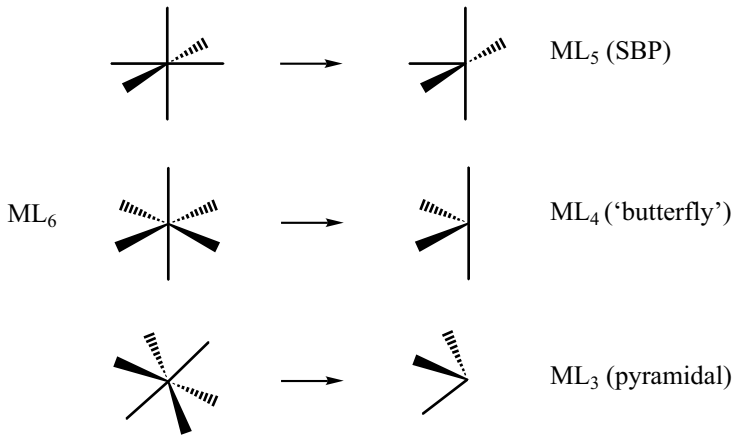

5-1

The same procedure can be applied to molecules of the type AH_n, where A is an element from the second or third row of the periodic table. In particular, starting from tetrahedral methane, CH_4, the archetype of organic molecules, one can obtain the organic fragments pyramidal $CH_3(C_{3v})$, bent $CH_2(C_{2v})$, and $CH(C_{\infty v})$, by removing one, two, or three atoms of hydrogen (**5-2**).

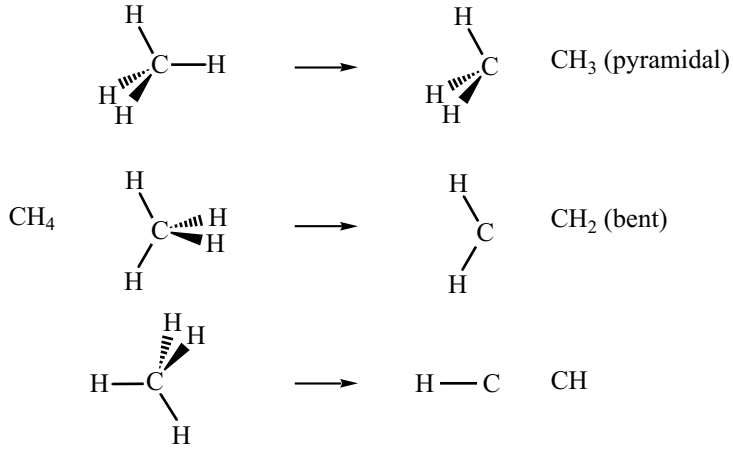

5-2

Even though these comments are purely geometrical in nature, it turns out that they have profound chemical consequences. Thus, an ML_5 complex (SBP) possesses *a vacant site*, and it is likely to bind an additional ligand to form an octahedral complex. In the same way, the $ML_4(C_{2v})$ and $ML_3(C_{3v})$ fragments have two and three available sites, respectively, with respect to the initial octahedron. In the organic series,

the CH_3, CH_2, and CH fragments possess the same characteristics, with the potential to form one, two, or three new bonds.

This similarity in the capacities of inorganic and organic fragments to form new bonds can be expressed in orbital terms, particularly if we consider *the number, the shape, and the electronic occupation* of the orbitals that are available to form these new bonds. The resemblances between these orbitals are at the heart of the theory of the isolobal analogy, developed by R. Hoffmann, which enables us to build bridges between the electronic structures of inorganic and organic molecules.

5.1.1. Fragment orbitals by the valence-bond method

The orbitals of methane, CH_4, and those of the related fragments CH_3, CH_2, and CH can be described using the molecular orbital method, as we have done for all the systems studied so far in this book. But the *valence-bond approach*, introduced by L. Pauling,[3] can also be used; this is perhaps the simplest way to establish an initial relationship between the electronic structures of organic and inorganic fragments.

[3] L. Pauling *The Nature of Chemical Bond*, 3rd edn., Cornell University Press, Ithaca, NY (1960).

In CH_4, the carbon atom is at the centre of a tetrahedron defined by the four hydrogen atoms. The carbon atom's four valence orbitals (the 2*s* orbital and the three 2*p* orbitals) can be combined to give four equivalent hybrid orbitals (written sp^3) that point towards the vertices of the tetrahedron. Since carbon has four valence electrons, one electron can be placed in each hybrid orbital. A $1s_H$ orbital, which is also singly occupied, can interact with the sp^3 hybrid that points towards it, and in this way we can describe the four equivalent bonds in a tetrahedral arrangement.

Using this model, how can we describe the orbital structure of the CH_3, CH_2, and CH fragments that are obtained by *homolytic* rupture of one, two, or three C—H bonds? In the case of CH_3, three of the hybrid orbitals point towards three hydrogen atoms and interact strongly with the $1s_H$ orbitals. But the fourth orbital points in the direction where there is no hydrogen atom (**5-3a**). It is therefore a *nonbonding hybrid orbital*, which contains a single electron (from the homolytic rupture of the C—H bond). In the same way, there are two nonbonding singly occupied sp^3 hybrid orbitals in CH_2 (**5-3b**), and three in CH (**5-3c**).

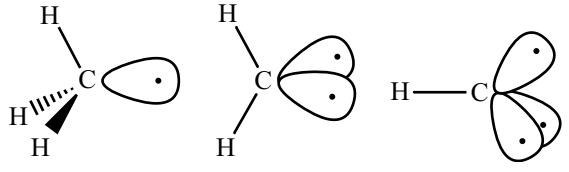

5-3a **5-3b** **5-3c**

We now turn to an octahedral ML_6 complex with a d^6 electronic configuration, which we shall consider as the starting point for inorganic fragments. This complex obeys the 18-electron rule, just as methane obeys the octet rule. To be a little more concrete, though this choice is in no way unique, we shall consider a chromium complex $[CrL_6]$, with *six neutral* L-type ligands (PR_3, CO, etc.), each of which supplies a pair of electrons to the metal. In this complex, chromium is in the oxidation state zero, and the electronic configuration is indeed d^6.

In the spirit of valence-bond theory, we must construct six hybrid orbitals that point towards the vertices of the octahedron. We must therefore combine just six of the nine valence orbitals of the metal: it turns out that these are the *s* orbital, the three *p* orbitals, and two of the *d* orbitals (this hybridisation pattern will be written d^2sp^3, see Chapter 2, § 2.1.2.3). Three *d* orbitals are therefore not involved in the hybridisation, and they stay unchanged (**5-4**). The link with MO theory is plain: these are the three nonbonding orbitals of the octahedral t_{2g} block. In a d^6 complex, these three non-hybridized orbitals are doubly occupied.

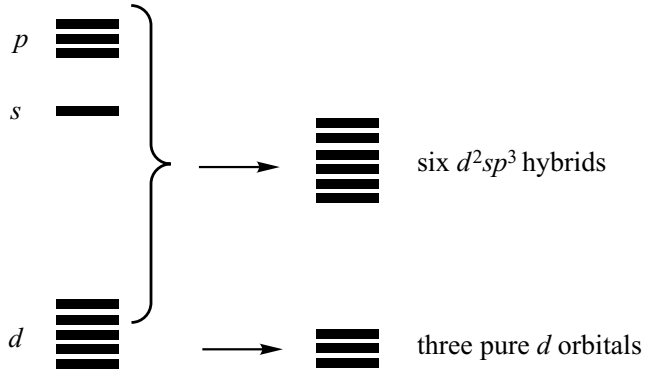

5-4

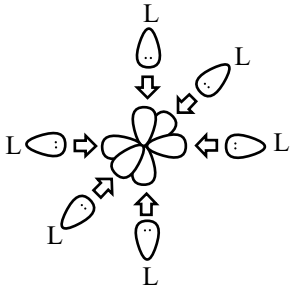

5-5

With the six metal electrons placed in this way, the hybrid orbitals are empty. Each of these interacts with the doubly occupied orbital of the ligand L towards which it points, thereby forming six bonds in an octahedral arrangement (**5-5**).

We now break one Cr—L bond *homolytically*, as we did above for methane. If the ligand is neutral, and of L type (CO, PR_3, ...), this homolytic rupture leaves one of the bonding electrons on the metal, forming the radicals $^{\cdot}L^{+}$ and $[^{\cdot}CrL_5]^{-}$. In the latter (**5-6a**, right-hand side), there are still five d^2sp^3 hybrid orbitals that interact strongly with the orbitals on the five ligands. The sixth orbital points towards the vacant site of the octahedron: it is therefore nonbonding, and it contains the electron that came from the homolytic rupture of the Cr—L bond. From this viewpoint, the resemblance with CH_3 is striking (**5-6a**): the

CH_3 and $[CrL_5]^-$ fragments are both characterized by the presence of a singly occupied nonbonding orbital which points towards a vacant site, of a tetrahedron for the former, of an octahedron for the latter.

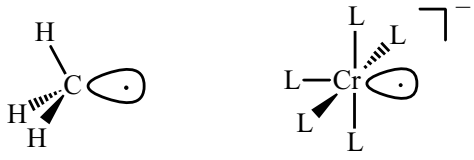

5-6a

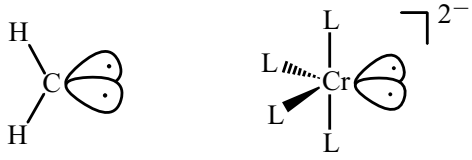

5-6b

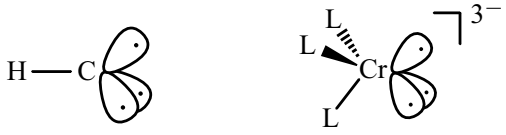

5-6c

In the same way, the homolytic rupture of a second Cr—L bond that leads to the complex $[CrL_4]^{2-}$ with a 'butterfly' geometry leaves two singly occupied nonbonding hybrid orbitals on the metal, as in the organic fragment CH_2 (**5-6b**). And the rupture of a third bond leads to the fragment $[CrL_3]^{3-}$ (**5-6c**), whose electronic structure is similar to that of the fragment CH with three nonbonding hybrid orbitals each containing one electron.

These organic and inorganic fragments, which have the same number of nonbonding hybrid orbitals occupied by the same number of electrons, are said to be *isolobal* analogues.[4] The isolobal analogy is represented by a double-headed arrow, underneath which is a symbol that can be described either as a small hybrid orbital or as a tear.[5]

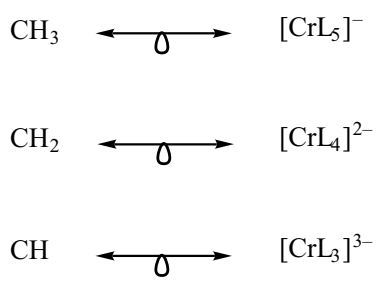

[4] This analogy establishes a link between fragments which are neither isostructural nor isoelectronic.

[5] T. A. Albright, J. K. Burdett, M.-H. Whangbo *Orbital Interactions in Chemistry*, John Wiley & Sons, NY (1985), chapter 21.

Our choice of a chromium complex was quite arbitrary. In each of the inorganic fragments above, we may obviously replace chromium by molybdenum or tungsten, as they have the same number of valence electrons. More generally, we may also consider a metal from another group in the periodic table, so long as the number of electrons is not changed. Thus, all d^7 ML_5 complexes with a square-based pyramidal (SBP) geometry possess a singly occupied nonbonding hybrid orbital; they are therefore isolobal analogues of the pyramidal fragment CH_3. As examples, we may consider the neutral complexes $[Mn(CO)_5]$, $[Tc(CO)_5]$, and $[Re(CO)_5]$, or the cationic complex $[Fe(CO)_5]^+$. In the same way, the complexes $[Mn(CO)_4]^-$ or $[Fe(CO)_4]$, with a 'butterfly' geometry, are, like $[CrL_4]^{2-}$, complexes with a d^8 electronic configuration and therefore isolobal analogues of the organic fragment CH_2. And pyramidal d^9 ML_3 complexes ($[Cr(CO)_3]^{3-}$, $[Mn(CO)_3]^{2-}$, $[Fe(CO)_3]^-$, and $[Co(CO)_3]$, for example) are all isolobal analogues of CH.

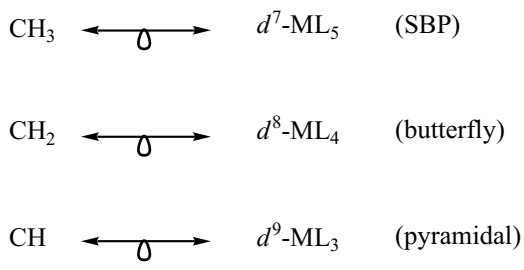

The same type of change may also be made on the organic fragment, by replacing CH_3 with BH_3^- or NH_3^+ (still with a pyramidal geometry). All these fragments are isolobal to d^7 ML_5 complexes such as $[Mn(CO)_5]$. One can also modify the charge on the organic or inorganic fragment. Since CH_3 is isolobal to $[Mn(CO)_5]$, CH_3^+ (pyramidal) is isolobal to $[Cr(CO)_5]$, and CH_3^- to $[Fe(CO)_5]$, if all these complexes are considered with a SBP geometry.[6] In these three pairs of analogous compounds, the single nonbonding hybrid orbital contains zero (CH_3^+ and $[Cr(CO)_5]$), one (CH_3 and $[Mn(CO)_5]$) or two electrons (CH_3^- and $[Fe(CO)_5]$).

[6] In the isolobal analogy, fragments (organic or inorganic) are considered with geometries which are not necessarily the most stable. For example, the most stable structure for $[Fe(CO)_5]$ is trigonal-bipyramidal (TBP) rather than square-pyramidal. Similarly, the CH_3^+ cation is planar.

5.1.2. Fragment molecular orbitals

The analogy between the electronic structures of two isolobal fragments is, of course, still present if we consider their molecular orbitals.

We start with the organic series CH_3, CH_2, and CH. Just as there were one, two, or three nonbonding hybrid orbitals, respectively, in the valence-bond model, the electronic structure in terms of

molecular orbitals shows the presence of one, two or three nonbonding or essentially nonbonding MO, respectively (Chapter 1, Figures 1.4–1.6). Moreover, the number of electrons to be placed in these orbitals is the same as in the nonbonding hybrid orbitals: one for CH_3 (**5-7a**), two for CH_2 (**5-7b**), and three for CH (**5-7c**). Notice that the electronic occupation of these MO can sometimes be problematical, as the orbital energies are quite close. For CH_2 and CH, we have chosen to place the electrons in the MO so as to create as many pairs as possible. This electronic occupation is indeed the ground state of CH, but it is not for methylene, CH_2, for which the ground state is a triplet, with one electron in each of the two nonbonding orbitals (parallel spins). In fact, this is not important when one is using the isolobal analogy. The capacity of a fragment to form new bonds depends more on the number of available nonbonding orbitals and the *total* number of electrons they contain, than on the more-or-less arbitrary initial distribution of the electrons in the fragment.

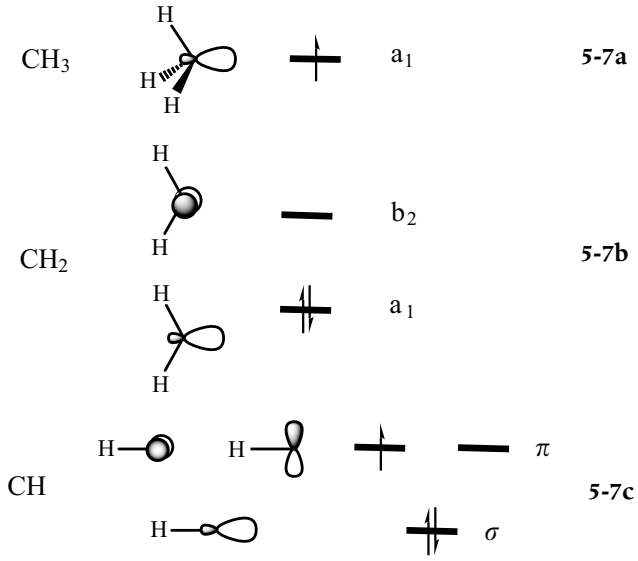

In contrast to hybrid orbitals, MO are adapted to molecular symmetry. Several features therefore arise that are new, compared to the previous description. First, even though the MO that are considered are always concentrated in the same region of space as the vacant site(s) of the tetrahedron, they do not always point directly towards these sites, except, of course, in the case of CH_3 where there is only a single vacant site. For example, the shapes of the a_1 and b_2 MO in the CH_2 fragment mean that the two sites of the initial tetrahedron are equivalent for these two MO (**5-7b**), but neither orbital points along the direction of the

broken C—H bonds. Moreover, in contrast to hybrid orbitals, the MO do not have the same shape or energy. Still using CH_2 as an example, the a_1 (a hybrid orbital) and b_2 (a pure *p* orbital) MO have different shapes, and the a_1 orbital is lower in energy than the b_2 orbital (**5-7b**). In CH, there is one hybrid orbital with σ symmetry and two pure *p* orbitals with π symmetry, the pair of degenerate orbitals (π) being higher in energy than the σ orbital (**5-7c**).

We shall now consider the inorganic fragments that are the isolobal analogues of CH_3, CH_2, and CH, that is, the SBP d^7 ML_5, 'butterfly' d^8 ML_4 and pyramidal d^9 ML_3 fragments (§ 5.1.1), and compare the MO that are concentrated around the vacant site(s) following the homolytic rupture of one, two, or three bonds in the initial structure (tetrahedral CH_4 or octahedral ML_6).

In the CH_3 and d^7 ML_5 fragments, there is only one orbital of this type. It is totally symmetric (a_1 symmetry) in both cases (C_{3v} for CH_3 and C_{4v} for ML_5) (**5-8**), it points towards the vacant site (of the tetrahedron or of the octahedron) and of course it has axial symmetry with respect to the main symmetry axis (C_3 and C_4, respectively). These two orbitals are *not identical*—the first is an sp^3 hybrid orbital, the second a polarized z^2 orbital—but *they are very similar*. Counting electrons, the nonbonding orbital of the methyl radical is singly occupied (**5-7a**). In a d^7 ML_5 fragment, such as $[Mn(CO)_5]$, six electrons occupy the nonbonding orbitals derived from the t_{2g} block of the octahedron, and the seventh occupies the polarized z^2 orbital (Chapter 2, Figure 2.7). In both fragments, the orbital pointing towards the vacant site is therefore singly occupied.

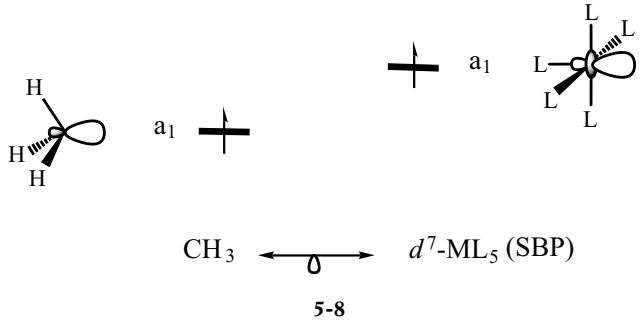

5-8

The set of all these characteristics—the same number of orbitals to be considered, similar symmetry properties, and the same number of electrons—allows us to establish that two fragments are isolobal in the framework of MO theory.

Comment

The hydrogen atom, with its atomic orbital 1_{s_H} singly occupied, is also an isolobal analogue of the d^7 ML_5 fragment.

The CH_2 and d^8 ML_4 ('butterfly') fragments, both with C_2v symmetry, provide a second illustration. Now there are two orbitals to consider for each fragment. For CH_2, these are the two orbitals shown in **5-7b**: the first, totally symmetric (a_1), has of course axial symmetry with respect to the C_2 axis; the second (a pure p orbital with b_2 symmetry)[7] is antisymmetric with respect to the molecular plane. For the metallic fragment, whose orbital structure was established in Chapter 2 (Figure 2.15), there is a polarized d orbital, with b_2 symmetry, and the s–p hybrid orbital on the metal, with a_1 symmetry. The orbitals involved in the two fragments have the same symmetries (**5-9**). Moreover, the same number of electrons must be placed in these orbitals: two in CH_2 (**5-7b**) and also in a d^8 ML_4 fragment, since there are six electrons in the three nonbonding d orbitals derived from the t_{2g} block of the octahedron (Chapter 2, Figure 2.15). Notice, however, that the energetic order of the orbitals is inverted (**5-9**), so that with the chosen electronic occupation (the lowest-energy MO doubly occupied) the electronic configuration is not the same for the two fragments (a_1^2 in CH_2, b_2^2 in d^8 ML_4). As long as one is mainly concerned by the fragments' capacity to form new bonds, this difference is of no real consequence (see § 5.3.1).

[7] This orbital (p_y) has b_2 symmetry (see the character table for the C_{2v} point group, Chapter 6, Table 6.5). If the x- and y-axes are interchanged (the z-axis stays as the C_2 axis), this orbital becomes p_x, which has b_1 symmetry (as was noted in Chapter 1, Figure 1.5). The choice is arbitrary. The important point is that this orbital is antisymmetric with respect to the molecular plane. This comment also applies to the polarized d orbital on the metallic fragment, whose symmetry is either b_1 or b_2, depending on the orientation chosen for the x- and y-axes.

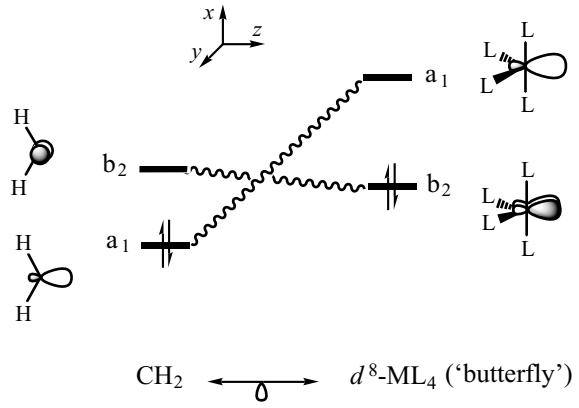

5-9

For the CH and pyramidal d^9 ML_3 fragments, three orbitals must be considered. For CH, these are the orbitals shown in **5-7c**: one orbital with σ symmetry and two degenerate orbitals with π symmetry, with three electrons in total. In a d^9 ML_3 complex, such as $Co(CO)_3$, six electrons occupy the three nonbonding orbitals derived from the t_{2g} block

of the octahedron (Chapter 2, Figure 2.13). At slightly higher energy, we find the three orbitals that are concentrated in the region of the vacant sites of the octahedron — a pair of degenerate orbitals (e symmetry in the C_{3v} point group) and one totally symmetric orbital (a_1)—in which we must place the three remaining electrons. If we compare the degenerate MO in the two fragments, we notice that in each case one orbital is antisymmetric with respect to the plane of the paper (p_y and e_y) but the other is symmetric with respect to this plane (p_x and e_x). Even though the symmetry labels in the $C_{\infty v}$ and C_{3v} point groups are different, the similarity between the orbitals in the two fragments is plain: the σ orbital in CH corresponds to the a_1 orbital in the metallic fragment, and the degenerate π pair to the degenerate e pair (**5-10**). It is true that the energetic ordering of the degenerate and the totally symmetric orbitals is inverted, but this detail has no more importance here than in the preceding example concerning the CH_2 and d^8 ML_4 fragments.

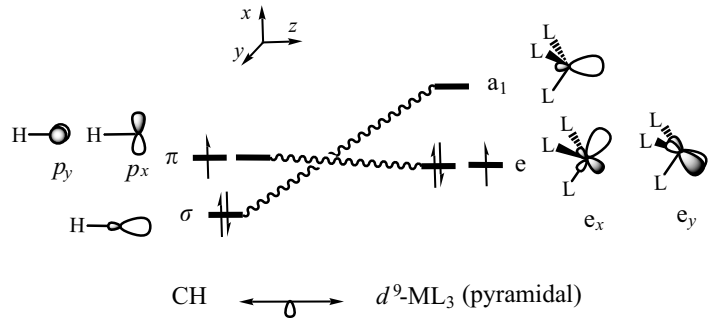

5-10

5.2. Other analogous fragments

An octahedral d^6 ML_6 complex, such as $[Cr(CO)_6]$, is not the only initial structure that can be used to construct inorganic fragments which are analogous to the organic fragments CH_3, CH_2, and CH (**5-11a** and **b**). Two other structures are often used as starting points.

The cyclopentadienyl ligand (Cp) is very widespread in organometallic chemistry. When it is coordinated in the η^5 mode, the most common situation, it behaves as an L_2X ligand (Chapter 1, § 1.1.1.3). $[CpML_3]$ complexes ($L = CO, PR_3, \ldots$) are therefore pseudo-octahedral complexes of the ML_5X type, which have 18 electrons when their electronic configuration is d^6. A d^6 $[CpML_3]$ complex may therefore be used as a new initial structure, very similar to that used previously. Since the presence of the cyclopentadienyl ligand oxidizes the metal by one unit, a metal with seven valence electrons (M = Mn, Tc, Re) must be used to obtain a neutral complex. The complex $[CpMn(CO)_3]$ is therefore a

possible starting point. Subsequently, the fragments d^7 $[CpMn(CO)_2]^-$, d^8 $[CpMn(CO)]^{2-}$, and d^9 $[CpMn]^{3-}$ are obtained by homolytic rupture of one, two, or three Mn—CO bonds. Neutral metallic fragments can be obtained, if the metal is taken from one group further to the right in the periodic table each time. Starting from the complex d^6 $[CpMn(CO)_3]$, we can thus deduce that the fragments d^7 $[CpFe(CO)_2]$, d^8 [CpCo(CO)], and d^9 [CpNi] are isolobal to CH_3, CH_2, and CH, respectively (**5-11a** and **c**).

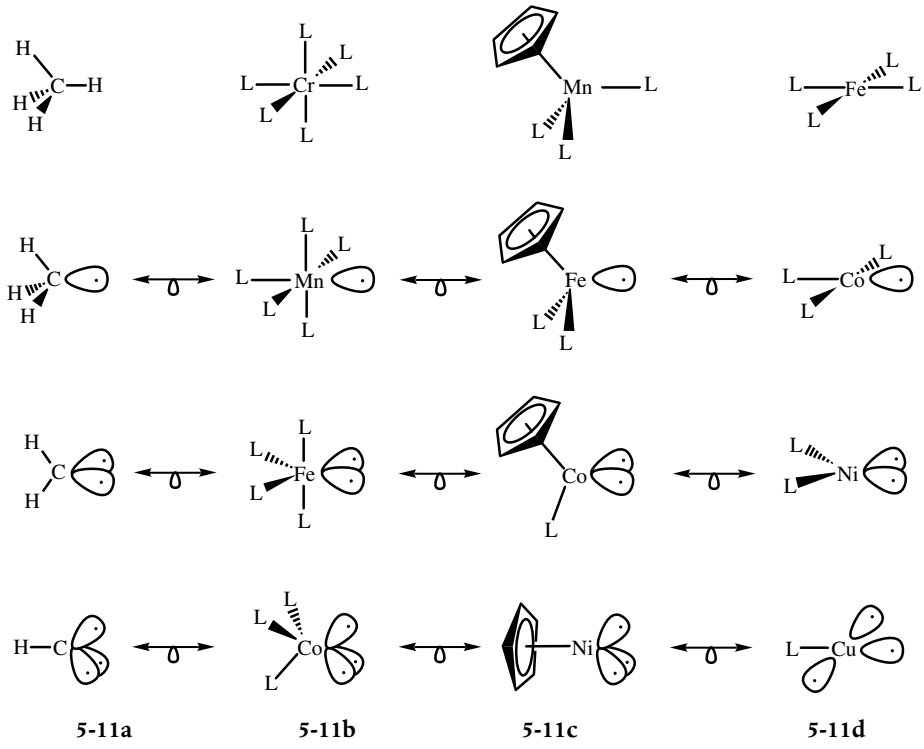

5-11a **5-11b** **5-11c** **5-11d**

Another starting point is sometimes used, taking a complex whose 'normal' number of electrons is 16 instead of 18. The most common example involves a square-planar complex with a d^8 electronic configuration (Chapter 2, § 2.2). Starting, for example, from $[Fe(CO)_4]$, and using the same method as above, one can show that the fragments $[Co(CO)_3]$, with a 'T-shaped' geometry, bent $[Ni(CO)_2]$ and [Cu(CO)] are isolobal analogues of CH_3, CH_2, and CH, respectively (**5-11a** and **d**).

5.3. Applications

5.3.1. Metal–metal bonds

Since the CH_3 and d^7 ML_5 fragments have analogous electronic structures, their chemical behaviour is similar in some respects. For example,

dimerization to form ethane (C_2H_6) is an important property of the methyl radical, as is its initiation of radical-type chain reactions. Similarly, species such as $[Mn(CO)_5]$ or $[Co(CN)_5]^{3-}$, both of which are d^7 ML_5 systems, have a very rich radical-type chemistry; in particular, they dimerize to form $[Mn_2(CO)_{10}]$ and $[Co_2(CN)_{10}]^{6-}$, respectively, (despite the presence, in the latter, of three negative charges on each monomer!). These bimetallic complexes are therefore isolobal analogues of the ethane molecule.

$$C_2H_6 \longleftrightarrow [Mn_2(CO)_{10}] \longleftrightarrow [Mn(CO)_5CH_3]$$

The main orbital interaction that occurs during the dimerization of the fragments (CH_3, $[Mn(CO)_5]$ or $[Co(CN)_5]^{3-}$) involves in all cases the singly occupied nonbonding orbital on each monomer. The interaction schemes for the orbitals on the $[Mn(CO)_5]$ (or $[Co(CN)_5]^{3-}$) and CH_3 fragments produce a doubly occupied bonding MO in the dimer, with axial symmetry around the internuclear axis, and the corresponding antibonding orbital which is empty (**5-12a** and **b**). There is therefore a single σ bond between the two metallic centres in the $[Mn_2(CO)_{10}]$ or $[Co_2(CN)_{10}]^{6-}$ dimers, which implies nearly free rotation around the metal–metal bond, as there is around the C—C single bond in ethane. The analogy can be extended to *mixed* inorganic–organic dimers such as $[Mn(CO)_5CH_3]$, formed by the combination of the metallic fragment $[Mn(CO)_5]$ and its organic analogue CH_3. In this last example, there is once again a single σ bond between the metal and the carbon, resulting from the combination of the singly occupied orbitals on the two fragments.

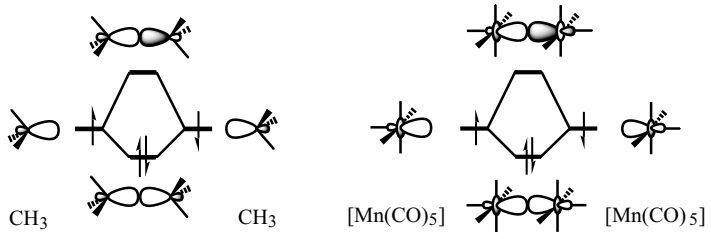

C_2H_6 $[Mn_2(CO)_{10}]$

5-12a **5-12b**

Another example involves the dimerization of the CH_2 and 'butterfly' d^8-ML_4 fragments. The dimer of CH_2 is just simply ethylene, a planar molecule characterized by a double bond between the two carbon atoms (a σ bond and a π bond). The isolobal analogy linking the CH_2 and 'butterfly' $[Fe(CO)_4]$ fragments (**5-9**) shows us that the

bimetallic complex $[Fe_2(CO)_8]$, in the conformation shown in **5-13**, is an isolobal analogue of ethylene, which implies the existence of a double bond between the two metallic centres.

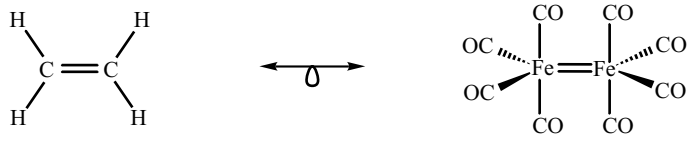

C_2H_4 $[Fe_2(CO)_8]$

5-13

The similarity in the electronic structures of the two molecules is confirmed by the interaction diagrams shown in **5-14a** for C_2H_4 and **5-14b** for $[Fe_2(CO)_8]$.

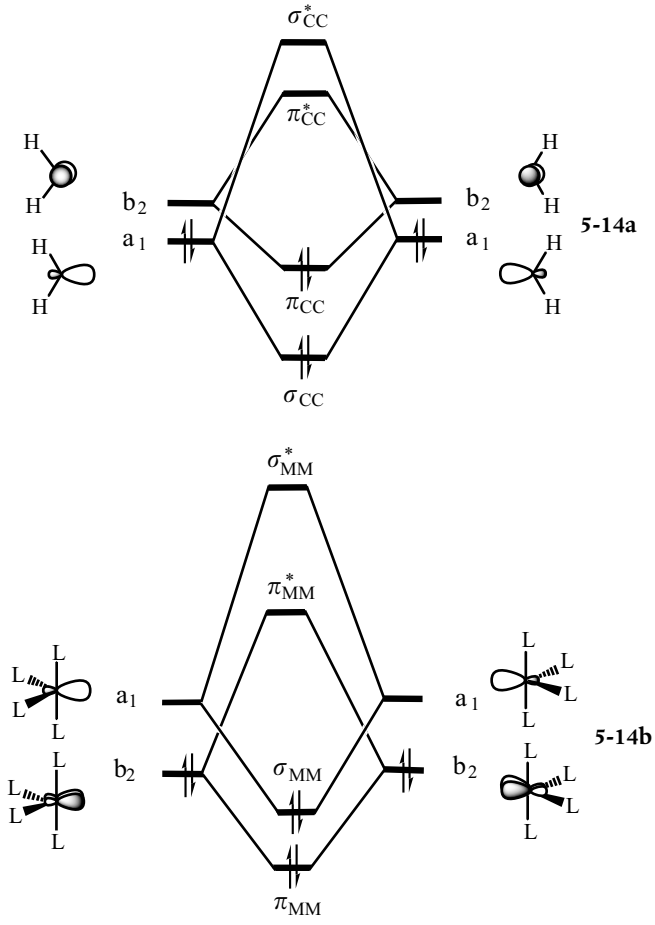

5-14a

5-14b

In ethylene, the interaction between the fragment orbitals leads to the formation of two bonding (σ_{CC} and π_{CC}) and two antibonding MO (σ^*_{CC} and π^*_{CC}). In the ground electronic state, the former are doubly occupied and characterize the σ and π bonds (**5-14a**). In the $[Fe_2(CO)_8]$ dimer, there are also two bonding MO, one of σ type with axial symmetry around the internuclear axis, the other of π type with a nodal plane in the plane of the paper, and the two corresponding antibonding MO (**5-14b**). There are still, *in total*, four electrons to be placed in these MO, so in the ground electronic state the two bonding MO (σ_{MM} and π_{MM}) are doubly occupied, just as in ethylene.

We noted above that the different orbital occupations in the two isolated fragments (a_1^2 for CH_2, b_2^2 for $[Fe(CO)_4]$, **5-9**) has no influence on their capacity to form new bonds and is therefore of little importance for the isolobal analogy. The example above illustrates this point nicely: independently of the energetic order of the fragment orbitals and the initial electronic occupation, the occupied and empty MO in the two dimers have analogous symmetry properties (**5-15**).

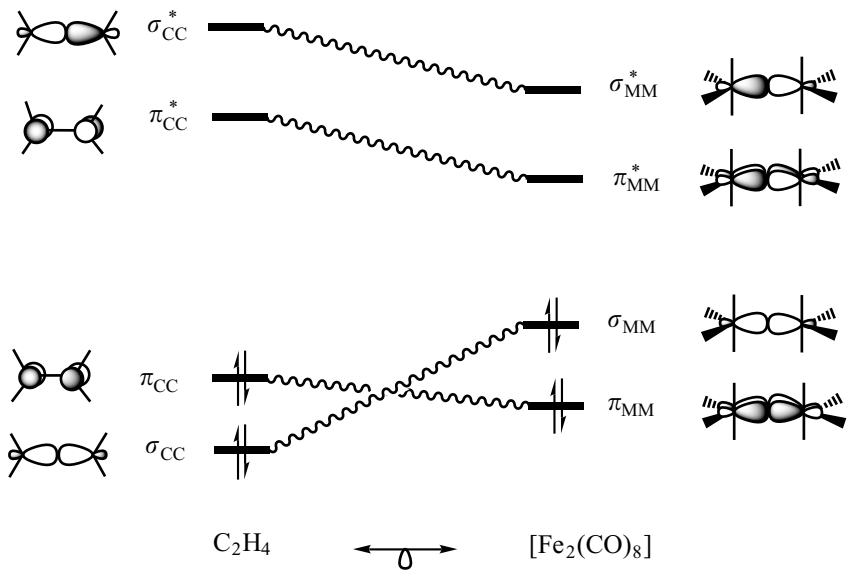

5-15

The analogy is not limited to molecules that are formed by the combination of two fragments. For example, the complex $[Os_3(CO)_{12}]$ can be considered as the combination of three $[Os(CO)_4]$ fragments with C_{2v} geometry. Each of these is of course isoelectronic to $[Fe(CO)_4]$, and therefore isolobal to the organic fragment CH_2. The $[Os_3(CO)_{12}]$ complex is therefore an isolobal analogue of cyclopropane (**5-16**). Each metallic centre is bound to two neighbours by a single bond, as in

the organic analogue. Other complexes, which appear to be very different, also have this property. The fragment [CpRhL] is isoelectronic to [CpCoL], and therefore isolobal to the $[Fe(CO)_4]$ and CH_2 fragments (**5-11**). As a result, the complex $[Cp_2Rh_2(CO)_2(\mu\text{-}CH_2)]$ can be described as a 'two-thirds inorganic' cyclopropane (**5-16**).

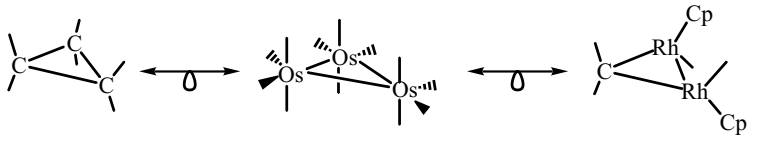

C_3H_6 $[Os_3(CO)_{12}]$ $[Rh_2(Cp)_2(CO)_2(\mu\text{-}CH_2)]$

5-16

5.3.2. Conformational problems

Several conformational properties that are well known in organic molecules reappear in inorganic complexes or in mixed organic/inorganic systems. The ethylene molecule provides a good example; it adopts a planar geometry that allows the formation of two bonds between the carbon atoms (a σ bond and a π bond). In the 'orthogonal' structure, where the two methylene groups lie in perpendicular planes, only the σ bond would be preserved. We now turn to the carbene complex $[Fe(CO)_4(CH_2)]$ in a TBP geometry, with the carbene in an equatorial position. Since the CH_2 and $[Fe(CO)_4]$ fragments are isolobal, this complex is an isolobal analogue of ethylene, C_2H_4. Two limiting conformations can be imagined, with the CH_2 ligand either perpendicular to the equatorial plane of the complex, or in this plane. The analogue of the first of these conformations is indeed a planar molecule of ethylene (**5-17a**), but the second corresponds to a strongly destabilized state of ethylene in the orthogonal geometry (**5-17b**). However,

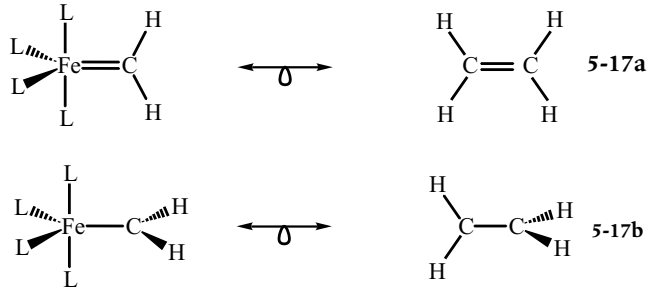

5-17a

5-17b

the similarity in electronic structures does not necessarily imply that the barriers to rotation (**5-17a** → **b**) will be comparable in the organic molecule and in the organometallic complex. About 64 kcal/mol are needed to twist ethylene from its planar to its orthogonal structure, but the rotation of the carbene ligand in a complex of d^8 $[ML_4(CR_2)]$ type needs only about 15–20 kcal/mol (see Exercise 5.8).

In the same way, we can predict (or rediscover) the conformational preferences of several ethylene complexes. If we replace the carbene in the preceding example by ethylene, still in an equatorial position, we obtain the complex $[Fe(CO)_4(C_2H_4)]$ which is isolobal to cyclopropane. The conformation shown in **5-18a** is isolobal to cyclopropane in its most stable geometry, with three carbon atoms on a tetrahedral environment, whereas that shown in **5-18b** is isolobal to a 'deformed' cyclopropane, in which the coordination around one of the carbon atoms is square-planar. The first of these conformations is therefore more stable: in contrast to the carbene, ethylene 'prefers' to lie in the equatorial plane of the complex. In a simple way, we come to the same conclusion concerning the conformational preference as we did in the preceding chapter (§ 4.1.1), when we examined the problem starting from the interaction diagrams between fragment orbitals.

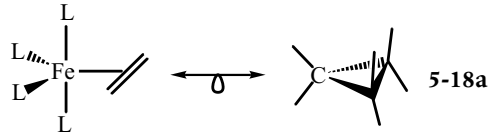

5-18a

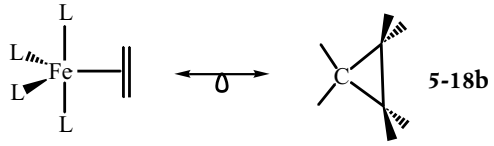

5-18b

5.4. Limitations

The isolobal analogy draws out similarities in the electronic structures of organic and inorganic molecules that can easily escape our attention. As a result of these similarities, we can discover resemblances in the number and nature of bonds, molecular geometries, and sometimes even reactivities. But analogies must not be pushed too far, and there can be significant differences between analogous molecules.

One of the limitations concerns the kinetic stabilities of analogous species. For example, in the analogous series of compounds ethylene, carbene complexes of iron tetracarbonyl and its dimer, $[Fe_2(CO)_8]$ (**5-19**), the first two are known, but the last is unstable and to date it

has only been observed in an inert matrix at very low temperatures. In other words, the analogy with a very stable organic molecule is not a guarantee that the inorganic species will be stable.

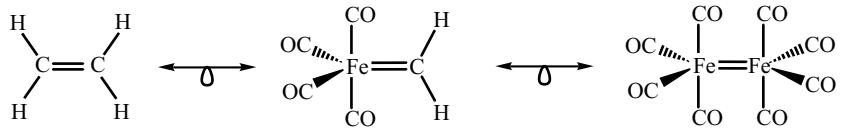

5-19

Another limitation concerns the capacity of some ligands, such as the carbonyl group, to coordinate in either terminal or bridging positions (μ-type coordination) in polynuclear complexes. Consider the bimetallic complex $[CpFe(CO)_2]_2$, for example, (**5-20b**). Each $[CpFe(CO)_2]$ fragment is analogous to the methyl radical (**5-11**), so the complex is isolobal to ethane (**5-20a**). However, it is known in two different forms: $[CpFe(CO)_2]_2$, where all the carbonyl ligands are in terminal positions, and $[CpFe(CO)(\mu\text{-}CO)]_2$, in which two carbonyl ligands are bridging (**5-20c**), and this latter form is the more stable. A structure of this type, with bridging hydrogen atoms, is of course unknown for ethane, the organic analogue of this complex.

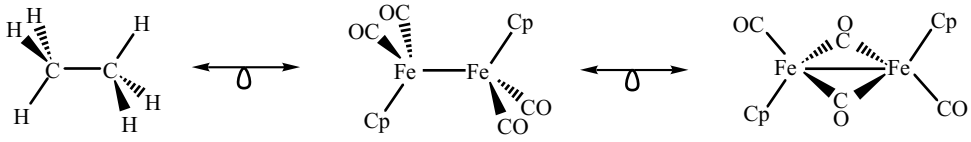

5-20a **5-20b** **5-20c**

In metallic complexes, the bridged and non-bridged structures are often very close in energy, and small changes can favour one geometry or the other. Thus, in the trimetallic complex $[Os_3(CO)_{12}]$, which is analogous to cyclopropane (**5-21a**), all the carbonyl ligands are terminal. However, in the isoelectronic iron complex, two carbonyl

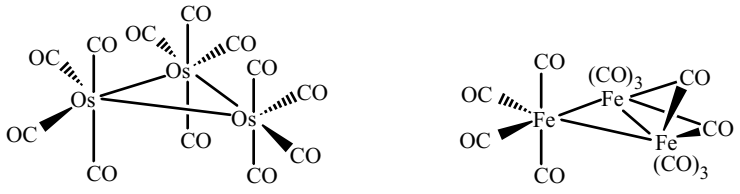

5-21a **5-21b**

ligands bridge the two metallic centres, giving the isomer $[Fe(CO)_4(Fe(CO)_3(\mu\text{-}CO))_2]$ (**5-21b**). As in the previous example, a

bridged structure of this type cannot be seriously imagined for the organic analogue, but that does not prevent the complex **5-21b**, like the complex **5-21a**, from being an isolobal analogue of cyclopropane.

Exercises

5.1

1. Give an organic and a bimetallic isolobal analogue of the complex $[Mn(CO)_5CH_3]$.
2. Suggest an orbital interaction diagram that is suitable for the description of the bond between the metallic centre and the methyl group in this mixed complex.

5.2

1. By using the isolobal analogy with an organic molecule, predict the number and nature (σ or π) of the metal–metal bond(s) in the bimetallic complex $[CpRh(CO)]_2$.
2. Suggest a structure for this compound.

5.3

1. How many carbonyl ligands (n) are necessary on each metal centre for the bimetallic complex of osmium (2) to be an isolobal analogue of cyclobutane (1)?

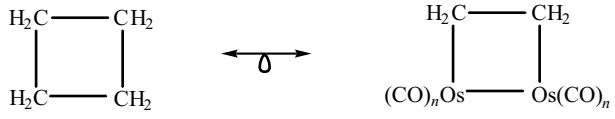

1 **2**

2. Indicate the geometrical arrangement of the ligands around the metal centres.

5.4

1. Show that the trimetallic complex $[(CO)_4Fe(Pt(CO)L)_2]$ ($L = PR_3$) is an isolobal analogue of cyclopropane.

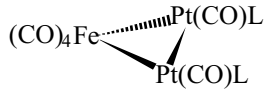

2. Deduce the positions of the ligands around each metallic centre.

5.5

In the complex below, $[Cr(CO)_4(BH_4)]^-$, the borohydride ligand is bound to the metal centre in the η^2 mode, that is, with two bridging hydrogen atoms.

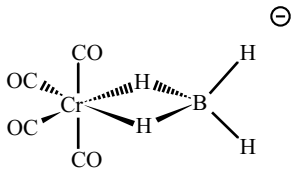

1. Give an organic isolobal analogue of the fragment $[Cr(CO)_4]^-$.
2. Give a boron-based analogue of this fragment.
3. Which boron-based compound is the isolobal analogue of the full complex?

Deduce (or rediscover) its geometrical structure.

5.6

Use the isolobal analogy to predict the more stable conformations for the following ethylene complexes (Cp = η^5-cyclopentadienyl).

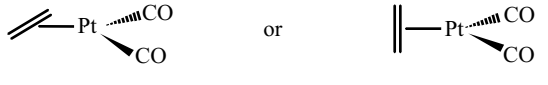

(a) or **(b)**

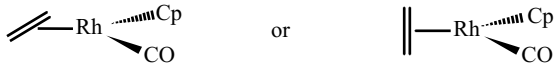

(a) **(b)**

5.7

1. Show that the complex $[Ir_4(CO)_{12}]$ (**1**) is an isolobal analogue of tetrahedrane (**2**).

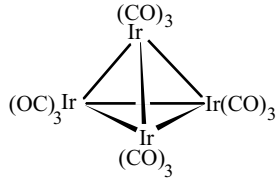

1

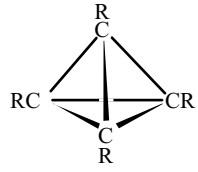

2

2. What can be said about the complex [(η^3-cyclopropenyl)$Co(CO)_3$] **3** and the bimetallic complex [μ-(η^2-alcyne)$(Co(CO)_3)_2$] **4**, in which the acetylenic bond is perpendicular to the metal–metal bond?

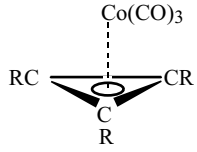

3

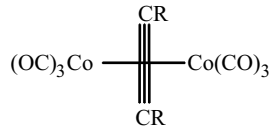

4

3. Give another limiting representation for the structures of complexes **3** and **4**.

5.8

Examine the analogies described in Scheme **5-17**. Does the double-bond really disappear on passing from structure **a** to structure **b** for (*i*) the organic molecule and (*ii*) the organometallic complex?

Elements of group theory and applications

Examination of the geometries of isolated molecules shows that there are four types of *symmetry elements*: reflection planes, axes of rotation, inversion centres, and improper axes of rotation. A *symmetry operation* moves a molecule from an initial configuration to another, equivalent configuration, either by leaving the position of the atoms unchanged, or by exchanging equivalent atoms. The ideas of symmetry element and symmetry operation are of course very closely linked, since a symmetry operation is defined with respect to a given element of symmetry, and, conversely, the presence of a symmetry element is established by the presence of one or more symmetry operations that are associated with that element.

6.1. Symmetry elements and symmetry operations

6.1.1. Reflection planes

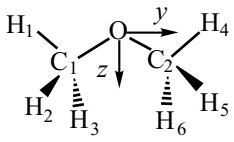

6-1

Consider the dimethylether molecule ($O(CH_3)_2$) in the conformation shown in **6-1**: the hydrogen atoms H_1 and H_4 lie in the plane C_1—O—C_2 (the plane of the paper), but the atoms H_2, H_5 and H_3, H_6 are 'above' and 'below' this plane.

The *xz* plane, which is perpendicular to the plane of the paper and which bisects the angle C_1—O—C_2, is a symmetry element of the molecule, written σ_v. Reflection in this plane leads to a configuration that is equivalent to the initial one: the position of the oxygen atom (located in the σ_v plane) stays unchanged, and the positions of the pairs of equivalent atoms (C_1, C_2), (H_1, H_4), (H_2, H_5), and (H_3, H_6) are interchanged (**6-2**).

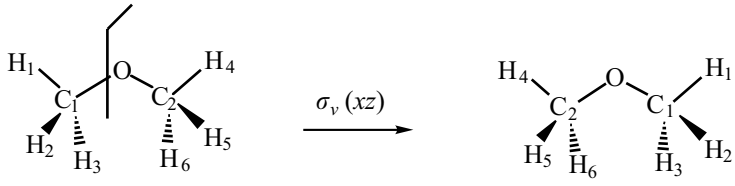

6-2

The *yz* plane (written σ_v'), which contains the three heavy atoms, is also a symmetry elements of the molecule, since reflection in this plane maintains the positions of the atoms O, C_1, C_2, H_1, and H_4, and exchanges the pairs of hydrogen atoms (H_2, H_3) and (H_5, H_6) (**6-3**).

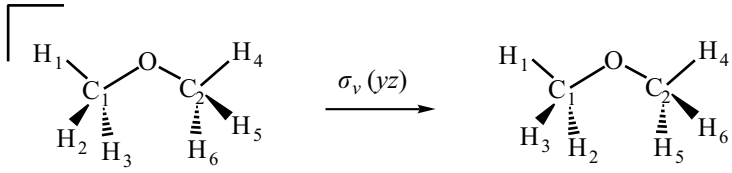

6-3

If the operation of reflection in either of these planes is performed twice (an operation which is written σ^2), a configuration is obtained that is *identical* to the initial one. This idea can be expressed as follows: $\sigma^2 = E$, where E represents the *identity operation*. A reflection plane is therefore associated with a *single symmetry operation* that leads to a configuration that is equivalent to but not identical with the initial configuration.

6.1.2. Inversion centre

If the change of the coordinates (x, y, z) for every atom to $(-x, -y, -z)$ leads to a molecular configuration that is equivalent to the initial one, the point at the origin of the frame of reference is an inversion centre (or centre of symmetry) for the molecule. The symbol i is used both for this symmetry element and for the associated operation. Two examples will illustrate the fact that the inversion centre may be located on one of the atoms of the molecule, but this is not necessary. In the octahedral complex $[FeCl_6]^{4-}$, the iron atom is situated at the inversion centre: the inversion operation leaves its position unchanged, whereas the chlorine atoms are exchanged in pairs: $Cl_{1,2}$, $Cl_{3,4}$, and $Cl_{5,6}$ (**6-4**). But in the ethylene molecule, the inversion centre is situated in the middle of the carbon–carbon bond, and all the atoms are exchanged by the inversion operation (**6-5**).

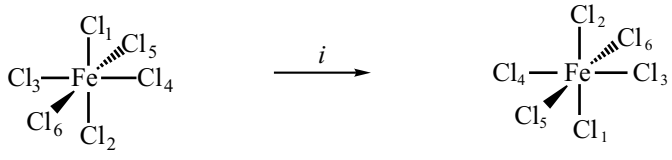

6-4

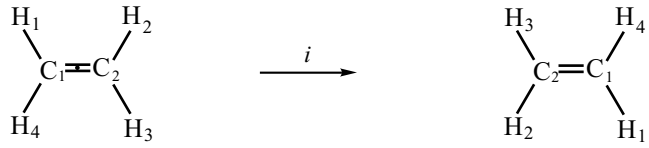

6-5

Notice that a molecule may not contain more than one inversion centre, and that there is only one symmetry operation associated with this element. If the inversion operation is performed twice (i^2), the resulting molecular configuration is identical to the initial one ($i^2 = E$).

6.1.3. Rotation axes

We return to the example of dimethylether (**6-1**). A rotation of 180° (π) around the z-axis leads to a molecular configuration that is equivalent to the initial one (**6-6**), with the following pairs of atoms being exchanged: (C_1, C_2), (H_1, H_4), (H_2, H_6), and (H_3, H_5). The z-axis is therefore a symmetry element of the molecule. The ratio between 360° and the rotation angle associated with the symmetry operation (180° in this example) defines the *order* of the axis. In this case it is therefore a two-fold axis (or of order two), written C_2. A single symmetry operation is associated with this axis, shown in **6-6** and written C_2^1 or simply C_2. If this operation is applied twice (a rotation of $2 \times 180° = 360°$, written C_2^2), we return to the initial molecular configuration ($C_2^2 = E$). Note that by convention, the rotation is performed in a clockwise sense.

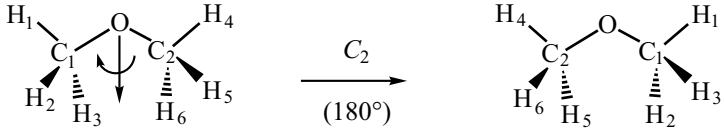

6-6

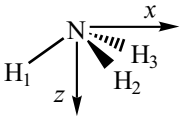

6-7

Ammonia (NH_3) is an example of a molecule that possesses a three-fold axis (C_3). This is the z-axis that passes through the N atom and is perpendicular to the equilateral triangle defined by the three hydrogen atoms (**6-7**).

A rotation of 120° (or $1 \times 2\pi/3$) around this axis leads to an equivalent configuration in which H_1, H_2, and H_3 have been replaced by H_2, H_3, and H_1, respectively (**6-8**). This operation is written C_3^1 or C_3. A rotation of 240° (or $2 \times 2\pi/3$) also leads to a configuration that is equivalent to the initial one ((H_1, H_2, H_3), replaced by (H_3, H_1, and H_2)), (**6-9**). This new operation is written C_3^2. A rotation of 360° (or $3 \times 2\pi/3$) brings us

back to the initial configuration, that is, $C_3^3 = E$. There are therefore *two* symmetry operations, different from the identity operation, that are associated with a C_3-axis.

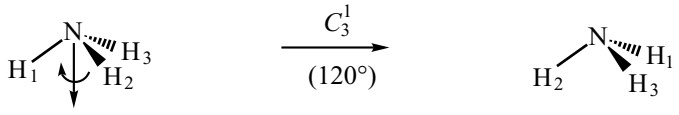

6-8

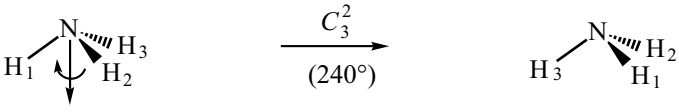

6-9

More generally, an axis of order n (C_n) is present if a rotation of $360°/n$ (or $2\pi/n$) leads to an equivalent configuration for the molecule. This axis generates $(n-1)$ symmetry operations, $C_n^1, C_n^2, \ldots, C_n^{n-1}$, the operation C_n^n being equivalent to the identity operation ($C_n^n = E$).

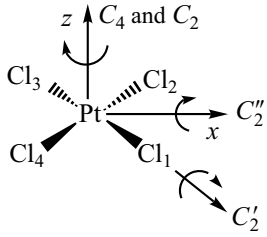

6-10

Some molecules have several rotation axes. The axis of highest order is called the *principal axis*. The complex $[PtCl_4]^{2-}$, in which the platinum atom is located in the centre of the square defined by the four chlorine atoms (**6-10**), possesses a C_4-axis, perpendicular to the plane of the square, and four C_2-axes in the plane of the square: two of these are co-linear with the bonds Cl_1—Pt—Cl_3 and Cl_2—Pt—Cl_4 (C_2'), and the two others bisect the angles Cl—Pt—Cl (C_2''). The principal axis is therefore four-fold (of order four). The existence of a four-fold rotation axis implies the presence of a co-linear two-fold axis, as the operation C_4^2 (a rotation of $2 \times 2\pi/4$) is identical to the operation C_2^1 (a rotation of $1 \times 2\pi/2$).

The set of operations associated with a rotation around the axis that is perpendicular to the molecular plane can thus be written: C_4^1, $C_4^2(=C_2^1)$, C_4^3 and $C_4^4(=E)$. Usually, the notation used for these is C_4^1, C_2, C_4^3, and E, or sometimes $2C_4$, C_2, and E, where the two operations C_4^1 and C_4^3 are grouped together. This type of situation occurs every time that there is an axis whose order is even and greater than 2 (in practice, 4, 6, or 8). For example, if a molecule possesses a C_6-axis, a C_3-axis and a C_2-axis are necessarily co-linear with this axis. The symmetry operations are thus: C_6^1, $C_6^2(=C_3^1)$, $C_6^3(=C_2^1)$, $C_6^4(=C_3^2)$, C_6^5 and $C_6^6(=E)$, which can also be written $2C_6$, $2C_3$, C_2, and E.

Comment

The $[PtCl_4]^{2-}$ example (**6-10**) allows us to make several ideas more precise about planes of symmetry. The z-axis defines the 'vertical' direction. The molecular plane (xy), which is perpendicular to the principal (z) axis, is written σ_h ('h' for 'horizontal'). The two planes which contain the principal axis and two Pt—Cl bonds are written σ_v ('v' for 'vertical'). And the two planes xz and yz, which contain the principal axis and which bisect the angles Cl—Pt—Cl, are written σ_d ('d' for 'dihedral').

6.1.4. Improper rotation axes

The symmetry operation associated with an improper axis of order n (written S_n) is performed in two steps: a rotation of $2\pi/n$ around this axis, followed by a reflection in a plane that is perpendicular to this axis. It is important to realize that the axis used is not necessarily a C_n-axis, nor is the plane that is involved necessarily a symmetry element of the molecule.

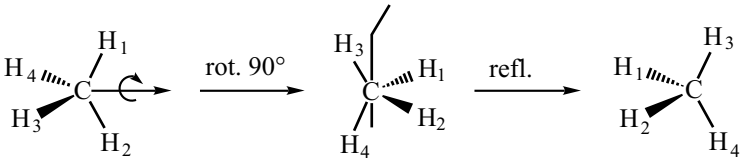

6-11

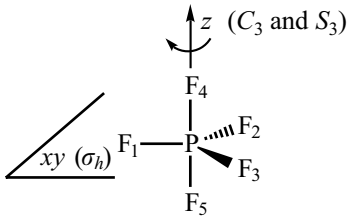

6-12

As a first example, we consider the methane molecule (CH_4), whose geometry is tetrahedral. If we perform a rotation of 90°($2\pi/4$) around the axis bisecting the angles H_1—C—H_2 and H_3—C—H_4, followed by a reflection in the plane perpendicular to this axis passing through the carbon atom, we obtain a configuration that is equivalent (but *not* identical) to the initial one (**6-11**). The axis which we used is therefore an improper four-fold axis (S_4), and the symmetry operation described in **6-11** is written S_4^1, or simply S_4. Notice that this axis is not a C_4-axis in the molecule (but a C_2-axis), and that the plane used is not a symmetry element in the molecule. As in the cases of C_n axes, the S_4 operation can be performed m times in succession, and these are written S_n^m. In the example above, it is easy to verify that $S_4^2 = C_2^1$ (a two-fold axis, co-linear with S_4) and that $S_4^4 = E$ (see Exercise 6.4). The only two operations that are unique to the S_4-axis are therefore S_4^1 and S_4^3.

The hypervalent molecule PF_5 adopts a trigonal-bipyramidal (TBP) geometry (**6-12**). The fluorine atoms F_1, F_2, and F_3 define the base of the bipyramid (the xy plane, written σ_h) and are situated at the vertices of an equilateral triangle (the angles between bonds are 120°). The atoms

F_4 and F_5 define the vertices of the bipyramid, the F_4—P—F_5 axis (the z-axis) being perpendicular to the plane σ_h.

A rotation of $120°(2\pi/3)$ around the z-axis, followed by a reflection in the xy plane, leads to an equivalent configuration for the molecule (**6-13**). The z-axis is therefore an improper three-fold axis (S_3). Notice that in this example both the axis and the plane that were used to perform the S_3 operation are themselves symmetry elements in the molecule: the z-axis is also a C_3-axis, and the σ_h plane is a reflection plane. A characteristic property of the S_3-axis (and, more generally, of improper axes whose order is odd) is that the S_3^3 operation does not lead to a configuration that is identical to the initial one (S_3^3 is different from E). Although a rotation of $3 \times 2\pi/3$ (=360°) around the z-axis does leave the positions of the five fluorine atoms unchanged, an odd number of reflections (three) in the xy plane interchanges the positions of the atoms F_4 and F_5($\sigma_h^3 = \sigma_h$). We therefore obtain $S_3^3 = \sigma_h$. To obtain the identity operation, the operation S_3^6 must be performed (a rotation of twice 360° and an even number (six) of reflections in the plane). Of the six $S_3^m(m = 1–6)$ that seem possible, only the S_3^1 and S_3^5 operation need to be considered, as the others are equivalent to symmetry operations associated with the C_3-axis the σ_h plane or the identity operation in the case of S_3^6.

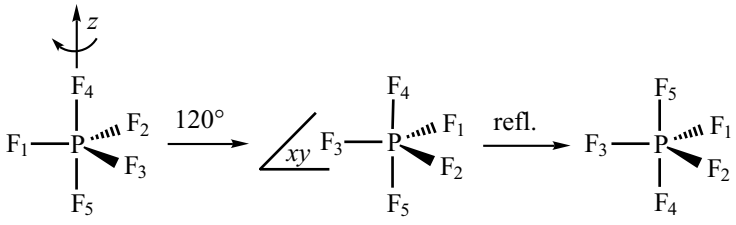

6-13

6.2. Symmetry groups

6.2.1. Definitions

The set of symmetry operations associated with a molecule makes up a *group*, in the mathematical sense of the term. One can indeed verify (*i*) If A, B, and C are three symmetry operations, the relation $A(BC) = (AB)C$ holds, that is, the combination of symmetry operations is associative, (*ii*) there is a null element (the identity operation E): $AE = EA = A$, (*iii*) for each symmetry operation A, there is an inverse operation A^{-1} such that $A^{-1}A = AA^{-1} = E$ (see Exercise 6.5).

Moreover, all the symmetry elements intersect at a single point (e.g. the oxygen atom in dimethylether (**6-1**), the nitrogen atom in ammonia (**6-7**), the middle of the carbon–carbon bond in ethylene (**6-5**)). The expression *point-group symmetry* is therefore used. For each molecule, there is a corresponding point group that completely characterizes its symmetry properties.

The different symmetry operations can be grouped into *classes*. From a mathematical point of view, two symmetry operations A and B belong to the same class if there is a symmetry operation X in the group, such that $B = X^{-1}AX$. Verification of this relationship can be tedious, and it will be sufficient for us to note that a class gathers together symmetry operations of the same 'nature', even if this term is rather vague: as examples, we may give the rotations C_3^1 and C_3^2 associated with a C_3-axis, the rotations C_4^1 and C_4^3 associated with a C_4-axis, and the reflections in two σ_v planes or in two σ_d planes in $[PtCl_4]^{2-}$ (see the comment in § 6.1.3). As far as notation is concerned, one often groups together the operations in a given class, for example, replacing C_3^1 and C_3^2 by $2C_3$, C_4^1 and C_4^3 by $2C_4$, etc.

6.2.2. Determination of the symmetry point group

A set of symmetry elements (or of symmetry operations) enables us to define a symmetry point group which is represented by a symbol. There is a simple method to determine the point group, and it is not necessary to establish a complete list of all the symmetry operations in the molecule under consideration.

1. Initially, check whether the molecule adopts one of the four most easily identifiable geometries: octahedral (e.g. $[FeCl_6]^{4-}$ (**6-4**)), tetrahedral (e.g. CH_4), linear with an inversion centre (e.g. CO_2), or linear without an inversion centre (e.g. HCN). If this is the case, the problem is solved; the symbols associated with these four point groups are O_h, T_d, $D_{\infty h}$, and $C_{\infty v}$ respectively.
2. If none of these groups is appropriate, *and if there is no rotation axis*, there are three possibilities: the molecule (*i*) does not possess and symmetry element (the point group C_1, in which the identity operation is the only symmetry operation); (*ii*) possesses a plane of symmetry (the point group C_s); (*iii*) possesses an inversion centre (the point group C_i).
3. If the molecule possesses *a single* rotation axis (of order n), there are four possibilities: (*i*) there is no other symmetry element besides this axis, with the possible exception of a co-linear axis of lower order. The point-group symbol is then C_n; (*ii*) the existence of a reflection plan σ_h (perpendicular to the C_n-axis) indicates that the point group is of the type C_{nh}; (*iii*) if there are $n\sigma_v$ planes (that contain the C_n

axis), the point-group symbol is C_{nv}; (*iv*) the presence of an improper axis S_{2n}, co-linear with the C_n-axis, indicates that the point group is of the type S_{2n}.

4. If the molecule possesses several rotation axes (the principal axis being of order n), there are three possibilities: (*i*) there are no other symmetry elements besides these axes (D_n point-groups); (*ii*) there are $n\sigma_d$ planes that bisect the C_2 axes (D_{nd} point groups); (*iii*) there is also a σ_h plane, perpendicular to the principal axis (D_{nh} point groups).

6.2.3. Basis of an irreducible representation

The application of group theory to the construction of molecular orbitals leads us to study the way in which atomic orbitals (or linear combinations of these orbitals) transform when the operations of the point group are applied. Several definitions, which are also appropriate for other types of function besides orbitals, will be presented and illustrated by some simple examples.

6.2.3.1. *Basis for a representation*

If a set of functions $f = \{f_1, f_2, \ldots, f_i, \ldots, f_n\}$ is such that any symmetry operation, R_k, of the group G transform one of the functions, f_i, into a linear combination of the various functions of the set f, the set is said to be globally stable and to constitute *a basis for the representation* of the group G. As the symmetry operations maintain the positions of the atoms or interchange the positions of equivalent atoms, *it can be shown that the set of atomic orbitals (AO) of a molecule constitute a basis for the representation of the point-group symmetry of the molecule*. In what follows, we shall adopt the usual notation in group theory, and indicate a basis for a representation by Γ.

6.2.3.2. *Basis for an irreducible representation*

Suppose that a basis Γ, of dimension n, can be decomposed into several bases Γ_i, whose dimensions are smaller (n_i), each of which is globally stable with respect to all the symmetry operations of the group. Suppose also that it is not possible to decompose any of the representations Γ_i into representations whose dimensions are smaller than n_i. The *reducible representation* Γ is said to have been *decomposed into a sum of irreducible representations* Γ_i, which is written:

$$\Gamma = a_1\Gamma_1 \oplus a_2\Gamma_2 \oplus \cdots \oplus a_m\Gamma_m \tag{6.1}$$

6.2.3.3. H_2O *as an example*

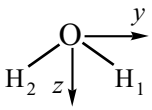

6-14

To illustrate this point, we shall consider the set of valence AO of the atoms in the water molecule: $1s_{H_1}$ and $1s_{H_2}$ on the hydrogen atoms and $2s$, $2p_x$, $2p_y$, and $2p_z$ on the oxygen atom. The water molecule possesses a two-fold rotation axis (z), and two planes of symmetry, xz and yz (**6-14**); its point group is therefore C_{2v}. The set of atomic orbitals constitutes a basis (Γ) for the representation of this point group.

We apply one of the symmetry operations of the group (E, ${C_2}^z$, σ_{xz}, and σ_{yz}) to these orbitals. A rotation by 180° around the z-axis (${C_2}^z$) interchanges the orbitals $1s_{H_1}$ and $1s_{H_2}$ (**6-15** and **6-16**). On the oxygen atom, the $2s$ and $2p_z$ are transformed into themselves (the axis of revolution for $2p_z$ is identical to the rotation axis) (**6-17** and **6-18**), whereas $2p_x$ and $2p_y$ are transformed into their opposites (**6-19** and **6-20**).

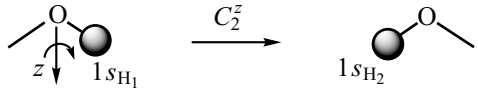

6-15

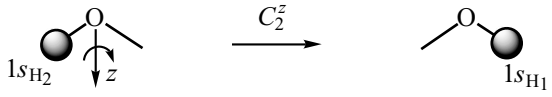

6-16

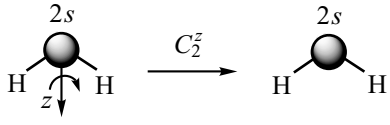

6-17

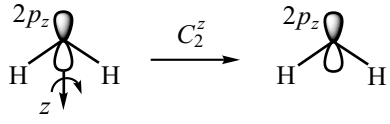

6-18

If the same exercise is undertaken for the three other symmetry operations, we obtain the results that are presented in Table 6.1.

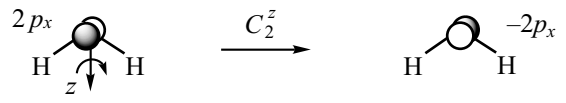

6-19

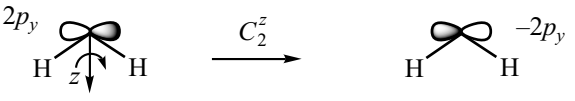

6-20

Table 6.1. Transformation of the atomic orbitals of the hydrogen and oxygen atoms of the H_2O molecule by the action of the symmetry operations of the C_{2v} point group

C_{2v}	E	C_2^z	σ_{xz}	σ_{yz}
$1s_{H_1}$	$1s_{H_1}$	$1s_{H_2}$	$1s_{H_2}$	$1s_{H_1}$
$1s_{H_2}$	$1s_{H_2}$	$1s_{H_1}$	$1s_{H_1}$	$1s_{H_2}$
$2s$	$2s$	$2s$	$2s$	$2s$
$2p_x$	$2p_x$	$-2p_x$	$2p_x$	$-2p_x$
$2p_y$	$2p_y$	$-2p_y$	$-2p_y$	$2p_y$
$2p_z$	$2p_z$	$2p_z$	$2p_z$	$2p_z$

No matter which symmetry operation is applied, it is clear that the $2s$ orbital on the oxygen atom is transformed into itself. It therefore constitutes *by itself* a set that is globally stable, and so it is a basis for the representation of the point group. As the dimension of this basis is 1, it is impossible to reduce it further: the $2s$ orbital is a basis of a one-dimensional irreducible representation in the C_{2v} point group. The same applies for the other AO of the oxygen atom ($2p_x$, $2p_y$, and $2p_z$): the action of the symmetry operations transforms each of them either into itself, or into its opposite (Table 6.1), so each of them constitutes a globally stable set.

We now examine the action of the symmetry operations on the $1s_{H_1}$ and $1s_{H_2}$ orbitals on the hydrogen atoms (the representation Γ_H). It is immediately clear that neither $1s_{H_1}$ nor $1s_{H_2}$ constitutes by itself a set that is globally stable, since some symmetry operations transform $1s_{H_1}$ into $1s_{H_2}$, and vice-versa (Table 6.1). However, the set $\{1s_{H_1}, 1s_{H_2}\}$ *is* stable, and so it is a basis for a representation of the group. Moreover, if the symmetry operations are applied to the two linear combinations $(1s_{H_1} + 1s_{H_2})$ and $(1s_{H_1} - 1s_{H_2})$, we see that they are globally stable towards the action of the symmetry operations, since each is transformed either into itself or into its opposite (Table 6.2). Both these linear combinations are

Table 6.2. Transformation of the linear combinations $(1s_{H_1} + 1s_{H_2})$ and $(1s_{H_1} - 1s_{H_2})$ of the atomic orbitals of the hydrogen atoms in the H_2O molecule by the action of the symmetry operations of the C_{2v} point group

C_{2v}	E	C_2^z	σ_{xz}	σ_{yz}
$1s_{H_1} + 1s_{H_2}$	$1s_{H_1} + 1s_{H_2}$	$1s_{H_2} + 1s_{H_1}$	$1s_{H_2} + 1s_{H_1}$	$1s_{H_1} + 1s_{H_2}$
$1s_{H_1} - 1s_{H_2}$	$1s_{H_1} - 1s_{H_2}$	$-(1s_{H_1} - 1s_{H_2})$	$-(1s_{H_1} - 1s_{H_2})$	$1s_{H_1} - 1s_{H_2}$

therefore bases for an irreducible representation whose dimension is 1 in the C_{2v} point group.[1]

[1] These two functions are also called *the symmetry-adapted linear combinations of the atomic orbitals* $1s_{H_1}$ and $1s_{H_2}$ (we shall return to this point in greater detail in § 6.4).

6.2.4. Characters

6.2.4.1. *Representation of the group*

As we have already remarked, the action of a symmetry operation R_k on a basis for a representation $f = \{f_1, f_2, \ldots, f_i, \ldots, f_n\}$ of the group transforms each of the functions f_i into a linear combination f_i' of the different functions of the set f. This action can be represented by a *matrix* $\mathbf{M}_k$ such that:

$$\mathbf{M}_k f_i = f_i' \tag{6.2}$$

This is an $(n \times n)$ matrix, where n is the dimension of the basis. The collection of matrices associated with the different symmetry operations constitutes a *representation* of the point group.

6.2.4.2. *Characters: the* C_{3v} *point group*

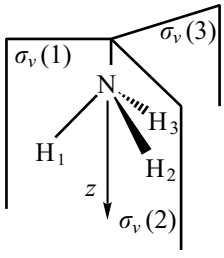

6-21

The following symmetry elements are present in the NH_3 molecule: a C_3 (z) axis and three planes $\sigma_v(i)$ that contain the N—H_i bonds and bisect the opposite H—N—H angle (**6-21**). These symmetry elements are characteristic of the C_{3v} point group.

Consider the orbitals $1s_{H_1}$, $1s_{H_2}$, and $1s_{H_3}$ which constitute a basis written Γ_H. The action of the symmetry operations (E, C_3^1, C_3^2, $\sigma_v(1)$, $\sigma_v(2)$, $\sigma_v(3)$) on these orbitals gives the results presented in Table 6.3.

Each (3×3) matrix associated with a symmetry operation (Figure 6.1) can easily be constructed from this table. Notice in particular that the matrix associated with the identity operation (E) is diagonal; all its non-zero terms lie on the diagonal and moreover, they are all equal to 1.

Each of these matrices can be characterized by its *trace*, that is the sum of its diagonal elements. In group theory, this trace is called the *character* of a matrix, written χ. Notice that the character in Figure 6.1

Table 6.3. Transformation of the atomic orbitals $1s_{H_1}$, $1s_{H_2}$, and $1s_{H_3}$ of the hydrogen atoms of the NH_3 molecule by the action of the symmetry operations of the C_{3v} point group

C_{3v}	E	C_3^1	C_3^2	$\sigma_v(1)$	$\sigma_v(2)$	$\sigma_v(3)$
$1s_{H_1}$	$1s_{H_1}$	$1s_{H_3}$	$1s_{H_2}$	$1s_{H_1}$	$1s_{H_3}$	$1s_{H_2}$
$1s_{H_2}$	$1s_{H_2}$	$1s_{H_1}$	$1s_{H_3}$	$1s_{H_3}$	$1s_{H_2}$	$1s_{H_1}$
$1s_{H_3}$	$1s_{H_3}$	$1s_{H_2}$	$1s_{H_1}$	$1s_{H_2}$	$1s_{H_1}$	$1s_{H_3}$

$$E \quad \begin{bmatrix}1&0&0\\0&1&0\\0&0&1\end{bmatrix}\begin{bmatrix}1s_{H_1}\\1s_{H_2}\\1s_{H_3}\end{bmatrix}=\begin{bmatrix}1s_{H_1}\\1s_{H_2}\\1s_{H_3}\end{bmatrix} \qquad \chi(E)=3$$

$$C_3^1 \quad \begin{bmatrix}0&0&1\\1&0&0\\0&1&0\end{bmatrix}\begin{bmatrix}1s_{H_1}\\1s_{H_2}\\1s_{H_3}\end{bmatrix}=\begin{bmatrix}1s_{H_3}\\1s_{H_1}\\1s_{H_2}\end{bmatrix} \qquad \chi(C_3^1)=0$$

$$C_3^2 \quad \begin{bmatrix}0&1&0\\0&0&1\\1&0&0\end{bmatrix}\begin{bmatrix}1s_{H_1}\\1s_{H_2}\\1s_{H_3}\end{bmatrix}=\begin{bmatrix}1s_{H_2}\\1s_{H_3}\\1s_{H_1}\end{bmatrix} \qquad \chi(C_3^2)=0$$

$$\sigma_v(1) \quad \begin{bmatrix}1&0&0\\0&0&1\\0&1&0\end{bmatrix}\begin{bmatrix}1s_{H_1}\\1s_{H_2}\\1s_{H_3}\end{bmatrix}=\begin{bmatrix}1s_{H_1}\\1s_{H_3}\\1s_{H_2}\end{bmatrix} \qquad \chi(\sigma_v(1))=1$$

$$\sigma_v(2) \quad \begin{bmatrix}0&0&1\\0&1&0\\1&0&0\end{bmatrix}\begin{bmatrix}1s_{H_1}\\1s_{H_2}\\1s_{H_3}\end{bmatrix}=\begin{bmatrix}1s_{H_3}\\1s_{H_2}\\1s_{H_1}\end{bmatrix} \qquad \chi(\sigma_v(2))=1$$

$$\sigma_v(3) \quad \begin{bmatrix}0&1&0\\1&0&0\\0&0&1\end{bmatrix}\begin{bmatrix}1s_{H_1}\\1s_{H_2}\\1s_{H_3}\end{bmatrix}=\begin{bmatrix}1s_{H_2}\\1s_{H_1}\\1s_{H_3}\end{bmatrix} \qquad \chi(\sigma_v(3))=1$$

Figure 6.1. Matrix representation of the action of the symmetry operations of the C_{3v} point group on the $1s_{H_1}$, $1s_{H_2}$, and $1s_{H_3}$ orbitals of the hydrogen atoms of the NH_3 molecule.

associated with the identity operation (three in this example) is equal to the dimension of the basis; this result is general. Notice also that the characters associated with the symmetry operations that belong to a given class (see § 6.2.1) are equal (to 0 for the operations C_3^1 and C_3^2, and to 1 for the operations $\sigma_v(1)$, $\sigma_v(2)$, and $\sigma_v(3)$).

From now on, the action of the symmetry operations on a basis will be represented by the set of characters associated with each symmetry operation; the operations may be grouped into classes where appropriate. The symmetry properties of the basis (Γ_H) formed by the $1s_{H_1}$, $1s_{H_2}$, and $1s_{H_3}$ orbitals of the hydrogen atoms of the NH_3 molecule can be summarized as follows (Table 6.4):

Table 6.4. Characters associated with the basis Γ_H formed by the orbitals $1s_{H_1}$, $1s_{H_2}$, and $1s_{H_3}$ of the hydrogen atoms in the NH_3 molecule (C_{3v} point group)

C_{3v}	E	C_3^1	C_3^2	$\sigma_v(1)$	$\sigma_v(2)$	$\sigma_v(3)$
Γ_H	3	0	0	1	1	1

Or alternatively

C_{3v}	E	$2C_3$	$3\sigma_v$
Γ_H	3	0	1

6.2.5. Character tables

A character table provides a complete list of the irreducible representations associated with a given point group, as well as other useful information. The appearance of these tables, which is identical for all point groups, is illustrated below for the C_{2v} (e.g. H_2O) and C_{3v} (e.g. NH_3) point groups.

6.2.5.1. *Character table for the C_{2v} point group*

This table can be described in the following ways (Table 6.5):

1. The symbol of the point group appears in the top left-hand corner.
2. The symmetry operations, grouped in classes, appear on the first line. However, in this point group, there is only one operation per class.
3. The symbols given to the different irreducible representations of the point group appear underneath the point-group symbol, in the first column. These are known as Mulliken symbols.
4. The characters associated with each irreducible representation are found in the central part of the table. For example, the characters for the A_1 representation are $(1, 1, 1, 1)$, for the B_2 representation

Table 6.5. Character table for the C_{2v} point group

C_{2v}	E	C_2^z	σ_{xz}	σ_{yz}		
A_1	1	1	1	1	z	x^2, y^2, z^2
A_2	1	1	−1	−1		xy
B_1	1	−1	1	−1	x	xz
B_2	1	−1	−1	1	y	yz

$(1, -1, -1, 1)$, etc. Every irreducible representation of this group is one-dimensional, since $\chi(E) = 1$ for each of them.

5. The last two columns on the right contain algebraic functions which are bases for the irreducible representations on the same line. For example, z is a basis for the A_1 irreducible representation, and xz a basis for the B_1 irreducible representation.

These last two points need further comment. The A_1 representation, for which every character is 1, is also known as the totally symmetric representation, since any of the possible symmetry operations of the group transforms a basis function into itself. There is a totally symmetric representation in each point group. The characters for the other representations are either 1 or −1, depending on whether the function is transformed into itself or into its opposite. The algebraic functions given in the last two columns on the right allow us to find immediately the symmetry of the AO on the 'central' atom, that is, the one whose position is unchanged by any of the symmetry operations, or the one located at the intersection of all the symmetry elements (the oxygen atom in the case of the water molecule). So the p_x, p_y, and p_z orbitals transform in the same way as x, y, and z, respectively, and the s orbital (with spherical symmetry) like $(x^2 + y^2 + z^2)$. The symmetries of these orbitals are therefore A_1 (s, p_z), $B_1(p_x)$, and $B_2(p_y)$. The character table for the C_{2v} point group therefore allows us to reduce the basis Γ_O formed by the valence orbitals of oxygen:

$$\Gamma_O = 2A_1 \oplus B_1 \oplus B_2 \tag{6.3}$$

Notice that the last column of the character table contains functions that are squares or second-order products of x, y, and z. The symmetries of these functions indicate the symmetries of the d orbitals on the central atom, which is clearly very useful for the study of transition metal complexes. Thus, in a complex with C_{2v} symmetry, the $d_{x^2-y^2}$ and d_{z^2} orbitals have A_1 symmetry, whereas the d_{xy}, d_{xz}, and d_{yz} orbitals have A_2, B_1, and B_2 symmetries, respectively (Table 6.5). The basis of dimension 5 formed by the d orbitals of the central atom (Γ_d) can therefore be

reduced as follows:

$$\Gamma_d = 2A_1 \oplus A_2 \oplus B_1 \oplus B_2 \tag{6.4}$$

6.2.5.2. *Character table for the C_{3v} point group*

We shall now examine a second character table, that associated with the C_{3v} point group (Table 6.6), the point group for the NH_3 molecule. It is presented in the same format as the previous one, but it illustrates several characteristics of the point groups in which a rotation axis is present whose order is higher than 2 (here, a C_3-axis).

Notice first that on the first line, the symmetry operations are grouped in classes. Thus, the two rotation operations around the C_3-axis (C_3^1 and C_3^2, **6-8** and **6-9**) are written $2C_3$, and the reflections in the three planes of symmetry, $\sigma_v(1)$, $\sigma_v(2)$, and $\sigma_v(3)$ (**6-21**) are written $3\sigma_v$. In general, the notation that is used indicates the number of symmetry operations in the class, followed by the symmetry element that is concerned. One of the irreducible representations in this point group has a character of two associated with the identity operation. This is therefore a two-dimensional irreducible representation, written E (be careful not to confuse this with the identity operation, E).

If we consult the last two columns of the character table, we can establish the symmetry properties of the orbitals on the central atom. The s orbital is a basis for the A_1 representation (or, more simply, it has A_1 symmetry), like the p_z orbital. The p_x and p_y orbitals form a basis for the two-dimensional representation (E). This indicates that from the symmetry point of view, these orbitals cannot be separated. Neither of them taken separately, nor any linear combination of them, forms a set that is stable to the action of the symmetry operations C_3^1 and C_3^2. If we consider the d orbitals on the central atom, the final column in the character table shows us that d_{z^2} has A_1 symmetry, whereas the orbital pairs $(d_{x^2-y^2}, d_{xy})$ and (d_{xy}, d_{yz}) have E symmetry.

To finish this section, we provide a few comments about the Mulliken symbols that are used for irreducible representations, though without full details. One-dimensional representations are indicated by the letters A or B, whereas the letters E and T are used for two- and

Table 6.6. Character table for the C_{3v} point group

C_{3v}	E	$2C_3$	$3\sigma_v$		
A_1	1	1	1	z	x^2+y^2, z^2
A_2	1	1	-1		
E	2	-1	0	(x, y)	$(x^2-y^2, xy), (xz, yz)$

three-dimensional representations, respectively. In the groups which contain an inversion centre, the subscript *g* (from the German *gerade*, which means even) is added to the representations that are symmetric with respect to inversion (a positive character in the column headed by *i*), and the subscript *u* (from the German *ungerade*, for odd) to the representations that are antisymmetric with respect to inversion (a negative character). Thus in the C_i point group, in which the inversion centre is the only symmetry element, the two (one-dimensional) irreducible representations are written A_g and A_u, and the functions that are bases of these representations transform into themselves or their opposites, respectively.

6.3. The reduction formula

As we have already seen (§ 6.2.5), the character table gives us information on orbital symmetry properties. If the molecule contains a central atom, the symmetries of the orbitals of this atom are indicated in the last two columns of the table. However, the orbitals on non-central atoms, for example the $1s_H$ orbitals in H_2O or NH_3, are not individually bases for an irreducible representation (Tables 6.1 and 6.3). These AO form a basis for a reducible representation that can be decomposed into a sum of irreducible representations of the point group. Although the character table does not give the result immediately, it does enable us to find it by using the *reduction formula*.

6.3.1. The reduction formula

If the characters χ_Γ associated with a reducible representation Γ are known, it can be decomposed into a sum of irreducible representations ($\Gamma = \sum_i a_i \Gamma_i$) of the point group by using the *reduction formula*:

$$a_i = \frac{1}{h} \sum_k \chi_\Gamma(R_k) \times \chi_i(R_k) \times n(R_k) \tag{6.5}$$

where the summation (k) is carried out over the classes, h is the number of symmetry operations in the point group, also known as its *order*, $\chi_\Gamma(R_k)$ is the character of the reducible representation for a given class, $\chi_i(R_k)$ is the character of the irreducible representation for that class, and $n(R_k)$ is the number of symmetry operations in that class.

Before being able to apply the reduction formula, it is therefore necessary to determine the characters of the reducible representation being studied.

6.3.2. Characters of a reducible representation

We need intially to establish the characters of a reducible representation Γ. For a given symmetry operation R, only the diagonal terms of the matrix associated with this operation contribute to the character χ_R (§ 6.2.4.2). If the symmetry operation transforms the orbital under consideration into itself, the contribution to the character is $+1$. If, however, it transforms the orbital into its opposite, the contribution is -1. If the orbital is transformed into another one, the contribution is zero. We have already given an example of the calculation of these characters for the $1s_H$ orbitals on the hydrogen atoms in NH_3 (Table 6.4). We shall now consider tow other examples, for the molecules H_2O and C_2H_4.

Consider the basis Γ_H constituted by the two orbitals $1s_{H_1}$ and $1s_{H_2}$ on the hydrogen atoms in the water molecule. From Table 6.1, we notice that the two orbitals are transformed into themselves by the operations E and σ_{yz} (characters equal to $1+1=2$), whereas they are interchanged by the operations C_2^z and σ_{xz} (characters equal to $0+0=0$). The characters associated with the basis Γ_H, listed in Table 6.7, do not correspond to any of the irreducible representations of the C_{2v} point group, which are all one-dimensional (Table 6.5). This is therefore a basis for a *reducible* representation.

The examples of H_2O and NH_3 (Table 6.4) illustrate a characteristic property of the Γ_H representations constituted by the set of $1s_{H_1}$ orbitals on the hydrogen atoms of a molecule. An orbital of this type can only be transformed either into itself (contribution to the character equal to $+1$) or into an orbital located on another hydrogen atom (contribution to the character of 0). To determine the character associated with a particular symmetry operation, it is therefore sufficient to *count the number of hydrogen atoms that are left unchanged by this operation*. This comment is also applicable to other orbitals that possess this property (e.g. the *s* orbitals on heavy atoms that are equivalent by symmetry).

In other cases, it is necessary to examine carefully the ways in which the orbitals are transformed by the symmetry operations. Consider, for example, the ethylene molecule (**6-22**). It belongs to the D_{2h} point group and contains the following symmetry elements: the C_2^x, C_2^y, and C_2^z axes,

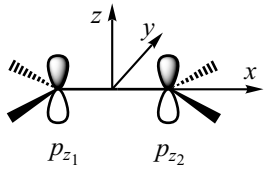

6-22

Table 6.7. Characters associated with the representation Γ_H constituted by the $1s_{H_1}$ and $1s_{H_2}$ orbitals of the hydrogen atoms in the H_2O molecule (C_{2v} point group)

C_{2v}	E	C_2^z	σ_{xz}	σ_{yz}
Γ_H	2	0	0	2

an inversion center i located in the middle of the carbon–carbon bond and the three planes σ_{xy}, σ_{xz}, and σ_{yz} (§ 6.2.2).

The results of applying the symmetry operations to the p_{z1} and p_{z2} orbitals are given in Table 6.8. It is clear that *an orbital can be transformed into its opposite even if the symmetry operations does not move the atom on which it is found* (e.g. the action of C_2^x transform p_{z1} into $-p_{z1}$, even though the position of the C_1 atom is unaltered). The characters associated with the basis Γ_{pz} cannot therefore be obtained simply by counting the number of carbon atoms whose position is left unchanged by each symmetry operation, in contrast to those of the Γ_H representation (Table 6.8).

Table 6.8. Transformation of the atomic orbitals p_{z1} and p_{z2} on the carbon atoms of the ethylene molecule (**6-22**) by the action of the symmetry operations of the D_{2h} point group, and the characters of the Γ_{pz} and Γ_H representations

D_{2h}	E	C_2^z	C_2^y	C_2^x	i	σ_{xy}	σ_{xz}	σ_{yz}
p_{z1}	p_{z1}	p_{z2}	$-p_{z2}$	$-p_{z1}$	$-p_{z2}$	$-p_{z1}$	p_{z1}	p_{z2}
p_{z2}	p_{z2}	p_{z1}	$-p_{z1}$	$-p_{z2}$	$-p_{z1}$	$-p_{z2}$	p_{z2}	p_{z1}
Γ_{pz}	2	0	0	−2	0	−2	2	0
Γ_H	4	0	0	0	0	4	0	0

6.3.3. Applications

6.3.3.1. H_2O *as an example*

We shall now apply the reduction formula (6.5) to some of the reducible representations that we have already studied. Table 6.9 contains the character table for the C_{2v} point group and the characters that we have obtained for the Γ_H basis that is formed by the two $1s_{H_1}$ and $1s_{H_2}$ orbitals in the H_2O molecule (Table 6.7).

Table 6.9. Characters of the irreducible representations of the C_{2v} point group and of the representation Γ_H in the H_2O molecule

C_{2v}	E	C_2^z	σ_{xz}	σ_{yz}
A_1	1	1	1	1
A_2	1	1	−1	−1
B_1	1	−1	1	−1
B_2	1	−1	−1	1
Γ_H	2	0	0	2

As the order of the group (h, the number of symmetry operations) is 4, we obtain:

$$a_{A_1} = \frac{1}{4}[(2 \times 1 \times 1) + (0 \times 1 \times 1) + (0 \times 1 \times 1) + (2 \times 1 \times 1)] = 1$$

$$a_{A_2} = \frac{1}{4}[(2 \times 1 \times 1) + (0 \times 1 \times 1) - (0 \times 1 \times 1) - (2 \times 1 \times 1)] = 0$$

$$a_{B_1} = \frac{1}{4}[(2 \times 1 \times 1) + (0 \times 1 \times 1) + (0 \times 1 \times 1) - (2 \times 1 \times 1)] = 0$$

$$a_{B_2} = \frac{1}{4}[(2 \times 1 \times 1) - (0 \times 1 \times 1) + (0 \times 1 \times 1) + (2 \times 1 \times 1)] = 1$$

which leads to the expression

$$\Gamma_H = A_1 \oplus B_2 \tag{6.6}$$

6.3.3.2. *NH_3 as an example*

In the same way, we can decompose the Γ_H basis in the NH_3 molecule (Table 6.10): its characters have already been obtained (Table 6.4):

Table 6.10. Characters of the irreducible representations of the C_{3v} point group and of the Γ_H representation in the NH_3 molecule

C_{3v}	E	$2C_3$	$3\sigma_v$
A_1	1	1	1
A_2	1	1	−1
E	2	−1	0
Γ_H	3	0	1

We obtain

$$a_{A_1} = \frac{1}{6}[(3 \times 1 \times 1) + (0 \times 1 \times 2) + (1 \times 1 \times 3)] = 1$$

$$a_{A_2} = \frac{1}{6}[(3 \times 1 \times 1) + (0 \times 1 \times 2) + (1 \times (-1) \times 3)] = 0$$

$$a_E = \frac{1}{6}[(3 \times 2 \times 1) + (0 \times (-1) \times 2) + (1 \times 0 \times 3)] = 1$$

so

$$\Gamma_H = A_1 \oplus E \tag{6.7}$$

The three-dimensional representation Γ_H is therefore decomposed into a one-dimensional (A_1) and a two-dimensional (E) irreducible representation.

6.3.4. Direct products

It is often useful to be able to determine the symmetry of a function that is a product of two (or more) functions whose symmetry is already known. This need arises, for example, when we consider a polyelectronic wave function that is written as a product of monoelectronic functions (atomic or molecular orbitals), or when we are interested in the overlap between two orbitals (see § 6.5.1).

Consider two functions ϕ_1 and ϕ_2, whose symmetries are B_1 and B_2, respectively, in the C_{2v} point group. The characters associated with the product function $(\phi_1 \times \phi_2)$ are obtained, for each symmetry operation R, from *the product* of the characters $\chi_R(B_1)$ and $\chi_R(B_2)$ of the B_1 and B_2 representations. Inspection of the character table for the C_{2v} point group (Table 6.5) shows that the characters that are obtained for the product function are identical to those of the A_2 irreducible representation (Table 6.11).

Table 6.11. Direct product of the B_1 and B_2 irreducible representations in the C_{2v} point group

C_{2v}	E	C_2^z	σ_{xz}	σ_{yz}
$\chi_R(B_1)$	1	−1	1	−1
$\chi_R(B_2)$	1	−1	−1	1
$\chi_R(B_1) \times \chi_R(B_2)$	1	1	−1	−1
$\chi_R(A_2)$	1	1	−1	−1

This result can be written as follows:

$$B_1 \times B_2 = A_2 \tag{6.8}$$

Note that if the two functions ϕ_1 and ϕ_2 have the same symmetry in a group whose irreducible representations are one-dimensional, the product of the characters is necessarily equal to 1 for all the symmetry operations. The product function is therefore a basis for the totally symmetric representation (A_1 in the case of the C_{2v} point group). But the situation is more complicated when the point group contains a two- or three-dimensional (degenerate) representation. Consider, for example, the product $E \times E$ in the C_{3v} point group (Table 6.12). The characters that are obtained do not correspond to any of the irreducible representations of this group (see Table 6.6). The representation $E \times E$ in fact forms a basis for a reducible four-dimensional representation; when this is reduced, the totally symmetric representation (A_1) of the C_{3v} group appears as one component.

$$E \times E = A_1 \oplus A_2 \oplus E \tag{6.9}$$

Table 6.12. The E × E direct product in the C_{3v} point group

C_{3v}	E	$2C_3$	$3\sigma_v$
$\chi_R(\mathrm{E})$	2	−1	0
$\chi_R(\mathrm{E}) \times \chi_R(\mathrm{E})$	4	1	0

In general, the *product of two functions of the same symmetry is either a basis for the totally symmetric representation of the group, or is a basis for a reducible representation that contains it*. In contrast, the product of two functions whose symmetries are different *never* contains the totally symmetric representation.

6.4. Symmetry-adapted orbitals

Once the decomposition of a reducible representation into a sum of irreducible representations has been achieved, the following step consists of finding the linear combination of orbitals that are bases for these irreducible representations. These are often referred to as symmetry-adapted linear combinations of orbitals (SALCO).

6.4.1. Projection operator

To find these combinations, we use a 'projection operator' P, whose action on a function ϕ is defined as follows (without considering normalization):

$$P\phi = \left[\sum_k \chi_i(R_k) R_k\right] \phi \tag{6.10}$$

where $\chi_i(R_k)$ is the character associated with the operation R_k for the irreducible representation being considered, Γ_i,[2] R_k is the symmetry operation whose character is $\chi_i(R_k)$ and ϕ is one of the orbitals of the reducible representation or a linear combination of these orbitals. It is called a *generating function*.

[2] If the character is complex, the complex conjugate is taken.

Note that the summation (k) in this formula is carried out over all the *symmetry operations*. If there are several operations in a given class of the group, we must take account of each of them.

6.4.2. Application

6.4.2.1. *The* Γ_{H} *basis in* H_2O

A simple example will show how this formula is used. Consider the Γ_{H} basis that is constituted by the two $1s_{\mathrm{H}_1}$ and $1s_{\mathrm{H}_2}$ orbitals in the H_2O

molecule. We have already show that Γ_H can be reduced to the sum of two irreducible representations, A_1 and B_2 (formula (6.6)). We shall now continue by finding the combination of these orbitals that forms a basis for the A_1 representation. We choose one of these orbitals, $1s_{H_1}$, for example, which will act as the generating function ϕ in equation (6.10). We then construct a table which contains (*i*) the result of the action of symmetry operation R_k on the generating function (the term $R_k\phi$ in equation (6.10)); (*ii*) the characters of the irreducible representation under consideration (the term $\chi_i(R_k)$) and last, the product of these two terms (Table 6.13). The sum of these products over all the symmetry operations (equation (6.10)) gives function ϕ_{A_1} that we seek, that is, the linear combination of the $1s_{H_1}$, and $1s_{H_2}$, orbitals that is a basis for the A_1 representation.

Table 6.13. Quantities necessary for the determination of the linear combination of the $1s_{H_1}$ and $1s_{H_2}$ orbitals that has A_1 symmetry in the H_2O molecule

C_{2v}	E	C_2^z	σ_{xz}	σ_{yz}
$R_k(1s_{H_1})$	$1s_{H_1}$	$1s_{H_2}$	$1s_{H_2}$	$1s_{H_1}$
A_1	1	1	1	1
Product	$1 \times 1s_{H_1}$	$1 \times 1s_{H_2}$	$1 \times 1s_{H_2}$	$1 \times 1s_{H_1}$

We therefore obtain: $\phi_{A_1} = (1 \times 1s_{H_1}) + (1 \times 1s_{H_2}) + (1 \times 1s_{H_2}) + (1 \times 1s_{H_1}) = 2 \times (1s_{H_1} + 1s_{H_2})$. It is clear that we would have obtained the same result if we had taken the $1sH_2$ orbital as the generating function, as this would merely have led to an interchange of the subscripts 1 and 2 in the second line of Table 6.13.

The linear combination that has B_2 symmetry is obtained in the same way, from the data in Table 6.14. It is: $\phi_{B_2} = (1 \times 1s_{H_1}) - (1 \times 1s_{H_2}) - (1 \times 1s_{H_2}) + (1 \times 1s_{H_1}) = 2 \times (1s_{H_1} - 1s_{H_2})$.

In summary, the linear combinations of the $1s_{H_1}$ and $1s_{H_2}$ orbitals that are adapted to the molecular symmetry of H_2O are the sum and difference of these two. If we include the normalization factor that is

Table 6.14. Quantities necessary for the determination of the linear combination of the $1s_{H_1}$ and $1s_{H_2}$ orbitals that has B_2 symmetry in the H_2O molecule

C_{2v}	E	C_2^z	σ_{xz}	σ_{yz}
$R_k(1s_{H_1})$	$1s_{H_1}$	$1s_{H_2}$	$1s_{H_2}$	$1s_{H_1}$
B_2	1	-1	-1	1
Product	$1 \times 1s_{H_1}$	$(-1) \times 1s_{H_2}$	$(-1) \times 1s_{H_2}$	$1 \times 1s_{H_1}$

given by Hückel theory, the expressions are:

$$\phi_{A_1} = \frac{1}{\sqrt{2}} (1s_{H_1} + 1s_{H_2}) \tag{6.11a}$$

$$\phi_{B_2} = \frac{1}{\sqrt{2}} (1s_{H_1} - 1s_{H_2}) \tag{6.11b}$$

[3] We have already shown (see Table 6.2) that these linear combinations are stable with respect to all the symmetry operations of the C_{2v} point group.

This result could have been anticipated, since we have only two equivalent functions to combine.[3] These symmetry-adapted orbital are shown in Figure 6.2.

Figure 6.2. Symmetry-adapted orbitals for H_2O (C_{2v} point group).

Comment

In the standard (non-extended) Hückel method, the overlap between orbitals (S) is neglected in the calculation of the normalization factor. As a result, the sum of the squares of the coefficients is 1. In what follows, when we describe symmetry-adapted orbitals as *normalized*, we shall always adopt that approximation.

6.4.2.2. *The* Γ_H *basis in* NH_3

We now consider a second example, one where the result is more difficult to predict: the three $1s_H$ orbitals in the NH_3 molecule. These orbitals form a basis $\Gamma_H = A_1 \oplus E$ (formula (6.7)). We shall proceed in the same way, taking the $1s_{H_1}$ orbital as the generating function. The second line of Table 6.3 shows how this orbital is transformed by the symmetry operation of the C_{3v} point group. We may use this result to construct Table 6.15, and hence find the linear combination that has A_1 symmetry.

By adding the terms in the last line, we obtain: $\phi_{A_1} = 2 \times (1s_{H_1} + 1s_{H_2} + 1s_{H_3})$. The (non-normalized) totally symmetric function is therefore simply the sum of the initial functions, the same result as that obtained for H_2O.

For the representation with E symmetry, we must find *two* independent linear combinations of the $1s_H$ orbitals (a two-dimensional

Table 6.15. Quantities necessary for the determination of the linear combination of the $1s_{H_1}$, $1s_{H_2}$, and $1s_{H_3}$ orbitals that has A_1 symmetry in the NH_3 molecule

C_{3v}	E	C_3^1	C_3^2	$\sigma_v(1)$	$\sigma_v(2)$	$\sigma_v(3)$
$R_k(1s_{H_1})$	$1s_{H_1}$	$1s_{H_3}$	$1s_{H_2}$	$1s_{H_1}$	$1s_{H_3}$	$1s_{H_2}$
A_1	1	1	1	1	1	1
Product	$1 \times 1s_{H_1}$	$1 \times 1s_{H_3}$	$1 \times 1s_{H_2}$	$1 \times 1s_{H_1}$	$1 \times 1s_{H_3}$	$1 \times 1s_{H_2}$

Table 6.16. Quantities necessary for the determination of the first linear combination of the $1s_{H_1}$, $1s_{H_2}$, and $1s_{H_3}$ orbitals with E symmetry in the NH_3 molecule

C_{3v}	E	C_3^1	C_3^2	$\sigma_v(1)$	$\sigma_v(2)$	$\sigma_v(3)$
$R_k(1s_{H_1})$	$1s_{H_1}$	$1s_{H_3}$	$1s_{H_2}$	$1s_{H_1}$	$1s_{H_3}$	$1s_{H_2}$
E	2	-1	-1	0	0	0
Product	$2 \times 1s_{H_1}$	$(-1) \times 1s_{H_3}$	$(-1) \times 1s_{H_2}$	$0 \times 1s_{H_1}$	$0 \times 1s_{H_3}$	$0 \times 1s_{H_2}$

Table 6.17. Quantities necessary for the determination of the second linear combination of the $1s_{H_1}$, $1s_{H_2}$, and $1s_{H_3}$ orbitals with E symmetry in the NH_3 molecule

C_{3v}	E	C_3^1	C_3^2	$\sigma_v(1)$	$\sigma_v(2)$	$\sigma_v(3)$
$R_k(1s_{H_2} - 1s_{H_3})$	$1s_{H_2} - 1s_{H_3}$	$1s_{H_1} - 1s_{H_2}$	$1s_{H_3} - 1s_{H_1}$	$1s_{H_3} - 1s_{H_2}$	$1s_{H_2} - 1s_{H_1}$	$1s_{H_1} - 1s_{H_3}$
E	2	-1	-1	0	0	0
Product	$2 \times (1s_{H_2} - 1s_{H_3})$	$(-1) \times (1s_{H_1} - 1s_{H_2})$	$(-1) \times (1s_{H_3} - 1s_{H_1})$	$0 \times (1s_{H_3} - 1s_{H_2})$	$0 \times (1s_{H_2} - 1s_{H_1})$	$0 \times (1s_{H_1} - 1s_{H_3})$

representation). If we use the $1s_{H_1}$ orbital once again as the generating function, and the characters of the E representation (Table 6.16), we obtain $\phi_E(1) = 2 \times (1s_{H_1}) - 1s_{H_2} - 1s_{H_3}$.

In this way, we have found one of the two linear combinations that we need. If we now change the generating function to $1s_{H_2}$ or $1s_{H_3}$, we shall clearly obtain the same type of function, but where the subscripts 1, 2, and 3 have been permuted. This function is acceptable, but it is not orthogonal to the previous one, and in general we prefer to use linear combinations of the orbitals that are mutually orthogonal.[4] In this example, the second linear combination can be obtained if the combination $(1s_{H_2} - 1s_{H_3})$ is used as the generating function. Action of the symmetry operations on this function gives the results in Table 6.17.

Taking the characters of the E representation into account, we obtain the function: $\phi_E(2) = 2 \times (1s_{H_2} - 1s_{H_3}) + (-1) \times (1s_{H_1} - 1s_{H_2}) + (-1) \times (1s_{H_3} - 1s_{H_1}) = 3 \times (1s_{H_2} - 1s_{H_3})$, that is, the generating function itself (without considering normalization).

In conclusion, the normalized linear combinations of the $1s_{H_1}$, $1s_{H_2}$, and $1s_{H_3}$ orbitals that are adapted to the molecular symmetry of NH_3 are:

$$\phi_{A_1} = \frac{1}{\sqrt{3}} (1s_{H_1} + 1s_{H_2} + 1s_{H_3}) \tag{6.12a}$$

$$\phi_E(1) = \frac{1}{\sqrt{6}} (2 \times (1s_{H_1}) - 1s_{H_2} - 1s_{H_3}) \tag{6.12b}$$

$$\phi_E(2) = \frac{1}{\sqrt{2}} (1s_{H_2} - 1s_{H_3}) \tag{6.12c}$$

[4] The second function can also be found by another method, from the requirement that it be orthogonal to the symmetry-adapted orbitals already found (ϕ_{A1} and $\phi_E(1)$) (see Exercise 6.7).

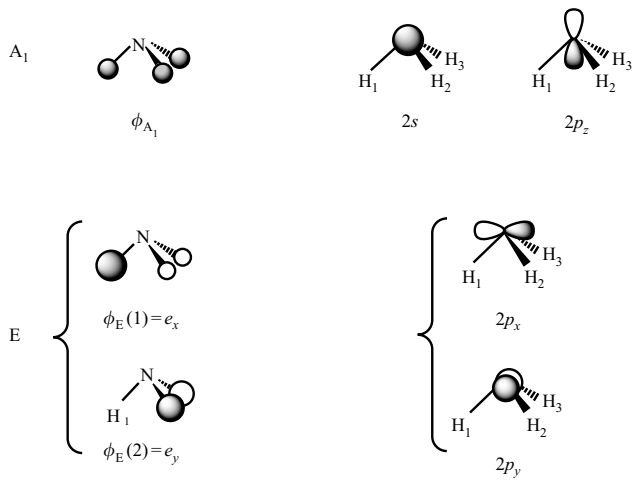

Figure 6.3. Symmetry-adapted orbitals for NH_3 (C_{3v} point group) and orbitals of the same symmetry on the central atom.

These orbitals are shown in Figure 6.3, together with the orbitals on the central atom whose symmetry is given in the character table for the C_{3v} point group (Table 6.6).

The set of orbitals that we have found for the E representations, $\phi_E(1)$ and $\phi_E(2)$, is not unique. Any pair of independent linear combinations of these two orbitals also constitutes a basis for this representation, and the same is true for the $2p_x$ and $2p_y$ orbitals on the central atom. The $\phi_E(1)$ and $\phi_E(2)$ orbitals shown here are, however, the set that is used most frequently. The first is transformed in the same way as $2p_x$ by all the symmetry operations of the C_{3v} point group and the second like $2p_y$. They are therefore often written e_x and e_y, respectively.

6.5. Construction of MO: H_2O as an example

The problem of allowing AO, or SALCO of these orbitals, to interact to form molecular orbitals (MO), is simplified considerably if the symmetry properties of the system are taken into account. The use of symmetry allows us to identify rapidly those interactions which are *exactly zero*, and therefore to consider only those which really do contribute to the formation of the MO.

6.5.1. Symmetry and overlap

Two orbitals ϕ_1 and ϕ_2 interact if their overlap is non-zero (Chapter 1, § 1.3). This overlap is equal to the integral over all space of the product of the functions ϕ_1 and ϕ_2:

$$S_{12} = \int_{\text{space}} \phi_1^* \phi_2 \mathrm{d}\tau \tag{6.13}$$

It can be shown that this integral is non-zero if the product function is a basis for the totally symmetric representation of the group (or of a

reducible representation that contains the totally symmetric representation). *It is therefore necessary for the two orbitals to have the same symmetry* (see § 6.3.4) for the integral to be non-zero. If their symmetries are different, the integral is rigorously equal to zero, and their overlap is said to be *zero by symmetry*.

Comment

These rules (that are not proved here) can be illustrated by two simple examples. Consider the function with a single variable $y = x^2$. The integral of this symmetric (or even) function between $-a$ and $+a$ is non-zero ($[x^3/3]_{-a}^{+a} = (a^3/3) - (-a^3/3) = 2a^3/3$). However, the integral of the antisymmetric (or odd) function $y = x^3$, which changes sign when x is replaced by $-x$, is equal to zero ($[x^4/4]_{-a}^{+a} = (a^4/4) - (a^4/4) = 0$).

6.5.2. Molecular orbitals for H_2O

To construct the MO of the H_2O molecule, we shall allow the atomic orbitals of the central oxygen atom to interact with the symmetry-adapted orbitals on the hydrogen atoms (the fragment method). We have already established the symmetry properties of the various orbitals (C_{2v} point group), and they are repeated in Figure 6.4. It is easy to check visually that the orbitals with the same symmetry on two different fragments have a non-zero overlap, whereas those with different symmetries have zero overlap ('by symmetry').

The interaction diagram is shown in Figure 6.5, where the orbitals on the fragments and in the full molecule are labelled by symmetry ($a_1, b_2, \ldots$).

There is an interaction between the two orbitals with B_2 symmetry that leads to the formation of a bonding MO, written $1b_2$, and an antibonding MO, written $2b_2$. As there are three orbitals with A_1

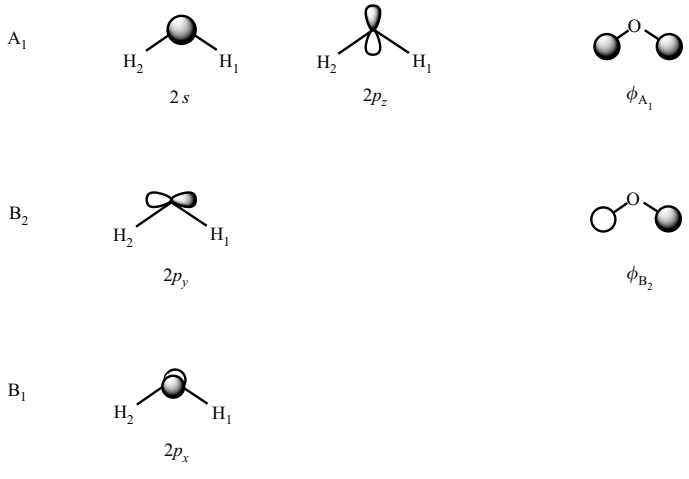

Figure 6.4. Symmetry-adapted orbitals for H_2O (C_{2v} point group) and orbitals with the same symmetry on the central atom.

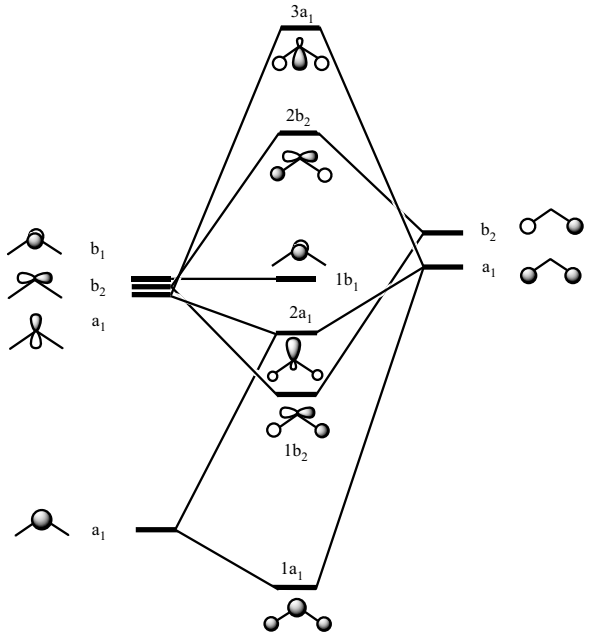

Figure 6.5. Construction of the MOs for H_2O from AO on oxygen and the symmetry-adapted orbitals on the hydrogen atoms.

symmetry, three molecular orbitals are formed: $1a_1$ (bonding), $2a_1$ (nonbonding), and $3a_1$ (antibonding). The atomic orbital with B_1 symmetry ($2p_x$) cannot, by symmetry, interact with any other, and so it stays unchanged in shape and in energy ($1b_1$, nonbonding).

6.6. Symmetry-adapted orbitals in several ML_n complexes

The aim of this section is to construct the symmetry-adapted orbitals for the principal ligand fields, making use of the reduction (6.5) and projection (6.10) formulae. In what follows, with the exception of § 6.6.6, we shall only consider a single orbital on each ligand, the one that is used to create the σ bond with the metal (Chapter 1, § 1.5.1). The orbital on ligand L_i will be written σ_i. We shall suppose that all the ligands, and thus all the orbitals σ_i, are identical.

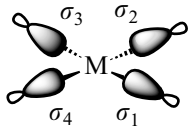

6-23

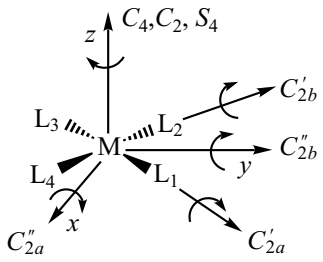

6-24

6.6.1. Square-planar ML_4 complexes

Consider a complex in which the metallic atom is surrounded by four ligands that are placed at the corners of a square (**6-23**). The symmetry elements of this system are characteristic of the D_{4h} point group. The axes are shown in **6-24**. The planes of symmetry are xy (σ_h), xz (σ_{da}), and yz (σ_{db}), respectively, together with the planes that bisect xz and yz and each contain two M—L bonds (σ_{va} and σ_{vb}, respectively). The inversion centre is of course at the origin, coincident with the central atom.

6.6.1.1. *Reduction of the Γ_σ representation*

The action of a symmetry operation on one of the orbitals σ_i can transform it only into itself or into an orbital σ_j on another ligand. Following the procedure that we have already established for bases Γ_H constituted by $1s_H$ orbitals located on hydrogen atoms (§ 6.3.2), the character of the representation Γ_σ is obtained simply by *counting the number of ligands whose position stays unchanged*. It is easy to see that the identity operation (E) and reflection in the molecular plane (σ_h) leave the positions of the four ligands unchanged ($\chi = 4$). Rotations around the C_2' axes and reflections in the σ_v planes maintain the positions of the two ligands situated on the symmetry element concerned ($\chi = 2$). The other symmetry operations move all the ligands ($\chi = 0$). The characters obtained for the representation are listed in Table 6.18, together with the characters of the irreducible representations of the D_{4h} point group.

The order of the group (h, the number of symmetry operations) is 16 (first line of Table 6.18). The reduction formula (6.5) enables us to decompose the four-dimensional representation Γ_σ into a sum of irreducible representations, $\sum_i a_i \Gamma_i$. The only non-zero values of a_i are:

$$a_{A_{1g}} = \frac{1}{16}[(4 \times 1 \times 1) + (2 \times 1 \times 2) + (4 \times 1 \times 1) + (2 \times 1 \times 2)] = 1$$
$$a_{B_{1g}} = \frac{1}{16}[(4 \times 1 \times 1) + (2 \times 1 \times 2) + (4 \times 1 \times 1) + (2 \times 1 \times 2)] = 1$$
$$a_{E_u} = \frac{1}{16}[(4 \times 2 \times 1) + (2 \times 0 \times 2) + (4 \times 2 \times 1) + (2 \times 0 \times 2)] = 1$$

hence

$$\Gamma_\sigma = A_{1g} \oplus B_{1g} \oplus E_u \tag{6.14}$$

Table 6.18. Character table for the D_{4h} point group and characters of the reducible representation Γ_σ of a square-planar complex ML_4

D_{4h}	E	$2C_4$	C_2	$2C_2'$	$2C_2''$	i	$2S_4$	σ_h	$2\sigma_v$	$2\sigma_d$		
A_{1g}	1	1	1	1	1	1	1	1	1	1		$x^2 + y^2, z^2$
A_{2g}	1	1	1	−1	−1	1	1	1	−1	−1		
B_{1g}	1	−1	1	1	−1	1	−1	1	1	−1		$x^2 - y^2$
B_{2g}	1	−1	1	−1	1	1	−1	1	−1	1		xy
E_g	2	0	−2	0	0	2	0	−2	0	0		(xz, yz)
A_{1u}	1	1	1	1	1	−1	−1	−1	−1	−1		
A_{2u}	1	1	1	−1	−1	−1	−1	−1	1	1	z	
B_{1u}	1	−1	1	1	−1	−1	1	−1	−1	1		
B_{2u}	1	−1	1	−1	1	−1	1	−1	1	−1		
E_u	2	0	−2	0	0	−2	0	2	0	0	(x, y)	
Γ_σ	4	0	0	2	0	0	0	4	2	0		

The representation Γ_σ is thus decomposed into two one-dimensional representations (A_{1g} and B_{1g}) and one degenerate two-dimensional representation (E_u).

6.6.1.2. *Symmetry-adapted orbitals*

Application of the projection formula (6.10) requires that we know how one of the ligand orbitals (the generating function) is transformed by *all the symmetry operations*. We shall consider two generating functions in turn, σ_1 and σ_2, where the numbering of the orbitals is shown in **6-23**. The results of the action of the symmetry operations on these two orbitals, $R_k(\sigma_1)$ and $R_k(\sigma_2)$, are given in Table 6.19, together with the characters of the irreducible representations A_{1g}, B_{1g}, and E_u.

The symmetry-adapted functions are obtained by multiplying the function $R_k(\sigma_1)$ (or $R_k(\sigma_2)$) for each symmetry operation by the character of the irreducible representation considered, and adding the sum of these products for all the symmetry operations (formula (6.10)).

By using σ_1 as a generating function for the symmetries A_{1g} and B_{1g}, then σ_1 and σ_2 successively for the symmetry E_u (a two-dimensional, degenerate representation), we obtain:

$$\phi_{A_{1g}} = 4 \times (\sigma_1 + \sigma_2 + \sigma_3 + \sigma_4)$$

$$\phi_{B_{1g}} = 4 \times (\sigma_1 - \sigma_2 + \sigma_3 - \sigma_4)$$

$$\phi_{E_u}(1) = 4 \times (\sigma_1 - \sigma_3)$$

$$\phi_{E_u}(2) = 4 \times (\sigma_2 - \sigma_4)$$

Table 6.19. Action of the symmetry operations of the D_{4h} point group on the orbitals σ_1 and σ_2 (see **6-23** and **6-24** for the numbering of the orbitals and the symmetry elements) and the characters of the irreducible representations A_{1g}, B_{1g}, and E_u

D_{4h}	E	C_4^1	C_4^3	C_2	C'_{2a}	C'_{2b}	C''_{2a}	C''_{2b}
$R_k(\sigma_1)$	σ_1	σ_4	σ_2	σ_3	σ_1	σ_3	σ_4	σ_2
$R_k(\sigma_2)$	σ_2	σ_1	σ_3	σ_4	σ_4	σ_2	σ_3	σ_1
A_{1g}	1	1	1	1	1	1	1	1
B_{1g}	1	−1	−1	1	1	1	−1	−1
E_u	2	0	0	−2	0	0	0	0

D_{4h}	i	S_4^1	S_4^3	σ_h	σ_{va}	σ_{vb}	σ_{da}	σ_{db}
$R_k(\sigma_1)$	σ_3	σ_4	σ_2	σ_1	σ_1	σ_3	σ_4	σ_2
$R_k(\sigma_2)$	σ_4	σ_1	σ_3	σ_2	σ_4	σ_2	σ_3	σ_1
A_{1g}	1	1	1	1	1	1	1	1
B_{1g}	1	−1	−1	1	1	1	−1	−1
E_u	−2	0	0	2	0	0	0	0

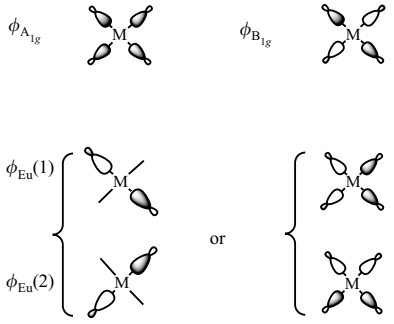

Figure 6.6. Symmetry-adapted σ orbitals for a square-planar ML_4 complex. Two different representations are shown for the degenerate E_u orbitals.

which gives the following normalized expressions for the orbitals:

$$\phi_{A_{1g}} = \frac{1}{2}(\sigma_1 + \sigma_2 + \sigma_3 + \sigma_4) \tag{6.15a}$$

$$\phi_{B_{1g}} = \frac{1}{2}(\sigma_1 - \sigma_2 + \sigma_3 - \sigma_4) \tag{6.15b}$$

$$\phi_{E_u}(1) = \frac{1}{\sqrt{2}}(\sigma_1 - \sigma_3) \tag{6.15c}$$

$$\phi_{E_u}(2) = \frac{1}{\sqrt{2}}(\sigma_2 - \sigma_4) \tag{6.15d}$$

These symmetry-adapted orbitals are shown in Figure 6.6. The solution found for the degenerate E_u orbitals is not unique, since any pair of independent linear combinations of these orbitals is also a basis for this representation. Another choice is often made, the (normalized) sum and difference of the two functions $\phi_{E_u}(1)$ and $\phi_{E_u}(2)$ (right-hand side of Figure 6.6).

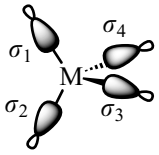

6-25

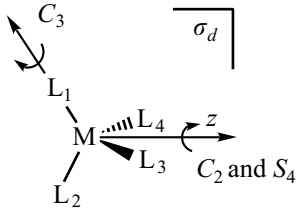

6-26

6.6.2. Tetrahedral ML_4 complexes

Consider a complex ML_4 in which the four ligands are situated at the apices of a tetrahedron. Each ligand has a σ orbital which points towards the metallic centre (**6-25**). The symmetry elements, which are characteristic of the T_d point group, are:

- four C_3 axes, each of which is co-linear with one of the M—L bonds;
- three C_2 axes that bisect the L—M—L angles;
- three S_4 axes that are co-linear with the C_2 axes;
- six σ_d planes, each of which contains two M—L bonds.

An example of each of these elements is shown in **6-26**.

6.6.2.1. *Reduction of the Γ_σ representation*

To obtain the characters that are associated with the reducible representation Γ_σ, we just need to count the number of ligands that are left unmoved by the various symmetry operations. For the identity operation, we clearly have $\chi = 4$. Rotation around a C_3-axis leaves one ligand in its original position ($\chi = 1$), the one located on that axis. Rotation around the C_2 and S_4 axes moves all the ligands ($\chi = 0$). Reflection in a σ_d plane leaves the two ligands that are in this plane in their original positions ($\chi = 2$). The characters that are obtained are given in Table 6.20, together with those for the irreducible representations of the T_d point group.

The order of the group (the number of symmetry operations, h) is 24 (first line of Table 6.20). Application of the reduction formula (6.5)

Table 6.20. Character table for the T_d point group and the characters of the reducible representation Γ_σ in a tetrahedral ML_4 complex

T_d	E	$8C_3$	$3C_2$	$6S_4$	$6\sigma_d$		
A_1	1	1	1	1	1		$x^2+y^2+z^2$
A_2	1	1	1	−1	−1		
E	2	−1	2	0	0		$(2z^2-x^2-y^2, x^2-y^2)$
T_1	3	0	−1	1	−1		
T_2	3	0	−1	−1	1	(x,y,z)	(xy,xz,yz)
Γ_σ	4	1	0	0	2		

gives:

$$a_{A_1} = \frac{1}{24}[(4\times1\times1)+(1\times1\times8)+(0\times1\times3)+(0\times1\times6)+(2\times1\times6)] = 1$$

$$a_{A_2} = \frac{1}{24}[(4\times1\times1)+(1\times1\times8)+(0\times1\times3)-(0\times1\times6)-(2\times1\times6)] = 0$$

$$a_{E} = \frac{1}{24}[(4\times2\times1)-(1\times1\times8)+(0\times2\times3)-(0\times0\times6)+(2\times0\times6)] = 0$$

$$a_{T_1} = \frac{1}{24}[(4\times3\times1)+(1\times0\times8)-(0\times1\times3)+(0\times1\times6)-(2\times1\times6)] = 0$$

$$a_{T_2} = \frac{1}{24}[(4\times3\times1)+(1\times0\times8)-(0\times1\times3)-(0\times1\times6)+(2\times1\times6)] = 1$$

hence

$$\Gamma_\sigma = A_1 \oplus T_2 \tag{6.16}$$

The representation Γ_σ is thus decomposed into a one-dimensional representation (A_1, the totally symmetric representation) and a degenerate three-dimensional representation (T_2).

6.6.2.2. *Symmetry-adapted orbitals*

The linear combinations of the σ_i orbitals that are bases for the A_1 and T_2 irreducible representations can be determined from the projection formula (6.10). Since there are many symmetry operations in this point group (24), the exercise is rather tedious, and we shall be content here

just to give the result. The symmetry-adapted orbitals are:

$$\phi_{A_1} = \frac{1}{2}(\sigma_1 + \sigma_2 + \sigma_3 + \sigma_4) \tag{6.17a}$$

$$\phi_{T_2}(1) = \frac{1}{\sqrt{2}}(\sigma_1 - \sigma_2) \tag{6.17b}$$

$$\phi_{T_2}(2) = \frac{1}{\sqrt{2}}(\sigma_3 - \sigma_4) \tag{6.17c}$$

$$\phi_{T_2}(3) = \frac{1}{2}(\sigma_1 + \sigma_2 - \sigma_3 - \sigma_4) \tag{6.17d}$$

These orbitals are shown in Figure 6.7.

The expression of the T_2 orbitals given in (6.17b–d) is not unique; as we have already seen for square-planar complexes in § 6.6.1.2, any independent linear combination of these functions is acceptable. One such, which 'favours' a vertical C_3-axis, is shown on the right-hand side of Figure 6.7 (see Exercise 6.10).

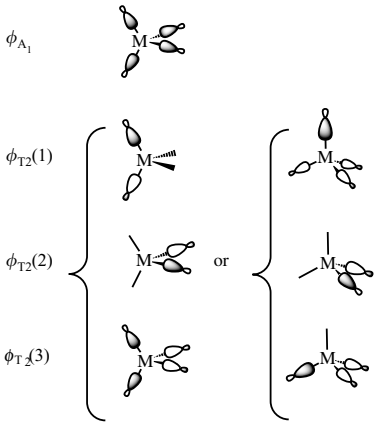

Figure 6.7. Symmetry-adapted σ orbitals in a tetrahedral ML_4 complex. Two different representations are given for the degenerate T_2 orbitals.

6.6.3. Trigonal-planar ML_3 complexes

A trigonal-planar ML_3 complex (**6-27**) belongs to the D_{3h} point group and contains the following symmetry elements: the molecular plane (σ_h), three perpendicular planes (σ_v), each of which contains one M—L bond, a C_3-axis and an S_3-axis which are co-linear and perpendicular to the σ_h plane, and three C_2 axes, each of which is co-linear with one of the bonds. Each type of symmetry element is illustrated in **6-28**.

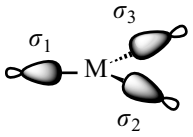

6-27

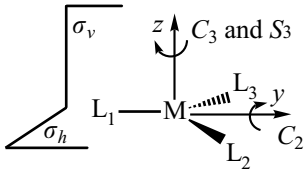

6-28

6.6.3.1. *Reduction of the representation* Γ_σ

Rotations around the C_3 and S_3 axes change the positions of all the ligands ($\chi = 0$), but a rotation around a C_2-axis leaves the ligand on that axis unmoved ($\chi = 1$). Reflections in the σ_h and σ_v planes leave all three ligands in their original positions ($\chi = 3$). The characters obtained from these considerations are given in Table 6.21 (Γ_σ), together

Table 6.21. Character table for the D_{3h} point group and the characters of the reducible representation Γ_σ for a trigonal-planar ML_3 complex

D_{3h}	E	$2C_3$	$3C_2$	σ_h	$2S_3$	$3\sigma_v$		
A_1'	1	1	1	1	1	1		$x^2 + y^2, z^2$
A_2'	1	1	−1	1	1	−1		
E'	2	−1	0	2	−1	0	(x, y)	$(x^2 - y^2, xy)$
A_1''	1	1	1	−1	−1	−1		
A_2''	1	1	−1	−1	−1	1	z	
E''	2	−1	0	−2	1	0		(xz, yz)
Γ_σ	3	0	1	3	0	1		

with those of the different irreducible representations of the D_{3h} point group.

As the order of the group (h) is 12, application of the reduction formula (6.5) leads to (products where at least one factor is zero have been omitted):

$$a_{A_1'} = \frac{1}{12}[(3 \times 1 \times 1) + (1 \times 1 \times 3) + (3 \times 1 \times 1) + (1 \times 1 \times 3)] = 1$$

$$a_{A_2'} = \frac{1}{12}[(3 \times 1 \times 1) - (1 \times 1 \times 3) + (3 \times 1 \times 1) - (1 \times 1 \times 3)] = 0$$

$$a_{E'} = \frac{1}{12}[(3 \times 2 \times 1) + (3 \times 2 \times 1)] = 1$$

$$a_{A_1''} = \frac{1}{12}[(3 \times 1 \times 1) + (1 \times 1 \times 3) - (3 \times 1 \times 1) - (1 \times 1 \times 3)] = 0$$

$$a_{A_2''} = \frac{1}{12}[(3 \times 1 \times 1) - (1 \times 1 \times 3) - (3 \times 1 \times 1) + (3 \times 1 \times 3)] = 0$$

$$a_{E''} = \frac{1}{12}[(3 \times 2 \times 1) - (3 \times 2 \times 1)] = 0$$

hence

$$\Gamma_\sigma = A_1' \oplus E' \tag{6.18}$$

The representation Γ_σ is thus decomposed into a one-dimensional representation (A_1', the totally symmetric representation) and a degenerate two-dimensional representation (E').

6.6.3.2. *Symmetry-adapted orbitals*

As in the previous examples, the orbital with A_1' symmetry (the totally symmetric representation) is a linear combination of all the σ_i orbitals with coefficients that are equal in sign and magnitude. The orbitals with E' symmetry are obtained by applying the projection formula to the functions σ_1 and $(\sigma_2 - \sigma_3)$, in turn (see Exercise 6.11), as for NH_3 (§ 6.4.2.2.). The results are:

$$\phi_{A_1'} = \frac{1}{\sqrt{3}}(\sigma_1 + \sigma_2 + \sigma_3) \tag{6.19a}$$

$$\phi_{E'}(1) = \frac{1}{\sqrt{6}}(2\sigma_1 - \sigma_2 - \sigma_3) \tag{6.19b}$$

$$\phi_{E'}(2) = \frac{1}{\sqrt{2}}(\sigma_2 - \sigma_3) \tag{6.19c}$$

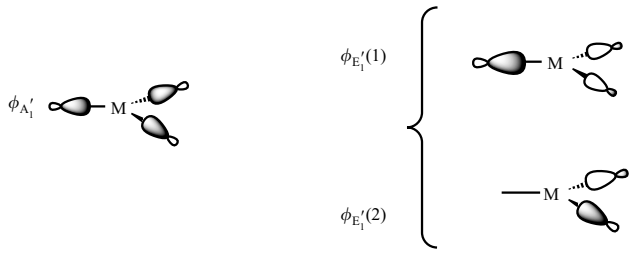

Figure 6.8. Symmetry-adapted σ orbitals for a trigonal-planar ML_3 complex.

These three orbitals are shown in Figure 6.8.

6.6.4. Trigonal-bipyramidal ML_5 complexes

In a trigonal-bipyramidal ML_5 complex, three of the ligands are found in equatorial positions (L_1, L_2, and L_3), whereas the other two (L_4 and L_5) are in axial sites (**6-29**). The apices of the bipyramid are defined by the axial ligands, its triangular base by the positions of the equatorial ligands. The angles between the equatorial bonds are 120° and the axial bonds are perpendicular to the equatorial plane. Like the trigonal-planar complex ML_3, a trigonal-bipyramidal molecule belongs to the D_{3h} point group (see **6-28** for the symmetry elements).

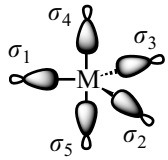

6-29

6.6.4.1. *Reduction of the representation* Γ_σ

The C_3-axis maintains the positions of the two axial ligands ($\chi = 2$), whereas the S_3-axis, which interchanges them, changes the positions of all the ligands ($\chi = 0$). A C_2-axis moves every ligand except the one placed on that axis ($\chi = 1$). The σ_h and σ_v planes do not move the three ligands found in these planes ($\chi = 3$). The characters of the Γ_σ representation are given in Table 6.22 (second line).

The reduction formula (6.5), in combination with the characters of the irreducible representations of the D_{3h} point group found in Table 6.21, leads to:

$$a_{A_1'} = \frac{1}{12}[(5\times1\times1)+(2\times1\times2)+(1\times1\times3)+(3\times1\times1)+(3\times1\times3)] = 2$$

$$a_{A_2'} = \frac{1}{12}[(5\times1\times1)+(2\times1\times2)-(1\times1\times3)+(3\times1\times1)-(3\times1\times3)] = 0$$

$$a_{E'} = \frac{1}{12}[(5\times2\times1)-(2\times1\times2)+(3\times2\times1)] = 1$$

$$a_{A_1''} = \frac{1}{12}[(5\times1\times1)+(2\times1\times2)+(1\times1\times3)-(3\times1\times1)-(3\times1\times3)] = 0$$

$$a_{A_2''} = \frac{1}{12}[(5\times1\times1)+(2\times1\times2)-(1\times1\times3)-(3\times1\times1)+(3\times1\times3)] = 1$$

$$a_{E''} = \frac{1}{12}[(5\times2\times1)-(2\times1\times2)-(3\times2\times1)] = 0$$

Table 6.22. Characters of the reducible representations Γ_σ, Γ_σ(eq) and Γ_σ(ax) of an ML_5 complex with a TBP geometry

D_{3h}	E	$2C_3$	$3C_2$	σ_h	$2S_3$	$3\sigma_v$
Γ_σ	5	2	1	3	0	3
Γ_σ(eq)	3	0	1	3	0	1
Γ_σ(ax)	2	2	0	0	0	2

hence

$$\Gamma_\sigma = 2A_1' \oplus A_2'' \oplus E' \tag{6.20}$$

The Γ_σ representation is thus decomposed into three one-dimensional representations ($2A_1'$ and A_2'') and one doubly degenerate representation (E').

It is important to note that *no* symmetry operation exchanges an axial ligands with an equatorial one. As these two types of ligands are therefore non-equivalent, both 'chemically' and according to group theory, they can be considered separately. The characters of the representations Γ_σ (eq) and Γ_σ (ax) are given in Table 6.22. From the reduction formula (6.5), we find:

$$\Gamma_\sigma(\text{eq}) = A_1{}' \oplus E' \tag{6.21}$$

$$\Gamma_\sigma(\text{ax}) = A_1{}' \oplus A_2{}'' \tag{6.22}$$

It is easy to check that $\Gamma_\sigma = \Gamma_\sigma(\text{eq}) \oplus \Gamma_\sigma(\text{ax})$.

6.6.4.2. *Symmetry-adapted orbitals*

The separation of Γ_σ into Γ_σ (eq) and Γ_σ (ax) leads to a considerable simplification of the determination of the symmetry-adapted orbitals. For the orbitals on the equatorial ligands, they are identical to those we have already determined for a trigonal-planar ML_3 complex (§ 6.6.3.2, 6.23a,b and c and Figure 6.9).

$$(\phi_{A_1'})_{\text{eq}} = \frac{1}{\sqrt{3}}(\sigma_1 + \sigma_2 + \sigma_3) \tag{6.23a}$$

$$(\phi_{E'})_{\text{eq}}(1) = \frac{1}{\sqrt{2}}(\sigma_2 - \sigma_3) \tag{6.23b}$$

$$(\phi_{E'})_{\text{eq}}(2) = \frac{1}{\sqrt{6}}(2\sigma_1 - \sigma_2 - \sigma_3) \tag{6.23c}$$

$$(\phi_{A_1'})_{\text{ax}} = \frac{1}{\sqrt{2}}(\sigma_4 + \sigma_5) \tag{6.23d}$$

$$(\phi_{A_2''})_{\text{ax}} = \frac{1}{\sqrt{2}}(\sigma_4 - \sigma_5) \tag{6.23e}$$

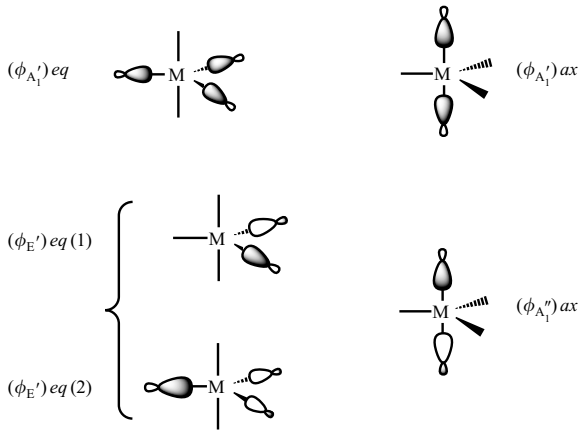

Figure 6.9. Symmetry-adapted σ orbitals for a TBP ML_5 complex.

For the axial ligands, we only need to make normalized sums (A_1' symmetry) and differences (A_2'' symmetry) (6.23d, 6.23e and Figure 6.9).

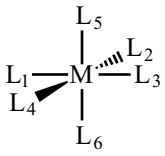

6-30

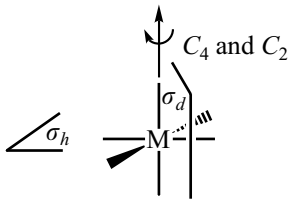

6-31

6.6.5. Octahedral ML_6 complexes

Of the numerous symmetry elements in an octahedral complex ML_6 (**6-30**), the only ones that leave the positions of certain ligands unchanged are shown in **6-31**. The three C_4 axes and their co-linear C_2 axes both conserve the positions of the two ligands situated on them ($\chi = 2$). Reflection in the three σ_h planes, which are perpendicular to the C_4 axes, does not move the four ligands in these planes ($\chi = 4$). Each of the six σ_d planes contains only two ligands, so reflection therein gives a character of 2.

6.6.5.1. *Reduction of the Γ_σ representation*

The characters of the resulting Γ_σ representation are given in Table 6.23 (Γ_σ), together with those of the irreducible representations of the O_h point group.

The order of this group (h) is 48. Use of the reduction formula (6.5) shows that the only non-zero contributions are:

$$a_{A_{1g}} = \frac{1}{48}[(6 \times 1 \times 1) + (2 \times 1 \times 6) + (2 \times 1 \times 3) + (2 \times 1 \times 6) + (4 \times 1 \times 3)] = 1$$

$$a_{E_g} = \frac{1}{48}[(6 \times 2 \times 1) + (2 \times 2 \times 3) + (4 \times 2 \times 3)] = 1$$

$$a_{T_{1u}} = \frac{1}{48}[(6 \times 3 \times 1) + (2 \times 1 \times 6) - (2 \times 1 \times 3) + (2 \times 1 \times 6) + (4 \times 1 \times 3)] = 1$$

Table 6.23. Character table for the O_h point group and the characters of the reducible representation Γ_σ for an octahedral ML_6 complex

O_h	E	$8C_3$	$6C_2'$	$6C_4$	$3C_2$	i	$8S_6$	$6\sigma_d$	$6S_4$	$3\sigma_h$		
A_{1g}	1	1	1	1	1	1	1	1	1	1		$x^2+y^2+z^2$
A_{2g}	1	1	−1	−1	1	1	1	−1	−1	−1		
E_g	2	−1	0	0	2	2	−1	0	0	2		(z^2, x^2-y^2)
T_{1g}	3	0	−1	1	−1	3	0	−1	1	−1		
T_{2g}	3	0	1	−1	−1	3	0	1	−1	−1		(xy, xz, yz)
A_{1u}	1	1	1	1	1	−1	−1	−1	−1	−1		
A_{2u}	1	1	−1	−1	1	−1	−1	1	1	−1		
E_u	2	−1	0	0	2	−2	1	0	0	−2		
T_{1u}	3	0	−1	1	−1	−3	0	1	−1	1	(x, y, z)	
T_{2u}	3	0	1	−1	−1	−3	0	−1	1	1		
Γ_σ	6	0	0	2	2	0	0	2	0	4		

hence

$$\Gamma_\sigma = A_{1g} \oplus E_g \oplus T_{1u} \tag{6.24}$$

The Γ_σ representation is therefore decomposed into a one-dimensional representation (A_{1g}), a doubly degenerate representation (E_g), and a triply degenerate representation (T_{1u}).

6.6.5.2. *Symmetry-adapted orbitals*

In view of the large number of symmetry operations, we shall limit ourselves here to giving the result of the application of the projection formula (6.10). The following orbitals are obtained; they are shown in Figure 6.10:

$$\phi_{A_{1g}} = \frac{1}{\sqrt{6}}(\sigma_1 + \sigma_2 + \sigma_3 + \sigma_4 + \sigma_5 + \sigma_6) \tag{6.25a}$$

$$\phi_{E_g}(1) = \frac{1}{2}(\sigma_1 - \sigma_2 + \sigma_3 - \sigma_4) \tag{6.25b}$$

$$\phi_{E_g}(2) = \frac{1}{\sqrt{12}}(-\sigma_1 - \sigma_2 - \sigma_3 - \sigma_4 + 2\sigma_5 + 2\sigma_6) \tag{6.25c}$$

$$\phi_{T_{1u}}(1) = \frac{1}{\sqrt{2}}(\sigma_1 - \sigma_3) \tag{6.25d}$$

$$\phi_{T_{1u}}(2) = \frac{1}{\sqrt{2}}(\sigma_2 - \sigma_4) \tag{6.25e}$$

$$\phi_{T_{1u}}(3) = \frac{1}{\sqrt{2}}(\sigma_5 - \sigma_6) \tag{6.25f}$$

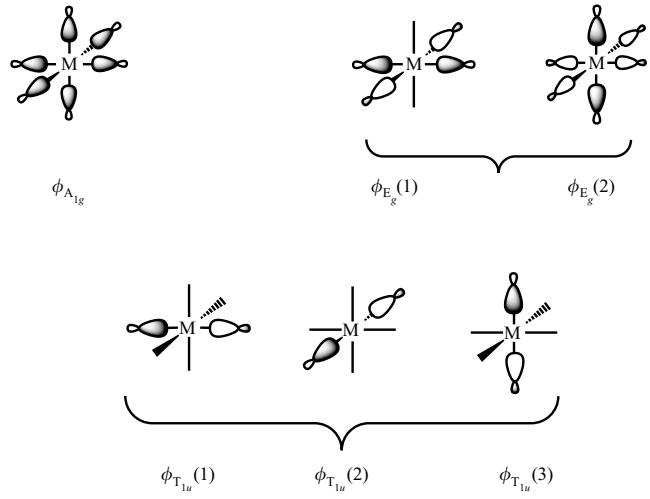

Figure 6.10. Symmetry-adapted σ orbitals in an octahedral ML_6 complex.

The degeneracy of the T_{1u} orbitals is obvious from the coefficients of the σ_i orbitals (6.25d–f), but the same is not true of the E_g orbitals, whose coefficients are very different (6.25b, c).

6.6.6. Trigonal-planar ML_3 complexes with a 'π system' on the ligands

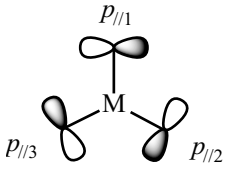

6-32

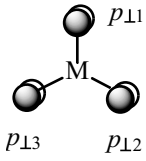

6-33

In this last example, we shall analyse a trigonal-planar ML_3 complex in which the ligands are considered to have two p orbitals perpendicular to the M—L bond as well as the σ orbital that points towards the metal (§ 6.6.3.). These p orbitals are written $p_\parallel$ (**6-32**) and $p_\perp$ (**6-33**), depending on whether they are in the plane of the complex or perpendicular to it. By convention, each orbital $p_{\parallel i}$ is oriented in a clockwise sense ($-p_{\parallel i}$ corresponds to the opposite orientation). This system can act as a model for a complex in which the three ligands are double-face π donors or π acceptors (Chapter 3).

6.6.6.1. *Reduction of the representations $\Gamma_{p\parallel}$ and $\Gamma_{p\perp}$*

To obtain the characters of the representations $\Gamma_{p\parallel}$ and $\Gamma_{p\perp}$, it is now not sufficient just to count the number of ligands whose position is unchanged by the action of the symmetry operations of the (D_{3h}) point group. Although that procedure was acceptable in the previous examples, the situation is more complicated now, since an orbital can be transformed into itself ($\chi = 1$) *or* into its opposite ($\chi = -1$).

We consider first the $\Gamma_{p\parallel}$ representation. Action of the C_3 and S_3 axes changes all three orbitals ($\chi = 0$), a C_2-axis transforms the orbital of the atom on that axis into its opposite and also interchanges the two others while changing their sign (**6-34** for the axis that passes through

the ligand L_1). The associated character is therefore -1. The molecular plane σ_h maintains the three orbitals ($\chi = 3$) in their original positions, whereas reflection in a σ_v plane has the same consequences as rotation around a C_2-axis (**6-35**, $\chi = -1$).

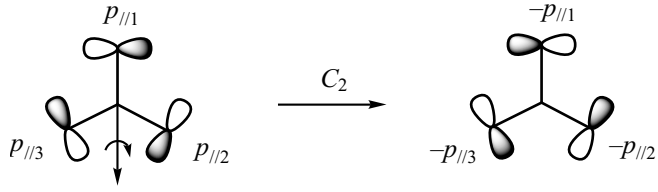

6-34

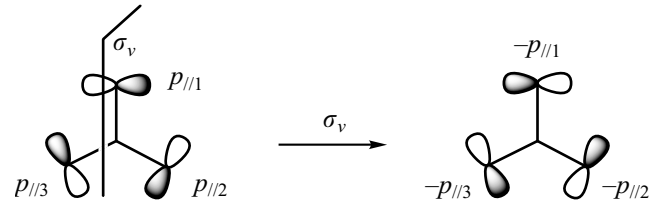

6-35

We now turn to the $\Gamma_{p\perp}$ representation. The character is still zero for the C_3 and S_3 axes, and still -1 for a C_2-axis (**6-36**). Reflection in the σ_h plane changes each orbital into its opposite (**6-37**, $\chi = -3$), whereas a σ_v plane maintains one orbital and interchanges the two others (**6-38**, $\chi = 1$).

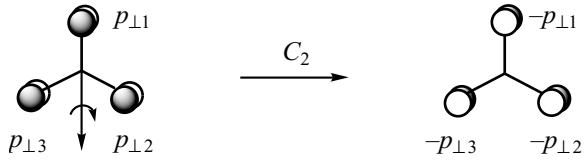

6-36

The characters associated with the $\Gamma_{p\parallel}$ and $\Gamma_{p\perp}$ representations are listed in Table 6.24, together with the characters of the irreducible representations of the D_{3h} point group.

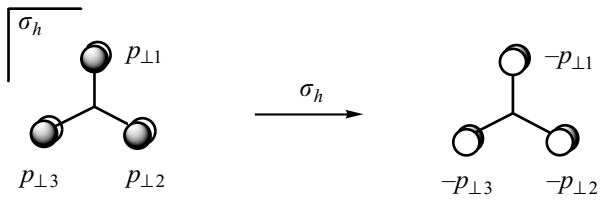

6-37

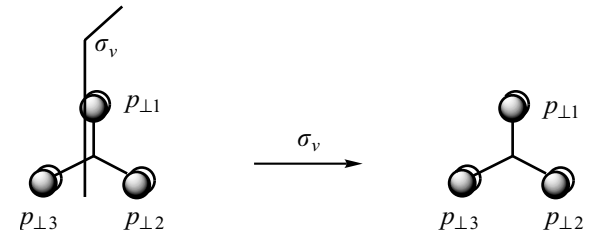

6-38

Table 6.24. Character table for the D_{3h} point group and the characters of the reducible representations $\Gamma_{p\parallel}$ and $\Gamma_{p\perp}$ for a trigonal-planar ML_3 complex

D_{3h}	E	$2C_3$	$3C_2$	σ_h	$2S_3$	$3\sigma_v$		
A_1'	1	1	1	1	1	1		x^2+y^2, z^2
A_2'	1	1	−1	1	1	−1		
E'	2	−1	0	2	−1	0	(x, y)	(x^2-y^2, xy)
A_1''	1	1	1	−1	−1	−1		
A_2''	1	1	−1	−1	−1	1	z	
E''	2	−1	0	−2	1	0		(xz, yz)
$\Gamma_{p\parallel}$	3	0	−1	3	0	−1		
$\Gamma_{p\perp}$	3	0	−1	−3	0	1		

For the $\Gamma_{p\parallel}$ representation, application of the reduction formula (6.5) gives:

$$a_{A_1'} = \frac{1}{12}[(3\times1\times1)-(1\times1\times3)+(3\times1\times1)-(1\times1\times3)] = 0$$

$$a_{A_2'} = \frac{1}{12}[(3\times1\times1)+(1\times1\times3)+(3\times1\times1)+(1\times1\times3)] = 1$$

$$a_{E'} = \frac{1}{12}[(3\times2\times1)+(3\times2\times1)] = 1$$

$$a_{A_1''} = \frac{1}{12}[(3\times1\times1)-(1\times1\times3)-(3\times1\times1)+(1\times1\times3)] = 0$$

$$a_{A_2''} = \frac{1}{12}[(3\times1\times1)+(1\times1\times3)-(3\times1\times1)-(1\times1\times3)] = 0$$

$$a_{E''} = \frac{1}{12}[(3\times2\times1)-(3\times2\times1)] = 0$$

hence

$$\Gamma_{p\parallel} = A_2' \oplus E' \tag{6.26}$$

For the $\Gamma_{p\perp}$ representation, we obtain:

$$a_{A_1'} = \frac{1}{12}[(3 \times 1 \times 1) - (1 \times 1 \times 3) - (3 \times 1 \times 1) + (1 \times 1 \times 3)] = 0$$
$$a_{A_2'} = \frac{1}{12}[(3 \times 1 \times 1) + (1 \times 1 \times 3) - (3 \times 1 \times 1) - (1 \times 1 \times 3)] = 0$$
$$a_{E'} = \frac{1}{12}[(3 \times 2 \times 1) - (3 \times 2 \times 1)] = 0$$
$$a_{A_1''} = \frac{1}{12}[(3 \times 1 \times 1) - (1 \times 1 \times 3) + (3 \times 1 \times 1) - (1 \times 1 \times 3)] = 0$$
$$a_{A_2''} = \frac{1}{12}[(3 \times 1 \times 1) + (1 \times 1 \times 3) + (3 \times 1 \times 1) + (1 \times 1 \times 3)] = 1$$
$$a_{E''} = \frac{1}{12}[(3 \times 2 \times 1) + (3 \times 2 \times 1)] = 1$$

hence

$$\Gamma_{p\perp} = A_2'' \oplus E'' \tag{6.27}$$

6.6.6.2. *Symmetry-adapted orbitals*

We shall limit ourselves here to the determination of the symmetry-adapted A_2'' and E'' orbitals in the $\Gamma_{p\perp}$ representation. Table 6.25 shows the action of all the symmetry operations of the D_{3h} point group on the generating functions $p_{\perp 1}$ and $(p_{\perp 2} - p_{\perp 3})$, as well as the characters of the A_2'' and E'' irreducible representations.

The symmetry-adapted orbitals are obtained from formula (6.10), by using the $p_{\perp 1}$ generating function for the $\phi_{A_2''}$ orbital and for the first degenerate orbital $\phi_{E''}(1)$, and the function $(p_{\perp 2} - p_{\perp 3})$ for the second degenerate orbital $\phi_{E''}(2)$. We obtain:

$$\phi_{A_2''} = 4 \times (p_{\perp 1} + p_{\perp 2} + p_{\perp 3})$$
$$\phi_{E''}(1) = 2 \times (2p_{\perp 1} - p_{\perp 2} - p_{\perp 3})$$
$$\phi_{E''}(2) = 6 \times (p_{\perp 2} - p_{\perp 3})$$

so the normalized orbitals are

$$\phi_{A_2''} = \frac{1}{\sqrt{3}} (p_{\perp 1} + p_{\perp 2} + p_{\perp 3}) \tag{6.28a}$$
$$\phi_{E''}(1) = \frac{1}{\sqrt{6}} (2p_{\perp 1} - p_{\perp 2} - p_{\perp 3}) \tag{6.28b}$$
$$\phi_{E''}(2) = \frac{1}{\sqrt{2}} (p_{\perp 2} - p_{\perp 3}) \tag{6.28c}$$

Table 6.25. Action of the symmetry operations of the D_{3h} point group on the $p_\perp$ orbitals (see **6-33**) and the characters of the A_2'' and E'' irreducible representations. [See Scheme **6-28** for the definition of the symmetry elements. A $C_2(i)$-axis is co-linear with the M—L_i bond, and a $\sigma_v(i)$ plane contains the M—L_i bond.]

D_{3h}	E	C_3^1	C_3^2	$C_2(1)$	$C_2(2)$	$C_2(3)$	σ_h	S_3^1	S_3^2	$\sigma_v(1)$	$\sigma_v(2)$	$\sigma_v(3)$
$R_k(p_{\perp 1})$	$p_{\perp 1}$	$p_{\perp 2}$	$p_{\perp 3}$	$-p_{\perp 1}$	$-p_{\perp 3}$	$-p_{\perp 2}$	$-p_{\perp 1}$	$-p_{\perp 2}$	$-p_{\perp 3}$	$p_{\perp 1}$	$p_{\perp 3}$	$p_{\perp 2}$
$R_k(p_{\perp 2} - p_{\perp 3})$	$p_{\perp 2} - p_{\perp 3}$	$p_{\perp 1} - p_{\perp 2}$	$p_{\perp 3} - p_{\perp 1}$	$p_{\perp 2} - p_{\perp 3}$	$p_{\perp 1} - p_{\perp 2}$	$p_{\perp 3} - p_{\perp 1}$	$p_{\perp 3} - p_{\perp 2}$	$p_{\perp 2} - p_{\perp 1}$	$p_{\perp 1} - p_{\perp 3}$	$p_{\perp 3} - p_{\perp 2}$	$p_{\perp 2} - p_{\perp 1}$	$p_{\perp 1} - p_{\perp 3}$
A_2''	1	1	1	−1	−1	−1	−1	−1	−1	1	1	1
E''	2	−1	−1	0	0	0	−2	1	1	0	0	0

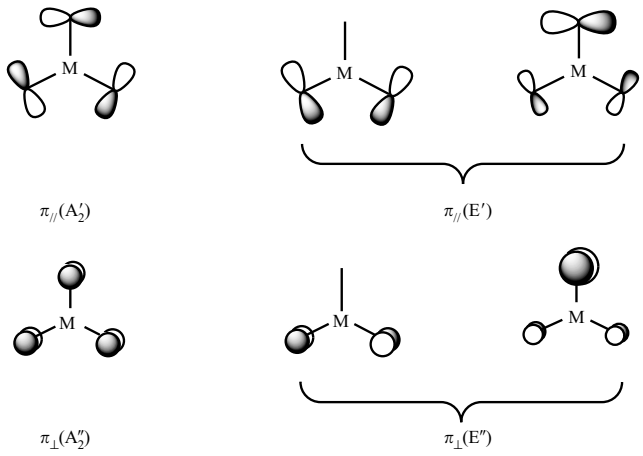

Figure 6.11. $\pi_{\parallel}$ and $\pi_{\perp}$ symmetry-adapted orbitals in a trigonal-planar ML_3 complex.

For the A_2' and E'' symmetry-adapted orbitals ($\Gamma_{p\parallel}$), we obtain (see Exercise 6.12):

$$\phi_{A_2'} = \frac{1}{\sqrt{3}}\,(p_{\parallel 1} + p_{\parallel 2} + p_{\parallel 3}) \tag{6.29a}$$

$$\phi_{E'}(1) = \frac{1}{\sqrt{6}}\,(2p_{\parallel 1} - p_{\parallel 2} - p_{\parallel 3}) \tag{6.29b}$$

$$\phi_{E'}(2) = \frac{1}{\sqrt{2}}\,(p_{\parallel 2} - p_{\parallel 3}) \tag{6.29c}$$

The different symmetry-adapted orbitals are shown in Figure 6.11.

Although the σ-type orbitals point along the M—L bonds, the orbitals above are constructed from ligand orbitals that are perpendicular to these bonds. This is why they are often written $\pi_{\parallel}$ and $\pi_{\perp}$, even though this notation is not strictly correct according to group theory.

Exercises

Symmetry elements and symmetry operations

6.1

How many reflection planes are there in the following molecules? (1) water (H_2O); (2) ammonia (NH_3); (3) ethylene (C_2H_4); (4) (*Z*)-1,2-difluoroethylene; (5) (*E*)-1,2-difluoroethylene; (6) aluminium trichloride ($AlCl_3$, a trigonal-planar molecule).

6.2

Which of the following molecules contain an inversion centre? (1) carbon dioxide (CO_2, linear); (2) hydrogen cyanide (HCN, linear); (3) dimethylether (shown in **6-1**); (4) benzene (C_6H_6, hexagonal);

(5) (*Z*)-1,2-difluoroethylene; (6) (*E*)-1,2-difluoroethylene; (7) aluminium trichloride ($AlCl_3$, a trigonal-planar molecule); (8) methane (CH_4, tetrahedral); (9) $[PtCl_4]^{2-}$ (a square-planar complex, Scheme **6-10**); (10) ethane (C_2H_6) in the staggered conformation; (11) ethane in the eclipsed conformation.

6.3

1. Are there any rotation axes in the ammonia molecule (**6-7**) in addition to the C_3-axis?
2. Locate the three C_3 axes and the four C_2 axes in the methane molecule.
3. How many C_2 axes are there in (*i*) ethylene; (*ii*) (*Z*)-1,2-difluoroethylene; (*iii*) (*E*)-1,2-difluoroethylene ?
4. Which rotation axes are present in $AlCl_3$?

6.4

1. Consider a C_2-axis and the co-linear S_4-axis in methane (see Scheme **6-11**). Show that $S_4^2 = C_2$ and that $S_4^4 = E$.
2. Carry out the S_3^2 and S_3^4 operations in the PF_5 molecule (see Scheme **6-12**). Show that these operations are equivalent to operations associated with the C_3-axis or the σ_h plane.
3. (i) Show that ethane (C_2H_6) in the *eclipsed* conformation possesses an improper axis that is co-linear with the C–C bond. What is the order of this axis? (*ii*) Repeat the question for ethane in the *staggered* conformation.

6.5

The symmetry elements present in the ammonia molecule (NH_3) are a C_3-axis (**6-7**) and three planes of symmetry ($\sigma_v(1)$, $\sigma_v(2)$, and $\sigma_v(3)$) (Exercise 6.1, question 2).

1. Perform the C_3 operation followed by $\sigma_v(1)$ (written $\sigma_v(1)C_3$); carry out $\sigma_v(1)$ followed by C_3 (written $C_3\sigma_v(1)$). What conclusion(s) can you draw?
2. Perform $(C_3\sigma_v(1))\sigma_v(2)$ then $C_3(\sigma_v(1)\sigma_v(2))$. What conclusion(s) can you draw?
3. Which operations are the inverses of E, C_3, C_3^2, $\sigma_v(1)$?

6.6

Determine the point-group symmetries of the following molecules: (1) O_2; (2) HCl; (3) ethylene (C_2H_4); (4) (*Z*)-1,2-difluoroethylene; (5) (*E*)-1,2-difluoroethylene; (6) $AlCl_3$, a trigonal-planar molecule; (7) tetrachloromethane (CCl_4); (8) dichloromethane (CH_2Cl_2); (9)

NH_3 (**6-7**); (10) $[PtCl_4]^{2-}$ (**6-10**); (11) PF_5 (**6-12**); 12) trifluoroethylene ($F_2C{=}CHF$, planar).

Symmetry-adapted orbitals

6.7

Show that in the NH_3 molecule, the functions $(1/\sqrt{3})(1s_{H_1}+1s_{H_2}+1s_{H_3})$, a basis for the A_1 representation, and $(1/\sqrt{6})(2\times(1s_{H_1})-1s_{H_2}-1s_{H_3})$, one of the basis functions for the E representation, are orthogonal. The $1s_H$ orbitals are assumed to be normalized, and the overlap between two $1s_H$ orbitals on different atoms is written S.

6.8

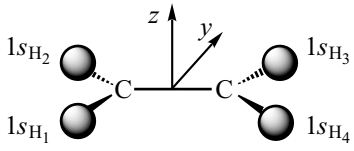

1. Reduce the Γ_H basis that is constituted by the $1s_H$ orbitals on the hydrogen atoms in the ethylene molecule (the characters of this representation are given in Table 6.8, and the character table for the D_{2h} point group is given below).
2. Find the linear combinations of these orbitals that are bases for irreducible representations.

D_{2h}	E	$C_2(z)$	$C_2(y)$	$C_2(x)$	i	$\sigma(xy)$	$\sigma(xz)$	$\sigma(yz)$		
A_g	1	1	1	1	1	1	1	1		x^2, y^2, z^2
B_{1g}	1	1	−1	−1	1	1	−1	−1		xy
B_{2g}	1	−1	1	−1	1	−1	1	−1		xz
B_{3g}	1	−1	−1	1	1	−1	−1	1		yz
A_u	1	1	1	1	−1	−1	−1	−1		
B_{1u}	1	1	−1	−1	−1	−1	1	1	z	
B_{2u}	1	−1	1	−1	−1	1	−1	1	y	
B_{3u}	1	−1	−1	1	−1	1	1	−1	x	

6.9

Construct the molecular orbitals of NH_3 from the symmetry-adapted orbitals that are given in Figure 6.3. To help you construct the interaction diagram, note that the energies of the orbitals on H_3 fragment and of the nitrogen $2p_N$ orbitals are close to −13.5 eV, and that the energy of the $2s_N$ orbital is −26.0 eV.

6.10

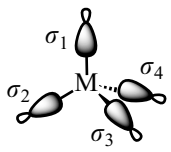

Calculate the coefficients of σ_1, σ_2, σ_3, and σ_4 (see below for the numbering of the atoms) in the symmetry-adapted T_2 orbitals given on the right-hand side of Figure 6.7. You should use the normalization relationships and the fact that these orbitals are mutually orthogonal and orthogonal to the symmetry-adapted A_1 orbital.

6.11

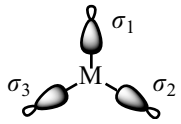

In a trigonal-planar ML_3 complex, the Γ_σ representation is reduced thus: $\Gamma_\sigma = A_1' \oplus E'$ (§ 6.6.3.1, formula (6.18)).

1. Characterize the A_1' symmetry-adapted orbital, using σ_1 as the generating function.
2. Characterize the E' symmetry-adapted orbitals, using σ_1 followed by $(\sigma_2 - \sigma_3)$ as the generating functions. The projection formula (6.10) and the character table for the D_{3h} point group (Table 6.21) should be helpful.

6.12

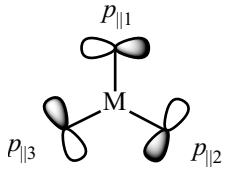

In a trigonal-planar ML_3 complex, the $\Gamma_{p\|}$ representation is reduced thus:

$\Gamma_{p\|} = A_2' \oplus E'$ (§ 6.6.6.1, formula (6.26)).

1. Characterize the A_2' symmetry-adapted orbital, using $p_{\|1}$ as the generating function.
2. Characterize the E' symmetry-adapted orbitals, using $p_{\|1}$ followed by $(p_{\|2}–p_{\|3})$ as the generating functions.

The projection formula (6.10) and the character table for the D_{3h} point group (Table 6.24) should be helpful. The complete set of symmetry operations is given in Table 6.25.

6.13

Consider a square-planar ML_4 complex in which each ligand possesses a π system made up of two p orbitals that are perpendicular to the M–L bonds. These orbitals are $p_\perp$ and $p_\|$, depending on whether they are perpendicular to the plane of the complex or in that plane. The orientation of these orbitals is shown below.

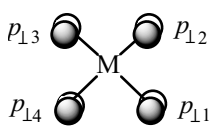

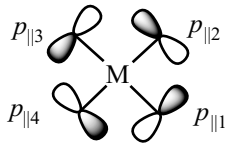

Tables 6.18 and 6.19, which give the character table for the D_{4h} point group and the full set of the symmetry operations of this group, should be helpful, as should Scheme **6-24** in which the different symmetry elements are shown.

1. Determine the characters of the $\Gamma_{p\perp}$ representation.
2. Decompose this representation into a sum of irreducible representations of the D_{4h} point group.

3. Characterize the symmetry-adapted orbitals in each of these representations. The generating function $p_{\perp 1}$ should be used for the one-dimensional representations, and the generating functions $p_{\perp 1}$ and $p_{\perp 2}$ in turn for the two-dimensional representation.
4. Sketch the resulting orbitals.
5. From an analysis of the interactions between the ligand orbitals, establish the energetic ordering of the symmetry-adapted MO.
6. Repeat questions 1–5 for the $\Gamma_{p\parallel}$ representation.

This page intentionally left blank

Answers to the exercises (in skeletal form)

Chapter 1: Setting the scene

1.1. The coordination modes are η^1 (X-type ligand) and η^3 (LX-type ligand).

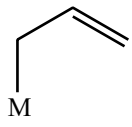

η^1-allyl

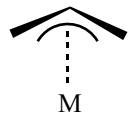

η^3-allyl

1.2.

	1	2	3	4	5	6	7	8	9	10	11	12	13	14	15	16	17	18	19	20	21	22	23	24
l	6	5	5	0	3	5	4	5	0	2	4	0	0	2	1	0	4	6	4	4	4	0	5	2
x	0	0	1	4	1	1	2	0	9	7	0	3	5	4	4	8	4	0	4	5	2	6	0	2
q	0	0	0	0	0	0	0	0	−2	0	0	−2	−3	−1	−1	−2	+1	+1	0	0	0	0	0	0
no	0	0	1	4	1	1	2	0	7	7	0	1	2	3	3	6	5	1	4	5	2	6	0	2
d^n	d^6	d^6	d^6	d^0	d^8	d^6	d^6	d^8	d^0	d^0	d^{10}	d^{10}	d^8	d^6	d^6	d^0	d^2	d^6	d^0	d^0	d^6	d^0	d^8	d^{10}
N_t	18	16	18	8	16	18	18	18	18	18	18	16	18	18	18	16	18	18	16	18	18	12	18	18

1.3. $no = 1$, d^8, $N_t = 16$; $no = 3$, d^6, $N_t = 18$; $no = 3$, d^6, $N_t = 16$; $no = 3$, d^6, $N_t = 18$; $no = 3$, d^6, $N_t = 16$; $no = 3$, d^6, $N_t = 18$; $no = 1$, d^8, $N_t = 16$.

1.4. (1) CO, Cl^-, Et^-, PR_3, H^-, H_2, SiR_3^-, SR^-, CN^-, I^-, Me^-, $COMe^-$, F^-, O^{2-}, NR_3, C_2H_4, C_6H_6, $C_5H_5^-$.

(2)

Complex	Ionic model	*no*
$[Fe(CO)_5]$	$[Fe(CO)_5]$	0
$[Ir(CO)(Cl)(PPh_3)_2]$	$[Ir^+(CO)(Cl^-)(PPh_3)_2]$	1
$[Mn(CO)_6]^+$	$[Mn^+(CO)_6]$	1
$[Ni(CN)_5]^{3-}$	$[Ni^{2+}(CN^-)_5]$	2
$[Zn(Cl)_4]^{2-}$	$[Zn^{2+}(Cl^-)_4]$	2
$[V(Cl)_4]$	$[V^{4+}(Cl^-)_4]$	4
$[Cr(CO)_3(\eta^6\text{-}C_6H_6)]$	$[Cr(CO)_3(\eta^6\text{-}C_6H_6)]$	0
$[Fe(\eta^5\text{-}C_5H_5)_2]$	$[Fe^{2+}(\eta^5\text{-}C_5H_5^-)_2]$	2
$[Cu(\eta^5\text{-}C_5H_5)(PR_3)]$	$[Cu^+(\eta^5\text{-}C_5H_5^-)(PR_3)]$	1
$[Zr(\eta^5\text{-}C_5H_5)_2(CH_3)]^+$	$[Zr^{4+}(\eta^5\text{-}C_5H_5^-)_2(CH_3^-)]$	4
$[Ti(PR_3)_2(Cl)_3(CH_3)]$	$[Ti^{4+}(PR_3)_2(Cl^-)_3(CH_3^-)]$	4
$[W(PR_3)_2(CO)_3(\eta^2\text{-}H_2)]$	$[W(PR_3)_2(CO)_3(\eta^2\text{-}H_2)]$	0
$[Ir(PR_3)_2(Cl)(H)_2]$	$[Ir^{3+}(PR_3)_2(Cl^-)(H^-)_2]$	3
$[Ni(H_2O)_6]^{2+}$	$[Ni^{2+}(H_2O)_6]$	2

1.5.

1. $[CrL_6]$, $no = 0$, d^6, $N_t = 18$; $[RuL]_5$, $no = 0$, d^8, $N_t = 18$.
2. The two compounds are 18-electron complexes. An η^6-coordination of the two ligands in the ruthenium complex would lead to a 20-electron organometallic (and thus strong-field) complex.
3. (i) η^5; (ii) η^3 ; (iii) η^1.

1.6. The borohydride ligand is of L-type in η^1-coordination, L_2-type in η^2-coordination, and L_3-type in η^3-coordination. In each case, the coordination mode of this ligand allows an 18-electron complex to be formed.

1.7. (1) $no = 0$; (2) $no = 3$; (3) $no = 2$; (4) $no = 2$ (each bridging Cl acts as an X-type ligand towards one metallic centre and as an L-type ligand towards the other); (5) $no = 2$ (SR = ligand of XL type (or LX), like Cl).

1.8.

1. The *s* orbitals have spherical symmetry, so their overlap is non-zero for any relative positions of the metal and the ligand. The bonding orbital is mainly concentrated on the ligand and the antibonding orbital on the metal.

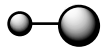

M–L bonding MO

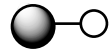

M–L antibonding MO

2. (*i*) On the x-axis; (*ii*) in the nodal plane *yz*: $S = 0$.
3. *xy*: the overlap is largest when the ligand is placed on the bisectors of the *x*- and *y*-axes, and smallest if it is in the *xz* or *yz* nodal planes ($S = 0$); z^2: largest overlap along the *z*-axis and smallest ($S = 0$) when the ligand is on the nodal cone.

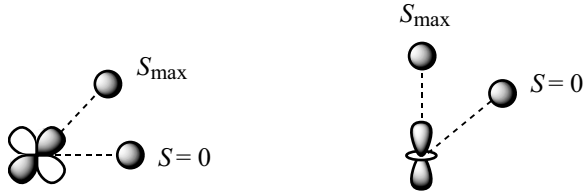

Chapter 2: Principal ligand fields: σ interactions

2.1. 1–*3*

M	Sc	Ti	V	Cr	Mn	Fe	Co	Ni	Cu	Zn
d^n	d^1	d^2	d^3	d^4	d^5	d^6	d^7	d^8	d^9	d^{10}
Electronic configuration	$t_{2g}^1 e_g^0$	$t_{2g}^2 e_g^0$	$t_{2g}^3 e_g^0$	$t_{2g}^3 e_g^1$	$t_{2g}^3 e_g^2$	$t_{2g}^4 e_g^2$	$t_{2g}^5 e_g^2$	$t_{2g}^6 e_g^2$	$t_{2g}^6 e_g^3$	$t_{2g}^6 e_g^4$
Unpaired electrons	1	2	3	4	5	4	3	2	1	0

2.2.

(1) d^6;
(2) Strong-field complex (organometallic): t_{2g}^6;
(3) The anion would be a 19-electron complex (d^7) with a very high-energy *d* MO (strong field) containing an electron. Dissociation gives a 17-electron ML_5 complex (d^7).

2.3.

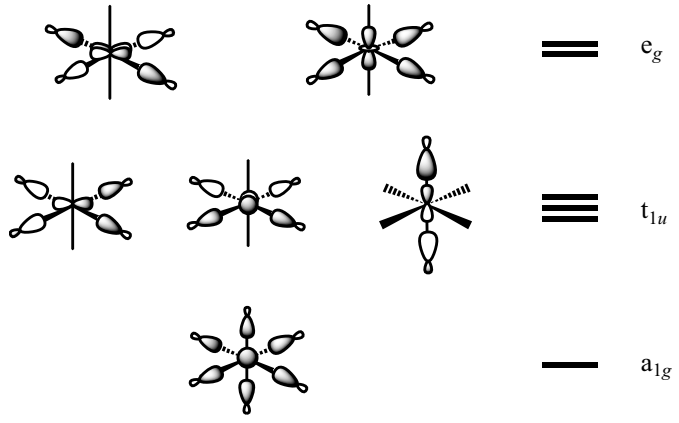

2.4. The xy and x^2-y^2 orbitals are interchanged compared to the description given in § 2.2.1.

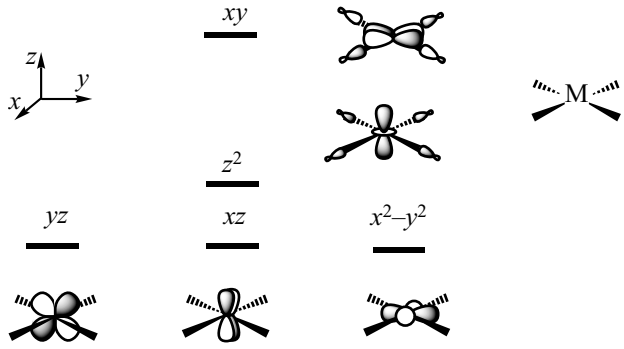

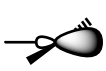 and 

2.5. (1) A fourteen-electron d^8 complex; (2) and (3) Two empty nonbonding MOs:

2.6. (1) and (2) For the orbitals of the square-planar complex, see § 2.2. The z^2 orbital becomes strictly nonbonding (ligands on the nodal cone).

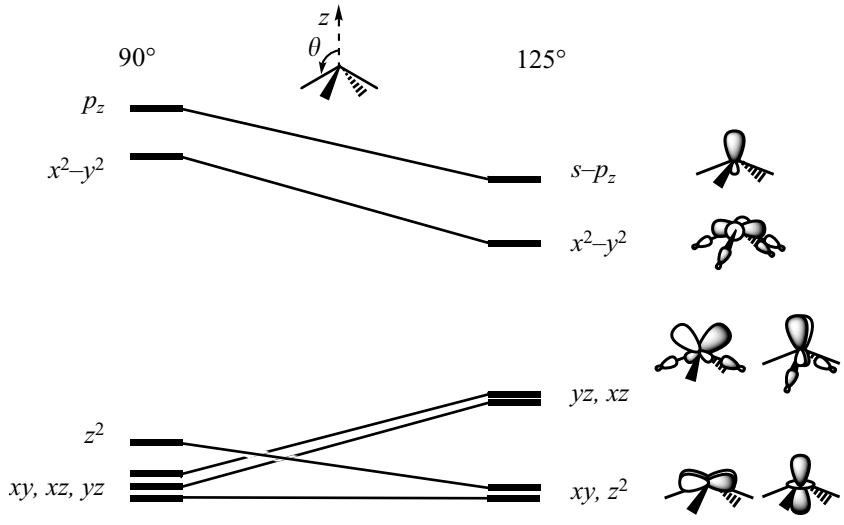

2.7.

1. See § 2.3.1.1, Figure 2.7.
2. (a) A low-spin d^7 complex with electronic configuration $(xy)^2(xz)^2(yz)^2(z^2)^1$. Compared to d^6 low-spin complexes, there is an additional electron in the z^2 orbital.

This orbital is particularly antibonding towards the apical ligand ⇒ substantial lengthening of this bond.

(b) Two electrons in z^2 (low-spin d^8): even greater lengthening of the apical bond.

3. A high-spin d^4 complex with electronic configuration $(xy)^1(xz)^1(yz)^1(z^2)^1$. The M—$Cl_a$ bond will be longer than M—Cl_b, due to the electron in z^2 (exp: M—Cl_a = 2.58 Å, M—Cl_b = 2.30 Å).
4. $(xy)^2(xz)^2(yz)^2(z^2)^2 \rightarrow (xy)^2(xz)^2(yz)^2(z^2)^1(x^2-y^2)^1$. Loss of an electron from z^2 (M—L_a antibonding) shortens the M—L_a bond. Addition of an electron to x^2-y^2 (M—L_b antibonding) lengthens the M—L_b bonds. Compared to the case of a low-spin complex (M—L_a > M—L_b), the bond lengths tend to become equal in a high-spin complex.

2.8.

1. See § 2.2.1, Figure 2.6 and § 2.3.1, Figure 2.9.
2. Low-spin d^8 $(b_{2g})^2(e_g)^4(a_{1g})^2$ for square-planar; d^8 high-spin $(e)^4(t_2)^4$ for the tetrahedron, with two unpaired electrons in the t_2 block.
3. Square-planar: six electrons in nonbonding orbitals, and two in very weakly antibonding orbitals, in the d block; tetrahedron: four electrons in nonbonding orbitals and four in weakly antibonding orbitals. The bonds are weaker in the tetrahedron.

2.9.

1.

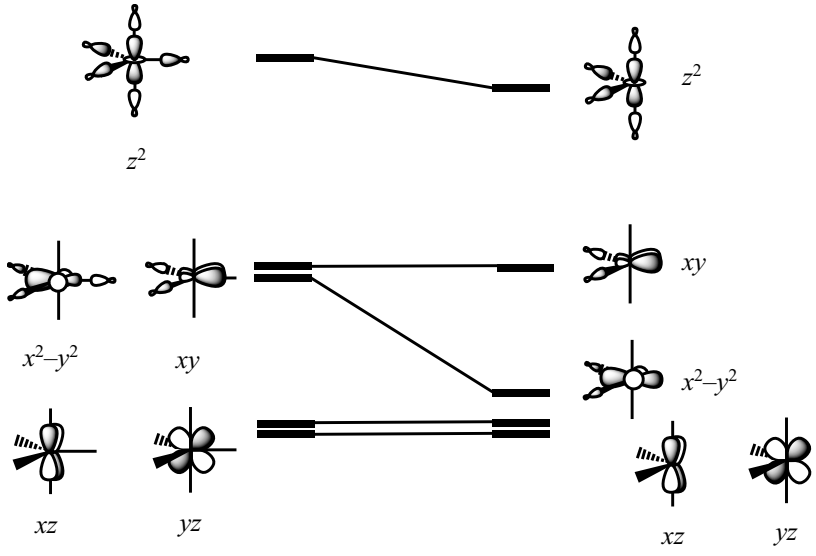

2. Compare with Figure 2.15 (right-hand side): the x^2-y^2 orbital ($1a_1$) is slightly antibonding, since the two ligands are not exactly on the nodal planes, as they are when $L_1—M—L_2 = 90°$. However, the *xy* orbital (b_2) is less antibonding, as in this case the three ligands are no longer pointing exactly towards the regions of greatest amplitude for *xy*. The gap between x^2-y^2 and *xy* therefore becomes smaller.

2.10. For the ML_4 complex, use the orientation given in Exercise 2.4. The result obtained is exactly the same as that established in § 2.8.4 (Figure 2.16), since the bond angles are 90° in both cases.

2.11. (1) and (2) The symmetry-adapted orbitals on the ligands have a_1 and t_2 symmetries (Chapter 6, § 6.6.2). Due to the (weakly) bonding overlaps, the a_1 orbital is lower in energy than the t_2 orbitals. The character table for the T_d point group (Chapter 6, § 6.6.2, Table 6.20) shows the symmetries of the metal orbitals: a_1 (*s*), t_2 (*p*), $e \oplus t_2$ (*d*). The following interaction diagram is obtained, characterized by a two-orbital interaction (a_1), interactions involving two sets of three orbitals (t_2), and nonbonding e orbitals (the order of the antibonding MOs $2a_1$ and $3t_2$ is not obvious, and may depend on the particular system considered):

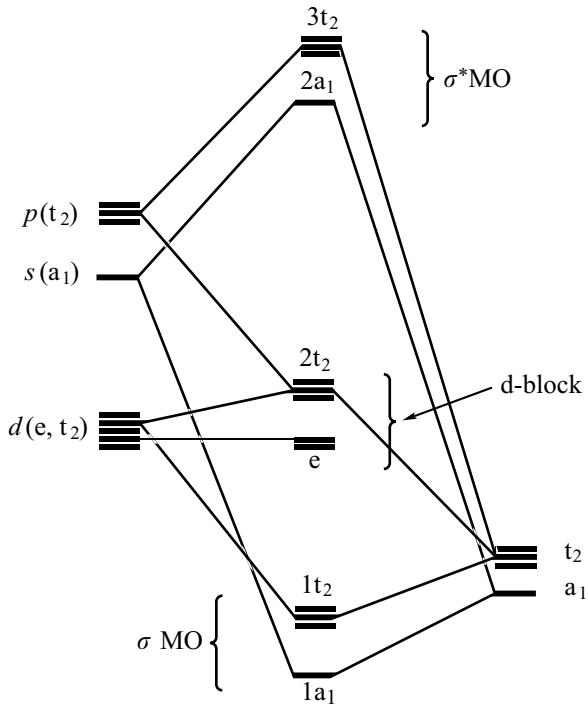

2.12. Trigonal-planar ML_3 complex

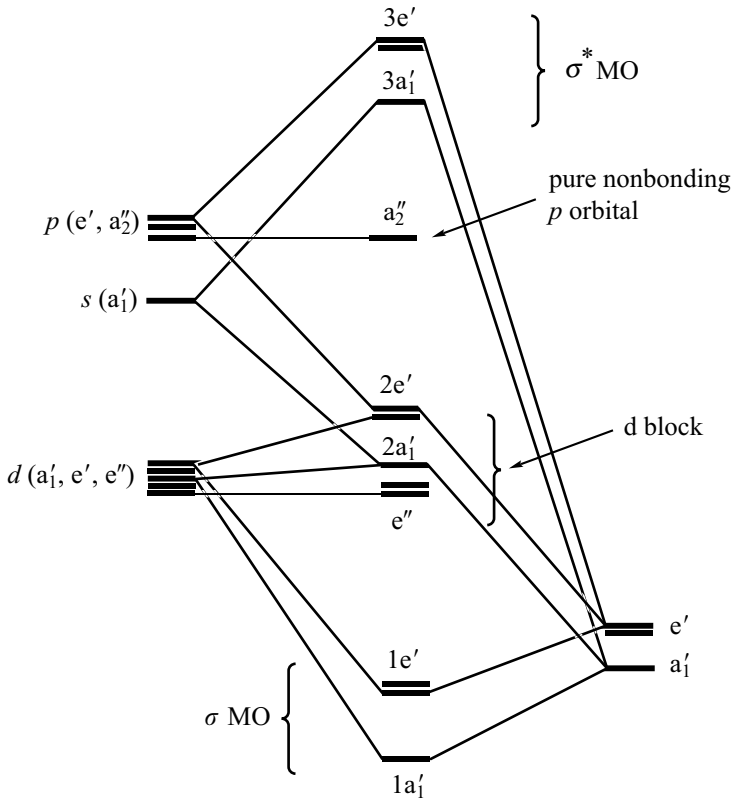

2.13.

1. The *s* orbital, which is totally symmetric like z^2 (a_1 symmetry).
2. The interaction between the *s* orbital on the metal and the ligand orbitals is bonding. As a result, the amplitude of z^2 decreases in the plane of the complex (*xy*) but increases along the *z*-axis. The metal–ligand interactions are therefore less antibonding after the polarization.

Chapter 3: π-type interactions

3.1.

1. See Figure 2.6 (right-hand side)
2. (a) z^2 is unchanged (overlap zero by symmetry with the lone pairs (p_{Cl}) on the chloride ligands); one orbital (*xy*) is destabilized by *four* antibonding interactions with p_{Cl}; two orbitals (*xz* and *yz*) are destabilized less strongly by

two antibonding interactions with p_{Cl}. Without detailed calculations, the position of z^2 with respect to the three other orbitals is not clear.

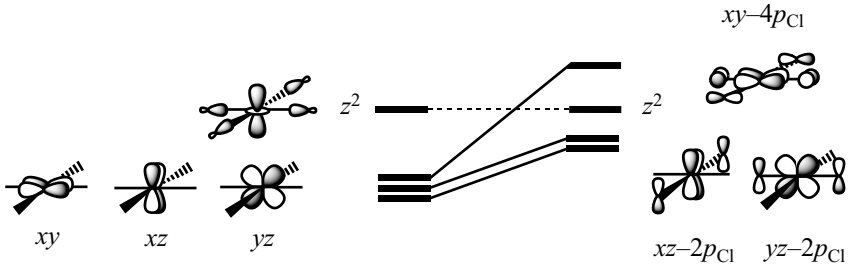

(b) *xy* is now stabilized by four bonding interactions with the π^*_{CN} orbitals (CN is a double-face π-acceptor, like CO), *xz* and *yz* by two bonding interactions.

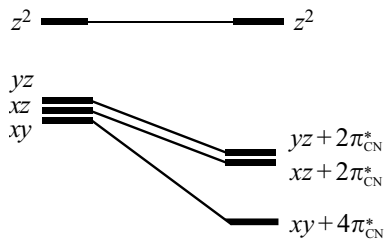

(c) z^2 and one of the three nonbonding MO are unchanged, but the two others are destabilized by an antibonding interaction with one p_{Cl}.

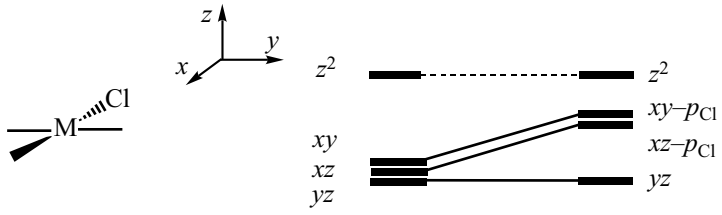

3.2. 1. See Figure 2.10.

2. 1a: Large overlaps between *yz* (nonbonding) and π^*_y, and between *xz* (nonbonding) and π^*_x; very small overlaps between x^2–y^2 and π^*_y (one bonding and one antibonding interaction, which do not completely cancel due to the

polarization of $x^2 - y^2$ (see question 1)); the same situation for xy and π_x^*.

1b: By symmetry (the xy and yz planes), there are interactions between yz (nonbonding) and π_z^*, and between xy (antibonding) and π_x^*.

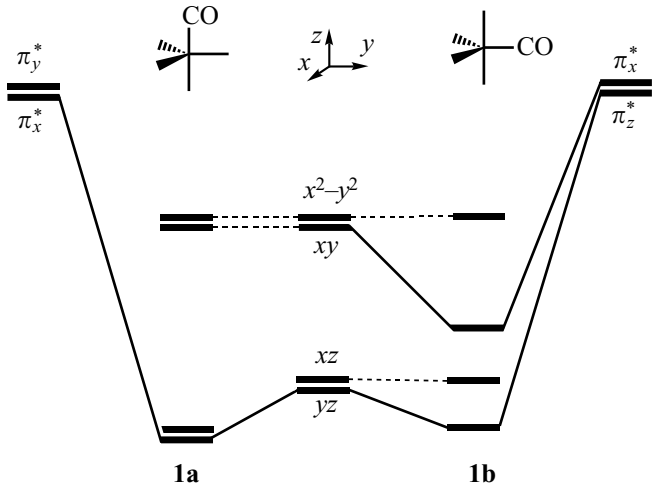

There are two stabilizing interactions in each case. The strongest interaction involves xy (antibonding) and π_x^* (these orbitals are closest in energy, and the overlap is larger due to the polarization of xy).

3. The most favourable site for substitution so far as the π interactions are concerned is axial for a d^4 complex and equatorial for a d^8 complex.
4. The same type of interactions, but antibonding (a double-face π-donor ligand).
5. d^4: equatorial substitution (one destabilizing interaction instead of two for axial substitution); d^8: two destabilizing interactions in both isomers, but axial substitution is favoured since one of the overlaps is larger for equatorial substitution.

3.3.

1. See Chapter 1, § 1.1.1.2
2. (i) a nonbonding σ orbital, concentrated on C; (ii) see Chapter 1, Figure 1.7; (iii) a π acceptor; (iv) through carbon.
3. The MO are similar to those in $[M(CO)_6]$ (see Scheme 3-35).
4. The bonds are shorter in $[Fe(CN)_6]^{4-}$ (an Fe(II) complex, with six electrons in π-bonding MO in the d block) than in $[Fe(CN)_6]^{3-}$ (an Fe(III) complex with only five electrons in π-bonding MO).

5. No, since the Fe^{3+} cation is smaller than the Fe^{2+} cation.
6. (i) d^3 for each of them; (ii) CN is a π acceptor, F a π donor (see Figure 3.8).

3.4.

1. $xz(P_1)$ and $xy(P_2)$.
2. x^2-y^2: **SS**; xz: **SA**; yz: **AA**
3.

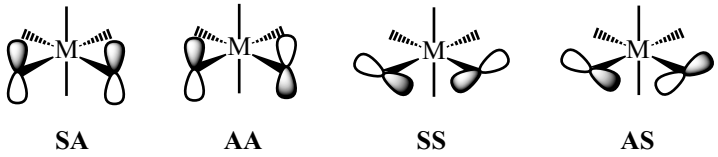

4. Three.
5. and 6.

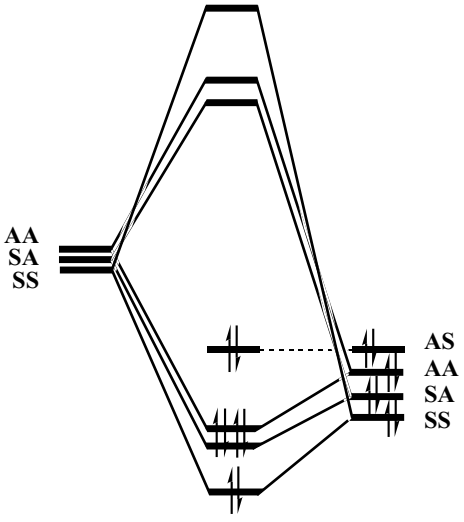

7. (i) 12; (ii) 18.

3.5.

1. Two, xz and yz.
2. (a) Two bonding interactions with the π^*_{CO} orbitals for axial substitution, only one for equatorial substitution;
   (b) axial.

3.6. Use the orbitals established in Exercise 6.13 (questions 4 and 6), but for $[Pt(CN)_4]^{2-}$, the p orbitals on the ligands should be replaced by the π^*_{CN} orbitals. The interaction diagram may be obtained by considering the symmetry properties of these orbitals and of the

metal *d* orbitals (see Table 6.18). There are three interactions: two involve e_g orbitals, and one concerns b_{2g} orbitals.

3.7.

1. See Chapter 2, Figure 2.11.
2. Use Figure 6.11.
3. Two interactions between e' orbitals and two between e'' orbitals.
4. It is not possible to establish easily the two-fold degeneracy of the orbitals.

Chapter 4: Applications

4.1.

1. Structure 2 (the same analysis as in § 4.1.1).
2. and 3.: See T. A. Albright, R. Hoffmann, J. C. Thibeault, D. Thorn *J. Am. Chem. Soc. 101*, 3801 (1979).

4.2.

1. See Chapter 2, § 2.8.2.
2. See Chapter 2, § 2.6.1 and Chapter 4, § 4.2.2.
3. A 'T-shaped' structure for $[Rh(PPh_3)_3]^+$ (d^8) and trigonal for $[Pt(PPh_3)_3]$ (d^{10}).

4.3.

1. See Chapter 2, § 2.1.2.4 (*trans*) and 2.1.2.5 (*cis*).
2. The same types of diagram as in the dichloro octahedral complexes (*trans*: see Chapter 3, § 3.3.1; *cis*: see Chapter 3, Exercise 3.4).
3. d^0: *cis*; d^2: *trans*; see D. M. P. Mingos *J. Organomet. Chem. 179*, C29 (1979).
4. $[OsO_2F_4]^{2-}$: *trans*; $[MoO_2Cl_4]^{2-}$: *cis*.

4.4.

1. d^6
2. See the analysis in Chapter 4, § 4.1.3 and A. Jarid, A. Lledos, D. Lauvergnat, Y. Jean *New J. Chem. 21*, 953 (1997).
3. (0, 0), (0, 90), and (90, 90).
4. Coplanar or perpendicular, the first being more stable.

4.5.

1. See the analysis for the bis-ethylene complexes (Chapter 4, § 4.1.3).
2. d^2: 1; d^4: 2; d^6: 2.
3. The back-donation interactions towards the carbenes decrease, so the rotation barrier also decreases.

4.6

1. For the *d* orbitals in the octahedron, use the sketches given in Figure 2.4. For those in the square-planar structure, use the representation in Exercise 2.4 (rotated by 90°). For the MO that characterize the broken M—H bonds, see Figure 4.12.
2. Yes.
3. An orbital in the reactant that characterizes a bond becomes a d-block orbital in the product.

Chapter 5: The isolobal analogy

5.1.

1. $CH_3—CH_3$; $[(CO)_5Mn—Mn(CO)_5]$
2. 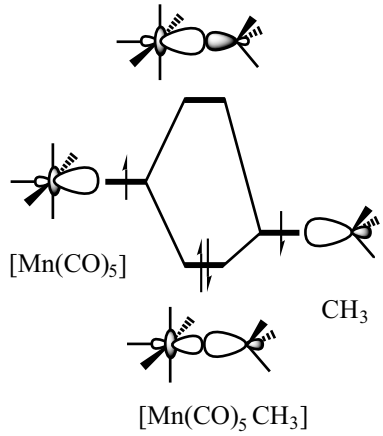

5.2.

1. 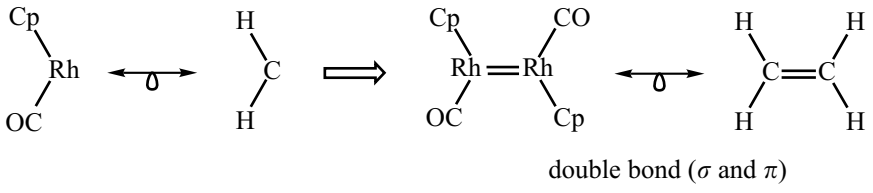

2. $[CpRh(\mu\text{-}CO)]_2$, with two bridging CO.

5.3.

1. and 2.

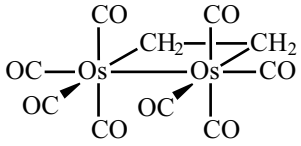

5.4.

1.

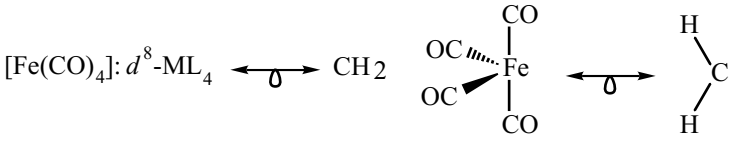

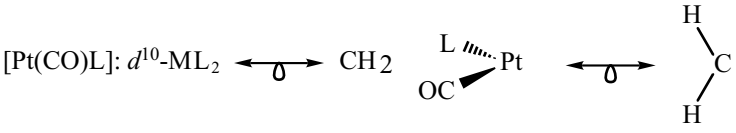

2.

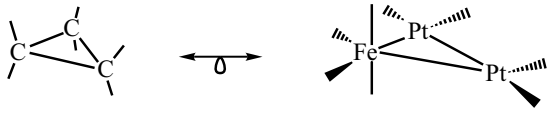

C_3H_6 $[Fe(CO)_4(Pt(CO)L)_2]$

Planar coordination around the platinum atoms, octahedral around the iron.

5.5.

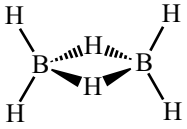

1. CH_2^+.
2. BH_2.
3. Diborane B_2H_6.

5.6.

1. (a).
2. (b) (analogues of cyclopropane).

5.7.

1.

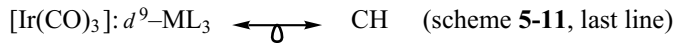

2. These are also isolobal analogues of tetrahedrane.
3. Tetrahedral representations, like structures 1 and 2 in the question.

5.8. Yes for the organic molecule ('orthogonal' ethylene), but not for the complex. There is a π interaction, weaker than that in conformation (a), which involves a nonbonding *d* orbital on the metal (see Chapter 4, § 4.1.1.).

Chapter 6: Elements of group theory and applications

6.1. (1) Two; (2) three, each of which contains an N—H bond and bisects the opposite H—N—H angle (planes written $\sigma_v(1)$, $\sigma_v(2)$, and $\sigma_v(3)$); (3) three: the molecular plane and two planes perpendicular to it, one perpendicular to the C—C bond, the other bisecting the H—C—H angles; (4) two, since the third plane described above for ethylene is not a symmetry element here (H—C—F angles); (5) one, the molecular plane; (6) four: the molecular plane and the three planes perpendicular to it which each contain an Al—Cl bond.

6.2. (1) Yes; (2) no; (3) no; (4) yes; (5) no; (6) yes; (7) no; (8) no; (9) yes; (10) yes; (11) no.

6.3.

1. No.
2. The C_3 axes are co-linear with one of the C—H bonds; the C_2 axes bisect two opposite H—C— H angles.
3. (a) three, at the intersections of the three planes found in Exercise 6.1 (question 3);
   (b) one, the intersection of the two reflection planes (Exercise 6.1, question 4);
   (c) one, perpendicular to the molecular plane.
4. a C_3 axis perpendicular to the molecular plane and three C_2 axes, each of which is co-linear with one of the Al—Cl bonds.

6.4.

1. $S_3^2 = C_3^2$ and $S_3^4 = C_3$.
2. (i) S_3; (ii) S_6.

6.5.

1. $\sigma_v(1)C_3 = \sigma_v(2)$; $C_3\sigma_v(1) = \sigma_v(3)$ (non-commutative).
2. $(C_3\sigma_v(1))\sigma_v(2) = C_3(\sigma_v(1)\sigma_v(2)) = C_3^2$ (associative).
3. E, C_3^2, C_3, $\sigma_v(1)$, respectively.

6.6. Consult § 6.2.2. (1) point 1: $D_{\infty h}$; (2) point 1: $C_{\infty v}$; (3) point 4: D_{2h}; (4) point 3: C_{2v}; (5) point 3: C_{2h}; (6) point 4: D_{3h}; (7) point 1: T_d; (8) point 3: C_{2v}; (9) point 3: C_{3v}; (10) point 4: D_{4h}; (11) point 4: D_{3h}; (12) point 2: C_s.

6.7.

$$\int_{\text{space}} [2(1s_{H_1}) - (1s_{H_2}) - (1s_{H_3})] \times [1s_{H_1} + 1s_{H_2} + 1s_{H_3}] d\tau$$
$$= (2 - 1 - 1) + S(2 + 2 - 1 - 1 - 1 - 1) = 0$$

6.8.

1. $\Gamma_H = A_g \oplus B_{1g} \oplus B_{2u} \oplus B_{3u}$.
2.

$$A_g : \frac{1}{2}(1s_{H_1} + 1s_{H_2} + 1s_{H_3} + 1s_{H_4})$$
$$B_{1g} : \frac{1}{2}(1s_{H_1} - 1s_{H_2} + 1s_{H_3} - 1s_{H_4})$$
$$B_{2u} : \frac{1}{2}(1s_{H_1} - 1s_{H_2} - 1s_{H_3} + 1s_{H_4})$$
$$B_{3u} : \frac{1}{2}(1s_{H_1} + 1s_{H_2} - 1s_{H_3} - 1s_{H_4})$$

6.9.

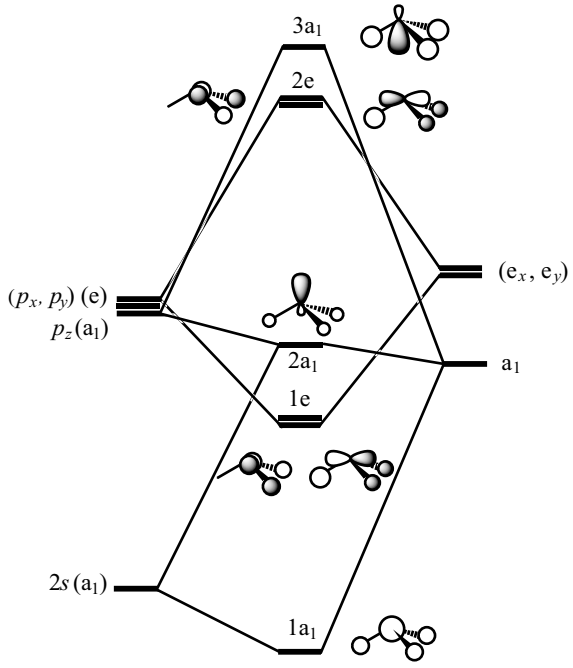

6.10.

$$\phi_{A_1} = \frac{1}{2}(\sigma_1 + \sigma_2 + \sigma_3 + \sigma_4)$$
$$\phi_{T_2}(2) = \frac{1}{\sqrt{2}}(\sigma_3 - \sigma_4)$$
$$\phi_{T_2}(1) = \lambda\sigma_1 - \mu(\sigma_2 + \sigma_3 + \sigma_4)$$

where $\lambda^2 + 3\mu^2 = 1$ (normalization)
$\phi_{T_2}(1)$ and ϕ_{A_1} orthogonal $\Rightarrow \lambda = 3\mu$

$$\Rightarrow \phi_{T_2}(1) = \frac{1}{\sqrt{12}}(3\sigma_1 - \sigma_2 - \sigma_3 - \sigma_4)$$

$$\phi_{T_2}(3) = \lambda\sigma_2 - \mu(\sigma_3 + \sigma_4)$$

where $\lambda^2 + 2\mu^2 = 1$ (normalization)
$\phi_{T_2}(3)$ and ϕ_{A_1} orthogonal $\Rightarrow \lambda = 2\mu$

$$\Rightarrow \phi_{T_2}(3) = \frac{1}{\sqrt{6}}(2\sigma_2 - \sigma_3 - \sigma_4)$$

6.11. 1. and 2.

D_{3h}	E	C_3^1	C_3^2	$C_2(1)$	$C_2(2)$	$C_2(3)$	σ_h	S_3^1	S_3^2	$\sigma_v(1)$	$\sigma_v(2)$	$\sigma_v(3)$
$R_k(\sigma_1)$	σ_1	σ_2	σ_3	σ_1	σ_3	σ_2	σ_1	σ_2	σ_3	σ_1	σ_3	σ_2
$R_k(\sigma_2 - \sigma_3)$	$\sigma_2 - \sigma_3$	$\sigma_3 - \sigma_1$	$\sigma_1 - \sigma_2$	$\sigma_3 - \sigma_2$	$\sigma_2 - \sigma_1$	$\sigma_1 - \sigma_3$	$\sigma_2 - \sigma_3$	$\sigma_3 - \sigma_1$	$\sigma_1 - \sigma_2$	$\sigma_3 - \sigma_2$	$\sigma_2 - \sigma_1$	$\sigma_1 - \sigma_3$
A_1'	1	1	1	1	1	1	1	1	1	1	1	1
E'	2	−1	−1	0	0	0	2	−1	−1	0	0	0

$\phi_{A_1'} = 4 \times (\sigma_1 + \sigma_2 + \sigma_3)$, so the normalized function is $(1/\sqrt{3})(\sigma_1 + \sigma_2 + \sigma_3)$.

$\phi_{E'}(1) = 2\sigma_1 - \sigma_2 - \sigma_3 + 2\sigma_1 - \sigma_2 - \sigma_3 = 4\sigma_1 - 2\sigma_2 - 2\sigma_3$, so the normalized function is $(1/\sqrt{6})(2\sigma_1 - \sigma_2 - \sigma_3)$.

$\phi_{E'}(2) = 2 \times (\sigma_2 - \sigma_3) - (\sigma_3 - \sigma_1) - (\sigma_1 - \sigma_2) + 2 \times (\sigma_2 - \sigma_3) - (\sigma_3 - \sigma_1) - (\sigma_1 - \sigma_2) = 6\sigma_2 - 6\sigma_3$ so the normalized function is $(1/\sqrt{2})(\sigma_2 - \sigma_3)$.

6.12. 1. and 2.

D_{3h}	E	C_3^1	C_3^2	$C_2(1)$	$C_2(2)$	$C_2(3)$	σ_h	S_3^1	S_3^2	$\sigma_v(1)$	$\sigma_v(2)$	$\sigma_v(3)$
$R_k(p_{\parallel 1})$	$p_{\parallel 1}$	$p_{\parallel 2}$	$p_{\parallel 3}$	$-p_{\parallel 1}$	$-p_{\parallel 3}$	$-p_{\parallel 2}$	$p_{\parallel 1}$	$p_{\parallel 2}$	$p_{\parallel 3}$	$-p_{\parallel 1}$	$-p_{\parallel 3}$	$-p_{\parallel 2}$
$R_k(p_{\parallel 2} - p_{\parallel 3})$	$p_{\parallel 2} - p_{\parallel 3}$	$p_{\parallel 3} - p_{\parallel 1}$	$p_{\parallel 1} - p_{\parallel 2}$	$p_{\parallel 2} - p_{\parallel 3}$	$p_{\parallel 1} - p_{\parallel 2}$	$p_{\parallel 3} - p_{\parallel 1}$	$p_{\parallel 2} - p_{\parallel 3}$	$p_{\parallel 3} - p_{\parallel 1}$	$p_{\parallel 1} - p_{\parallel 2}$	$p_{\parallel 2} - p_{\parallel 3}$	$p_{\parallel 1} - p_{\parallel 2}$	$p_{\parallel 3} - p_{\parallel 1}$
A_2'	1	1	1	−1	−1	−1	1	1	1	−1	−1	−1
E'	2	−1	−1	0	0	0	2	−1	−1	0	0	0

$\phi_{A_2'} = 4 \times (p_{\parallel 1} + p_{\parallel 2} + p_{\parallel 3})$, so the normalized function is $(1/\sqrt{3})(p_{\parallel 1} + p_{\parallel 2} + p_{\parallel 3})$.

$\phi_{E'}(1) = 2p_{\parallel 1} - p_{\parallel 2} - p_{\parallel 3} + 2p_{\parallel 1} - p_{\parallel 2} - p_{\parallel 3} = 2 \times (2p_{\parallel 1} - p_{\parallel 2} - p_{\parallel 3})$, so the normalized function is $(1/\sqrt{6})(2p_{\parallel 1} - p_{\parallel 2} - p_{\parallel 3})$.

$\phi_{E'}(2) = 2 \times (p_{\parallel 2} - p_{\parallel 3}) - (p_{\parallel 3} - p_{\parallel 1}) - (p_{\parallel 1} - p_{\parallel 2}) + 2 \times (p_{\parallel 2} - p_{\parallel 3}) - (p_{\parallel 3} - p_{\parallel 1}) - (p_{\parallel 1} - p_{\parallel 2}) = 6 \times (p_{\parallel 2} - p_{\parallel 3})$, so the normalized function is $(1/\sqrt{2})(p_{\parallel 2} - p_{\parallel 3})$.

6.13. 1. and 2.

D_{4h}	E	$2C_4$	C_2	$2C_2'$	$2C_2''$	i	$2S_4$	σ_h	$2\sigma_v$	$2\sigma_d$
$\Gamma_{p\perp}$	4	0	0	−2	0	0	0	−4	2	0

$\Rightarrow \Gamma_{p\perp} = A_{2u} \oplus B_{2u} \oplus E_g$

3.

D_{4h}	E	C_4^1	C_4^3	C_2	C_{2a}'	C_{2b}'	C_{2a}''	C_{2b}''
$R_k(p_{\perp 1})$	$p_{\perp 1}$	$p_{\perp 4}$	$p_{\perp 2}$	$p_{\perp 3}$	$-p_{\perp 1}$	$-p_{\perp 3}$	$-p_{\perp 4}$	$-p_{\perp 2}$
$R_k(p_{\perp 2})$	$p_{\perp 2}$	$p_{\perp 1}$	$p_{\perp 3}$	$p_{\perp 4}$	$-p_{\perp 4}$	$-p_{\perp 2}$	$-p_{\perp 3}$	$-p_{\perp 1}$
A_{2u}	1	1	1	1	−1	−1	−1	−1
B_{2u}	1	−1	−1	1	−1	−1	1	1
E_g	2	0	0	−2	0	0	0	0

D_{4h}	i	S_4^1	S_4^3	σ_h	σ_{va}	σ_{vb}	σ_{da}	σ_{db}
$R_k(p_{\perp 1})$	$-p_{\perp 3}$	$-p_{\perp 4}$	$-p_{\perp 2}$	$-p_{\perp 1}$	$p_{\perp 1}$	$p_{\perp 3}$	$p_{\perp 4}$	$p_{\perp 2}$
$R_k(p_{\perp 2})$	$-p_{\perp 4}$	$-p_{\perp 1}$	$-p_{\perp 3}$	$-p_{\perp 2}$	$p_{\perp 4}$	$p_{\perp 2}$	$p_{\perp 3}$	$p_{\perp 1}$
A_{2u}	−1	−1	−1	−1	1	1	1	1
B_{2u}	−1	1	1	−1	1	1	−1	−1
E_g	2	0	0	−2	0	0	0	0

$\phi_{A_{2u}} = 4 \times (p_{\perp 1} + p_{\perp 2} + p_{\perp 3} + p_{\perp 4})$, so the normalized function is

$$\phi_{A_{2u}} = \frac{1}{2} \times (p_{\perp 1} + p_{\perp 2} + p_{\perp 3} + p_{\perp 4})$$

$$\phi_{B_{2u}} = \frac{1}{2} \times (p_{\perp 1} - p_{\perp 2} + p_{\perp 3} - p_{\perp 4}) \quad \text{(normalized)}$$

$$\phi_{E_g}(1) = \frac{1}{\sqrt{2}}(p_{\perp 1} - p_{\perp 3}) \quad \text{(normalized)}$$

$$\phi_{E_g}(2) = \frac{1}{\sqrt{2}}(p_{\perp 2} - p_{\perp 4}) \quad \text{(normalized)}$$

4.

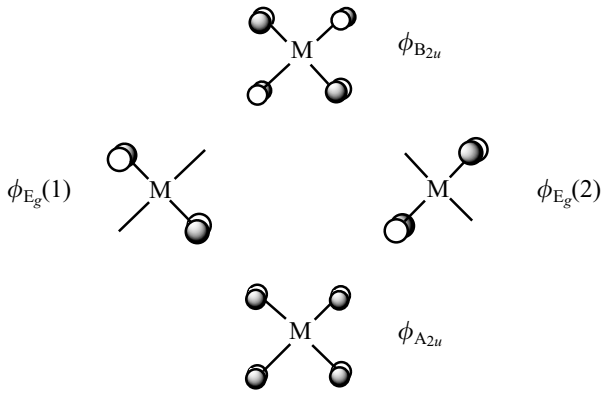

5. $\varepsilon_{A_{2u}} < \varepsilon_{Eg} < \varepsilon_{B_{2u}}$

6.

D_{4h}	E	$2C_4$	C_2	$2C_2^{'}$	$2C_2^{''}$	i	$2S_4$	σ_h	$2\sigma_v$	$2\sigma_d$
$\Gamma_{p\parallel}$	4	0	0	−2	0	0	0	4	−2	0

$\Rightarrow \Gamma_{p\parallel} = A_{2g} \oplus B_{2g} \oplus E_u$

Normalized functions:

$$\phi_{A_{2g}} = \frac{1}{2} \times (p_{\parallel 1} + p_{\parallel 2} + p_{\parallel 3} + p_{\parallel 4})$$

$$\phi_{B_{2g}} = \frac{1}{2} \times (p_{\parallel 1} - p_{\parallel 2} + p_{\parallel 3} - p_{\parallel 4})$$

$$\phi_{E_u}(1) = \frac{1}{\sqrt{2}}(p_{\parallel 1} - p_{\parallel 3})$$

$$\phi_{E_u}(2) = \frac{1}{\sqrt{2}}(p_{\parallel 2} - p_{\parallel 4})$$

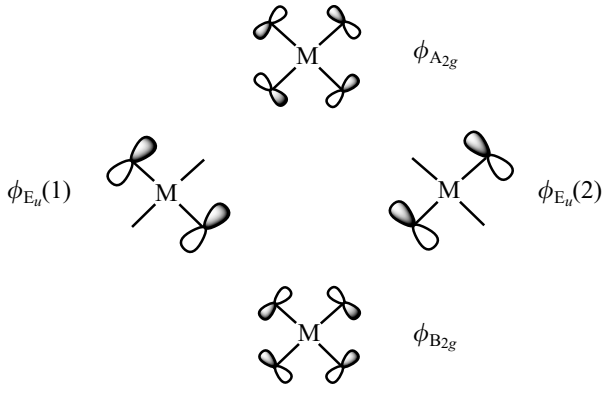

where $\varepsilon_{B2g} < \varepsilon_{E_u} < \varepsilon_{A_{2g}}$

Bibliography

In addition to the references given in the different chapters,several books have been useful for the preparation of this work.The following deserve a particular mention:

T. A. Albright, J. K. Burdett, and M.-H. Whangbo *Orbital Interactions in Chemistry*, Wiley (1985).

François Mathey and Alain Sevin, *Chimie moléculaire des éléments de transition*, Les Editions de l'Ecole Polytechnique (2000).

J. K. Burdett *Chemical Bonds: A Dialog*,Wiley (1997).

J. K. Burdett *Molecular Shapes*, Wiley (1980).

R. H. Crabtree *The Organometallic Chemistry of Transition Metals*, Wiley (1988).

J. E. Huheey, E. A. Keiter, and R. L. Keiter *Inorganic Chemistry: Principles of Structure and Reactivity*, fourth edition, Harper Collins College Publishers (1993).

E. W. Abel, F. Gordon A. Stone, and G. Wilkinson, *Comprehensive Organometallic Chemistry*, 2nd edn., vol. 13, Pergamon Press (1995).

F. A. Cotton, *Chemical Applications of Group Theory*, 3rd edn., Wiley (1990).

P. H. Walton, *Beginning Group Theory for Chemistry*, Oxford University Press (1998).

This page intentionally left blank

Index